



US Army Corps
of Engineers
Construction Engineering
Research Laboratories

AD-A266 778



3

USACERL Technical Report FM-92/03
August 1992

2

Vibro-Acoustic Analysis of an Aircraft Maintenance Dock

by
James Wilcoski
Louis Sutherland

DTIC
ELECTE
JUL 09 1993
S B D

This report documents an analysis of the effects of high-level acoustic environments on an Aircraft Maintenance Dock (AMD) designed for the U.S. Air Force by the U.S. Army Corps of Engineers. The analysis includes detailed estimation of the maximum sound levels inside the facility, identification of facility components that are potentially sensitive to high-level vibro-acoustic loads, and a summary of design considerations appropriate for this environment. The high noise levels represent the sum of direct sound pressures on the facility shell radiated by internal noise sources and the corresponding reverberant sound field inside the facility.

The maximum equivalent static pressures that would be expected to produce the same peak stress as the actual acoustic pressures inside the facility (including fatigue considerations) range from ± 32 pounds per square foot (psf) on the walls to ± 27 psf on the roof, and an average of ± 36 psf on the draft curtain.

Dynamic response and fatigue effects are incorporated into these estimated acoustic loads. Dynamic (g) load factors for equipment components mounted on the facility structure vary widely depending on location and equipment weight, ranging from ± 1.7 to ± 17 g's.

Additional details on vibro-acoustic design loads, including reaction loads on supporting structure due to acoustically induced vibration of wall and roof panels, vibration loads on the heating and ventilating (HV) system, and random vibration test specifications for equipment mounted inside the AMD, have also been determined.

Several critical components of the AMD were analyzed. Design modifications have been recommended as a result of this analysis for this facility, including increases in ductwork thickness, a new ductwork joint design, and vibration isolation for ductwork, exhaust fans, pipe systems, light fixtures, and wind truss supports. A summary of recommended design practices to minimize potential structural damage or equipment malfunction due to the high vibro-acoustic environments was developed.

Operation of the enclosed test equipment at higher levels was evaluated. This evaluation resulted in a table of allowable number of cycles of operation to produce the same impact on the facility as the original operational requirements.

The type of standard steel construction to be employed for this facility, typical of high bay test facilities, is not normally exposed to the type of intermittent high intensity vibro-acoustic loading anticipated from the planned test operations. However, if proper consideration is given to the vibro-acoustic loads specified herein for the design of the building shell and the mounting and/or qualifications of internal equipment, the planned use of the facility should not be significantly impaired.

Approved for public release; distribution is unlimited.

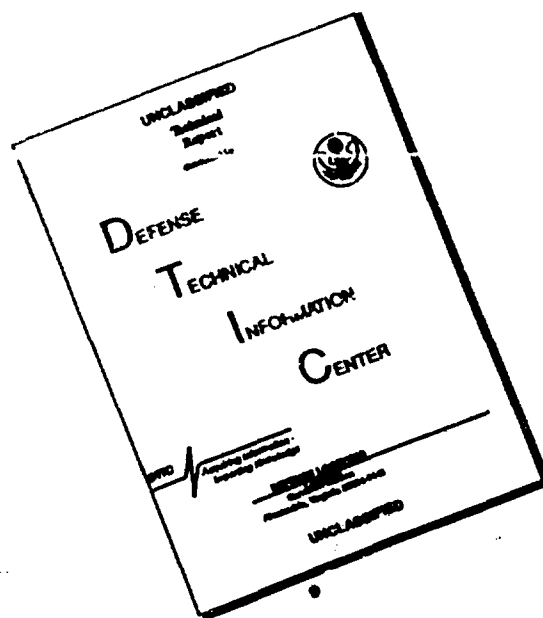
93 7 08 13 9

93-15557



25308

DISCLAIMER NOTICE



**THIS DOCUMENT IS BEST
QUALITY AVAILABLE. THE COPY
FURNISHED TO DTIC CONTAINED
A SIGNIFICANT NUMBER OF
PAGES WHICH DO NOT
REPRODUCE LEGIBLY.**

The contents of this report are not to be used for advertising, publication, or promotional purposes. Citation of trade names does not constitute an official endorsement or approval of the use of such commercial products. The findings of this report are not to be construed as an official Department of the Army position, unless so designated by other authorized documents.

DESTROY THIS REPORT WHEN IT IS NO LONGER NEEDED

DO NOT RETURN IT TO THE ORIGINATOR

USER EVALUATION OF REPORT

REFERENCE: USACERL TR FM-92/03, *Vibro-Acoustic Analysis of an Aircraft Maintenance Dock*

Please take a few minutes to answer the questions below, tear out this sheet, and return it to USACERL. As user of this report, your customer comments will provide USACERL with information essential for improving future reports.

1. Does this report satisfy a need? (Comment on purpose, related project, or other area of interest for which report will be used.)

2. How, specifically, is the report being used? (Information source, design data or procedure, management procedure, source of ideas, etc.)

3. Has the information in this report led to any quantitative savings as far as manhours/contract dollars saved, operating costs avoided, efficiencies achieved, etc.? If so, please elaborate.

4. What is your evaluation of this report in the following areas?

a. Presentation: _____

b. Completeness: _____

c. Easy to Understand: _____

d. Easy to Implement: _____

e. Adequate Reference Material: _____

f. Relates to Area of Interest: _____

g. Did the report meet your expectations? _____

h. Does the report raise unanswered questions? _____

i. General Comments. (Indicate what you think should be changed to make this report and future reports of this type more responsive to your needs, more usable, improve readability, etc.)

5. If you would like to be contacted by the personnel who prepared this report to raise specific questions or discuss the topic, please fill in the following information.

Name: _____

Telephone Number: _____

Organization Address: _____

6. Please mail the completed form to:

Department of the Army
CONSTRUCTION ENGINEERING RESEARCH LABORATORIES
ATTN: CECER-IMT
P.O. Box 9005
Champaign, IL 61826-9005

REPORT DOCUMENTATION PAGE			Form Approved OMB No. 0704-0188
Public reporting burden for this collection of information is estimated to average 1 hour per response, including the time for reviewing instructions, searching existing data sources, gathering and maintaining the data needed, and completing and reviewing the collection of information. Send comments regarding this burden estimate or any other aspect of this collection of information, including suggestions for reducing this burden, to Washington Headquarters Services, Directorate for Information Operations and Reports, 1215 Jefferson Davis Highway, Suite 1204, Arlington, VA 22202-4302, and to the Office of Management and Budget, Paperwork Reduction Project (0704-0188), Washington, DC 20503.			
1. AGENCY USE ONLY (Leave Blank)	2. REPORT DATE August 1992	3. REPORT TYPE AND DATES COVERED Final	
4. TITLE AND SUBTITLE Vibro-Acoustic Analysis of an Aircraft Maintenance Dock		5. FUNDING NUMBERS MIPR ENM9486 dated 19 April 1989	
6. AUTHOR(S) James Wilcoski, Louis Sutherland			
7. PERFORMING ORGANIZATION NAME(S) AND ADDRESS(ES) USACERL PO Box 9005 Champaign, IL 61826-9005		8. PERFORMING ORGANIZATION REPORT NUMBER USACERL TR FM-92/03	
9. SPONSORING/MONITORING AGENCY NAME(S) AND ADDRESS(ES) U.S. Army Engr. District, Omaha ATTN: CEMRO-ED-MB 215 North 17th Street Omaha NE 68102-4978		10. SPONSORING/MONITORING AGENCY REPORT NUMBER	
11. SUPPLEMENTARY NOTES Copies are available from the National Technical Information Service, 5285 Port Royal Road, Springfield, VA 22161.			
12a. DISTRIBUTION/AVAILABILITY STATEMENT Approved for public release; distribution is unlimited.		12b. DISTRIBUTION CODE	
13. ABSTRACT (Maximum 200 words) This report documents an analysis of the effects of high-level acoustic environments on an Aircraft Maintenance Dock (AMD) designed for the U.S. Air Force by the U.S. Army Corps of Engineers. The analysis includes detailed estimation of the maximum sound levels inside the facility, identification of facility components that are potentially sensitive to high-level vibro-acoustic loads, and a summary of design considerations appropriate for this environment. Several critical components of the AMD were analyzed. Design modifications have been recommended as a result of this analysis for this facility, including increases in ductwork thickness, a new ductwork joint design, and vibration isolation for ductwork, exhaust fans, pipe systems, light fixtures, and wind truss supports. A summary of recommended design practices to minimize potential structural damage or equipment malfunction due to the high vibro-acoustic environments was developed. The type of steel construction to be employed for this facility is not normally exposed to high-intensity vibro-acoustic loading. However, if proper consideration is given to the vibro-acoustic loads specified here for building design and qualifications of internal equipment, the planned use of the facility should not be significantly impaired.			
14. SUBJECT TERMS aircraft maintenance dock (AMD) vibro-acoustic environment vibro-acoustic analysis structural engineering		15. NUMBER OF PAGES 252	
		16. PRICE CODE	
17. SECURITY CLASSIFICATION OF REPORT Unclassified	18. SECURITY CLASSIFICATION OF THIS PAGE Unclassified	19. SECURITY CLASSIFICATION OF ABSTRACT Unclassified	20. LIMITATION OF ABSTRACT SAR

FOREWORD

This study was conducted for the U.S. Army Corps of Engineers, Omaha District, Special Projects Branch and Design Branch, under MIPR ENM9486, dated 19 April 1989; Work Unit SD9 R-D/N-Omaha, "Vibro-Acoustic Analysis." The Omaha District technical monitor was Larry Sand, CEMRO-ED-MB.

The research was performed by the Engineering and Materials Division (EM) of the U.S. Army Construction Engineering Research Laboratories (USACERL). Portions of this research were conducted by Louis Sutherland with the assistance of John Kaytor and Ron Brown, all of Wyle Research, El Segundo, CA. Dr. Paul A. Howdyshell is Chief of USACERL-EM. The USACERL technical editor was Gordon L. Cohen, Information Management Office.

The authors gratefully acknowledge the considerable efforts of Elizabeth C. Golish of USACERL, who formatted equations, tables, and figures for this report. The authors also thank Mr. Saniuk, Mr. Sand, and Kevin Howe, Omaha District, for providing information in support of this work.

COL Daniel Waldo, Jr. is Commander and Director of USACERL, and Dr. L.R. Shaffer is Technical Director.

DTIC COPY 11-11-1989 5

Accession For		<input checked="checked" type="checkbox"/>
NTIS	GRA&I	<input type="checkbox"/>
DTIC	TAB	<input type="checkbox"/>
Unannounced		
Justification		
By		
Distribution/		
Availability Codes		
Avail and/or		
Special		
Dist		
A-1		

CONTENTS

	Page
SF298	1
FOREWORD	2
LIST OF FIGURES AND TABLES	6
 1 INTRODUCTION	 13
Background	13
Objective	13
Approach	13
Scope	14
 2 FACILITY DESCRIPTION	 15
 3 ACOUSTIC ANALYSIS	 22
"Quick Look" at Noise Environment to Evaluate the Need for Model Test	22
Test Evaluation of Acoustic Data Reports	22
Development of Analysis Approach	23
Results of Acoustic Analysis	24
Baseline Environment for Reference Source Position	24
Variation in Baseline Acoustic Environment	27
Acoustic Design Environment	34
 4 VIBRO-ACOUSTIC RESPONSE TO THE AMD ACOUSTIC ENVIRONMENT	 37
Development of Vibro-Acoustic Design Environments	37
Equivalent Static Pressure Loads for AMD Acoustic Environment	43
Equivalent Static Pressures for Wall Panels	43
Equivalent Static Pressures for Other AMD Structural Panels	50
Vibration Loads for Design of AMD Equipment and Mounting Structure	53
Vibration Load Factors	53
Vibration Reaction Loads	56
Additional Details From Studies of Vibro-Acoustic Loads on Specific AMD Elements	57
Vibration and Acoustic Environmental Test Specifications	61
Acoustic Test Specifications	61
Vibration Test Specifications	62
Combined Environmental, Snow, Seismic, and Wind Loads	68
Effective Loading on Roof Deck and Rigid Insulation Fasteners	68
Summary: Design for Vibro-Acoustic Environments in the AMD	70
 5 RESPONSE OF EQUIPMENT TO ACOUSTIC AND VIBRATION ENVIRONMENTS	 71
Response of Equipment Packages to Acoustic Excitation	71
Rigid-Body Response to Acoustic Excitation	71
Vibro-Acoustic Response of Flexible Equipment Panels	73
General Criteria for Threshold of Equipment Malfunction from Acoustic Environments	75
Response of Equipment to Random Vibration Environments	78
Rigid-Body Response to Vibration	78

CONTENTS (Cont'd)

	Page
Vibration Response of Nonrigid Equipment	79
General Criteria for Equipment Malfunction from Vibration Environments	80
6 RECOMMENDED VIBRO-ACOUSTIC ENVIRONMENT DESIGN PRACTICES FOR AMD COMPONENTS	83
7 BUILDING COMPONENT RESPONSE AND STRENGTHENING RECOMMENDATIONS	85
Hangar Door Panels	85
Personnel Door	86
Roof Deck	87
Dynamic Response of the Roof System	87
HV Unit Dynamic Behavior	87
Ductwork	89
Duct Gage Thickness	90
Duct Connection Details	90
Control Panels	94
Fire Protection Oscillating Monitor Nozzles	94
Louvers and Dampers	94
Wall Mounted Emergency Shower and Eye Wash	95
Carbon Monoxide/Carbon Dioxide Detector Sensors	95
Thermostats and Other Small Controls	95
Miscellaneous Detectors, Switches and Other Electrical Equipment	96
Conduit, Connectors, Fittings, and Mineral-Insulated Cable	96
Combustible Vapor Sensors	97
8 BUILDING COMPONENT VIBRATION ISOLATION RECOMMENDATIONS	98
Horizontal Wind Braces	98
Heating and Ventilating Units	102
Ductwork	104
Exhaust Fans	108
Pipe Systems	110
Steam and Condensate Pipes	110
Hot Water and Heating Pipes	112
Fire Protection Pipes	114
General Recommendations for Pipe Systems	117
Lighting Fixtures	117
HID Lights	117
Fire Protection Strobe and Beacon Lights	119
Emergency Exit Lights	120
General Recommendations for Lighting Fixtures	121
9 CONCLUSIONS AND RECOMMENDATIONS	122
Conclusions	122
Recommendations	122
REFERENCES	123

CONTENTS (Cont'd)

	Page
APPENDIX A: List of AMD Components and Initial Indication of Potential Sensitivity to Vibro-Acoustic Loads	125
APPENDIX B: Calculation of the Acoustic Environment Inside the AMD	128
APPENDIX C: Near Field and Approximate Angle of Incidence Effects on Acoustic Loads on Walls and Roof of AMD	151
APPENDIX D: Review of Structural Response for Wide Band Random Noise Field	156
APPENDIX E: Experimental Measurement and Analysis of Typical Pre-Insulated Wall Panel Structural Characteristics	170
APPENDIX F: Extract From AISC Code for Steel Building Construction Fatigue	177
APPENDIX G: Reaction Loads on Supporting Structures for Beams and Plates Subject to Vibration	181
APPENDIX H: Detailed Data on Vibro-Acoustic Loads on Specific AMD Elements	183
APPENDIX I: Equipment Response Calculations	223
APPENDIX J: Qualification of Alternate Isolators	247

DISTRIBUTION

FIGURES

Number		Page
1	AMD Exterior	16
2	AMD Interior	17
3	Typical roof assembly (preliminary design concept)	18
4	Typical wall assembly (preliminary design concept)	19
5	Back door (representative of preliminary design concept)	20
6	Draft curtain (preliminary design concept)	21
7	Variation with rpm of primary source in one-third octave band sound pressure level at 3 ft above top center of back door	24
8	Variation in one-third octave band sound pressure level at 200 Hz near edge or corner in AMD (sources at 40 ft, 6820 rpm)	25
9	Variation across back wall in one-third band sound pressure level at 200 Hz (sources at 40 ft, 6820 rpm)	26
10	Variation across roof in one-third octave band sound pressure level at 200 Hz (sources at 40 ft, 6820 rpm)	26
11	Potential specific noise zones for interior surfaces of the AMD	28
12	Average one-third octave band sound pressure levels on AMD interior surface divided into noise zones according to Figure 11 (sources at 40 ft, 6820 rpm)	29
13	Change in one-third octave band sound level at 200 Hz along roof centerline for change in forward direction of main engine (at 6820 rpm)	31
14	Variation in sound level at 200 Hz due to change in position of source. (Sound level along line on roof directly over one pair of sources; all four operating at 6820 rpm.)	31
15	Effect of increasing absorption on one-third octave band sound pressure level near back center of roof	32
16	Sound levels on back, center of draft curtain with only auxiliary power sources operating for different values of absorption	33
17	Effect of increasing interior absorption on one-third octave band sound pressure level near back center of roof	35
18	Conceptual illustration of resonant vibration response of plate to uniform oscillating acoustic pressure	38

FIGURES (Cont'd)

Number		Page
19	Industrial wall sample mounted in test opening of Wyle 100,000 cu ft reverberation facility	41
20	Typical failures of steel panel in Figure 18 near panel-to-girt fastener	41
21	Normalized acceleration response of 26 gage corrugated steel industrial wall: (a) Response measured on panel between girts (b) Response measured on girts	42
22	Frequency spectrum of estimated spatial maximum deflection response for all modes at center of AMD wall panels (below 1000 Hz) subjected to environment in Table 3	45
23	Evaluation of fatigue damage under random loading, at stress levels above fatigue limits	47
24	Sinusoidal and random S/N curves in mild steel	48
25	Fatigue damage for steel-sinusoidal loading	49
26	Envelope of estimated average modal acceleration levels on wall panels of AMD exposed to acoustic design environment in Table 3	54
27	Decrease in baseline load factors in Table 5 for wall-mounted equipment	57
28	Vibration design and test envelope for components mounted on (a) wall panels, (b) girts, and (c) columns	63
29	Vibration design and test envelope for IR sensors mounted on (a) columns and (b) on 3x3x3/16 in. tube spanning girts	64
30	Vibration design and test envelope for components mounted on (a) roof deck/bar joists or (b) roof truss	65
31	Vibration design and test envelope for components mounted on (a) draft curtain panels or (b) truss frame supporting draft curtain	66
32	Vibration design and test envelope for components mounted on (a) door panels and (b) frame of door	67
33	Statistical variation in dynamic magnification factor for resonant response of complex structural systems	74
34	Design envelope for acoustic mobility of baffled flat panel with mounted equipment	75

FIGURES (Cont'd)

Number		Page
35	Maximum acoustical mobility of equipment cabinets measured in one-third octave bands in direction normal to cabinet walls from acoustic test of ground computer system	76
36	Modal vibration of roof truss 4	88
37	Modal vibration of roof truss C	89
38	Duct connection detail	93
39	Detail for attaching conduit to mechanical equipment	96
40	Examples of good and poor flexible cable connection details	97
41	Horizontal wind truss support	104
42	HV unit isolation	105
43	HV horizontal ductwork isolator locations	107
44	Horizontal duct vibration isolation support	108
45	Vertical ductwork vibration isolation support	109
46	Exhaust fan isolation support	109
47	Vertical support for steam and condensate pipes	111
48	Guided support for steam and condensate pipe	111
49	Horizontal pipes supported by bar joists	113
50	Vertical pipe support and isolation	113
51	HID light fixture support detail	118
52	Strobe light fixture support detail	119
53	Emergency exit light fixture	120
54	Shockproof designs for lights	121
B1	Rear view of one high bay area of AMD	132
B2	Composite reverberant sound level spectra on walls of AMD facility for various power settings (rpm) of main engines or for auxiliary power units operating at maintenance power	134

FIGURES (Cont'd)

Number		Page
B3	One-third octave band sound pressure levels at radius of 2.5 ft from center of auxiliary power unit	136
B4	Near field sound pressure level contours for one of four main engines	137
B5	Location of positions where sound levels on the inside of the AMD structure are tabulated	139
D1	Comparison of joint acceptance for the first ten (a) odd and (b) even modes of a simply supported beam in a diffuse sound field	162
E1	Photographs of vibration test setup on representative 2 in. wall panel	171
E2	Vibration response of test panel	172
E3	Vibration mode shapes of test panel	173
E4	Allowable wind load for typical preinsulated panel versus span based on maximum deflection = span/180	176
H1	Spectrum of acceleration response of roof deck/bar joist with and without loading by 6 in. diameter, Schedule 80 pipe	201
H2	Lumped mass mobility model for HV system	212
H3	Acceleration response spectrum for roof deck used as input to mobility model for HV vibration response	216

TABLES

1	Change in Total One-Third Octave Band Reverberant Plus Direct Sound Level at 200 Hz as Absorption Coefficient (α) for Roof is Increased	32
2	Allowable Personnel Exposure Time for a Range of Absorption Coefficients for AMD with Auxiliary Power Sources Operating at Maintenance Power	34
3	Acoustic Design Environment for AMD (One-Third Octave Band Sound Pressure Levels)	36
4	Summary of Wall Panel Characteristics	44
5	Summary of Equivalent Static Pressure for Design of Lightweight Structural Elements on AMD Subjected to Acoustic Design Environments in Table 3	52
6	Summary of Dynamic Response Loads for Design of AMD Supporting Structures or Attachment Hardware	55

TABLES (Cont'd)

Number		Page
7	Roof Vibro-Acoustic Loads for Alternative Bar Joists	58
8	Detailed Total Baseline Load Factors for Roof-Mounted Equipment	59
9	Summary of Vibration Response Parameters for Alternative Gages and Lengths of Draft Curtain	59
10	Summary of Vibro-Acoustic Response Parameters for 18 Gage Galvanized Steel Walls of HV Ducts	60
11	Summary of Calculated Vibration Response Parameters at Base of HV Unit	61
12	Summary of Vibration Test Specifications for AMD Equipment	62
13	Summary of Roof Live Loads (psf)	69
14	Trend in Threshold Levels for Malfunction of Equipment Exposed to Acoustic Environments*	77
15	Estimated Acoustically Induced Malfunction Rate of Sensitive Equipment Manufactured in the 1960's as a Function of Average One-Third Octave Sound Level	78
16	Cumulative Probability of a_p Exceeding $Y \times \bar{a}$	79
17	Failure Modes and Fragilities of Some Electronic Components from Vibration and Shock Environments	81
18	Hangar Door Panel Loading	86
19	Truss 4 Natural Frequencies (Hz)	88
20	Natural Frequencies for Roof Truss C	89
21	Ductwork Loading and Motion	91
22	Support Condition Specifications	99
23	Isolator Characteristics	103
24	Lowest Natural Frequency of Ductwork	106
B1	Sample Calculation of One-Third Octave Band Sound Power Level at 200 Hz (Input Data Provided by Main Engine Manufacturer)	130
B2	Interior Surface Acoustic Absorption for AMD	132

TABLES (Cont'd)

Number		Page
B3	Summary of Calculation of Reverberant Sound Pressure Levels	133
B4	Composite Reverberant Plus Direct One-Third Octave Band Sound Pressure Levels on Roof	140
B5	Composite Reverberant Plus Direct One-Third Octave Band Sound Pressure Levels on Back Wall	142
B6	Composite Reverberant Plus One-Third Octave Band Sound Pressure Levels Across Bottom Edge of Draft Curtain	143
B7	Composite Reverberant Plus Direct One-Third Octave Band Sound Pressure Levels Along Line from Center of Back Door Opening Up to Roof and Then Along Roof Centerline	144
B8	Composite Reverberant Plus Direct One-Third Octave Band Sound Pressure Levels Along Line from Center of Back Door Opening Up to Roof and Then Along Roof Centerline (for three different positions of source: 40 ft, 60 ft, and 80 ft, all at idle power [3215 rpm])	145
B9	Composite Reverberant Plus Direct One-Third Octave Band Sound Pressure Levels At Lower Midpoint of Back Side at Draft Curtain	147
B10	Effect of Changing Absorption Coefficient for Walls and Roof From 0 (Hard) to 0.1 (Soft) On Sound Levels On the Roof Centerline, 5 ft Forward	148
B11	Effect of Closing Doors with Only APUs Operating on Level at Bottom Center of Back of Draft Curtain	148
B12	Change in Level for Operation at Idle, 6820, and 8060 rpm	149
D1	Variation in Constant K' in Eq D32 with Panel Aspect Ratio a/b	168
E1	Observed and Predicted Modal Frequencies	174
H1	Summary of Calculation of Vibro-Acoustic Response of Wall Panels	184
H2	Load Factors for Equipment Mounted on Wall Panels, Girts and Columns	188
H3	Effective Structural Weights for Wall-Mounted Equipment	189
H4	Roof Vibro-Acoustic Loads for Alternative Bar Joists	191
H5	Summary of Calculations of Vibro-Acoustic Response of Roof	192
H6	Schematic Diagram of Analysis of Vibro-Acoustic Load Factors on Truss-Mounted Equipment	194

TABLES (Cont'd)

Number		Page
H7	Effective Weights of Roof Truss Mounting Structure	197
H8	Summary of Vibro-Acoustic Response Calculations of Door Panels	203
H9	Summary of Vibro-Acoustic Response Calculations for Draft Curtain	205
H10	Summary of Vibration Response Parameters for Alternative Gages and Lengths of Draft Curtain	206
H11	Summary of HV Enclosure Panel Vibro-Acoustic Response Parameters	208
H12	Summary of Vibro-Acoustic Response Parameters for 18 Gage Galvanized Steel Walls of HV Ducts	209
H13	Summary of Calculated Vibration Response Parameters at Base of HV	217
H14	Engine Power Level Calculations	222
I1	Calculated Weight for Horizontal Wind Brace Supports	224
I2	Effective Acceleration Calculations for Each Modal Contribution for Equipment Supported by the Roof Bar Joists	224
I3	Ductwork Support Reaction Calculations and Isolator Selection	227
I4	Effective Acceleration Calculations for Each Modal	235
I5	Steam and Condensate Pipe Support Reactions Calculations	237
I6	Pipe Weight and Frequency Calculations	238
I7	Effective Acceleration Calculations for Each Modal Contribution for Equipment Supported by the Roof Truss	240
I8	Effective Acceleration Calculations for Each Modal Contribution for Oscillating Monitor Fire Protection Pipes	241
I9	Effective Acceleration Calculations for Each Modal Contribution for Equipment Supported by the W8 x 28 Beams That Support the Heating and Ventilating Unit and Catwalk	242

VIBRO-ACOUSTIC ANALYSIS OF AN AIRCRAFT MAINTENANCE DOCK

1 INTRODUCTION

Background

The U.S. Army Corps of Engineers, Omaha District, has been tasked to design and construct facilities for housing and maintaining critical assets of the U.S. Air Force at Whiteman Air Force Base, MO. These facilities, known as Aircraft Maintenance Docks (AMDs), are typically constructed of lightweight metal frame and panel materials. The most severe loading on these facilities typically results from static snow or equivalent static wind loads. For the AMD that is the subject of this study, however, the Air Force requires that the aircraft to be housed and maintained in the facility must be able to taxi out under their own power. This means the AMD must withstand intermittent high-intensity vibro-acoustic loads from the aircraft engines as the vehicle taxis out. Such operation will load the facility with much greater dynamic loads than normally encountered by this type of lightweight building. If this loading were to damage any of the structural, nonstructural, or auxiliary systems—or cause them to fail—the occupying personnel and the aircraft housed there would be at risk. Because these sound levels may damage the structure or cause the malfunction of other components in the facility, precautions must be taken in the design of the secondary building structure and internal equipment mounting.

Objective

The objective of this study was to evaluate the vibro-acoustic environment acting on the AMD; define the equivalent static and dynamic load factors for sensitive structural components, nonstructural components, and all auxiliary systems; and recommend modification of design details to ensure the integrity of the components under the prescribed service life.

Approach

The following steps were taken to accomplish the objective:

1. The acoustic environment created in the AMD by engine operation during taxiing was determined
2. The components and equipment subjected to the vibro-acoustic loading were identified
3. The response of the AMD to the acoustic environment in terms of equivalent static pressures and dynamic load factors for each sensitive component was defined
4. Recommendations were developed for modifications to strengthen or isolate components found to be inadequately designed.

The report includes 10 appendixes containing data, analyses, and important supplementary reference material. Appendix A lists the AMD's potentially sensitive components. Appendix B provides a detailed discussion of the acoustic analysis methodology employed to define interior sound levels. Appendix C presents details of near-field and angle-of-incidence effects on the estimated AMD acoustic loads.

Appendix D presents details of structural response to wide-band random noise. Appendix E presents details of the experimental measurements and analysis of a typical preinsulated wall panel. Appendix F reprints material about fatigue considerations from the American Institute of Steel Construction (AISC) "Specifications for Structural Steel for Buildings," from the AISC *Manual of Steel Construction*. Appendix G presents details for reaction loads on supporting structures for beams and plates subjected to vibration. Appendix H presents detailed data on vibro-acoustic loads on specific AMD elements. Appendix I presents equipment response calculations. Appendix J presents the qualification of alternate isolators from those recommended in Chapter 8.

Scope

This analysis applies to a specific AMD designed for the Air Force by Omaha District in Fiscal Year (FY) 1989. However, this document is also expected to provide valuable information for analyses of the response of similar structures subjected to the same kind of vibro-acoustic environment.

2 FACILITY DESCRIPTION

The AMD consists of two identical test bays, A and C as illustrated in Figure 1, separated by a space of approximately 90 ft which contains the support utility systems. Figure 2 schematically shows one of the AMD high bay areas, identifying several major building components.

A typical test bay is composed of elements listed in the inventory of major facility components in Appendix A. For each item, the inventory lists quantity and weight (if known), the location, and the sheet reference number of the facility drawings from which this information was obtained. Also shown in the inventory is a preliminary indication of those elements expected to be sensitive to the vibro-acoustic environment. The following text outlines general features of the AMD structure as developed at an early design stage, but the details illustrated are not necessarily representative of final design.

As can be seen in Figure 2, the building is composed of steel framing with braced perimeter columns supporting roof trusses that span east and west. Parallel to the trusses are steel joists to which the steel roof decking is attached. The metal decking is covered with thermal insulation and an ethylene, propylene, diene monomer (EPDM) roofing membrane (Figure 3). The walls are sheathed with 2 in. thick insulated panels that were initially to be attached to horizontal steel girts by concealed clips and bolts similar to those shown in Figure 4. Subsequent evaluation of the potential vibration sensitivity of this fastening concept has indicated the potential need for a more accessible panel-to-girt fastener method. The method shown in Figure 4 represents one possibility of many that are available. Figures 5 and 6 show details of door and draft curtain design concepts that were assumed for purposes of this report. All steel members are connected to each other by welded and bolted connections not detailed in the source documents, but that can be sensitive to the acoustic environment and, therefore, should be designed accordingly.

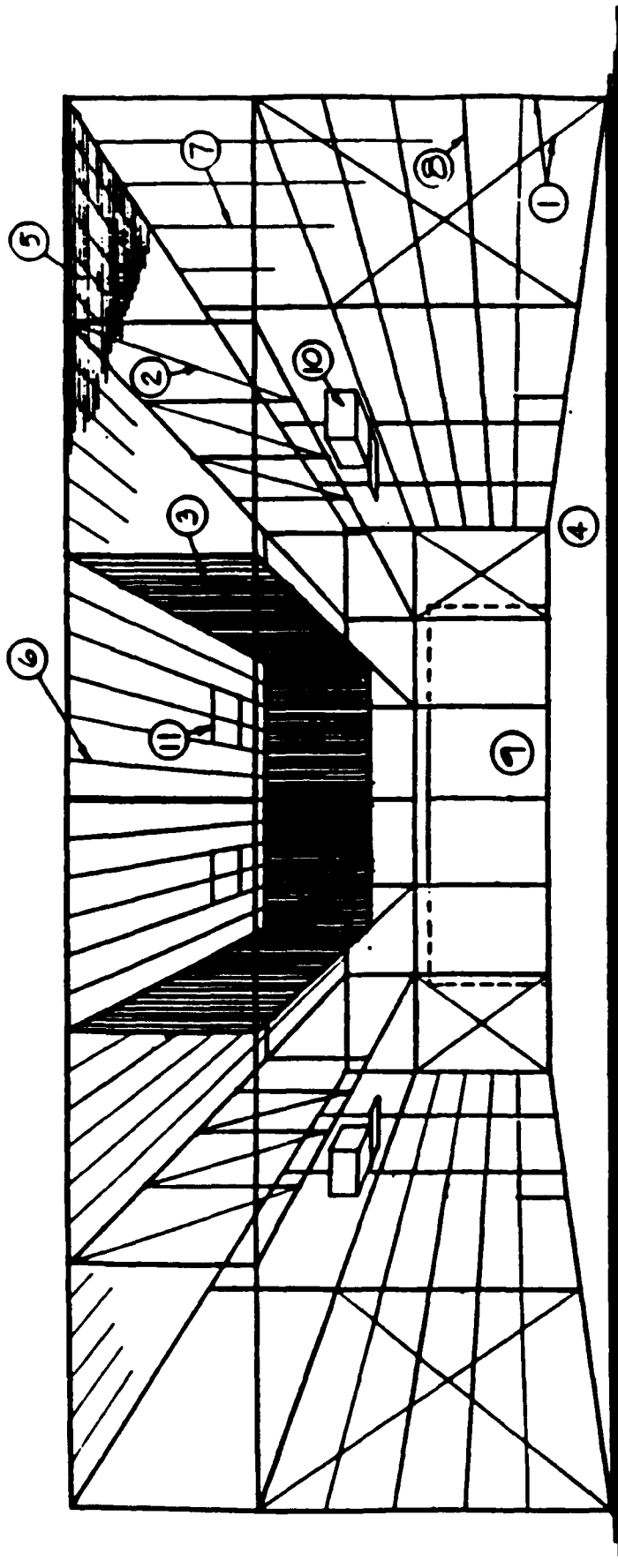
The inventory in Appendix A lists components of the catwalks (which provide service access to the heating and ventilating equipment located below the roof on the north and south walls), the draft curtains, and the test facility doors. All of these items may be sensitive to the vibration environment at their connections to the supporting structure.

The mechanical equipment listed on the last page of Appendix A may be sensitive to the acoustic environment in two ways: (1) any lightweight panels that are part of, or are an enclosure of, the equipment itself must be capable of withstanding the anticipated high noise levels and (2) equipment supports and support connectors are a point of sensitivity to structural vibrations.

The air-handling units can be designed to inherently resist acoustic vibration, or they can be shielded if necessary. Due to its low surface weight and high surface area, exposed air ducts must be carefully designed to sustain anticipated acoustic loads.

The piping and electrical equipment listed on the last page of Appendix A may also be sensitive to vibro-acoustic loads in two ways. The light fixtures must be designed for high noise levels, and the piping hangers and light fixture supports and support connectors must be capable of carrying the vibration loads without failure during periods of high noise. Similarly, any lightweight electrical panels must be capable of operating in the high vibro-acoustic environment involved.

The construction contractors are responsible for the design or improvement of many items shown in the inventory list that were not specifically detailed in the preliminary drawings. The contractors should take into account the additional dynamic loads caused by noise. Design information for these loads, in



- | | | | |
|----|--------------------|-----|------------------------------|
| 1. | Column and Bracing | 7. | Wall Panels |
| 2. | Truss | 8. | Girt |
| 3. | Draft Curtain | 9. | Rear Door |
| 4. | Concrete floor | 10. | Mechanical Equipment |
| 5. | Roof Decking | 11. | Auxiliary Power Unit Exhaust |
| 6. | Steel Joists | | |

Figure 2. AMD Interior.

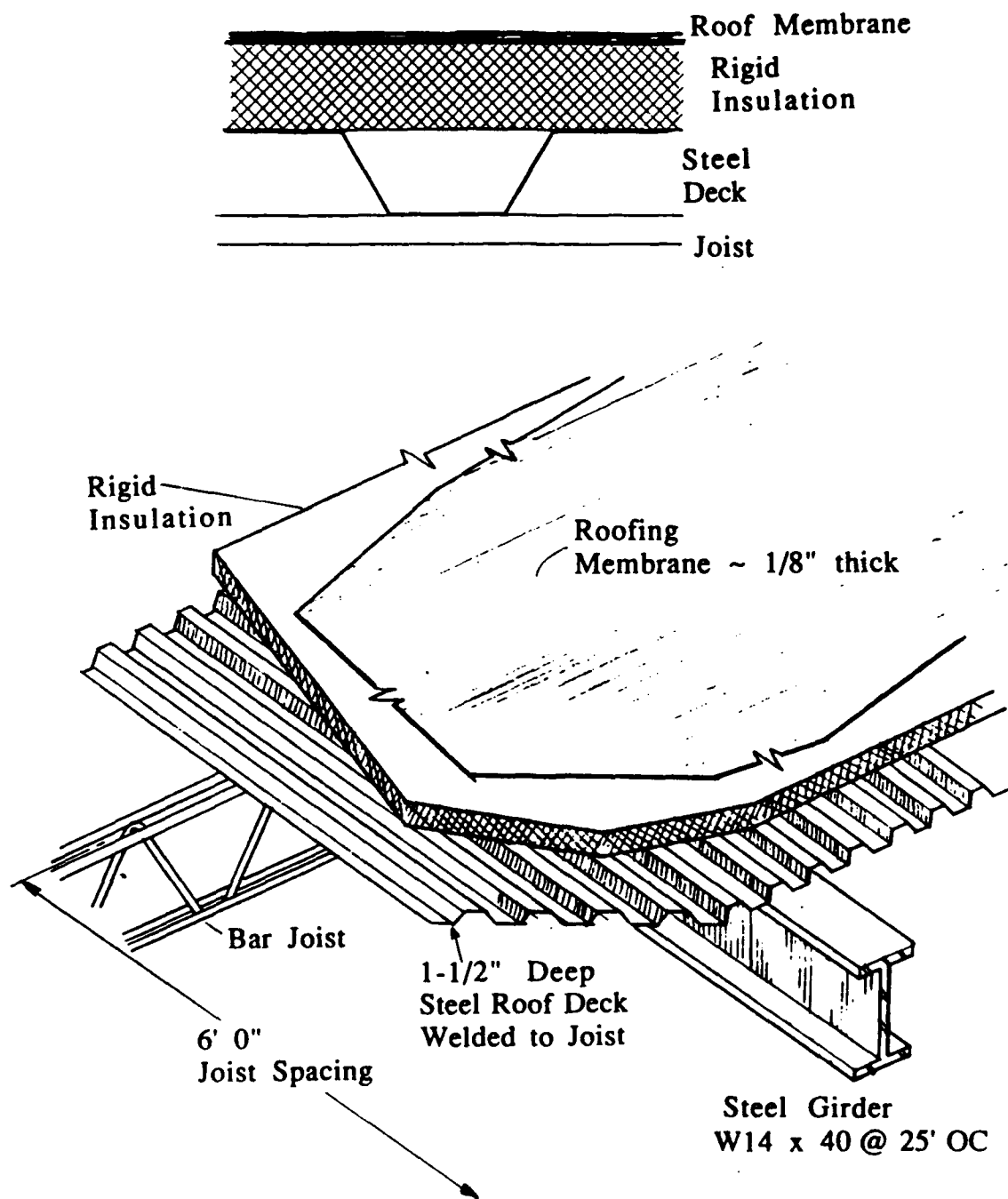


Figure 3. Typical roof assembly (preliminary design concept).

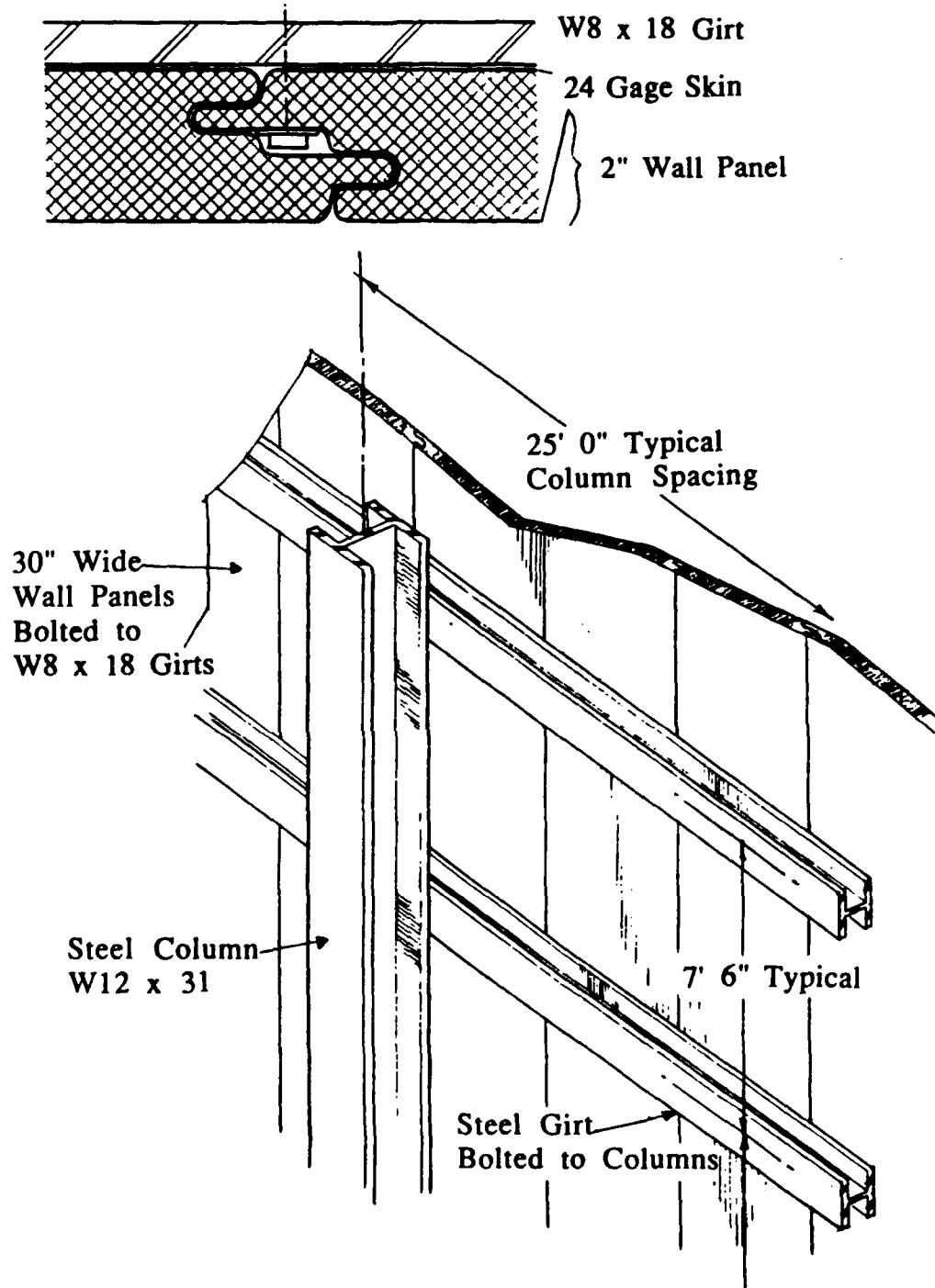


Figure 4. Typical wall assembly (preliminary design concept).

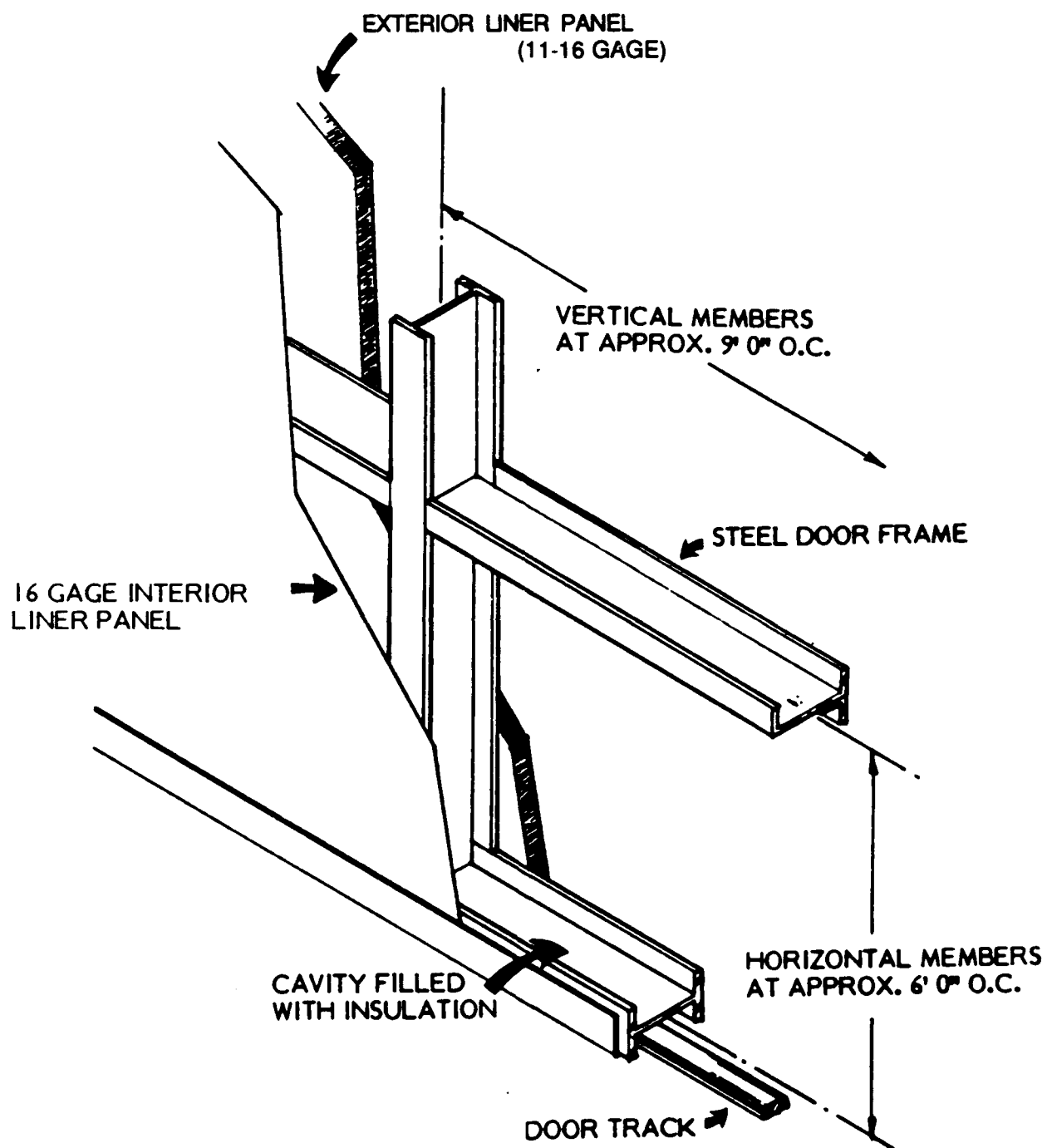


Figure 5. Back door (representative of preliminary design concept).

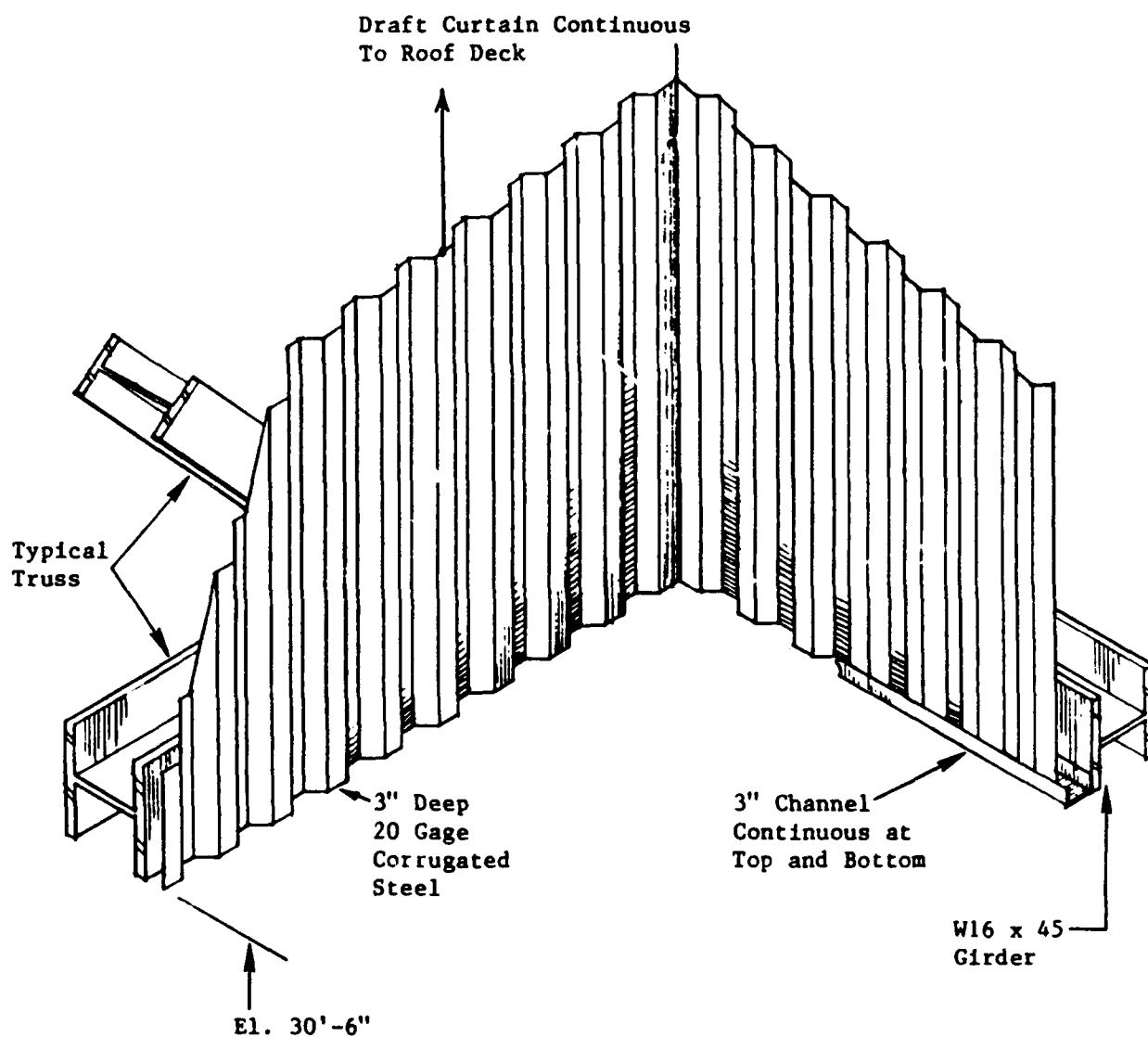


Figure 6. Draft curtain (preliminary design concept).

the form of equivalent static pressure (for external skin structure) or dynamic load factors* (for nonstructural components) is provided in Chapters 4 and 7. Chapter 5 includes additional details about the potential vibration sensitivity of AMD equipment. Chapter 8 provides vibration isolation recommendations for sensitive building and equipment components.

* g loads.

3 ACOUSTIC ANALYSIS

The analysis of the internal acoustic environment of the AMD involved the following steps.

- An initial "quick look" to evaluate whether a model study was critically needed
- Detailed review and evaluation of the acoustic data reports provided for the main engines and auxiliary power units (APUs)
- Development of an approach to use these data for definition of the acoustic environment inside the AMD
- Application of this approach to define the environment.

The results obtained from each of these steps are briefly summarized here. The vibro-acoustic environmental design analyses in this study are based on a maximum operating condition of 6820 revolutions per minute (rpm) for four main engines and two APUs operating simultaneously at maintenance power. The 6820 rpm condition for the main engines was the power condition specified for design purposes of this study. Limited information is also provided on the acoustic environment for 3215 rpm and 8060 rpm for the main engines.

"Quick Look" at Noise Environment to Evaluate the Need for Model Test

The unusual nature and potential severity of the acoustic loading in the AMD suggested initially that an acoustic model test might be required to help refine the environmental estimates. However, after a quick initial evaluation, it was decided that such a test was not required. This decision was based on two facts:

1. In the primary position of the aircraft, the extended sound source associated with the main engine jet exhaust will extend back from the source exit plane by 20 to 40 ft, but it is still expected to be contained almost entirely within the AMD enclosure. Thus, on the basis of the data provided, conventional methods for evaluating the acoustic environment inside a reverberant space containing a noise source were considered adequate for design purposes.

2. The initial evaluation of the data indicated that a model test would not be required to refine the estimated environment. (Although subsequent analysis indicated that the acoustic loads were higher than initially expected on certain portions of the AMD, it was still not considered necessary or practical to conduct a model test.)

A full-scale acoustic test of the primary noise source(s) in a simulated AMD might be conducted at a later date if considered necessary to refine the estimated noise levels contained herein.

Test Evaluation of Acoustic Data Reports

Acoustic data reports prepared by the manufacturer were provided for the two types of noise sources involved. For the primary noise source, the data report was very complete and thorough, and with one exception it appeared to be accurate in every detail. The exception was the tabulation of sound power levels provided in the test report. From a casual examination of these calculated sound power levels,

computed on the basis of sound level measurements at a 150 ft radius, it was very apparent that the computed sound power levels were in error, at least at very high frequencies. Thus it was necessary to repeat these calculations for all of the source power settings of interest, since the total sound power levels were a vital part of the input data needed to estimate AMD acoustic loads.

The simplified data report provided for the smaller APUs was quite adequate since the sound levels from these sources are much lower and will normally be negligible.

Development of Analysis Approach

For the various operating conditions of the acoustic sources involved in the AMD, the acoustic pressures on the AMD structure are the sum of:

1. Direct radiation from each sound source, accounting for the effect of the first reflection (i.e., pressure doubling) at the interior surfaces of the AMD but not including the reverberant sound field, and
2. The reverberant sound field due to the acoustic energy remaining within the AMD after the first reflection of the direct sound.

The direct sound field was determined from the noise contours provided by the data report on the primary noise source or calculated from the measured sound power levels for the smaller auxiliary power sound source. For the former, contours were available for one-third octave band levels at octave frequency intervals from 50 to 6300 Hz.

The reverberant sound levels depend on the total sound power generated by the sources and the acoustic absorption at the interior surfaces of the AMD. The following baseline assumptions were made for these acoustic absorption coefficients to establish conservative acoustic design environments.

<u>Surface</u>	<u>Acoustic Absorption Coefficient</u>
Floor	0
Walls, Roof	0
Open Doors	1.0
Volume (Air Absorption)	Computed according to ANSI S1.26 (1978)

Limited analysis was also made of the change in interior levels for higher absorption coefficients on the walls (0.1) and roof (0.1 to 0.8). For the reverberant sound field, the following corrections were applied to the calculated free (diffuse) field levels to account for the expected increase in these sound levels at the interior surfaces: +3 dB at walls, an additional 0 to +3 dB within one wavelength of wall-roof or wall-floor edges, and an additional +3 to +6 dB (for a maximum of +9 dB) at three-way corners due to reflection of the diffuse sound field by the enclosing surfaces (Waterhouse and Cook, 1965).

Initially, therefore, the net acoustic levels were defined in terms of one-third octave band levels by an energy summation of the direct and reverberant sound fields at frequencies spaced one octave apart over a frequency range from 50 to 8000 Hz. Subsequently, one-third octave band levels at all band center frequencies from 1 to 8000 Hz were determined by interpolation from 50 to 8000 Hz and by extrapolation for frequencies from 1 to 40 Hz. The extrapolation of sound levels over the lower frequency range was quite reasonable due to the well-behaved shape of the noise spectrum typical of similar noise sources.

Appendix B provides a detailed discussion of the acoustic analysis methodology employed to define the interior sound levels.

Appendix C reviews details on potential near-field and angle-of-incidence effects on the estimated AMD acoustic loads. These second-order effects are shown to be negligible to a first approximation.

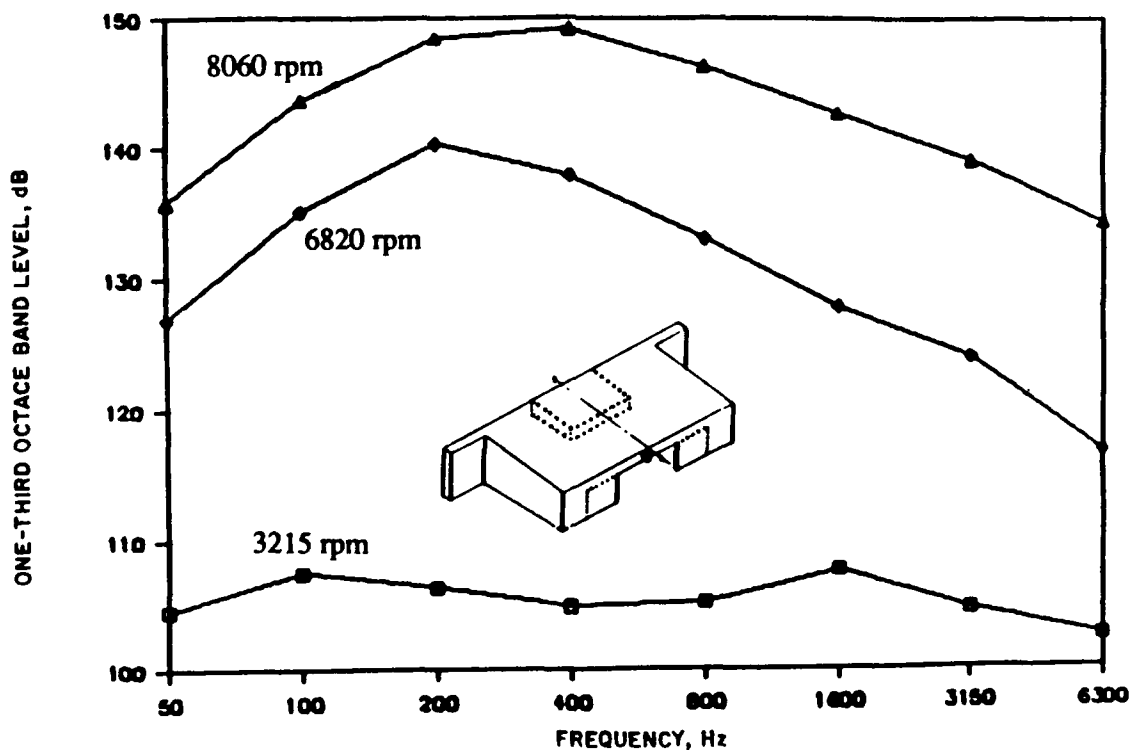
Results of Acoustic Analysis

A detailed tabulation of the one-third octave band sound levels computed in this study is given at the end of Appendix B. A summary of the principal results is presented in the following sections.

Baseline Environment for Reference Source Position

The internal acoustic environment varies over frequency, location on the AMD structure, source positions, and source power setting. It is neither practical nor desirable to consider all combinations of these parameters. Therefore, a design environment based on a conservative envelope of maximum levels was established.

Consider, first, the variation in level with the operating condition. Figure 7 shows the variation in one-third octave band level at a typical location of maximum levels (on the center of the back wall above the door opening) as the main engine is changed from 3215 rpm to 6820 rpm to 8060 rpm. The operating condition upon which this report is based is 6820 rpm. An increase to 8060 rpm as the design condition



(Note: source exit plane 40 ft forward of rear door.)

Figure 7. Variation with rpm of primary source in one-third octave band sound pressure level at 3 ft above top center of back door.

would increase sound levels in the structurally significant frequency range (below 1000 Hz) by about 8 to 12 dB, for an average increase in acoustic pressure (and corresponding structural response) of a factor of 3.2. The increase in sound level and the stress ratio relative to the stresses at the baseline (BL) of 6820 rpm was calculated for several levels of engine fan speeds. These values are presented in Table H-14. Such an increase in structural vibration response to the higher acoustic environment could lead to frequent structural failure of secondary structural components (i.e., wall or ceiling panels) or component/primary structure mounting points.

Note that in Figure 7, the one-third octave band sound level data points are shown at octave frequency intervals. This is because the direct sound field, which is included in the composite one-third octave band levels shown in Figure 7, was specified only at these frequency intervals in the manufacturer's acoustic test report.

The basic shape of the frequency spectrum in Figure 7 is representative for all locations. Therefore, it is sufficient to examine the spatial variation in sound level at only one frequency—in this case, 200 Hz, which is the frequency of maximum one-third octave band levels for 6820 rpm.

Figure 8 illustrates how the sound level varies with position near an edge formed by a wall/roof or wall/floor juncture, or near a three-plane corner. The fine structure of this variation is ignored from here on, and only the maximum increase at an edge (+3 dB) and a corner (+6 dB) is portrayed.

Figures 9 and 10 illustrate the spatial variation in sound level at 200 Hz over the back wall (and inside of stowed back door) and over the middle section of the roof, respectively. In each figure, a sketch

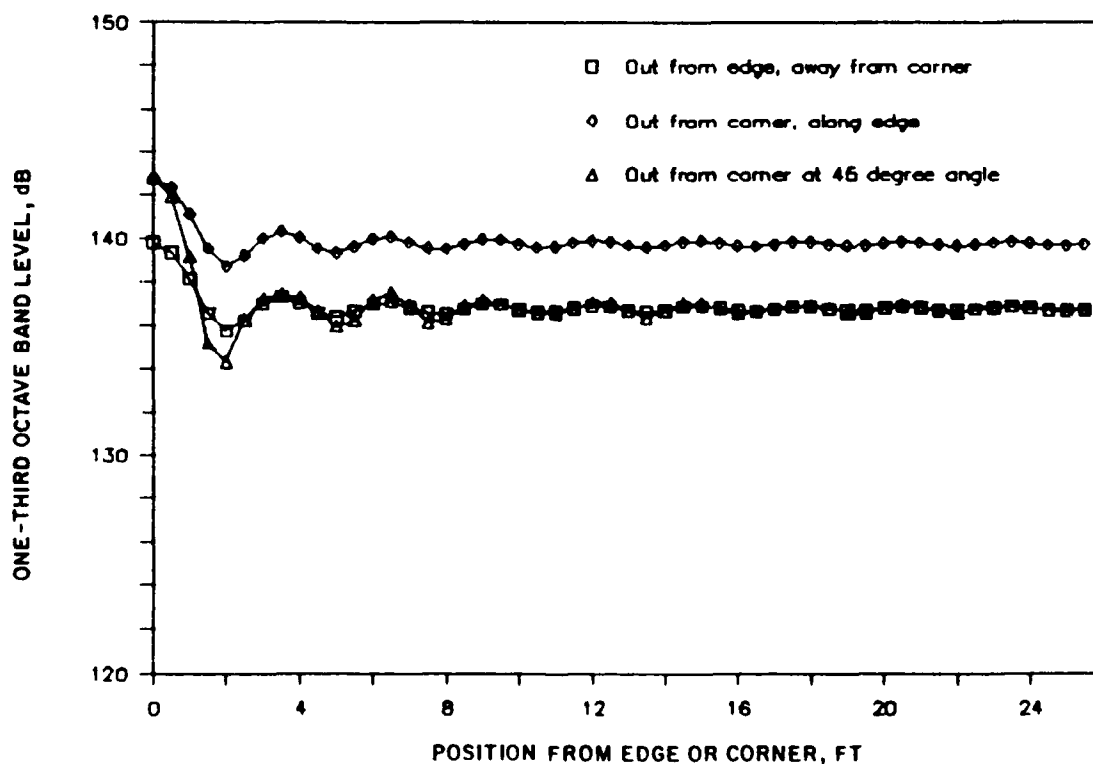


Figure 8. Variation in one-third octave band sound pressure level at 200 Hz near edge or corner in AMD (sources at 40 ft, 6820 rpm).

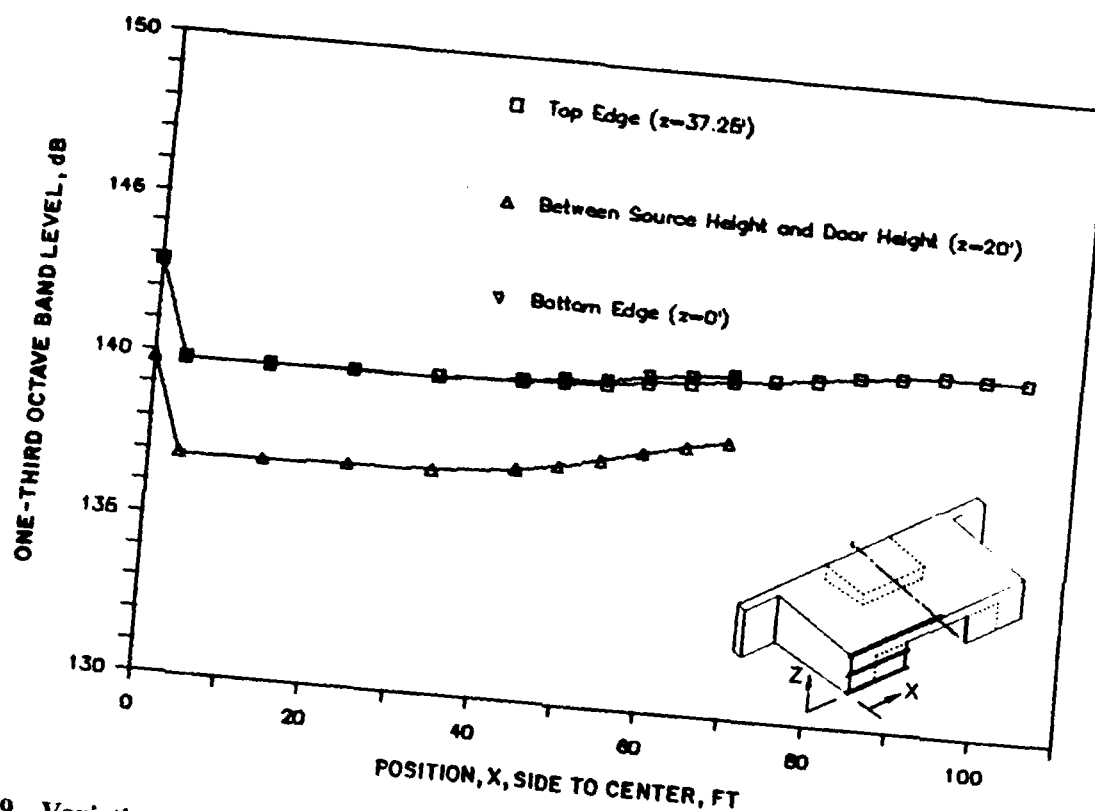


Figure 9. Variation across back wall in one-third band sound pressure level at 200 Hz (sources at 40 ft, 6820 rpm).

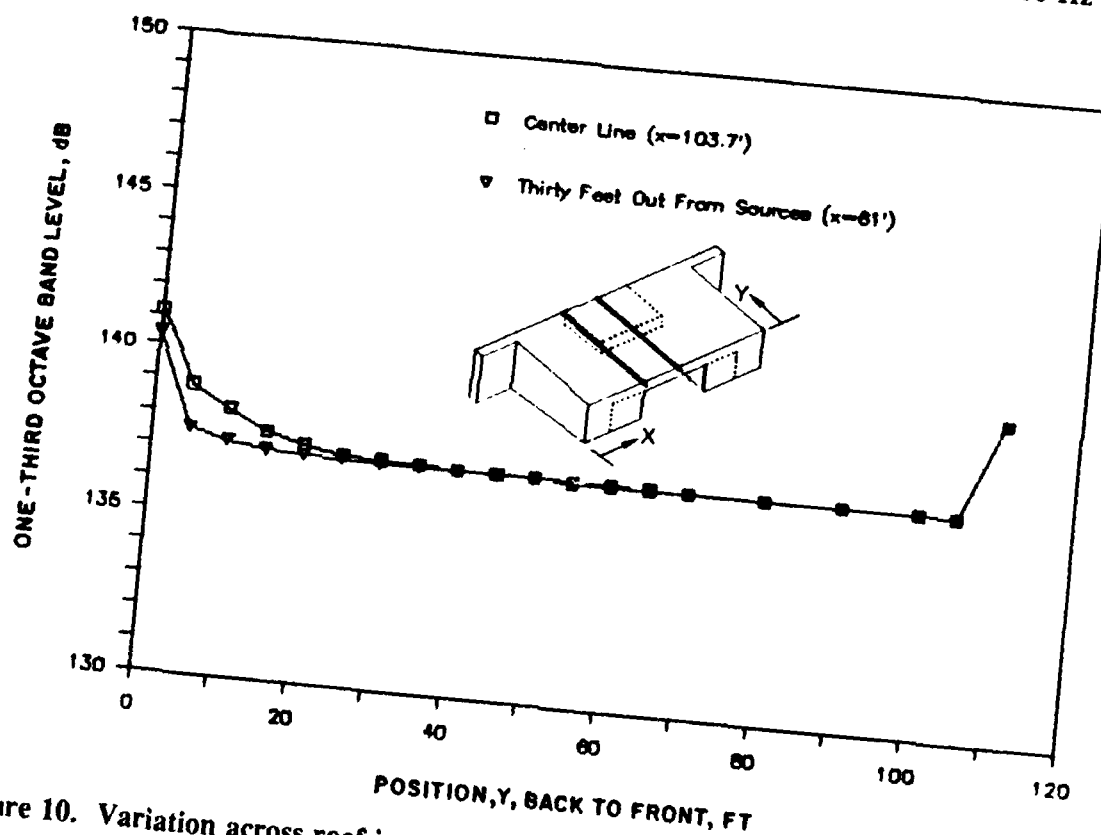


Figure 10. Variation across roof in one-third octave band sound pressure level at 200 Hz (sources at 40 ft, 6820 rpm).

shows the lines and coordinate systems along which the variation in level is portrayed. In all cases—in these and subsequent figures—the origin of the x (lateral position), y (fore and aft position), and z (vertical position) axes lies at the bottom left hand corner of the back wall (as viewed from outside). For both of these figures, the main engines are located at their initial reference position, corresponding to $y = 40$ ft.

An extensive evaluation of the type of data shown in these figures indicates that the interior surfaces of the AMD may be broken down into noise zones, as illustrated in Figure 11. They are defined in the key to the figure. If the separate noise zones were to be employed, the front and side walls of the AMD structure would have the same design environment as the roof zone R3.

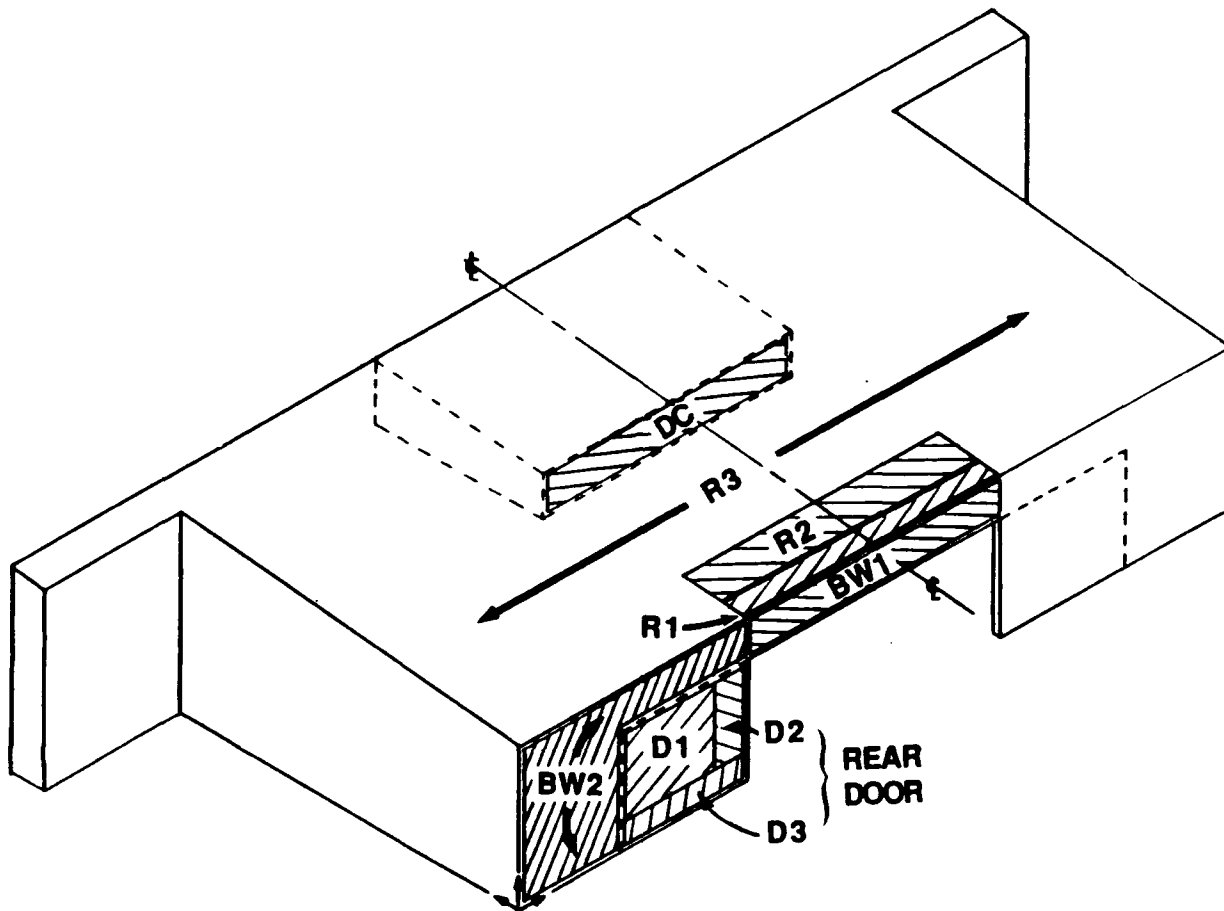
Figure 12 shows the average one-third octave band sound pressure levels for each of these noise zones, based on the detailed data in Appendix B and on interpolation to obtain one-third octave band levels at all frequencies from 31 to 6300 Hz.

Variation in Baseline Acoustic Environment

These figures have been based on the main engines located at their (initial) reference position corresponding to their exit planes 40 ft forward of the back wall (i.e., $y = 40$ ft). Figure 13 illustrates the effect of a forward shift in position of the main engines on the one-third octave sound level at 200 Hz. As the main engine position is shifted forward, the *average direct field* sound level on the roof forward of the back wall will change substantially due to the highly directional sound field of the main engine (see Figure B4 in Appendix B.) However, the maximum direct field level at any position on the roof above the source will not change appreciably for a wide range of source positions. Furthermore, the reverberant sound level will tend to remain constant until the positions of the exit planes of the main engines are well outside the AMD. The net result, illustrated in Figure 14, is that the maximum composite sound level (direct and reverberant) along the roof directly above the centerline of one of the main engines will be nearly constant for a large variation in the position of the main engines. Thus, it is practical to base the acoustic design levels upon the maximum levels applicable for the reference source position (i.e., $y = 40$ ft) but to ignore the change in levels in the y direction for this source position and use the maximum values over the full fore and aft span of the roof. Referring to the noise zones illustrated in Figure 11, noise zone R1 will be retained as is, since it involves the additional corner effects (e.g., total correction of +6 dB to reverberant sound levels). However, the levels in noise zone R2 will now be assumed to apply across the rest of the roof covering the area with x coordinates of 69 to 139 ft and y coordinates of 0 to 111 ft. Outside this middle band, the levels in noise zone R3 will still apply.

Effect of Increasing Surface Absorption. The possibility of reducing the interior acoustic environment by using acoustically absorbent panels for the ceiling was briefly explored. Figure 15 shows the estimated change in the one-third octave band sound pressure level spectrum as the interior acoustic absorption is changed. The baseline absorption assumed no absorption by the metal walls and ceiling (i.e., $\alpha = 0$). Increasing the absorption coefficient α to 0.1 for both the walls and ceiling decreases the sound level at a representative position near the back center of the roof by an average of about 1 dB.

As shown in Table 1, if the average absorption coefficient on the roof could be increased to as much as 0.8—not very likely for the low-frequency range of concern for structural loading—the total reverberant plus direct sound level at the point near the back center of the roof illustrated in Figure 15 would decrease by less than 3 dB. This is because the direct field, which is not sensitive to surface absorption, tends to control the sound level in this region near the back wall. As indicated above, when the source position is moved forward, the maximum levels in the middle third of the roof structure and in the draft curtain will tend to be controlled by the direct field, so that *increasing the roof absorption (or adding acoustic absorption on any internal surfaces, including the walls) will not have a marked effect on maximum (design) sound levels in this middle portion of the roof.*



KEY

<u>Zone</u>	<u>Code</u>	<u>Location</u>
Back Wall	BW1	Above back door opening
	BW2	From left side to edge of back door opening
Roof	R1	First 5 ft of roof immediately in front of door ($x = 69-104$ ft, $y = 0-5$ ft)
	R2	Next 15 ft of part of roof immediately in front of door opening ($x = 69-104$ ft, $y = 5-20$ ft)
	R3	Remainder of roof
Back Door (Inside Surface)	D1	All except inner 9 ft and lower 6 ft of door
	D2	Inner 9 ft from 6 ft above floor to top of door
	D3	Lower 6 ft from left to right side
Draft Curtain	DC	All portions of draft curtain

Figure 11. Potential specific noise zones for interior surfaces of the AMD.

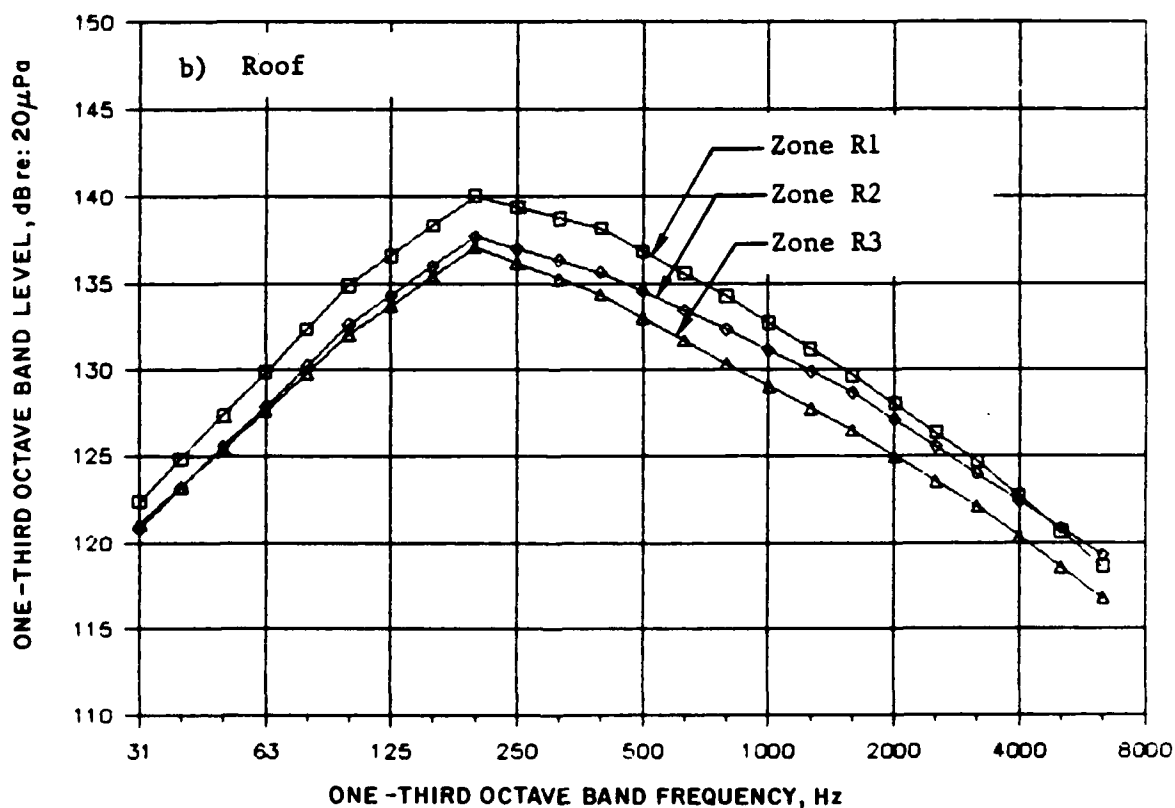
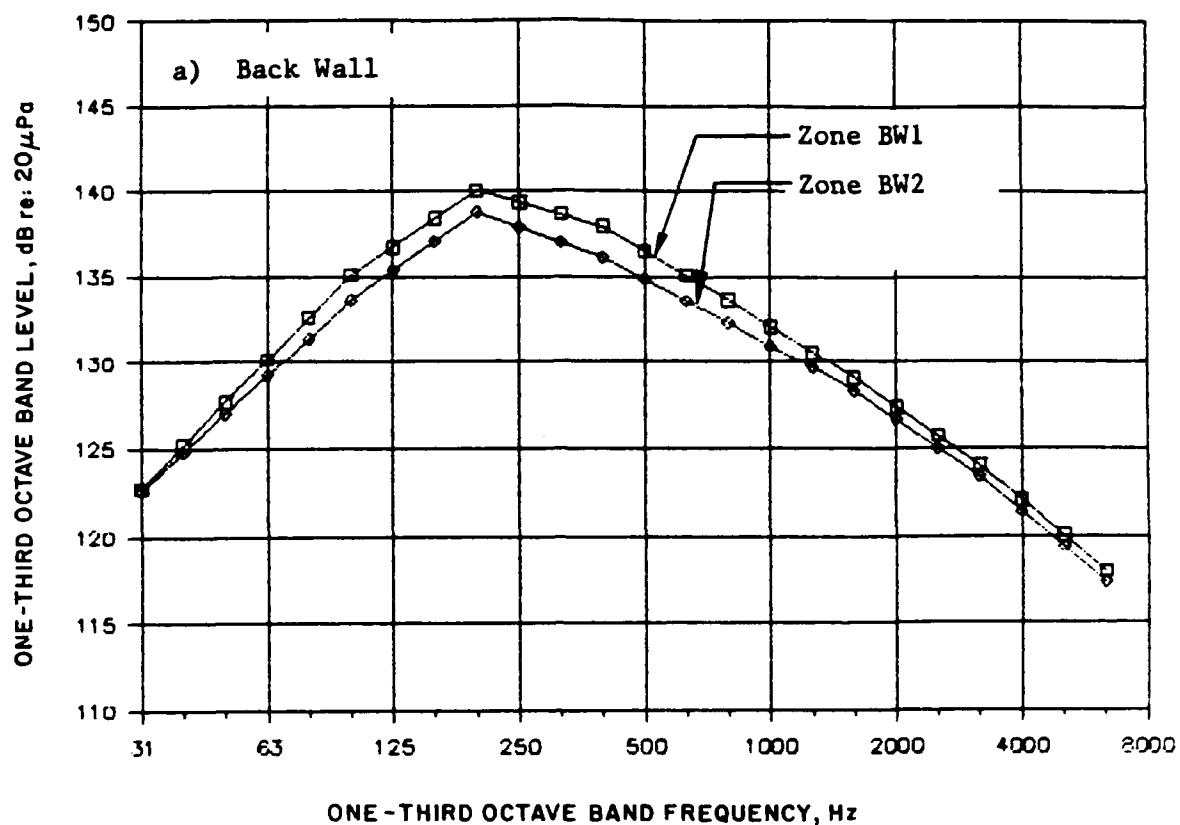


Figure 12. Average one-third octave band sound pressure levels on AMD interior surface divided into noise zones according to Figure 11 (sources at 40 ft, 6820 rpm).

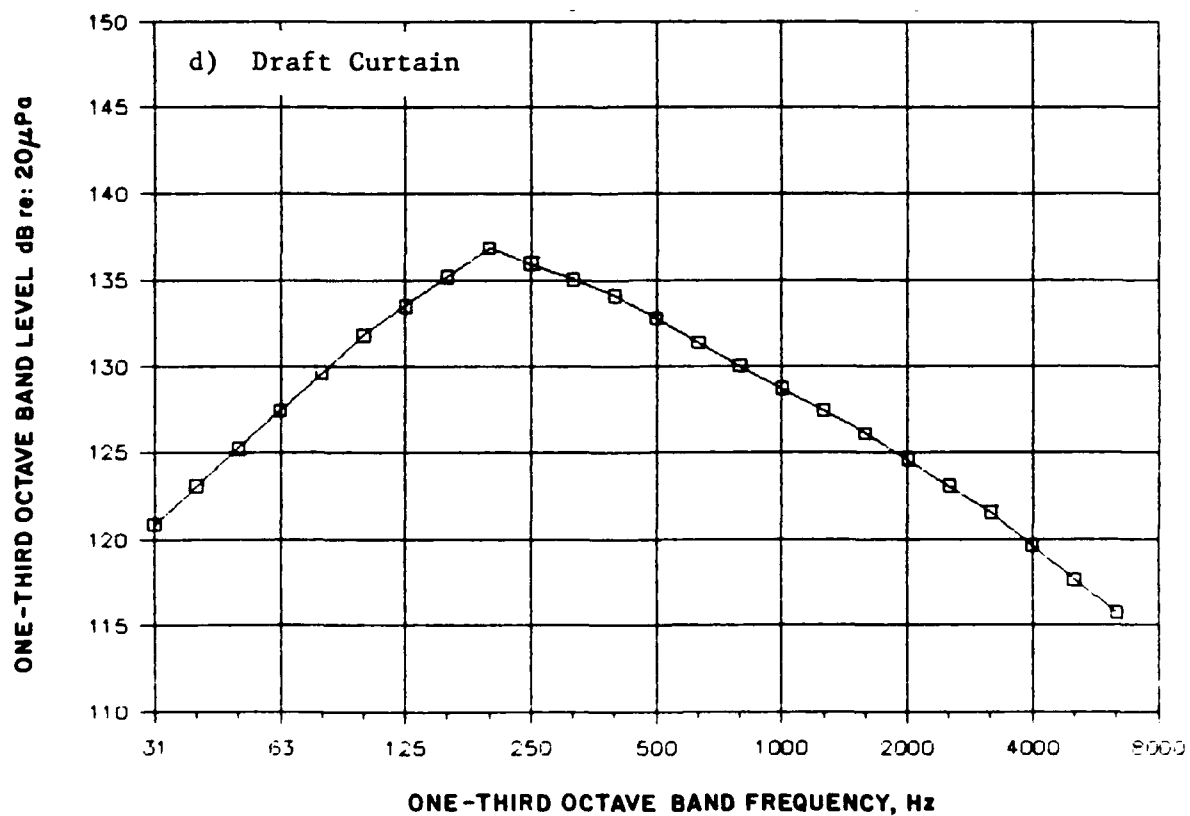
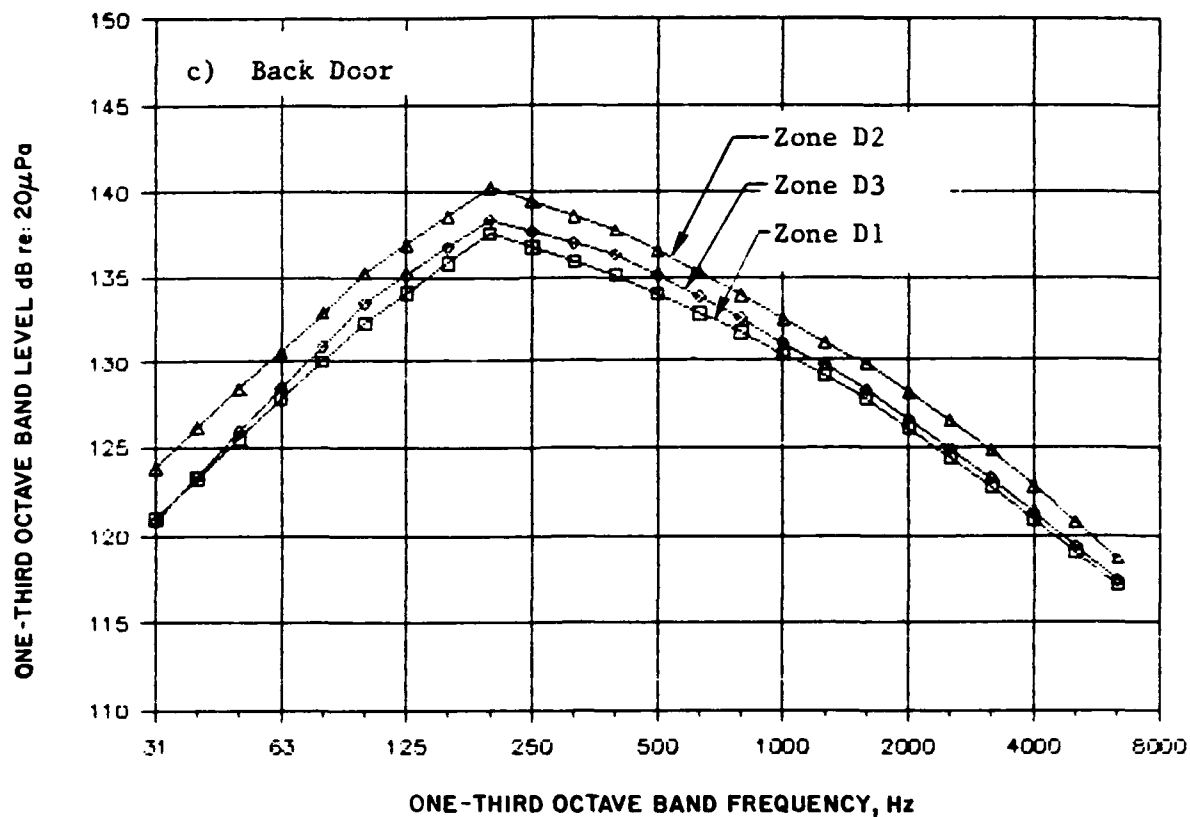


Figure 12. (Cont'd)

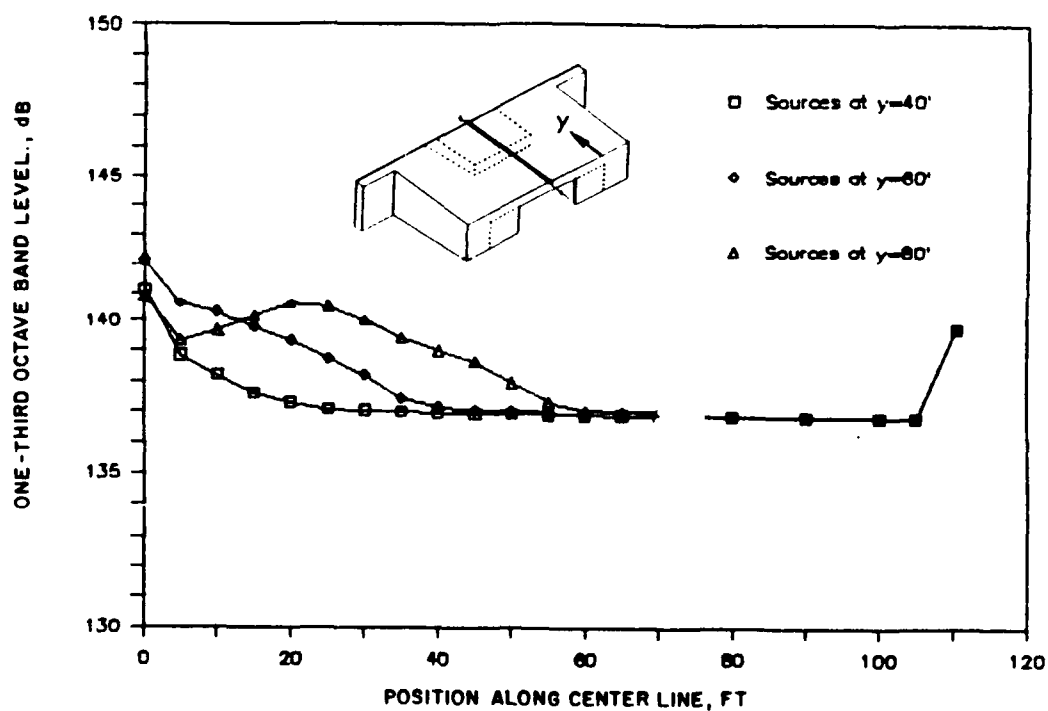


Figure 13. Change in one-third octave band sound level at 200 Hz along roof centerline for change in forward direction of main engine (at 6820 rpm).

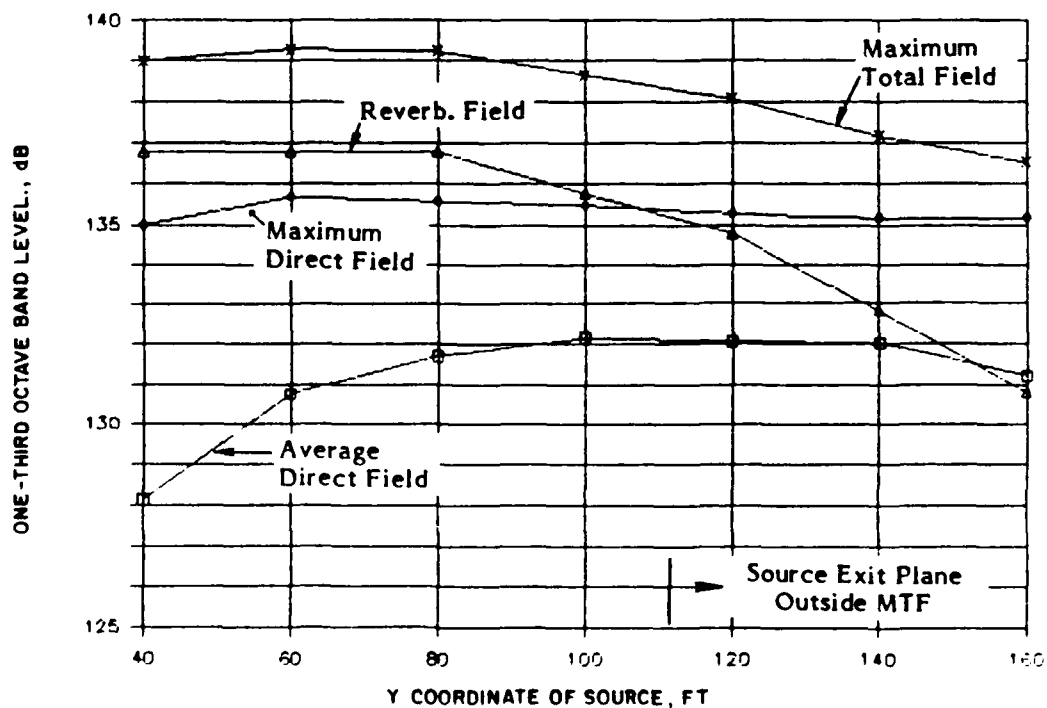
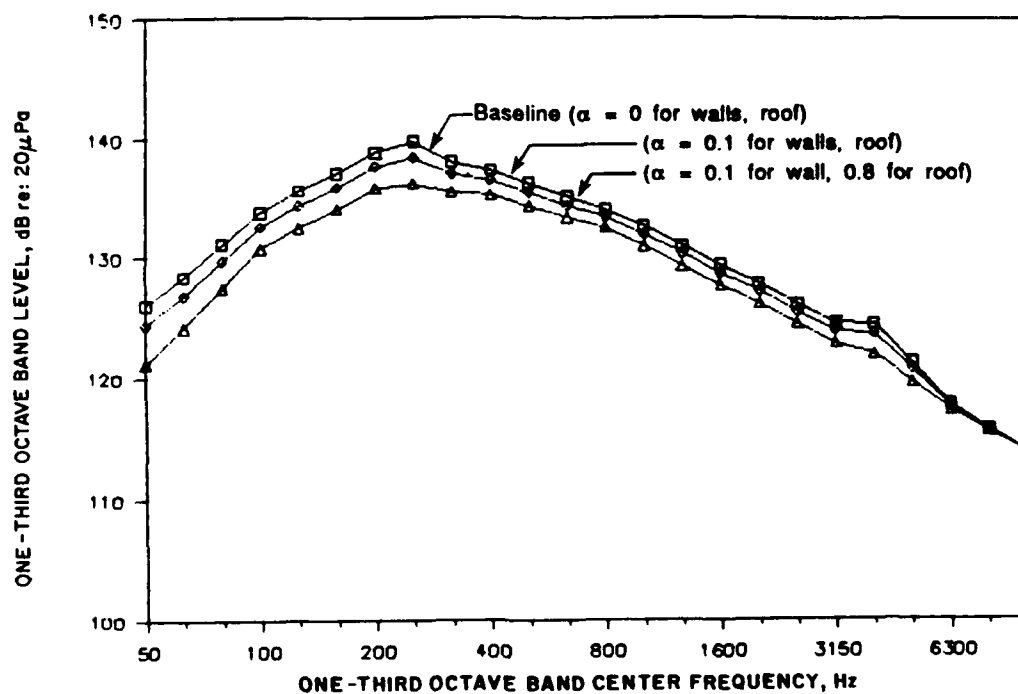


Figure 14. Variation in sound level at 200 Hz due to change in position of source. (Sound level along line on roof directly over one pair of sources; all four operating at 6820 rpm.)



(Note: $x = 103.7$ ft, $y = 5$ ft, sources at 40 ft, 6820 rpm.)

Figure 15. Effect of increasing absorption on one-third octave band sound pressure level near back center of roof.

Table 1

Change in Total One-Third Octave Band Reverberant Plus Direct Sound Level at 200 Hz as Absorption Coefficient (α) for Roof is Increased

Absorption Coefficients						
$\alpha(\text{roof})$	0	0.1	0.1	0.2	0.5	0.8
$\alpha(\text{walls})$	0	0	0.1	0.1	0.1	0.1
$L_T(\text{roof})^*$	138.8	138.1	137.6	137.2	136.3	135.8
$\Delta L \text{ re } (\alpha=0)$	0	-0.7	-1.2	-1.6	-2.5	-3.0
L_R^{**}	136.8	135.6	134.7	133.8	131.5	129.7
$\Delta L \text{ re } (\alpha=0)$	0	-1.2	-2.1	-3.0	-5.3	-7.1

Note: Figures apply to roof centerline 5 ft forward of back wall and other areas where reverberant field dominates.

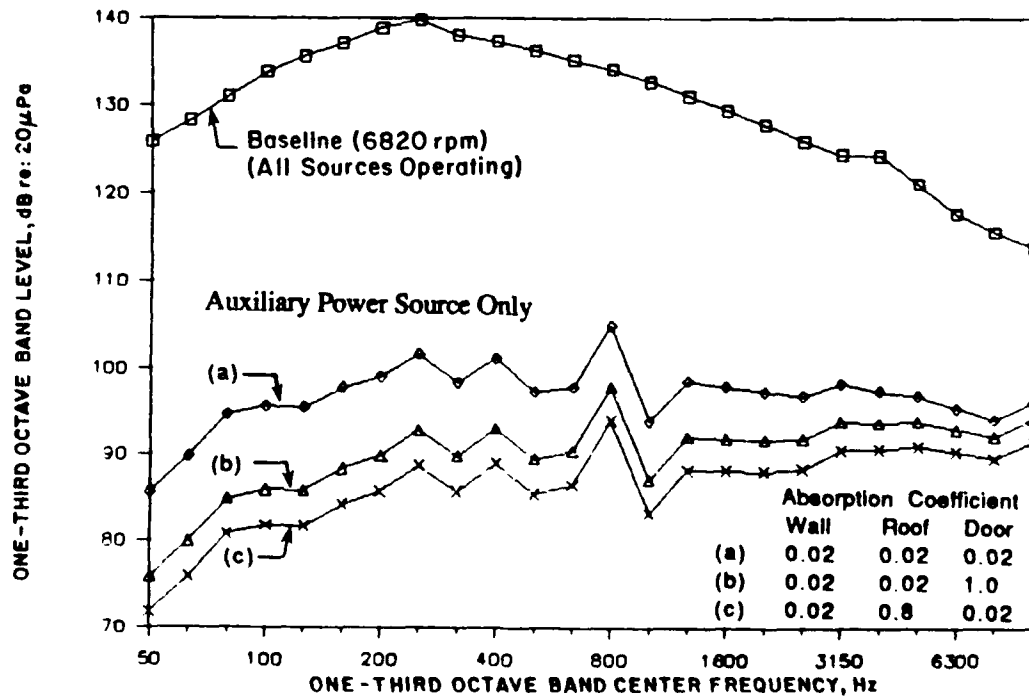
* Composite reverberant plus direct field sound level at roof centerline 5 ft forward of back wall, in dB.

** Reverberant field sound level on side, front walls or outer areas of roof, back door, in dB (see text).

However, as indicated in the table, for surfaces where the reverberant sound field is dominant, i.e., the front and side walls and outer two-thirds of the roof ($x = 0$ to 69 ft and 139 to 208 ft) and outer portions of the back wall ($x = 0$ to 34 ft and 174 to 208 ft), *increasing the roof absorption coefficient will decrease the reverberant sound levels substantially in these areas*. It is not possible at this point to establish the cost tradeoff involved in this option. The cost of adding absorption to the roof structure is definable. Initial estimates are that acoustically absorbent ceiling panels would cost approximately 30 percent more than the currently proposed design illustrated in Figure 3. (An entirely different option for increasing interior absorption would be to hang light volume-absorber panels from the existing ceiling.) However, any potential cost benefit of decreasing acoustic loads on portions of the interior AMD structure where reverberant sound levels dominate, by increasing interior acoustic absorption, cannot be defined until the cost implications of the acoustic loads (developed in Chapter 4) have been evaluated.

Environment When Operating APUs Only With Doors Closed. A potential use for the AMD could involve operating only the APUs with the facility doors closed. In this case, it is no longer reasonable to assume a value of 0 for the interior absorption coefficient for the walls and roof. Figure 16 shows the reverberant field sound levels for three assumed interior absorption conditions with only the APUs operating at maintenance power. Also shown for comparison are the basic design levels on the draft curtain with all sources operating.

Clearly the noise levels with only the APUs on are well below the design conditions, so structural effects would not be of concern while they are operating.



(Note: a = doors closed, minimum absorption, b = doors open, minimum absorption, c = doors closed, maximum absorption on roof; baseline is for sources at 40 ft, 6820 rpm.)

Figure 16. Sound levels on back, center of draft curtain with only auxiliary power sources operating for different values of absorption.

The primary constraint would be the limitations on hearing damage risk criteria for maintenance personnel as specified in Air Force Regulation (AFR) 161-35. This regulation specifies allowable working time in an 8-hour day as a function of A-weighted sound level (U.S. Air Force 1976). An A-weighted sound level is the overall sound level with low frequency levels attenuated (i.e., weighted) to correspond approximately to the human response to noise. The change in reverberant field A-weighted noise levels to which personnel would be exposed is compared in Table 2 for the exposure times allowed by AFR 161-35.

Clearly, extensive use of this mode of operation would indicate the need to consider increasing the interior absorption. Note, however, that even with the highest reasonable estimate of absorption ($\alpha = 0.8$ for walls and roof and 1.0 for open doors), the interior reverberant sound level with only the APUs operating is high enough to limit exposure time to just over 1 hour per day for maintenance personnel inside a high bay part of the AMD. In all cases, of course, such personnel would have to wear hearing protection (U.S. Air Force 1976).

Acoustic Design Environment

A review of the average composite (reverberant plus direct) sound levels for the various noise zones shown in Figure 11 indicates that the actual range in levels is relatively small (Figure 17). Thus, regardless of the potential noise zoning suggested earlier in Figure 11, it is considered reasonable design practice simply to use the upper bound of this range as the acoustic design environment throughout the AMD. The spread in average sound levels illustrated in Figure 17 (about ± 1.8 dB) corresponds to a range in acoustic pressures of only ± 23 percent. This is believed to be too small a range to justify, at this point, establishing location-dependent design values for the acoustic design environments. Note that since Figures 12 and 17 are based on average values over the various noise zones, the design envelope indicated

Table 2
Allowable Personnel Exposure Time for a Range of Absorption Coefficients for AMD
with Auxiliary Power Sources Operating at Maintenance Power

----Absorption Coefficients-----			$L_{(reverb.)}$ dB(A)	Allowed Exposure Time/Day*
Roof	Walls	Doors		
0.8 **	0.8	1.0 ***	95.3	68 min.
0.8	0.02	1.0 ***	99.0	36 min.
0.8	0.02	0.02	101.3	24 min.
0.02	0.02	1.0 *	104.6	14 min.
0.1 †	0.1	0.1	106.2	10 min.
0.02 ‡	0.02	0.02	110.0	5 min.

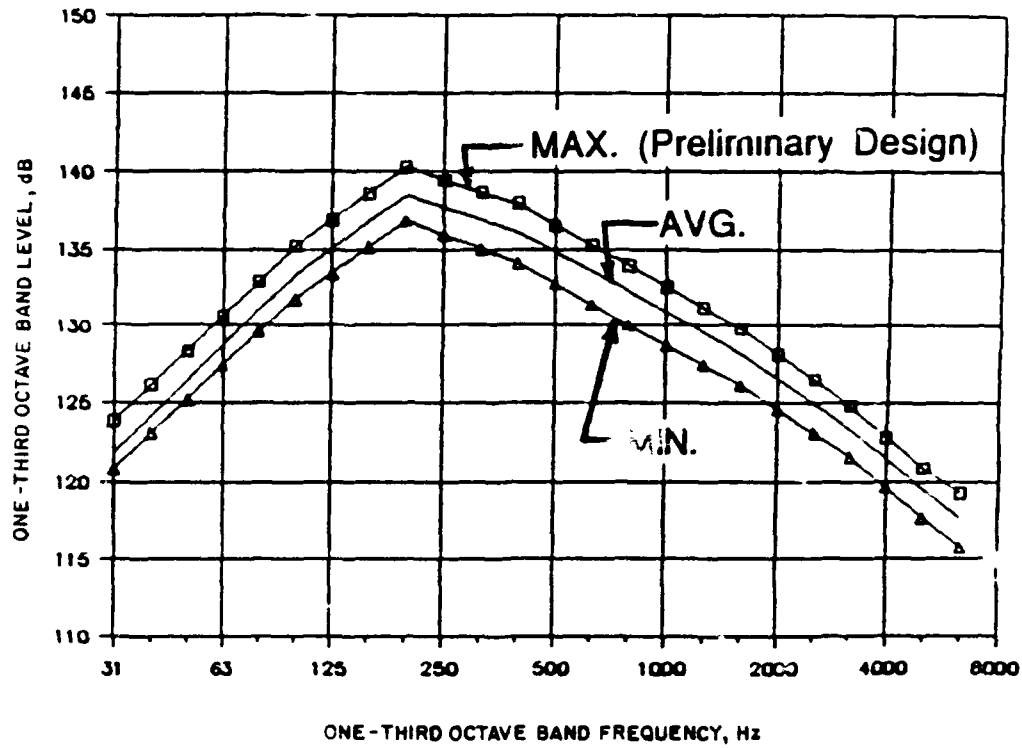
* According to AFR 161-35

** $\alpha = 0.8$ for major acoustic absorption treatment

*** Doors open

† $\alpha = 0.1$ for light treatment

‡ $\alpha = 0.02$ for no treatment



(Note: $x = 103.7$ ft, $y = 5$ ft, sources at 40 ft, 6820 rpm.)

Figure 17. Effect of increasing interior absorption on one-third octave band sound pressure level near back center of roof.

in Figure 17 does *not* represent the highest potential levels that will occur at two- and three-plane edges and corners. However, this is not considered a problem since the structural rigidity of the AMD wall and roof panels will be highest at these junctures and, therefore, most resistant to acoustic loads.

For reference purposes, the acoustic design environment for the AMD corresponding to the upper line in Figure 17 is listed in Table 3. Values are estimated by extrapolation down to a frequency of 1 Hz.

Table 3
Acoustic Design Environment for AMD (One-Third Octave Band
Sound Pressure Levels)
dB re: 20μPa

Frequency Hz	Sound pressure L_p^* dB	Frequency Hz	Sound pressure L_p^* dB
1	92.0	125	136.9
1.2	94.0	160	138.6
1.6	96.0	200	140.3
2	98.0	250	139.5
2.5	100.0	315	138.7
3.2	102.0	400	137.9
4	104.0	500	136.5
5	106.0	630	135.3
6.3	108.0	800	134.0
8	110.0	1000	132.6
10	112.0	1250	131.2
12	114.4	1600	129.8
16	116.9	2000	128.2
20	119.2	2500	126.5
25	121.2	3150	124.8
31	123.9	4000	122.8
40	126.1	5000	120.8
50	128.4	6300	119.2
63	130.7		
80	133.0		
100	135.2		

* root mean square (rms) acoustic pressure, in pounds per square foot (psf) = $(2117) \times 10^{(L_p - 194)/20}$

4 VIBRO-ACOUSTIC RESPONSE TO THE AMD ACOUSTIC ENVIRONMENT

The acoustic environment described in the previous chapter will result in significant structural vibration of the AMD shell structure, and in the corresponding vibro-acoustic response of equipment inside and attached to the AMD. It should be noted that this analysis considers only structure and structure-mounted equipment within the high bay areas of the AMD. Potential excessive vibro-acoustic response of vibration-sensitive portable equipment brought into these areas and used during operation of the main engines may require separate consideration.

Vibro-acoustic response is considered here in three forms: (1) acoustically equivalent static pressure loads on secondary wall, roof, and door panels of the AMD shell and lightweight equipment covers, (2) vibration (seismic) load factors for design of mounting structure for internal mechanical, electrical, and hydraulic equipment, and (3) vibration or acoustic test environment specifications that may be required in procurement specifications for equipment that cannot be preselected to be assuredly capable of withstanding the vibro-acoustic environment arising from normal operations in the AMD.

Before defining these various design environments, it is desirable to briefly review the basis for their development.

Development of Vibro-Acoustic Design Environments

The secondary skin structure elements of the AMD and lightweight enclosures of AMD equipment share one common characteristic that is the primary cause of the acoustically induced vibration response: their large surface area in combination with low surface weight.

The basic principles involved in the vibro-acoustic response of such structures are illustrated conceptually in Figure 18. When a panel is driven by a sinusoidal oscillating pressure load (i.e., pure tone), such as that generated by an acoustic wave striking the panel, the panel surface deflects in nearly the same manner as for a static (nonoscillating) pressure load, except the deflection is oscillatory. When the frequency of oscillation is very low—well below the first resonance frequency of the panel—the peak magnitude of the panel deflection is, in fact, essentially equal to that induced by a static pressure load with the same peak pressure. This is illustrated by the graph in Figure 18 where the frequency approaches zero. However, as the frequency of the oscillating (acoustic) pressure wave increases, the panel deflection for the same peak pressure input increases and reaches a maximum value equal to the dynamic magnification factor (Q) multiplied by the static pressure response. The dynamic magnification factor is the ratio of the response at resonance to the static response of a resonant system.

Thus, the panel deflection, $X(f)$, at any frequency f , can be expressed with a simplified model, as:

$$X(f) = R(f) \times P(f) \times A/K \quad [\text{Eq 1}]$$

where

$R(f)$	=	the dynamic deflection response function of the panel to a unit sinusoidal pressure at frequency f
$P(f)$	=	the effective pressure, in psi, at frequency f
A	=	the panel area, in sq in.
K	=	the panel stiffness, in lb/in.

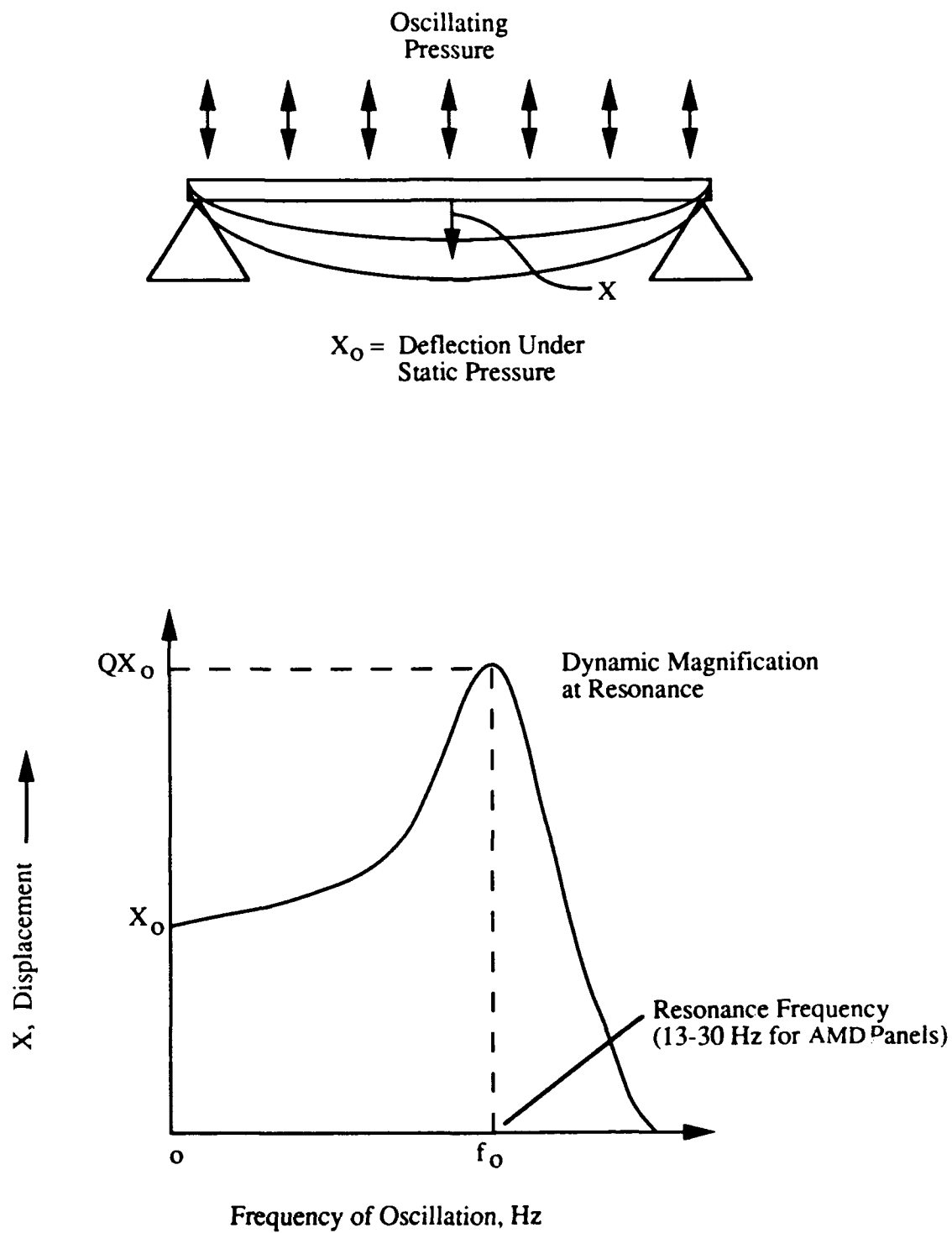


Figure 18. Conceptual illustration of resonant vibration response of plate to uniform oscillating acoustic pressure.

The panel acceleration response, $a(f)$, in g's at any sinusoidal frequency f , can be defined from Eq 1 using two basic relationships for vibration:

$$a(f) = \frac{\omega^2 \times X(f)}{g} = (2\pi f)^2 \times \frac{X(f)}{g} \quad [\text{Eq 2}]$$

and

$$f_o = \frac{1}{2\pi} \sqrt{\frac{Kg}{W}}$$

where f_o = panel resonance frequency, in Hz
 g = acceleration of gravity (386 in/sec²)
 W = panel weight, in lb
 ω = frequency, in rad/sec = $2\pi f$
 $X(f)$ = displacement (in.) at frequency f .

Thus, it is convenient to define a nondimensional vibro-acoustic acceleration response parameter called the specific acoustic mobility, expressed as $M_{SA}(f)$, to predict the acceleration response of a panel to acoustic excitation. In other words, the panel acceleration response at any frequency f can be expressed as:

$$a(f) = M_{SA}(f) \times \frac{P(f)}{w} \quad [\text{Eq 3}]$$

where $w = W/A$, the panel surface weight, in psi

and

$$M_{SA}(f) = R(f) \left(\frac{f}{f_o} \right)^2$$

If the acoustic excitation were sinusoidal (i.e., contained only one frequency) and uniform over the panel surface, the function $M_{SA}(f)$ would have the dimensionless value Q at the panel resonance frequency f_o . For the type of random, wideband acoustic excitation of a panel that will occur in the AMD, the value of M_{SA} is more complex, as discussed in detail in Appendix D.

In the simplest case, for excitation of a simply supported panel by a normally incident plane wave (i.e., when the direct sound field arrives along a line at 90 degrees to the panel surface), or for excitation by a reverberant sound field for which the acoustic wavelength is much longer than the average panel

length or width, the root mean square (rms) acceleration response, *averaged over the panel surface*, is given by (see Eq D12, Appendix D):

$$a(f_o) \equiv 1.06 \tilde{P}_b(f_o) \frac{\sqrt{Q}}{w}, \text{ g's} \quad [\text{Eq 4}]$$

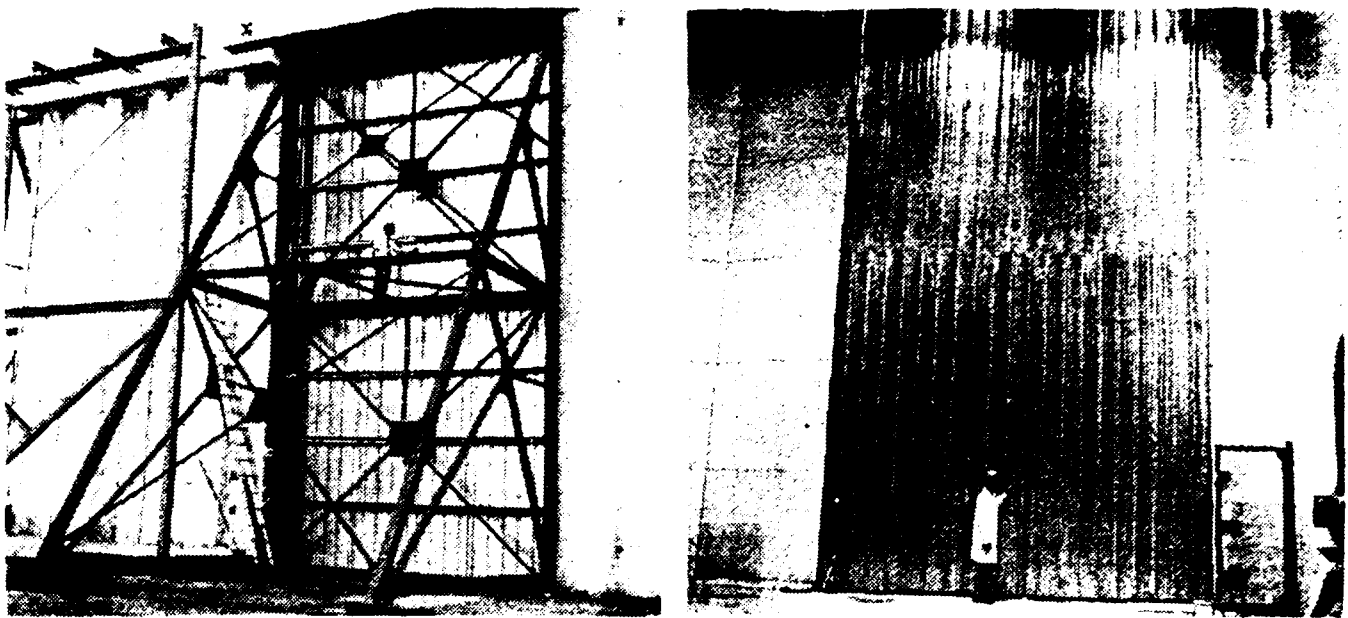
where $P_b(f_o)$ equals the rms sound pressure in the one-third octave band centered on the panel resonance frequency (f_o).

For a simply supported panel, the *maximum* rms acceleration occurs at the panel center, and is four times the *space-averaged* rms value given by Eq 4. However, the latter is considered a practical value for use in estimating average acceleration design environments.

Values for specific acoustic mobility, $M_{SA}(f)$, can be derived analytically as is done in Appendix D. Fortunately, however, validating experimental data on the vibro-acoustic response of large, lightweight industrial walls are also available from a unique series of acoustic tests conducted in 1968 for National Aeronautics and Space Administration (NASA). These tests involved exposure of the outside surface of several different variations on a basic corrugated steel industrial wall. The tests were designed to evaluate ground structure sensitivity to noise near rocket test and launch sites; the fact that the outside surface rather than the inside was the one exposed to the sound is not significant. Two test walls were tested simultaneously in one large opening of Wyle's 100,000 cubic feet acoustic reverberation test chamber, as illustrated in Figure 19. Each test wall measured 20 ft wide by 18 ft high, and was supported on 6.5 Z 2.9 or 2.9 Z 3.3 steel girts spaced 4.5 ft apart, designed to carry wind loads of 10 or 20 pounds per square foot (psf) respectively. Each wall unit, consisting of seven 3 ft wide 26-gage galvanized corrugated steel panels, was supported top and bottom by an eave strut and base angle respectively, which were connected by vertical sag rods. Some of the walls were lined with fiberglass batts loosely fastened on the inside. The panels were fastened to the girts and to each other with three different types of fasteners, varying from sheet metal screws to blind rivets.

The sound levels involved in this test varied from an overall sound pressure level of 139 dB to 153 dB re: 20 μ Pa. However, the noise spectrum peaked at a lower frequency than for the AMD environment so that the range of test levels equaled or exceeded the AMD design environment in Figure 17 only for frequencies below 150 Hz. Some failures of panel fasteners, such as those illustrated in Figure 20, occurred after 10 minutes of exposure to the highest test level of 153 dB, or after about 3 hours of exposure to test levels of 143 dB (Sutherland 1968, Appendix A). However, the most pertinent results from this test are not the observed fastener failures (since neither the panel design nor the test sound levels are representative for the AMD) but the data on the vibration response for validation of a prediction model.

Figure 21 shows the values of the $M_{SA}(f) = a(f)w/P(f)$ derived from the measurements of acceleration response on the center of the panels (Figure 21a), and the center of the girts (Figure 21b). In both cases, the acceleration response and pressure spectra were measured in the same narrow frequency band. The abscissa scale for each figure is a relative scale equal to the frequency normalized by the fundamental resonance frequency of the wall panels. As indicated in Figure 21, the values for M_{SA} are lower for the panels lined with fiberglass insulation, due to the added damping effect (and consequent decrease in Q) of the insulation. However, the general trend of these data is consistent with theoretical predictions and helps to support the detailed multimodal model outlined in Appendix D. $M_{SA}(f)$ increases rapidly with frequency from just below the fundamental resonance frequency and then, for the measurements on the panel, tends to flatten out with frequency as the response in higher modes is included. For a typical value



(Source: Sutherland 1968, Appendix A.)

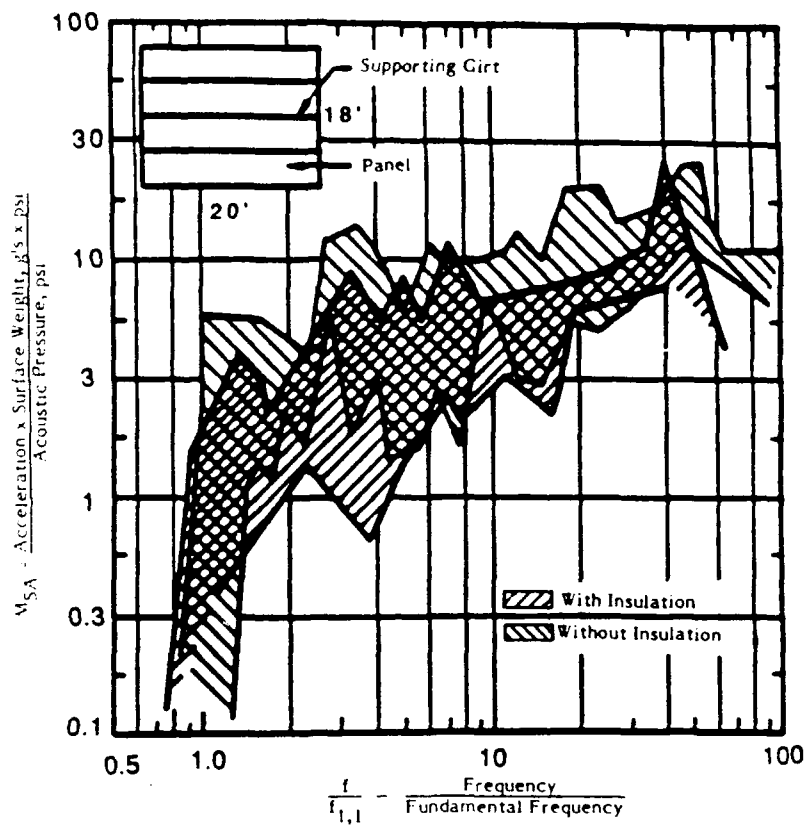
Figure 19. Industrial wall sample mounted in test opening of Wyle 100,000 cu ft reverberation facility.



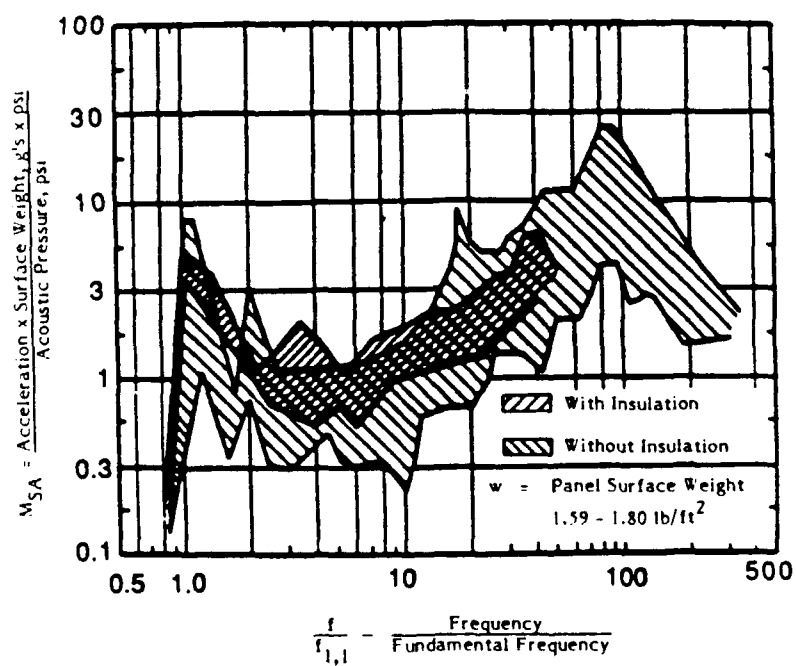
(Source: Sutherland 1968, Appendix A.)

Figure 20. Typical failures of steel panel in Figure 18 near panel-to-girt fastener.

(a)



(b)



(Source: Sutherland 1968, Appendix A.)

Figure 21. Normalized acceleration response of 26 gage corrugated steel industrial wall:
(a) Response measured on panel between girts (b) Response measured on girts.

of Q of about 10, applying Eq 4 and including the increase by a factor of four for the maximum response in the center of the panel, the predicted value of M_{SA} is about 13.4, which is very close to the upper bound of the data in Figure 21a. For Figure 21b, the value of M_{SA} has a more complex behavior, reflecting the reduced response of the girts at frequencies just above the fundamental frequency.

Equivalent Static Pressure Loads for AMD Acoustic Environment

An equivalent static pressure load can be determined which produces the same peak stress response as that produced by the actual dynamic load created by the acoustic environment. Two different approaches are used here. The first, used for wall panels, is based in part on experimental data for prototypes of these panels. The second method, used for the other structural elements, is semi-empirical but based on sound physical principles.

Equivalent Static Pressures for Wall Panels

For wall panels, experimental vibration response data (reviewed in Appendix E) were available from a dynamic vibration test of a sample preinsulated panel similar to the type under consideration for the AMD. The panel tested was an H. H. Robertson Co. type S30-2.00 26/26 sandwich panel 2 in. thick with 26 gage outer skins of galvanized steel. Similar wall panels, available from several manufacturers, but with 24 gage skins, are proposed for the AMD according to preliminary Corps of Engineers design specifications.

The key results obtained from this test, graphed in Figure E2 of Appendix E, were:

- Fundamental resonance frequency (f_0) = 30 Hz
- Dynamic magnification factor (Q) = 25 for the fundamental 1.0 mode, and an rms average of 15.0 for all higher modes.

The observed resonance frequency was in close agreement with a value predicted from the effective stiffness of the panel based on the manufacturer's specifications for the allowed static (wind) load. This analysis made it possible to reliably predict the resonance frequency of the other wall panels planned for use in the AMD. A summary of the results follows.

Analysis of Wall Panel Characteristics. Table 4 summarizes the analysis made of the basic static and dynamic characteristics of the test wall panel and the anticipated 7.5 ft span panel design for the AMD.

The value of effective stiffness of a homogeneous beam that has the same maximum deflection ($L/180$) specified by maximum allowable static load (P_s) was calculated as

$$(EI)_{eff} = 900L^3 \times a \times \frac{P_s}{384} \quad [Eq 5]$$

The effective spring rate was calculated as the ratio of static pressure to maximum deflection.

Table 4
Summary of Wall Panel Characteristics

Parameter	Units	Test Panel	AMD Panel
Width, a	in.	30	30
Length, L	in.	72	90
Outer skin area, A	sq in.	2160	2700
Skin gage		26	24
Skin thickness	in.	0.0179	0.0239
Total panel thickness	in.	2.0	2.0
Weight, W	lb	33.2	52.1 (Est.)
Allowable deflection	in.	0.40	0.50
Design wind load, P _s	psi psf	0.403 58.0	0.298 42.9
Effective stiffness, (EI) _{eff}	lb in ²	8.14x10 ⁶	15.3x10 ⁶
Effective spring rate	psi/in	NA	0.596
Resonance frequency, f _o	Hz		
Predicted		29.8	19.6
Measured		31	N/A

The resonance frequency (f_o) for the panel as a beam was calculated as

$$f_o = \left(\frac{\pi}{2L^2} \right) \sqrt{(EI)_{eff} \times L \frac{g}{W}} \quad [\text{Eq 6}]$$

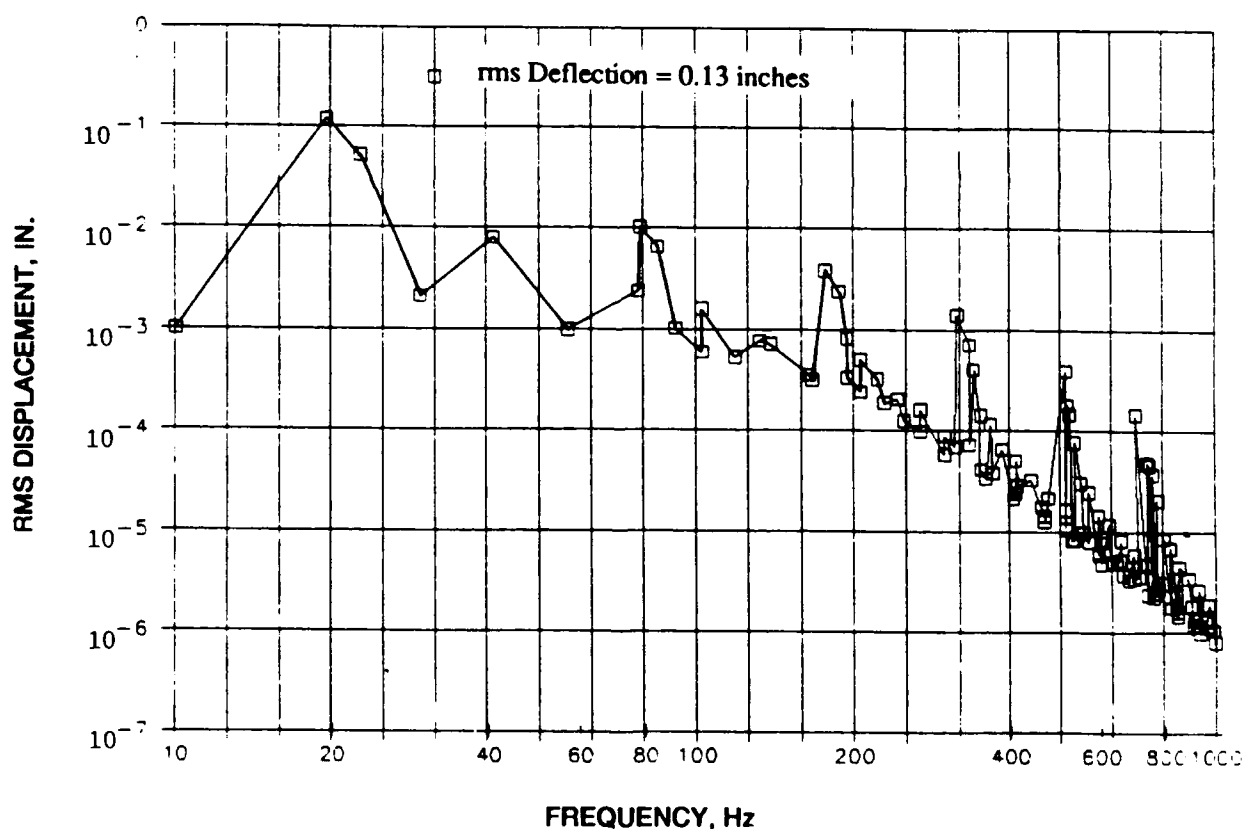
As the last entry in Table 4 shows, there was good agreement between the measured and predicted resonance frequency of the test panel. The predicted resonance frequency was based on the allowable static pressure load on the panels to limit the maximum deflection to 1/180th of the span. Thus, based on this validated model, the fundamental frequency of the AMD design wall panel is expected to be approximately 20 Hz. The second entry from the bottom in Table 4 provides the key parameter—the spring rate—needed to establish an effective static pressure load for the panel. All that remains, then, is to estimate the maximum deflection of the actual wall panel for the acoustic environment inside the AMD.

Estimated RMS Vibro-Acoustic Response of Wall Panels. Eq D11 (Appendix D) provides a general expression for the *space average* rms acceleration a(f_{m,n}) for the m,nth mode of a panel under excitation by a random acoustic noise. Given this rms acceleration (in g's), Eq 2 can be used to find the corresponding *space average* rms displacement X(f_{m,n}) at this frequency, f_{m,n}. The total *space average*

rms displacement (X_o) over all modes is then simply equal to the square root of the sum of the mean square displacements, or:

$$X_o = \sqrt{\sum x^2(f_{m,n})} \quad [\text{Eq 7}]$$

The results of carrying out this analysis for the wall panels, using the acoustic design environment described in Table 3 and Eq D11, D13, D14, and D15 (Appendix D) are illustrated in Figure 22 by the envelope of the mean square displacement response as a function of frequency. For this analysis, it was necessary to assume that the wall panels behaved as simply supported panels, but with the first mode at 19.6 Hz and the lowest modes corresponding to those for a simply supported (short-edge) and free (long-edge) plate acting as a beam included to approximate the complex modal behavior of the wall panel indicated by the data in Appendix E. Using Eq 7, the total *spatial maximum* rms displacement for the response spectrum in Figure 22 was found to be 0.138 in.



(Note: each point on the figure is the estimated rms deflection response at the center of the panel for just one vibration mode.)

Figure 22. Frequency spectrum of estimated spatial maximum deflection response for all modes at center of AMD wall panels (below 1000 Hz) subjected to environment in Table 3.

Adjustments to RMS Response to Define Effective Static Load. Three adjustments must be made to this *spatial maximum* rms displacement in order to establish an effective maximum displacement to apply to the determination of an effective static load. These are:

1. Correction to account for the difference between the rms and peak value of the random response
2. Correction to account for the long-term fatigue effects of this response
3. Correction to account for the difference between the *spatial average* response and the *spatial maximum* response.

Strictly speaking, the first two factors should be considered together because they are interrelated. However, they will be considered separately at this point for purposes of discussion.

Correction for Random Peaks. The acoustic pressure driving the wall panels is a random noise which has a statistical distribution of peak pressures described by a Rayleigh distribution. As explained in Appendix D, to define the peak response that will not be exceeded more than 10 percent of the time, the rms response must be multiplied by a factor (F_p) of 2.15.

This is a reasonable first approximation to account for the peak distribution of the random response. If a different probability of peak exceedance were desired, the factor would vary as follows (see Eq D21 in Appendix D):

Probability of Exceedance:	%	20	10	5	2.5	1
	F_p	1.79	2.15	2.45	2.72	3.03

Correction for Fatigue Effects. The fatigue effects due to repetition of the acoustic loading require some consideration of the potential duty cycles for operation of the AMD. The following estimates were provided to Wyle Research for preliminary design purposes:

Main engines - 4000 operations

Duration at 6820 rpm - 7-15 seconds per operation

Duration at idle rpm - 200-600 seconds per operation

APUs - 5000 hours of operation

For fatigue considerations, only operations at 6820 rpm for the main engines are expected to contribute to any potential vibration-fatigue-induced damage or malfunction of AMD structure or equipment. For the wall panels with a fundamental resonance frequency of about 20 Hz, the maximum number of stress cycles for these operations would be $4000 \times 15 \times 20$, which equals 1.2×10^6 cycles, or about 1 million cycles.

The vibro-acoustic responses of the AMD systems for the lower (idle or auxiliary power) conditions are expected to be well below the fatigue limit of AMD structure and equipment. The fatigue limit is the vibratory stress level which can be endured indefinitely. This is illustrated in Figure 23 along with a

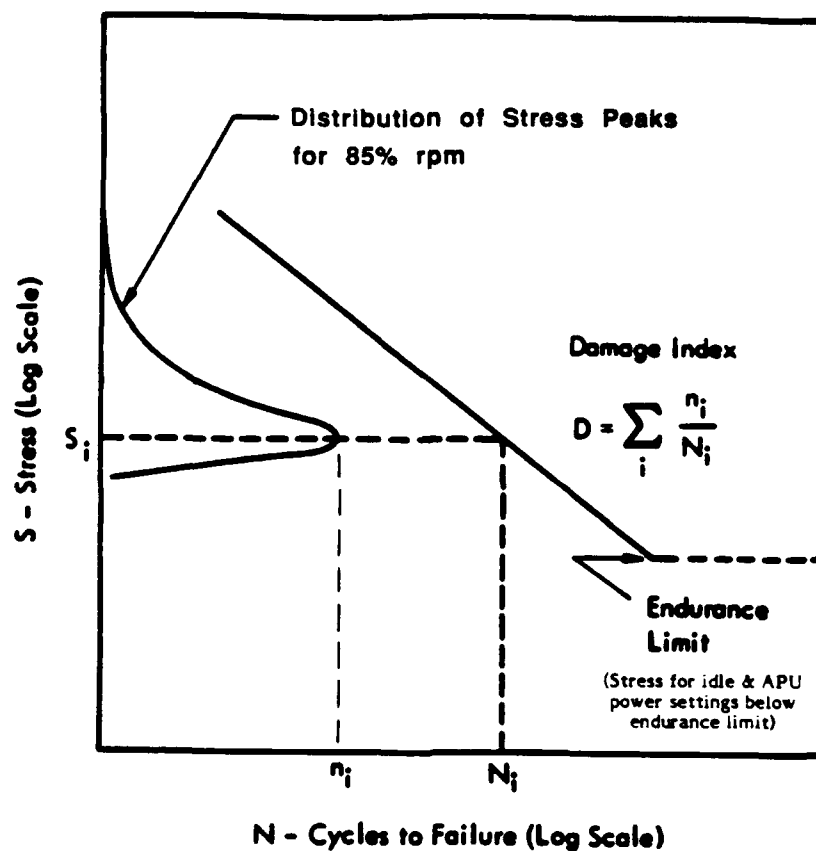


Figure 23. Evaluation of fatigue damage under random loading, at stress levels above fatigue limits.

conceptual illustration of how fatigue under random loading can be evaluated using Miner's Rule (Miner 1945). This rule can be stated as:

$$N_T = \frac{1}{\sum_i \left(\frac{P_i}{N_i} \right)} \quad [\text{Eq 8}]$$

where

- N_T = the total number of stress cycles of varying stress level.
- P_i = the probability of the i th stress level occurring
- N_i = the fatigue life (number of life cycles) at the i th stress level.

The general validity of this rule is limited by the following necessary, but potentially oversimplifying, assumptions (Richards and Mead 1968):

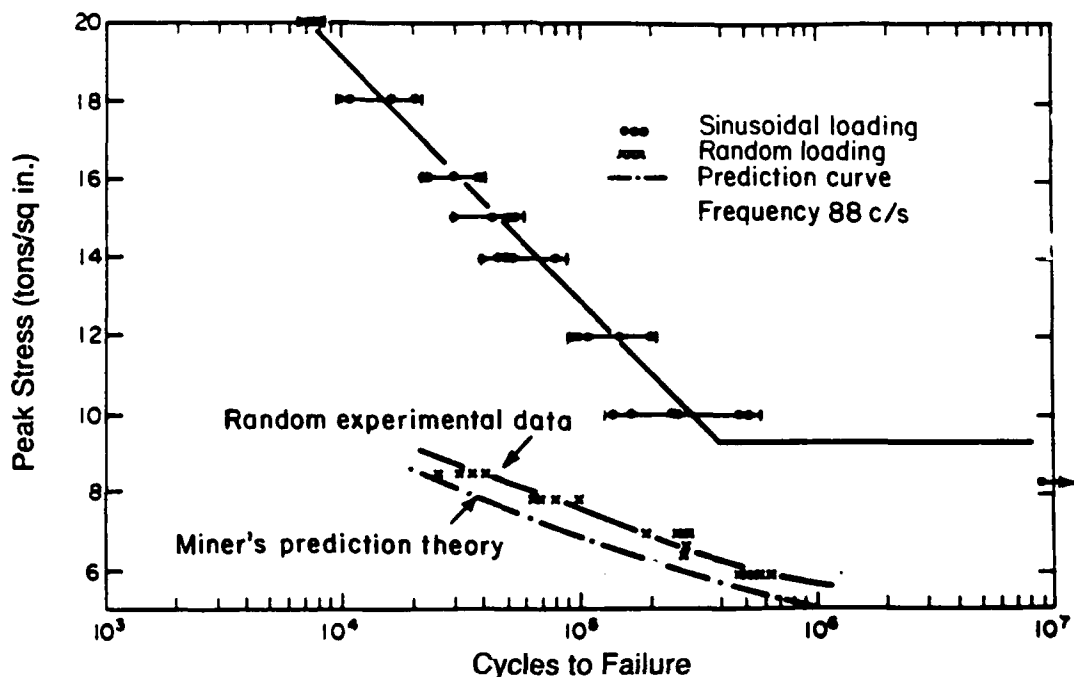
- No effect on fatigue life is accounted for as a result of the sequence of varying stresses
- No fatigue damage occurs for stress levels below the fatigue limit—the stress level sustainable for an infinite number of cycles

- Superposition of static tension or compression loads on top of the vibratory loads may be important but cannot be assessed.

Regardless of these limitations, Miner's Rule provides a reasonable engineering basis for evaluating fatigue at random stress levels.

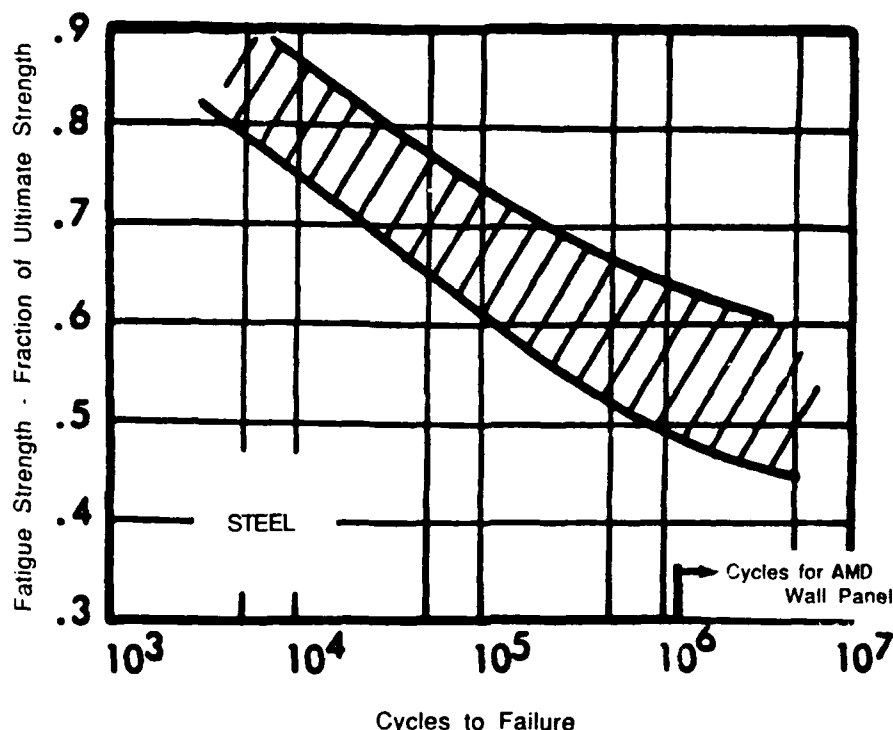
In effect, the model states that fatigue failure will occur after a total of N_T cycles if the sum of the fractions of fatigue life used up at each (i th) stress level adds up to one. Each fractional fatigue life is simply equal to the ratio of the number of stress cycles ($P_i N_T$) occurring at a given stress level to the actual fatigue life (N_i) at this stress level.

A precise evaluation of the fatigue life under random loading requires that an S/N (stress/fatigue life cycles) curve be available for the material in question. In the absence of such specific data on the wall panels, the experimental fatigue data on mild steel for sinusoidal and random loading shown in Figure 24 and the generic fatigue data on steel for sinusoidal loading shown in Figure 25 are used for guidance. Comparing the sinusoidal and random fatigue life data in Figure 24, it can be shown that for approximately the same *peak stress* (equal to 1.4 times the rms sinusoidal stress and 2.15 times the rms random stress, corresponding to 10 percent exceedance peaks), the two experimental sets of data become very similar. From Figure 25, for 1.2 million cycles of sinusoidal loading, the average ratio of (peak) stress at failure to ultimate strength is about 0.56. If the yield strength is assumed to be about 75 percent of the ultimate strength for the wall panel material, then the ratio of peak sinusoidal stress at failure to the yield strength would be about $0.55/0.75$ or about 0.75. Thus, for design purposes, the static pressure corresponding to the rms displacement (or rms stress) in the wall panels will be increased by a factor of



(Note: notched test-pieces $K_t=1.5$. Push-pull testing with zero mean load.)
(Source: Richards and Mead 1968. Reprinted by permission of John Wiley and Sons, Ltd.)

Figure 24. Sinusoidal and random S/N curves in mild steel.



(Adapted from data in Lipson and Juvinal 1963 and Cummings 1960.
Reproduced with the permission of Macmillan Publishing Company, Inc.)

Figure 25. Fatigue damage for steel-sinusoidal loading.

2.15 to account for peaks of the random loading and further increased by $1/0.75$ to account for the reduction in loading necessary to account for fatigue effects. This procedure is necessarily approximate but is considered a reasonable engineering approach in the absence of fatigue data for wall panel specimens under actual or simulated acoustic loading. The influence of fatigue effects for alternative power settings for the main engine is considered further in Appendix H.

Correction for Maximum Response Instead of Space Average. The overall maximum displacement for the wall panels under acoustic loading is shown to occur at frequencies near the fundamental frequency at about 20 Hz (Figure 22). However, the maximum displacement can only be approximated from the rms value. Exact phase relationships, which influence peak responses, are not retained in Eq 7 to compute the overall rms response from the sum of the responses in each mode. For design purposes, it will be assumed that the *spatial maximum* rms displacement response of the panel (0.13 in.) will be four times the *spatial average* rms value.

Summary of Computation of Equivalent Static Pressures for Wall Panels. The equivalent static pressure load for the wall panels is computed as follows:

1. For the acoustic design levels in Figure 17, the *spatial maximum* rms displacement is 0.13 in. (rounded to 2 significant figures)
2. The ratio of static pressure load to displacement for this panel is 0.596 psi/in (see "Analysis of Wall Panel Characteristics" earlier in this chapter)

3. The nominal static pressure (P_s) corresponding to this rms displacement is 0.596 psi/in. x 0.13 in., or 0.0775 psi (11.2 psf)

4. Applying the peak-to-rms and fatigue correction factors, the design equivalent static pressure (P_{seq}) is:

$$P_{seq} = P_s \times 2.15 \times (1/.75)$$
$$P_{seq} = 32 \text{ psf, the design value.}$$

Note that this equivalent static pressure load must be applied as either a positive or negative static pressure.

By designing the panel and attachment hardware to support this equivalent static load, in combination with any other time-coincident load(s), the wall panels should be able to withstand the internal acoustic design environment of the AMD. Note that no stress concentration factors or design margins have been included in the above equivalent acoustic load. Although there is already a considerable degree of conservatism built into this number, the structural designer should take into consideration standard structural design codes for alternating fatigue loads represented by the type of equivalent alternating static pressures specified above. Appendix F provides an extract from the AISC *Manual of Steel Construction* "Specification for Structural Steel for Buildings" (AISC 1980). This appendix contains the section on fatigue design, and includes recommended maximum ranges in fluctuating fatigue stresses to be considered in conjunction with basic allowable stresses ordinarily considered in building design.

This technical report does not, and cannot, provide detailed specifications for structural design that supersede standard building design codes. The latter must obviously take precedence. However, the unique nature of high-intensity acoustic loads on the type of lightweight building construction planned for the AMD shell dictates the need to give careful consideration to the guidance provided herein in order to avoid recurring fatigue problems with secondary structure or equipment malfunction problems due to vibro-acoustic response. Such problems, if allowed to occur, could at the very least increase building maintenance and operation costs significantly. At worst, these problems could cause significant damage to the test systems used inside the AMD.

Equivalent Static Pressures for Other AMD Structural Panels

Supplemental test data were not available for any of the other structural elements considered potentially susceptible to acoustic loading. The elements in this category are:

- Roof panels
- Inside surface of back door
- Draft curtain
- Enclosures for major mechanical equipment such as the heating and ventilating (HV) system
- HV ducts.

Equivalent static pressure loads for each of these secondary structure or equipment elements are considered in this section. The method used to estimate these static pressure loads is slightly different from the one described above. Instead of relating static pressure to displacement, the more general relationship developed in the section "Equivalent Static Pressure" (Appendix D) is used. This method relates the rms dynamic stress to the *spatial maximum* rms velocity of the panel and then, after again accounting for

random peaks and fatigue effects, an equivalent static pressure is defined which should produce approximately the same peak stress. The key steps in this process may be summarized as follows:

1. For each panel mode, find the *spatial average* rms acceleration response $\bar{a}(f_{mn})$ using Eq D11 (Appendix D)
2. Compute the *spatial average* rms velocity $v(f_{mn})$ for each mode, i.e., $v(f_{mn}) = \bar{a}(f_{mn}) \cdot g / 2\pi f_{mn}$
3. Compute the maximum rms stress $\sigma(f_{mn})_{\max}$ in each mode using Eq D17 (Appendix D), being sure to account for the difference between the *spatial average* and *spatial maximum* velocity response
4. Compute the overall maximum rms stress σ_{\max} as the square root of the sum of the squares of the mean square *spatial maximum* stresses in each mode
5. Using Eq D35 (Appendix D), define the equivalent static pressure (P_s) that produces the same peak stress, taking into account the random peaks of the excitation and fatigue effects.

For the draft curtain, an additional refinement was necessary to define the effective static pressure. This refinement is needed to account for the fact that for loading by the reverberant field, the effective acoustic pressure on the draft curtain approaches zero in the limit as frequency approaches zero. This is because as frequency approaches zero, the phase difference between the pressure on both sides of the draft curtain approaches zero. This phenomenon can be accounted for in the following manner. The net rms differential acoustic pressure (ΔP) in the reverberant sound across the draft curtain is:

$$\Delta P = \sqrt{[P_1 - P_2]^2} = \sqrt{2} \bar{P} \sqrt{1 - C(\Delta x)} \quad [\text{Eq 9}]$$

where

P_1, P_2 = *reverberant field* acoustic pressures on each side of the draft curtain that have the same rms magnitude (\bar{P})

$C(\Delta x)$ = space correlation coefficient in the reverberant field (Waterhouse 1955, pp 247-258) equal to:

$$\frac{\sin(2\pi \Delta x f / c)}{(2\pi \Delta x f / c)}$$

Δx = the length of the path from the middle of one side to the middle of the other side of the draft curtain which is nominally equal to its height, in ft

f = frequency, in Hz

c = speed of sound (1117 ft/sec).

For the draft curtain, with $\Delta x = 14$ ft, for frequencies greater than about 30 Hz the space correlation coefficient $C(\Delta x)$ approaches zero and the net acoustic design load on the draft curtain is 41 percent greater than on wall or ceiling panels. Conversely, for frequencies below 30 Hz, the net acoustic load reduces to zero since the correlation coefficient $C(\Delta x)$ approaches unity as frequency approaches zero.

This correction for the draft curtain acoustic load is accomplished by multiplying the rms modal response to the reverberant acoustic field at each frequency by:

$$\sqrt{2[1-C(\Delta X)]}$$

However, it must be emphasized that this acoustic load for the draft curtain is a conservative value since it would occur only for a few seconds during the time the test system moves forward towards the front door.

Table 5 summarizes the results of these calculations of equivalent static pressures for the different types of structure defined at the beginning of this section. The fundamental resonance frequencies for the corrugated roof and draft curtain panels were estimated by assuming that these nonhomogeneous structures could be treated as equivalent beams given available data on their bending stiffness (EI). For the back door panels and HV enclosure equipment, simply supported panels were assumed and resonance frequencies calculated from standard equations for such structures. Tabulations of the detailed calculations involved in completing Table 5 are given in Appendix H. Note that in all cases, these equivalent static pressures are to be applied in each direction normal to the applicable surface.

Table 5
Summary of Equivalent Static Pressure for Design of Lightweight Structural Elements
on AMD Subjected to Acoustic Design Environments in Table 3

Element	Estimated Maximum Deflection		Estimated Maximum rms Velocity in./sec	Equivalent Static Press. psf
	rms in.	Peak [*] in.		
Wall Panels	0.13	0.38	19	±32 **
Roof Panels ***	0.13	0.36	5.7	±27
Inside Back Door ^{†,***}	0.12	0.33	9.2	±7.8
Draft Curtain ^{‡,***,1†}	0.075	0.22	15	±34
HV Equipment ^{2†,***} Enclosure	0.183	0.52	13.3	±7.5

Note: design power condition for main engine is 6820 rpm.

- * Includes factor of 2.15 for random peaks plus 1/0.75 to allow for fatigue effects. No stress concentration factors included.
- ** The same equivalent static pressure load should be applied to the personnel doors that penetrate the AMD walls.
- *** For more details, see the section "Additional Details from Studies of Vibro-Acoustic Loads on Specific AMD Elements" in this chapter and Appendix H.
- † For typical 24 x 72 in. frame spacing, 16 gage skin.
- ‡ For average 13 ft length, 18 gage panel.
- 1† Design acoustic loads on draft curtain are transitory and strictly applicable only for a few seconds during forward movement of the test system.
- 2† For 18 gage 2 x 4 ft panel braced with 1 in. angle.

Vibration Loads for Design of AMD Equipment and Mounting Structure

Vibration loads for AMD equipment and mounting structures are defined, in this section, in terms of (1) vibration load factors (i.e., g-loads) to be applied to the design of any structure-mounted AMD equipment and its mounting attachment, and (2) reaction loads on secondary framing structure due to vibration of wall or roof panels. In all cases, these loads are bidirectional—applied in both directions along any one axis.

At the end of this section, results of more detailed studies are summarized for:

- Roof structure and roof-mounted equipment (page 57)
- Draft curtain (page 59)
- HV system (page 59).

The foundation for methods of computing the vibration loads for design of AMD equipment and mounting structure has been laid in the previous section. The starting point for the calculations was the determination of the acceleration response of the various types of structural walls or roof panels. However, the response levels for individual panels, for example, do not accurately represent the reduced acceleration levels at the panel boundaries (i.e., girts, bars, joists, etc.). The vibration loads on structural elements that support the AMD's external skin structure and serve as the mounting points for internal equipment are lower, as explained later.

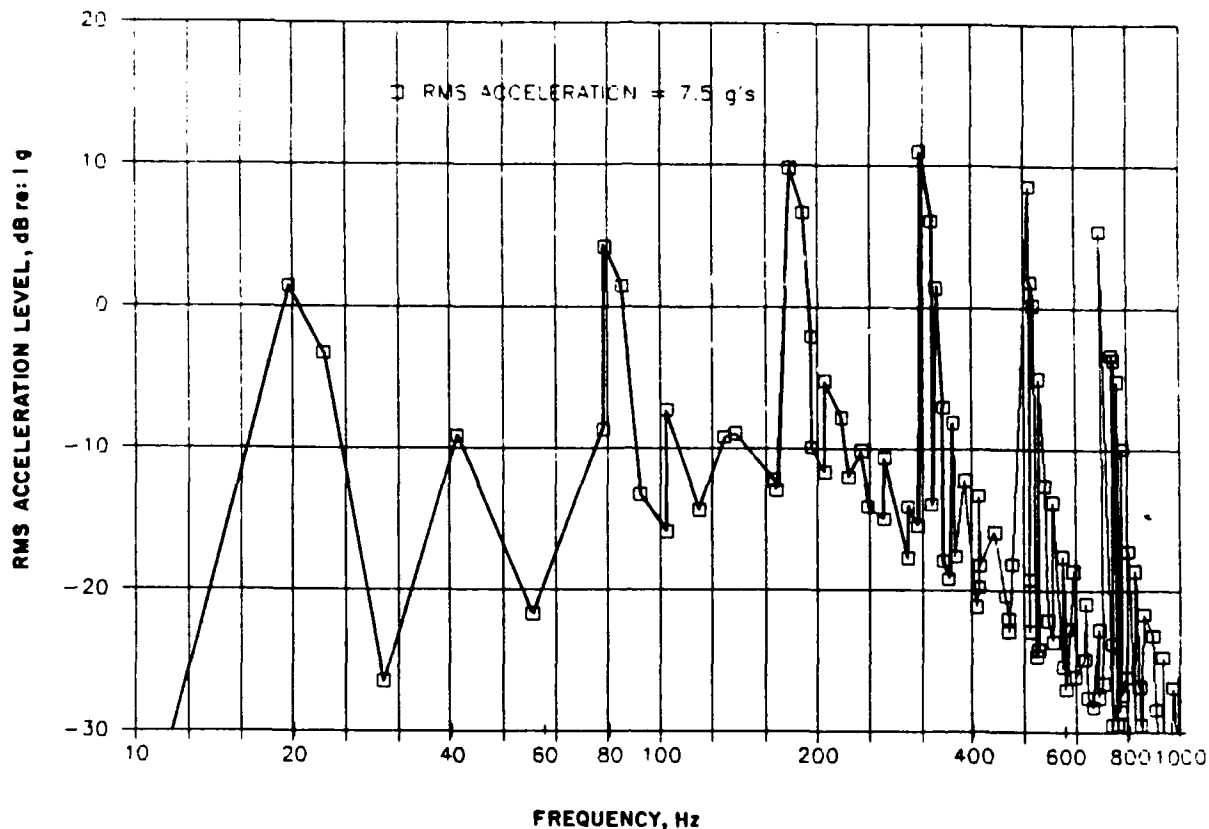
Vibration Load Factors

Two basic modifications to the preceding calculations provide a reasonable basis for establishing the desired load factors. First the *spatial average* response levels are computed instead of the spatial maximum response levels. Second, the surface weight parameter used in the response equations (see Appendix D) now includes the added weight of the support structure distributed over the surface of the acoustically loaded structure in question. Thus, the *space average* acceleration levels for the wall structure are based on the total average weight of the entire wall system, panels plus girts and columns distributed over the surface. This is a rough, but reasonable and generally conservative, approximation for estimating vibration load factors for equipment mounting points.

Finally, a third modification serves to further reduce the acceleration levels and corresponding vibration (seismic) load factors. This modification stems from the inherent reduction in vibration levels when mass-loading effects of heavy equipment mounted on the building frame structure are accounted for.

It should be pointed out that more sophisticated methods might have been used for this part of the analysis. These include (1) the Statistical Energy Analysis (SEA) method (Lyon 1975; Cremer 1973), useful for evaluating vibration energy flow through a structure, and (2) classical finite element methods. However, finite element methods were not considered well suited for predicting environmental vibration at frequencies well above the lowest vibration modes of the AMD building frame. The SEA method would have been more useful for this study, but its successful application requires knowledge (or reasonable estimates) of structural vibration transmission across many different types of joints as well as estimates of structural damping factors. Since this type of information was not well defined for the AMD, the accuracy of the method was expected to be limited for application to this program.

Summary of Vibration Load Factors. Figure 26 shows the estimated acceleration response spectrum at wall mounting points based on application of the concepts outlined above. Note how this figure compares to the displacement response spectrum for the wall panels alone shown in Figure 22. Based on this type of analysis, it is possible to estimate vibration load factors for several basic types of mounting



(Note: each point is the estimated space average rms acceleration in one vibration mode of the wall panels for Q of 25 in the first 1,0 mode, and 15 for all higher modes.)

Figure 26. Envelope of estimated average modal acceleration levels on wall panels of AMD exposed to acoustic design environment in Table 3.

locations in the AMD. The results of these calculations are summarized in Part (a) of Table 6. The detailed calculations are presented in Appendix H.

Note that the vibration load factors in Table 6 do not include any allowance for fatigue failures of the mounted equipment or of the mounting hardware. It is assumed that the equipment or structural design will account for potential fatigue effects when final stress design or test specifications are established for each item.

Also, as indicated by a footnote in Table 6, the specified load factors apply to vibration loads in a direction normal to the plane of the panel surface in question. For an estimate of in-plane vibration loads, the tabulated values should be multiplied by 0.5.

Mass-Loading Effects. The baseline load factors given in Table 6 do not take into account the reduction in vibration response due to mass loading. The trend illustrated in Figure 27 can be used to estimate this reduction. The abscissa is the total weight (W_e) of all the equipment mounted on the structure. The parameter on the three curves is the total effective weight (W_m) of the basic structure on which the equipment is mounted. The relative vibration load factor is given by the ratio $W_m/(W_e + W_m)$. The values of W_m defined in Table 6 are developed in detail in Appendix H for the typical primary and secondary structural elements listed in the table. The *effective weight* (W_m) of the mounting structure represents the dynamically effective weight of a vibrating beam, which is 50 percent of the true weight.

Table 6

**Summary of Dynamic Response Loads for Design of AMD
Supporting Structures or Attachment Hardware**

(a) Vibration (Seismic) Load Factors

----- Mounting Location-----		W_m , Effective Weight of Mounting Structures, lb	Baseline Vibration Design* Load Factor**
Walls	On Wall Panel (2.5 x 7.5 ft)	26 (per panel)	17
	On Girt, Back Wall***	715	8
	On Girt, Side & Front Wall †	505	8
	On Columns, Back Wall ‡	5035	5.4
	On Columns, Side & Front Walls ‡	4265	5.4
Roof	On Roof Panel/Bar Joist Section	520 (per section)	5.2
	On Roof Truss 1†	5017	3.1
Back Door	On Door Panes (16 gage)		5.4 ^{2†}
	On Frame Joints (2 x 6 ft)		5.4 ^{2†}
Draft Curtain	On Draft Curtain Panel (18 gage)	300	21 ^{3†}
	On Bottom Channel (W16 x 45)	1260	5.0
	On Roof Girders	5300	2.8

(Note: subjected to acoustic design environment in Table 3 with main engines at 6820 rpm.)

* Applicable without change in direction perpendicular to surface when equipment weight, W_e , is less than 10 percent of weight, W_m , of mounting structure. For heavier equipment, reduce baseline load factor by $W_m/(W_e+W_m)$.

** Load factors in direction normal to plane of surface (i.e., wall, roof, etc.). For in-plane vibration loads, multiply factors by 0.5.

*** Average effective weights for girts on back wall varying from W10 x 33 to W10 x 39. (See Table H3 in Appendix H.)

† Average effective weights for girts on side wall (W8 x 21) and front wall (W8 x 18).

‡ Average for columns varying from W12 x 53 on front and side walls to W12 x 65 on back wall.

1† Average values per roof truss section. See Tables H6 and H7 for detailed breakdown of values for baseline load factors and W_m respectively for each section of roof truss structure.

2† No allowance is made for reduction in load factor due to mass loading since only very light components should be mounted on the door surface and only if necessary.

3† For average section of draft curtain between column lines or trusses.

Table 6 (Cont'd)

(b) Vibration Reaction Loads for Secondary Structural Connection Due to Acoustic Loading

Joint Vertical Surfaces	Perpendicular to Surface	Co-Planar with Surface		
		Up	Down	Horizontal
Wall Panel/Girt	$\pm 610^{**}$	$\pm 160^{**}$	-440^{**}	$\pm 303^{**}$
Girt/Column	$\pm 123^{5**}$	0	-1300	± 176
Rear Door Panel/ Frame	$\pm 14 \text{ lb/ft}^{**}$	-	-	$\pm 7 \text{ lb/ft}$
Draft Curtain Panel/ Truss	$\pm 207 \text{ lb/ft}$	$+83 \text{ lb/ft}^{***}$	-124 lb/ft^{***}	$\pm 104 \text{ lb/ft}$
Horizontal Surfaces		Co-Planar with Surface		Perpendicular to Surface
		Up	Down	Horizontal
Roof Deck/Bar/Joist		$+25 \text{ lb/ft}^{**}$	-610 lb/ft^{**}	$\pm 160 \text{ lb/ft}^{**}$
Bar Joist/Roof/Truss		$+310^{**}$	-7610^{**}	$\pm 1980^{**}$

* For vibration reaction loads on HV duct joints see Tables 10 and 21.

** Reaction load increased for stress concentration, by factor of 3.5.

*** Vertical reaction loads on draft curtain = $\pm 1/2$ (reaction load perpendicular to surface) $- 1/2$ (surface weight)(average height).

For example, for a 1000 lb equipment item mounted on a column on the back wall, the relative change in vibration load factor from the baseline value in Table 6 for the unloaded structure would be $5035/(5035+1000)$, or 0.83; this is a 17 percent reduction in load factor due to mass loading.

Vibration Reaction Loads

In some cases two different methods were used to develop reaction loads at various structural joints or connections of secondary structures to account for acoustically induced vibration.

The first method is based on Appendix G, which addresses the topic of reaction loads at support points of beams or plates subject to various types of vibratory loads. As shown by the expressions in Appendix G, reaction loads at beam and panel support points tend to decrease with mode number.

The second method estimated a vibration reaction load as the product of the effective weight of a structure (W_m) times the vibration load factor in Table 6. This estimated total vibration reaction load would then be distributed over the number or length of the structural joints involved. The higher of the two estimates of reaction load, which were usually quite close, was used for design.

Part (b) of Table 6 presents a summary of the vibration reaction loads estimated for the major structural joints in the AMD that would be subject to significant vibration loads. Reaction loads in the vertical direction are defined for the up and down direction taking into account the inherent -1 g download due to gravity.

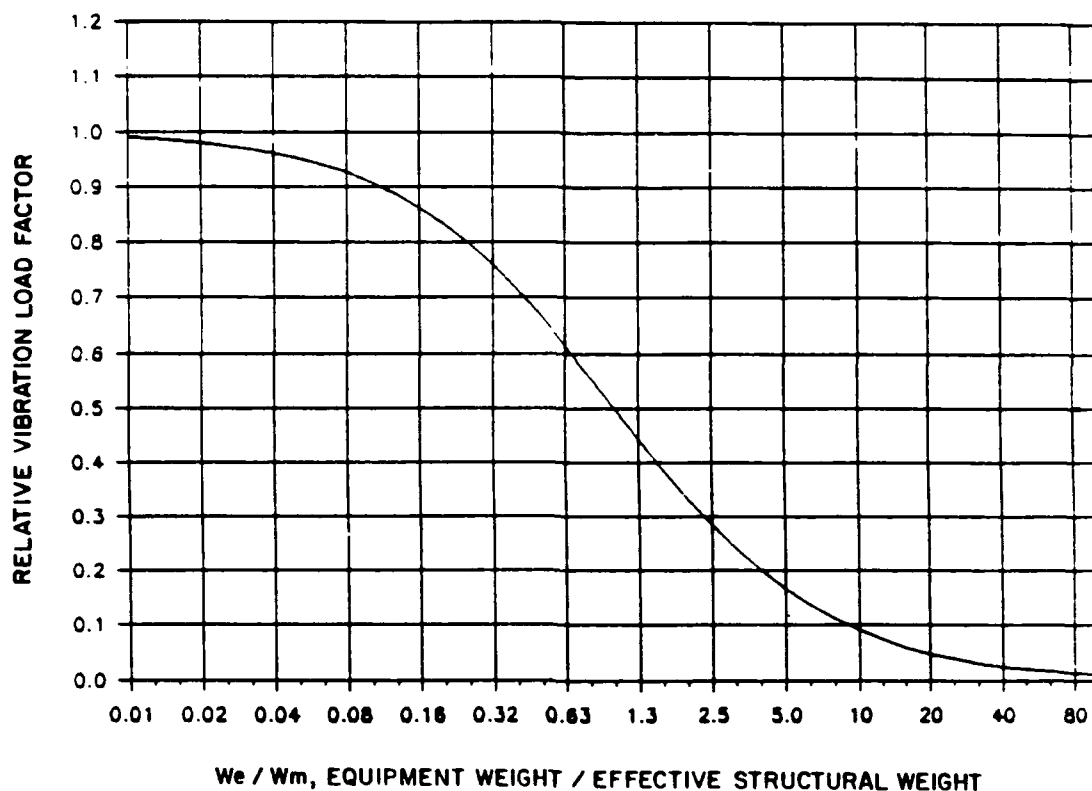


Figure 27. Decrease in baseline load factors in Table 5 for wall-mounted equipment.

Vibration reaction loads in directions parallel to, or co-planar with, a basic vibrating surface such as a wall panel or roof deck are taken as 50 percent of the basic value in the direction perpendicular to the surface.

Additional Details From Studies of Vibro-Acoustic Loads on Specific AMD Elements

Principal results of the detailed studies of vibro-acoustic loads on AMD structural elements have been provided in Table 6 (a) and (b). Additional details from the analyses carried out in Appendix H may be summarized as follows.

Roof Structure and Roof-Mounted Equipment. Vibro-acoustic loads on the roof deck for alternative bar joist configurations, summarized in Table H4 (Appendix H) are presented for reference here as Table 7. The fundamental frequency (f_1) for the roof deck/bar joist system in Table 7 is expressed by the following equation:

$$f_1 = \frac{\pi}{2 \times 144 \times L^2} \sqrt{\frac{EI}{\rho A_{\text{eff}}}} \cdot (\rho A)_{\text{eff}} = w_{\text{TOT}} \times \frac{b}{12 \times 386} \quad [\text{Eq 10}]$$

where

- L = is the bar joist span, in feet
- E = is the modulus of elasticity, in psi
- I = is the bar joist moment of inertia, in in.⁴
- b = bar joist spacing in feet = 5.7 ft.

Table 7
Roof Vibro-Acoustic Loads for Alternative Bar Joists

Bar Joist	Span(L) ft	I in ⁴	W/L lb/ft	w _{BJ} [*] psf	w _{ROOF} ^{**} psf	w _{TOT} ^{***} psf	f [†] Hz	LF g	P _s psf	R/b [†] lb/ft
8K1	8	6.6	5.1	0.89	5.9	6.79	26.2	4.52	63.4	447
14K6	25	70	7.7	1.35	5.9	7.25	8.47	5.34	23.4	384
16K4	25	78.4	7.0	1.23	5.9	7.13	9.04	5.37	24.9	389
16K5	25	88	7.5	1.32	5.9	7.22	9.51	5.23	26.1	394
16K6	25	95.6	8.1	1.42	5.9	7.32	9.85	5.15	27.0	397
16K7	25	106	8.6	1.51	5.9	7.41	10.31	5.04	29.7	406
16K9	25	125	10.0	1.75	5.9	7.65	11.0	4.86	31.6	413
22K5	25	172	8.8	1.54	5.9	7.44	13.1	4.85	36.9	425

* Average surface density of bar joist over average spacing of 5.7 ft.

** Surface density of roofing (steel deck, 2.2 psf) + (insulation + EPDM, 3.5 psf) + (fire protection piping, 0.2 psf) = 5.9 psf.

*** w_{BJ} + w_{ROOF}

† Reaction load per foot width (b) of roof panel.

This analysis shows that the vibration load factors (LF) and the reaction load (R/b) on the roof are not very sensitive to selection of the bar joists. However, the equivalent static pressure (P_s) varies significantly with the choice of bar joist.

The average load factors for roof-mounted equipment shown in Table 6 are for vibration only. A more complete definition of the baseline load factors for roof-mounted equipment including the effect of dead load, is specified in Table 8.

It is important to recognize that mass loading only reduces the vibratory portion of these load factors. Thus, for a 250 lb weight supported on one bar joist, the corrected total load factor (using W_m = 520 lb from Table 6) would be the following:

$$\begin{aligned}
 \text{Vibration LF} &= \pm 5.2 \times 520 / (250 + 520) &= \pm 3.5 \text{ g} \\
 \text{Dead Load} &&= - 1 \text{ g} \\
 \text{Total Load Factor} &\quad \text{Up} &= + 2.5 \text{ g} \\
 &\quad \text{Down} &= - 4.5 \text{ g}
 \end{aligned}$$

Pipe Hanger Vibration Load Factors. A more detailed analysis was also carried out of vibration loads for pipe hangers hung from bar joists (Appendix H). One method employed in the analysis used a combined lumped parameter mechanical mobility model for a mass-spring equivalent to the roof deck/bar joist system and a distributed mechanical mobility model for the supported pipe system. The result of this analysis indicates that the pipe hanger vibration load factor would reduce from a baseline value of $\pm 5.15 \text{ g}$ (the actual value before rounding to a value of 5.2 g as specified in Table 6a) to $\pm 1.85 \text{ g}$.

A different approach simply using the mass-loading concept indicated a value of $\pm 4.22 \text{ g}$. It is recommended that for now, a vibration load factor of $\pm 3 \text{ g}$ be used for design of 6 in. diameter pipe hanger loads.

Table 8
Detailed Total Baseline Load Factors for Roof-Mounted Equipment

Direction	--- Location ---	
	Roof Deck or Bar Joists	Roof Trusses*
Vertical, Up	+4.2 g	+ 2.1 g
Vertical, Down	-6.2 g	- 4.1 g
Lateral	±2.6 g	± 1.6 g

*Average

Draft Curtain. Vibration response was evaluated in Appendix H for two different gages (18 and 20) of draft curtain panels and for different lengths (varying from 10 to 16 ft). The results, given in Table H10, are shown for reference here as Table 9.

Only the equivalent static pressure (P_s) varies significantly with length. However, the highest average load factor, 28.5 g, occurs as expected for the lightest gage.

HV System. Vibro-acoustic loads on the HV mechanical equipment enclosure carried out in Appendix H are specified in Table 5 in terms of equivalent static pressures. The loads are not considered severe.

In addition, vibro-acoustic loads were evaluated in Appendix H for the HV ducts and for the base of the HV mechanical equipment unit itself.

HV Ducts. Table 10 lists the vibro-acoustic response parameters for the various sizes of HV ducts (18 gage thickness only; Chapter 7 provides similar information for other thicknesses). The values presented in the table correspond to vibro-acoustic response of the four walls of a rectangular duct where the wall was treated as a simply supported panel with a width (W) equal to the duct width (in either

Table 9
**Summary of Vibration Response Parameters for
Alternative Gages and Lengths of Draft Curtain**

Gage*	Length, ft	10	12	14	16	Avg
18 Gage $I = 1.325 \text{ in}^4/\text{ft}$ $w = 3.46 \text{ psf}$	f_o , hz	24.8	17.2	12.7	9.7	16.1
	P_s , psf	104	68	48	34	63.5
	LF, g	22	21	22	21	21.5
	R/b lb/ft	192	202	216	221	208
20 Gage $I = 0.959 \text{ in}^4/\text{ft}$ $w = 2.61 \text{ psf}$	f_o , hz	24.2	16.8	12.3	9.5	15.7
	P_s , psf	101	66	46	33	61.5
	LF, g	29	28	29	28	28.5
	R/b lb/ft	191	200	212	219	206

*Based on properties specified for Vulcraft Type 3N20 or 3N18 Acoustical Deck

Table 10

**Summary of Vibro-Acoustic Response Parameters for 18 Gage
Galvanized Steel Walls of HV Ducts**

Duct Size In.	Panel Size		$(f_o)^*$ Hz	P_s psf	LF psf	Q^{***} In.	X_{pk}^{**} psi	$W/120^\dagger$ In.	R/W^\ddagger lb/ft
	W In.	L In.							
8 x 14	8	90	71.6	156	24	7990	0.18	0.067	88
10 x 12	10	90	46.0	111	32	8835	0.28	0.083	117
12 x 12	12	90	32.1	58	23	6640	0.33	0.10	84
8 x 14	14	90	23.7	36	19	5625	0.35	0.12	69
12 x 16	16	90	18.3	27	21	5435	0.37	0.13	77
16 x 42	42	90	3.1	1.9	6.5	2280	0.49	0.35	24
16 x 50	50	90	2.4	1.4	5.4	2085	0.54	0.42	20
8 x 14	14	90	23.7	33	20	5110	0.30	0.12	73
20 x 24	20	133	11.6	17.4	24	5530	0.52	0.17	128
22 x 24	22	133	9.6	10.2	17	3915	0.48	0.18	90
24 x 24	24	133	8.1	7.7	17	3535	0.50	0.20	92
30 x 30	30	133	5.3	4.1	16.6	2855	0.53	0.25	90
36 x 36	36	133	3.8	2.7	9.5	2690	0.57	0.30	57

* Fundamental frequency for one side of duct wall with specified panel size.

** rms stress in duct wall. Peak stress will be 2.15 times greater 10 percent of the time.

*** Effective peak displacement allowing a peak/rms deflection of 2.15 and an additional increase of 1/0.75 for fatigue effect.

† Nominal desirable limit in deflection based on panel width.

‡ Conservative estimate of reaction load/ft along each joint.

direction) and a length (L) between duct supports. Due to the wide range in values of duct width (W), duct wall resonance frequencies varied substantially, causing a large variation in the equivalent static pressures (P_s) in pounds per square ft, load factors (LF) in g, and reaction loads (R/W) in pounds per foot-width. As indicated in Table 10, the estimated peak deflections (X_{pk}) of the duct wall were 2 to 3 times a conservative estimate for a nominally allowed deflection equal to $W/120$.

The conclusion to be drawn from this analysis is that duct joints may be very susceptible to acoustically induced fatigue and should be designed conservatively to minimize potential problems.

HV Mechanical Equipment Unit. A detailed analysis of the acoustically-induced vibration of the base of the HV mechanical equipment unit used a simplified lumped parameter mechanical mobility model defined in Figure H2 of Appendix H. The vibration excitation for this model was provided by the acoustic loads on the roof deck/bar joists which, in turn, will vibrate the underlying roof trusses. The model treated the W8 x 28 HV mounting beams spanning the 25 ft spacing between roof trusses C and D as a lumped mass-spring system loaded by the additional weight of the catwalk and HV system. Only the fundamental vibration mode of this lumped mass-spring could be treated by the model, but an empirical procedure was used to estimate an upper bound to vibration responses of the HV base for higher modes of the mounting structure.

The analysis model also treated the roof trusses in terms of an equivalent lumped mass-spring system using alternative values for the fundamental frequency of this system. (These frequencies are given in Chapter 7, Table 20.)

The net result of this simplified analysis is summarized in Table 11.

Table 11

Summary of Calculated Vibration Response Parameters at Base of HV Unit

f₂ Hz	LF g	Peak Displacement in.
24.6	1.26	0.020
32	1.24	0.018
55.4	1.20	0.008
72.1	1.20	0.008

The results were found to be relatively insensitive to the dynamic magnification factors assumed. Based on these results, it is recommended that the HV unit be designed for the following vibration load factors:

Vertical Direction	Up	+ 0.3 g
	Down	- 2.3 g
Horizontal Direction		± 0.63 g

Based on these results, it does not appear that vibration isolation of the HV unit will be required to avoid acoustically induced fatigue. However, vibration isolation of the HV mechanical equipment unit is recommended as good engineering practice to minimize structure-borne noise radiation and related ambient noise levels inside the AMD during routine maintenance operations when the test systems are not operating.

Vibration and Acoustic Environmental Test Specifications

For vibration- or acoustically-sensitive equipment, it may not be possible to determine with a reasonable degree of confidence that the item is capable of withstanding the noise and vibration environments specified for the AMD. In this case, it may be necessary to include a corresponding environmental test specification in the procurement package for this equipment. This section briefly outlines the principal elements that should appear in such environmental test specifications. More specific details may be found in MIL STD 810-D, *Method 515.3 Acoustic Noise and 514.3 Vibration*.

Acoustic Test Specifications

1. Acoustic test levels (as in Figure 17) with a specified frequency range (typically 50 to 5000 Hz for practical tests) and tolerance bands around the target specification. Alternatively, the standard spectrum shape contained in Method 515.3 of MIL STD 810-D could be used since it is similar to the AMD design environment.

2. Type and minimum size of test chamber. A reverberant acoustic test chamber would ordinarily be used and should have a volume of at least 10 times that of the test article.

3. Test duration. The design environmental levels in Figure 17 are not expected to have a cumulative duration over the life of the AMD of more than about 16.7 hours. A test duration of at least 10 hours would be recommended as a minimum.

4. Acoustic data acquisition and reporting. Specific guidelines should be provided as to the location, number, and characteristics of microphones used to verify the test environment. Microphone systems should conform with the performance standards of American National Standards Institute (ANSI) Standard S1.4 (ANSI 1983). According to MIL STD 810-D, three microphones are required, each to be located away from the test chamber walls and the test article. For small equipment tests in a relatively small reverberation chamber, one microphone may be an acceptable deviation from the requirements of the standard. The duration of the noise measurement signal and other "good practice" procedures for noise measurement, such as calibration, etc., should be called out. The measured test environment should be reported in terms of one-third octave band levels measured with a filter set conforming to ANSI Standard S1.11 (ANSI 1986).

5. Pass/fail test performance criteria should be clearly spelled out along with minimum procedures for the presentation of the test results. (Ordinarily, monitoring of satisfactory operation of the equipment during an environmental test is left up to the equipment manufacturer, not the test laboratory.)

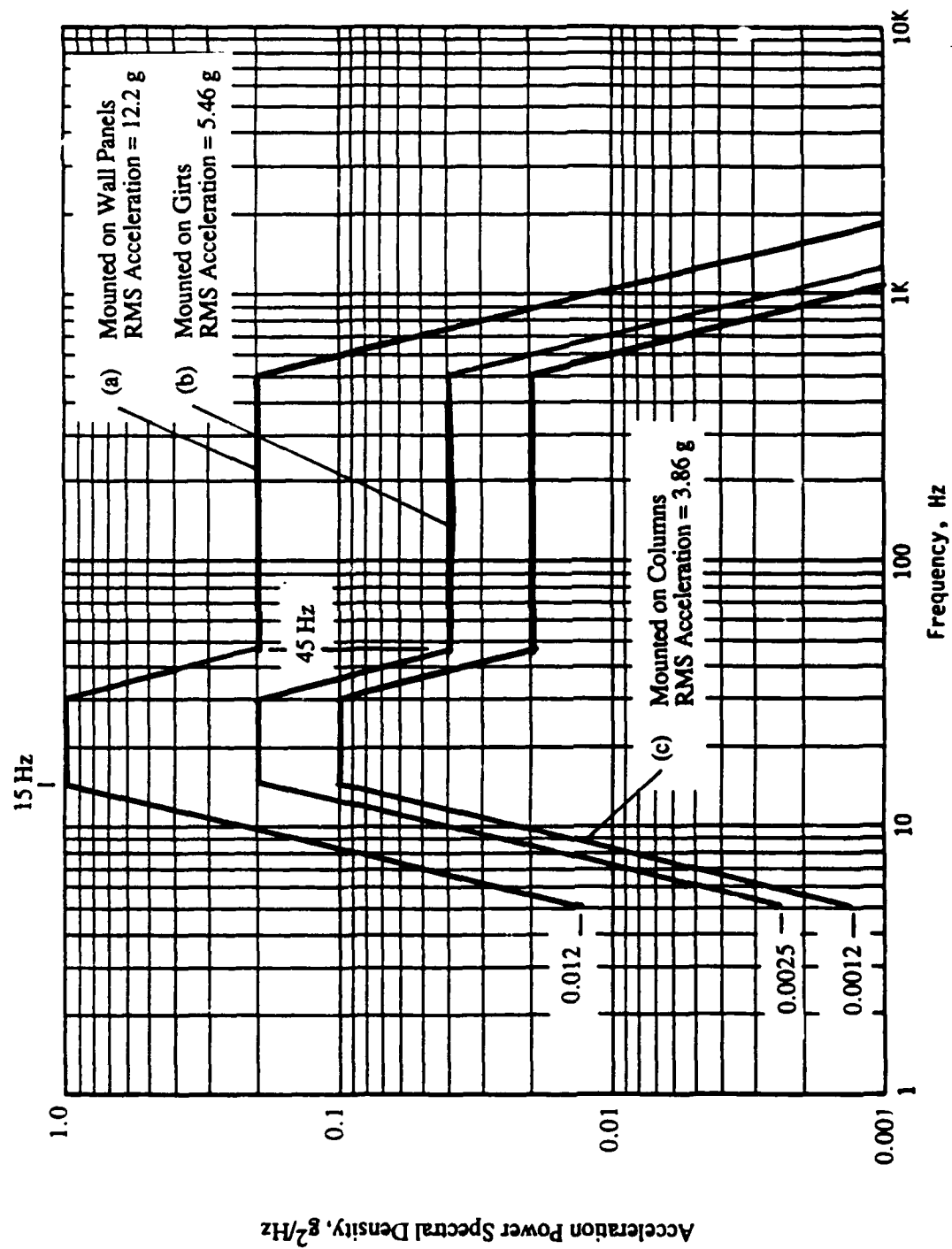
Vibration Test Specifications

1. Estimates have been prepared for the equipment mounting areas shown in Table 12. The corresponding vibration test specifications for these areas are shown in Figures 28 through 32 (see Appendix H for procedures employed). Table 12 also lists the rms acceleration for each test envelope,

Table 12
Summary of Vibration Test Specifications for AMD Equipment

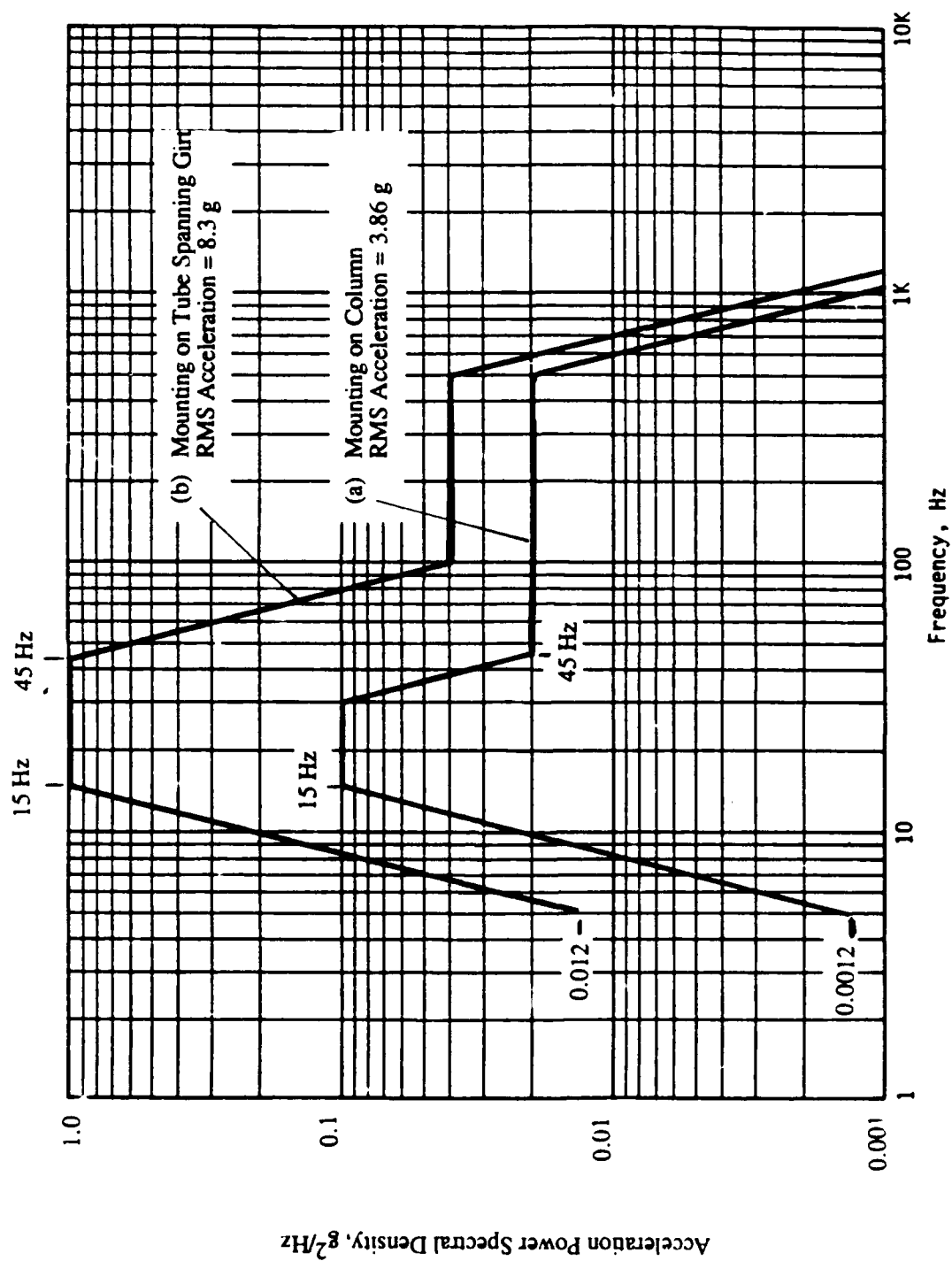
Location of Equipment	Vibration Test Specifications Figure No.	rms Acceleration Perpendicular to Surface	Co-Planar with Surface
Wall Panels	28a	12.2	x1/2
Panel Girts	28b	5.46	x1/2
Columns	28c	3.86	x1/2
IR* Sensors-			
on Columns	29a	3.86	x1/2
on Tube Spanning			
Panel Girts	29b	8.3	x1/2
Roof			
Roof Deck/			
Bar Joists	30a	6.49	x1/2
Roof Truss	30b	2.65	x1/2
Draft Curtain Panels	31a	29.9	x1/2
Draft Curtain Support			
Frame	31b	7.72	x1/2
Door Panels	32a	13.0	x1/2
Door Support Frames	32b	6.5	x1/2

* IR = infrared.



(Note: applicable for vibration normal to surface of wall. For vibration in either direction in plane of wall, multiply APSD by 0.25.)

Figure 28. Vibration design and test envelope for components mounted on (a) wall panels, (b) girts, and (c) columns.



(Note: applicable for direction normal to wall. For vibration in either direction in plane of wall, multiply APD by 0.25.)

Figure 29. Vibration design and test envelope for IR sensors mounted on (a) columns and (b) 3x3x3/16 in. tube spanning girts.

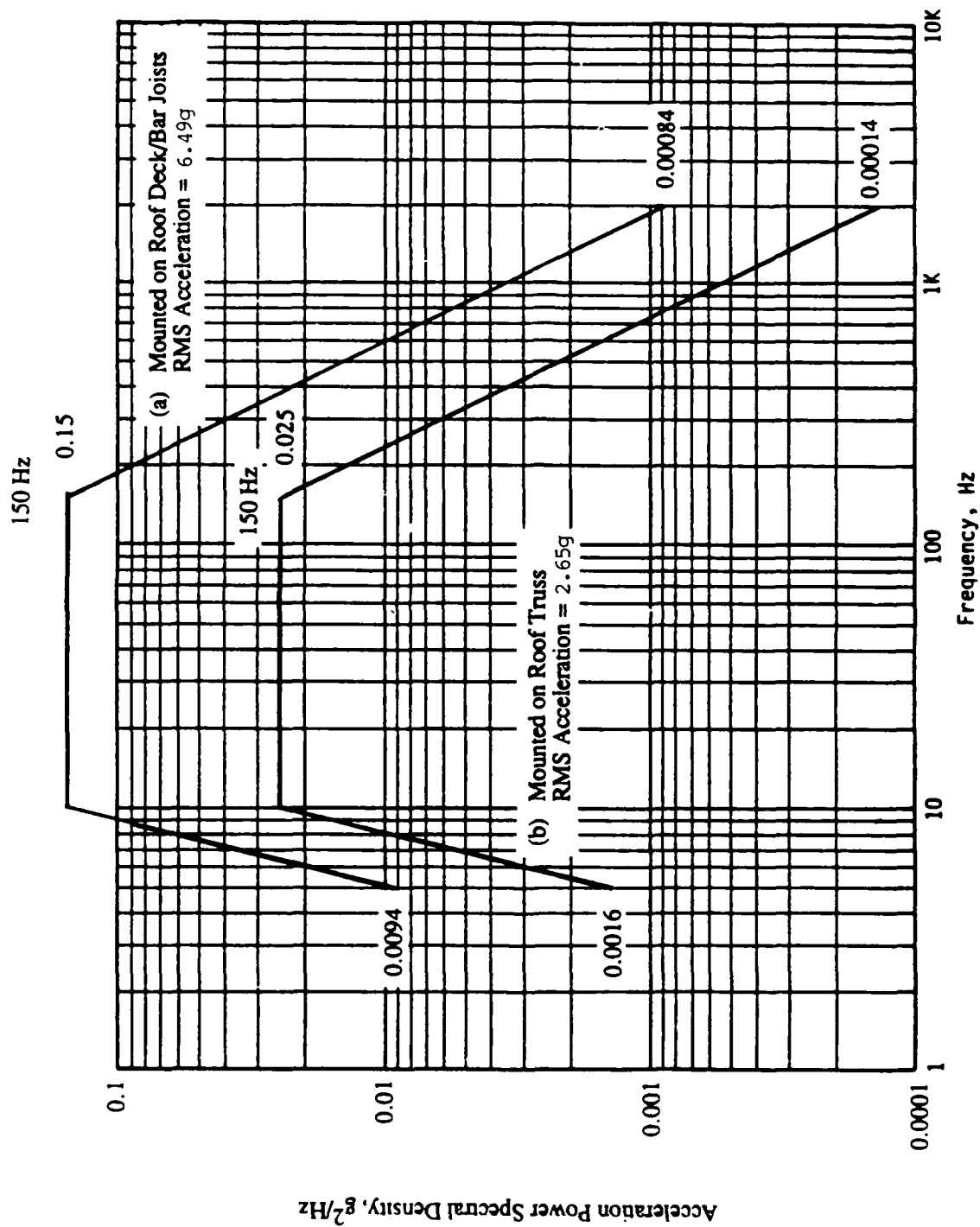
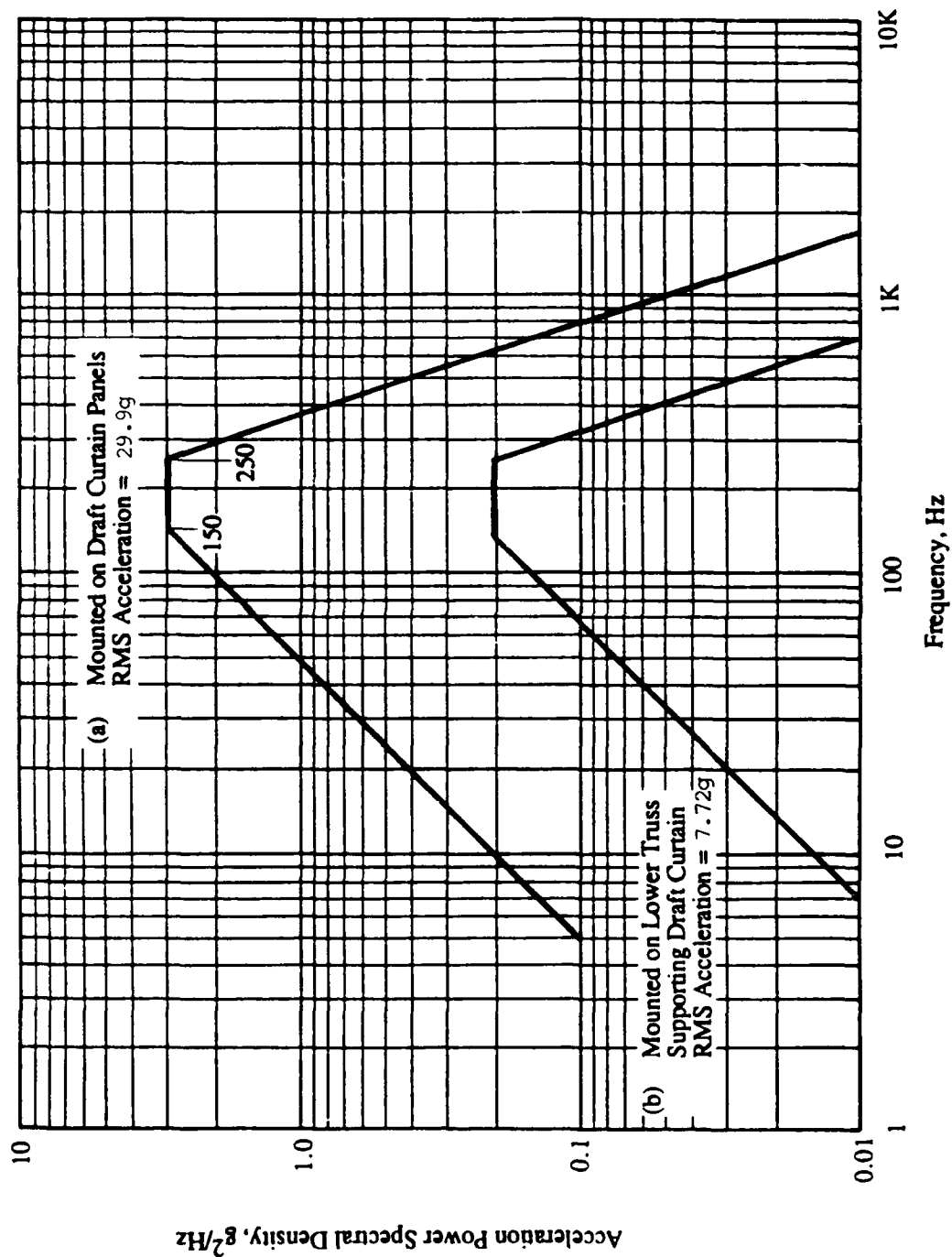
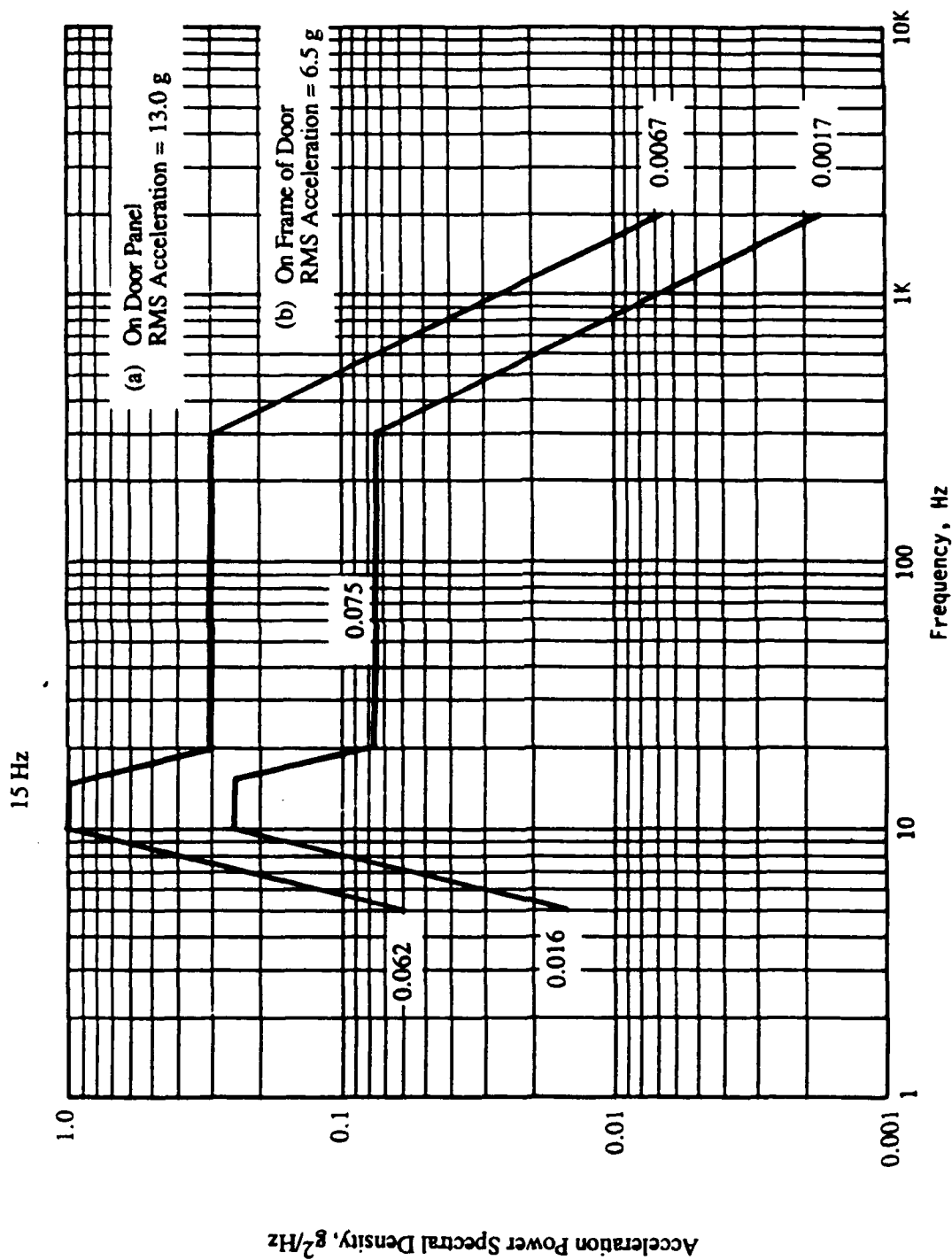


Figure 30. Vibration design and test envelope for components mounted on (a) roof deck/bar joists or (b) roof truss.



(Note: applicable for vibration normal to plane of draft curtain. For vibration in either direction in the plane of draft curtain, multiply APSD by 0.25. Each point is the estimated space average rms acceleration in one vibration mode of the wall panels for Q of 25 in the first 1.0 mode, and 15 for all higher modes.)

Figure 31. Vibration design and test envelope for components mounted on (a) draft curtain panels or (b) truss frame supporting draft curtain.



(Note: applicable for direction normal to door plane. For either direction in plane of door or door frame, multiply APSD by 0.25.)

Figure 32. Vibration design and test envelope for components mounted on (a) door panels and (b) frame of door.

which is determined by taking the square root of the integral of the acceleration power spectral density (APSD) over the frequency range (5–2000 Hz) for which the test specification is defined. As indicated in the table and in the figure legends, the figures specify the vibration test levels in the direction normal to the basic surface involved (i.e., wall, roof, draft curtain, or doors). The acceleration spectral density test levels perpendicular to this surface are reduced to one quarter so the corresponding rms acceleration levels are reduced to one half. A suitable tolerance in APSD levels for compliance with these random vibration test specifications is ± 100 percent, or ± 3 dB. For example, if the nominal test level is $0.1 \text{ g}^2/\text{Hz}$ at 100 Hz, a permissible APSD at this frequency would lie between 0.05 and $0.2 \text{ g}^2/\text{Hz}$. However, the rms acceleration of the overall test spectrum should be within ± 12 percent (± 1 dB) of the values specified in Table 12.

2. Vibration fixture. This is a vital part of the test specification since it is critical that the fixity of the test item be reasonably well simulated for the vibration test.

3. Test duration. A test duration of at least 10 hours is recommended. An accelerated (shorter) test at higher test levels should only be allowed after special care has been taken to ensure that a valid tradeoff between test level and duration has been used. This would require some knowledge of estimated fatigue characteristics of the component under test (see Appendix H).

4. Vibration test data acquisition and reporting. Again, the requirements are similar to that for acoustic tests except that spectrum analysis is ordinarily done with a narrow band spectrum analyzer. In this case, good practice calls for a data sample length, in seconds, equal to at least $50/df$, where df is the bandwidth of the spectrum analyzer. Current technology spectrum analysis instrumentation normally satisfies this requirement.

5. Pass/Fail test performance criteria are required as for the acoustic tests.

Combined Environmental, Snow, Seismic, and Wind Loads

In theory, it would be necessary to combine the environmental loads developed above with the conventional snow, seismic, and wind loads specified for the AMD structure. Realistically, the wind loads represent extreme conditions (70 mph winds) which would probably preclude operations in the AMD anyway, so it is not considered reasonable to combine wind and acoustical loads. Seismic loads are also based on rare conditions. Specifically, they are intended primarily for design of the main building structure, which is not expected to be significantly loaded by the internal acoustic environment. That leaves only the potential for combining snow loads on the roof with the environmental acoustic loads on this part of the AMD structure. The maximum snow load specified for the roof of high bay areas of the AMD is 24 psf. Note that the snow loads are downward only while the static pressure loads equivalent to the acoustic pressures are bidirectional. If these loads are to be combined, it is recommended that an rms average load be developed equal to the square root of the sum of the squares of the two components. The following section evaluates the impact of combining wind, snow, and acoustic loading for determining the effective loading on the roof deck and rigid insulation fasteners.

Effective Loading on Roof Deck and Rigid Insulation Fasteners

Worst-case live-load conditions must be considered by combining the effects of the vibro-acoustic load with the design wind load, and the vibro-acoustic load with the design snow load. The design wind load, at the location for the AMD, applied to the roof is 27.8 psf, and the design snow load is 24 psf.* Table 13 summarizes the equivalent static load acting on the roof panels subjected to the vibro-acoustic

* Telephone conversations with Mr. Kevin Howe, U.S. Army Corps of Engineers (USACE), Omaha District, Special Projects Branch, in April 1989.

Table 13
Summary of Roof Live Loads (psf)

		Wind	Snow	Acoustic	Combined*
Upward -	8K1 Bar Joist	27.8	----	63.4	65.1
	16K4 Bar Joist	27.8	----	24.9	29.0
	16K6 Bar Joist	27.8	----	27.0	30.9
Downward -	8K1 Bar Joist	----	24.0	63.4	64.7
	16K4 Bar Joist	----	24.0	24.9	28.0
	16K6 Bar Joist	----	24.0	27.0	29.9

* The combined loads are for information only, and the roof and insulation fasteners should be designed for the acoustic, snow, or wind live load independently.

loading. This table gives several load levels for a range of bar joist sizes supporting the roof panels. The current building design uses only 8K1, 16K4, and 16K6 bar joists.* The loads are combined in a way that assumes the rms wind or snow load is one fourth their peak load. The peak combined wind and acoustic load is then calculated as the square root of the sum of the squares of the rms wind load and acoustic load times the ratio of peak to rms load (F_P) for a randomly occurring load. The probability of exceedance is taken as 10 percent, which gives F_P a value of 2.15. The combined wind and acoustic load (L_W) then becomes:

$$L_W = F_P \sqrt{\left[\left(\frac{\text{Wind}}{4}\right)^2 + \left(\frac{\text{Acoustic}}{F_P}\right)^2\right]} \quad [\text{Eq 11}]$$

Table 13 summarizes the results of these calculations for each bar joist. The vehicle inside the AMD will not be operating during such high winds, except in an extreme emergency, so the most critical upward live load will be the acoustic load by itself.

The peak combined snow and acoustic load is calculated in a similar manner. The combined snow and acoustic load (L_S) becomes:

$$L_S = F_P \sqrt{\left[\left(\frac{\text{Snow}}{4}\right)^2 + \left(\frac{\text{Acoustic}}{F_P}\right)^2\right]} \quad [\text{Eq 12}]$$

* AMD Structural Drawing No. 5 and 7. The drawings referred to in this report are taken from *Maintenance Dock Hydrant Fuel System Aircraft Apron/Taxiway*, Vol. II FY 90/91 (USACE, Omaha District, April 1991), and are the same as the As Built FY 89 Maintenance Dock Drawings.

The snow load may dampen and mass load the roof such that the most critical downward live load will again be the acoustic load by itself. Table 13 summarizes the roof live load combinations.

Summary: Design for Vibro-Acoustic Environments in the AMD

In summary, design tools are provided for use by the structural, mechanical, and electrical equipment designer to prevent or minimize the potential for vibro-acoustic failure or malfunction of AMD secondary structure or internal equipment. The tools are provided in terms of (1) equivalent static pressures for the design of secondary structural skin elements or internal equipment with inherent lightweight panel elements such as HV ducts and HV equipment enclosures, (2) vibration load factors for the design of equipment mounting systems or fasteners, and (3) acoustic or vibration environmental test specifications.

5 RESPONSE OF EQUIPMENT TO ACOUSTIC AND VIBRATION ENVIRONMENTS

An equipment package and/or its components immersed in a high-intensity sound field can respond to the acoustic environment in three ways: (1) the complete package assembly can vibrate as a "rigid body" on its mounting attachments, (2) the sound pressure field can excite the housing panels, component-laden mounting panels, or other relatively thin substructure within the package into vibration, and (3) the equipment can respond to the alternating compression and decompression of the acoustic pressure. This section briefly reviews the characteristics and possible significance of each of these forms of response.

Response of Equipment Packages to Acoustic Excitation

Rigid-Body Response to Acoustic Excitation

The most fundamental structural response an equipment package can have under the action of an external acoustic field is a rigid-body motion of the entire package when it is located in free air without any baffling between front and back.

The coupling of an acoustic field and a rigid equipment package is achieved by the diffraction of sound waves about the equipment package. The resulting effect is a nonuniform distribution of sound pressures over the surface area of the equipment package, resulting in a net fluctuating pressure on the rigid equipment package. The net force (F) on an equipment package of cross-section area S , normal to the direction of a progressive sound wave with a pressure of P_o , can be stated in the form:

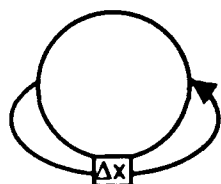
$$F = P_o S L_f \quad [\text{Eq 13}]$$

where the acoustic loading factor (L_f) depends on the relationship between the equipment package dimensions and the sound wavelength (λ). For initial estimates, the value of P_o can be computed from the one-third octave band sound pressure levels (L_b) in Table 3 at the resonance frequency of the equipment mounting. The conversion from band sound pressure levels (L_b) to the corresponding band sound pressure (P_b), in pounds per square inch, is:

$$P_b = 14.7 \times 10^{\frac{(L_b - 194)}{20}} \quad [\text{Eq 14}]$$

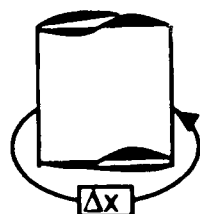
The maximum acoustic loading (L_f) occurs when the distance around the rigid equipment package (Δx) is approximately equal to a half wavelength ($\lambda/2$) of the exciting sound wave. At this condition, the sound pressures at opposite sides are 180 degrees out of phase so that one side is being pushed by the incident sound pressure while the other side is being pulled. The resulting acoustic load factor (L_f) in this case will be approximately 2 (+6 dB). Assuming typical equipment can be approximated as spherical or

cylindrical shapes, the acoustic loading factor (L_f) for rigid body excitation can be approximated by the following expressions in terms of a characteristic body dimension (Δx) in ft and frequency (f) in Hz:



$$L_f = \begin{cases} 0.0036 \Delta x \cdot f \\ 2 \\ 2230/(\Delta x \cdot f) \end{cases}, \quad \begin{matrix} \Delta x \cdot f < 500 \\ 500 \leq \Delta x \cdot f < 1000 \\ \Delta x \cdot f \geq 1000 \end{matrix} \quad [\text{Eq 15}]$$

Cylindrical Shape



$$L_f = \begin{cases} 0.006 \Delta x \cdot f \\ 2.1 \\ 60/(\Delta x \cdot f)^{1/2} \end{cases}, \quad \begin{matrix} \Delta x \cdot f < 350 \\ 350 \leq \Delta x \cdot f < 780 \\ \Delta x \cdot f \geq 780 \end{matrix} \quad [\text{Eq 16}]$$

The above expressions assume the incident sound field is a plane progressive wave such as would exist in the free (direct) field near, and aft of, the main engines.

For excitation by the reverberant field, the above expressions for L_f must be modified by the same factor used in Eq 14 to describe the net acoustic force on an un baffled draft curtain. That is,

$$L_f(\text{reverb.}) = \sqrt{2} L_f(\text{plane wave}) \sqrt{1 - C \Delta x} \quad [\text{Eq 17}]$$

where

$$C(\Delta x) = \frac{\sin(2\pi f \Delta x / c)}{2\pi f \Delta x / c}$$

Δx = the front-to-back dimension (i.e., one half the circumference) illustrated in the sketches for Eq 15 and 16, in ft

c = speed of sound (1117 ft/sec)

f = frequency, Hz

and $L_f(\text{plane wave})$ is given by Eq 15 or 16.

Eq 13 through 17 provide a simple way to estimate the net acoustic force on an otherwise rigid equipment package. If the equipment is vibration-isolated where f_o is the isolator resonance frequency, then the direct acoustically induced peak acceleration (a_p) of the package (in g's) could be estimated by:

$$a_p = F_p \sqrt{\frac{\pi P_b^2(f_o) S^2 L_f^2 Q}{2 (0.236) W^2}} \quad [\text{Eq 18}]$$

where

- $P_b(f_o)$ = rms pressure in one-third octave band at frequency f_o (from Table 3), psf
- W = the total weight of the equipment
- L_f = the acoustic loading factor estimated from Eq 15 through 17
- Q = the dynamic magnification factor for mechanical vibration
- F_p = 2.15 for 10 percent exceedance peak
- S = cross-sectional area of equipment package normal to the incident sound wave, ft^2 .

Based on a substantial amount of measured data, an approximate statistical model for the dynamic magnification factor Q can be defined by:

$$P(\geq Q) \cong 10^{-\frac{Q}{13}} \quad [\text{Eq 19}]$$

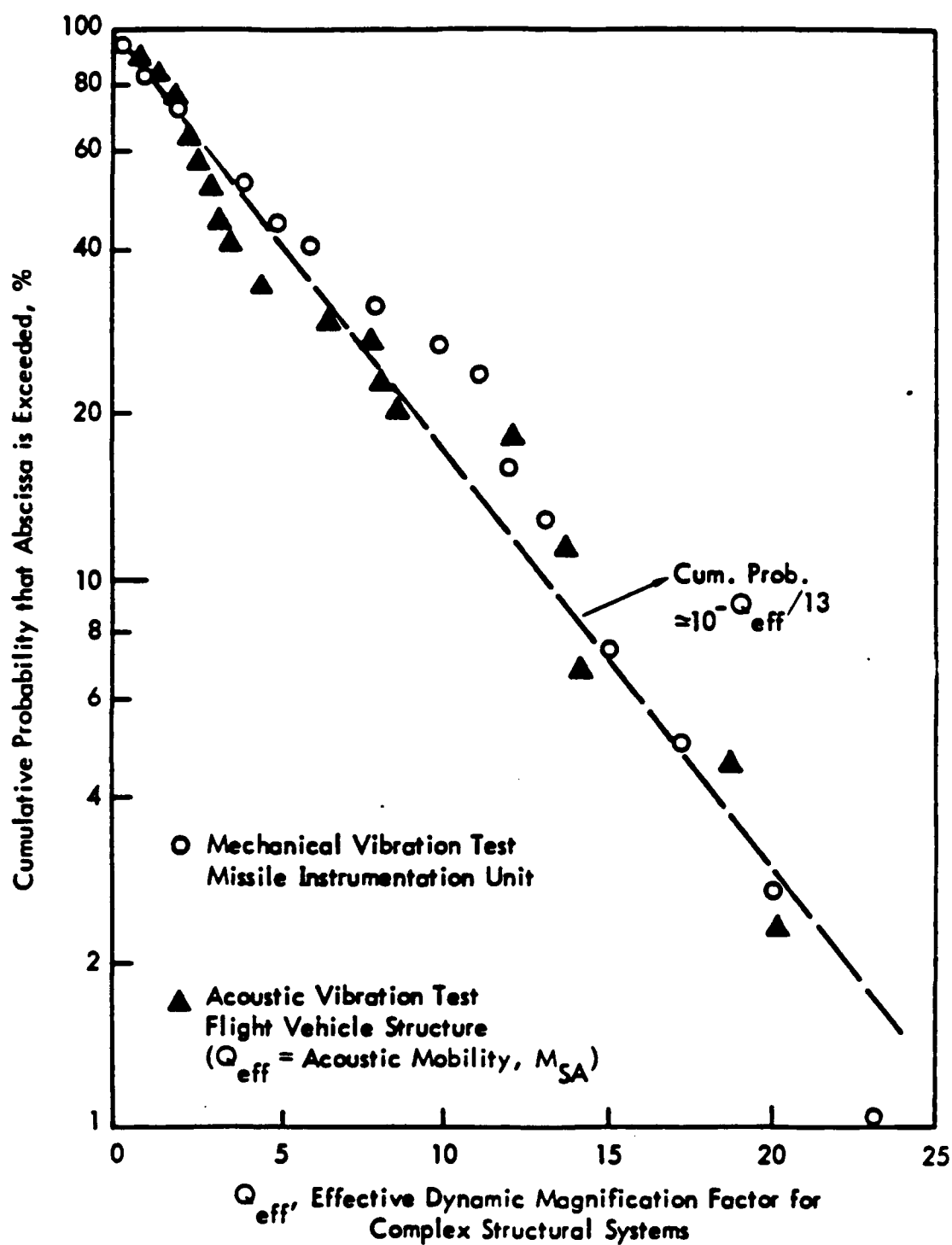
where $P(\geq Q)$ is the cumulative probability that a given value of Q will be exceeded for a large sample of equipment (Sutherland 1968). Thus, for $P(\geq Q) = 0.1$ (10 percent exceedance), $Q = 13$. Some of the data upon which this statistical model for Q is based are shown in Figure 33.

It should be pointed out that rigid-body response of high-density equipment packages (e.g., motors, hydraulic valves, etc.) due to direct acoustic excitation is unlikely to be a problem in most cases. Vibration input to such equipment is more likely to be caused by the vibration transmitted to the equipment mounting from the vibro-acoustic response of AMD walls or roof panels.

Vibro-Acoustic Response of Flexible Equipment Panels

Acoustic excitation of any wall of a lightweight equipment enclosure can result in significant vibration response to the sound. A more detailed analysis of this type of response was provided in Chapter 4 in terms of a general vibro-acoustic response factor called specific acoustic mobility (M_{SA}).

To illustrate one application of this vibro-acoustic response parameter to equipment vibration, Figure 34 shows how this specific acoustic mobility is expected to vary with frequency relative to the lowest fundamental mode of the equipment structure for a typical equipment cabinet. Figure 35 shows



(Source: Wyle Research)

Figure 33. Statistical variation in dynamic magnification factor for resonant response of complex structural systems.

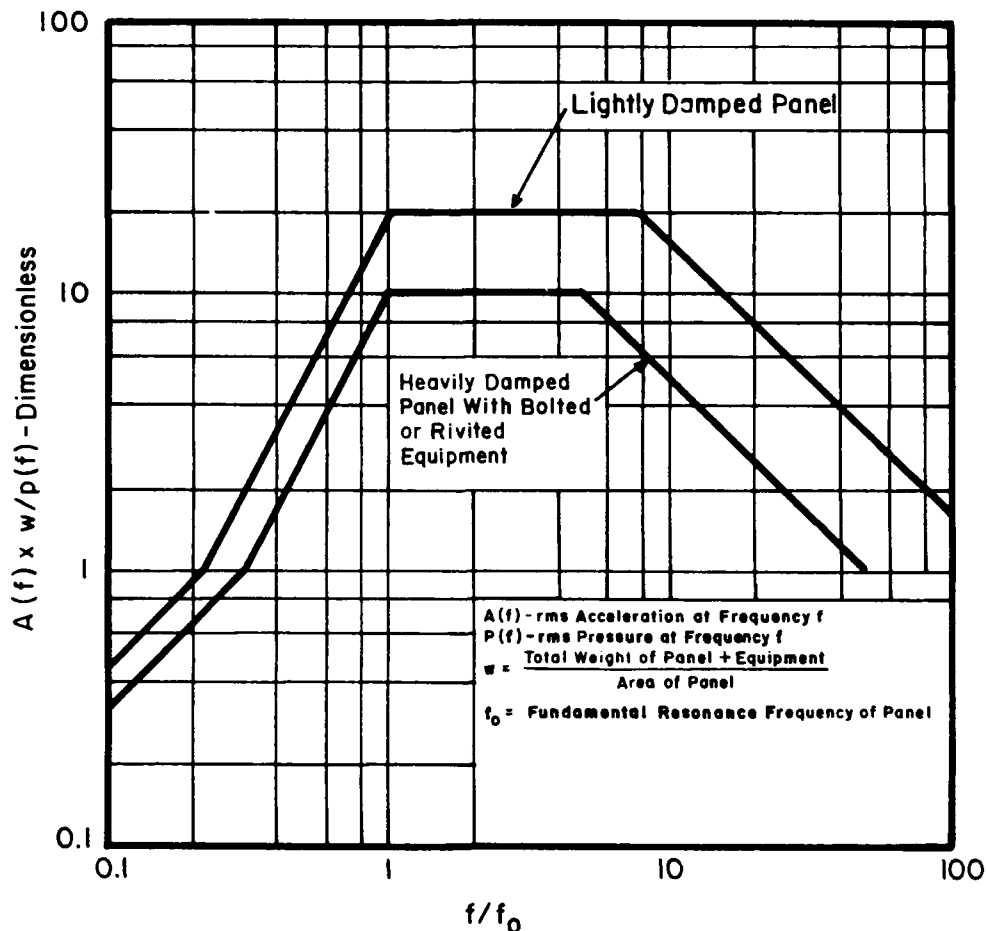


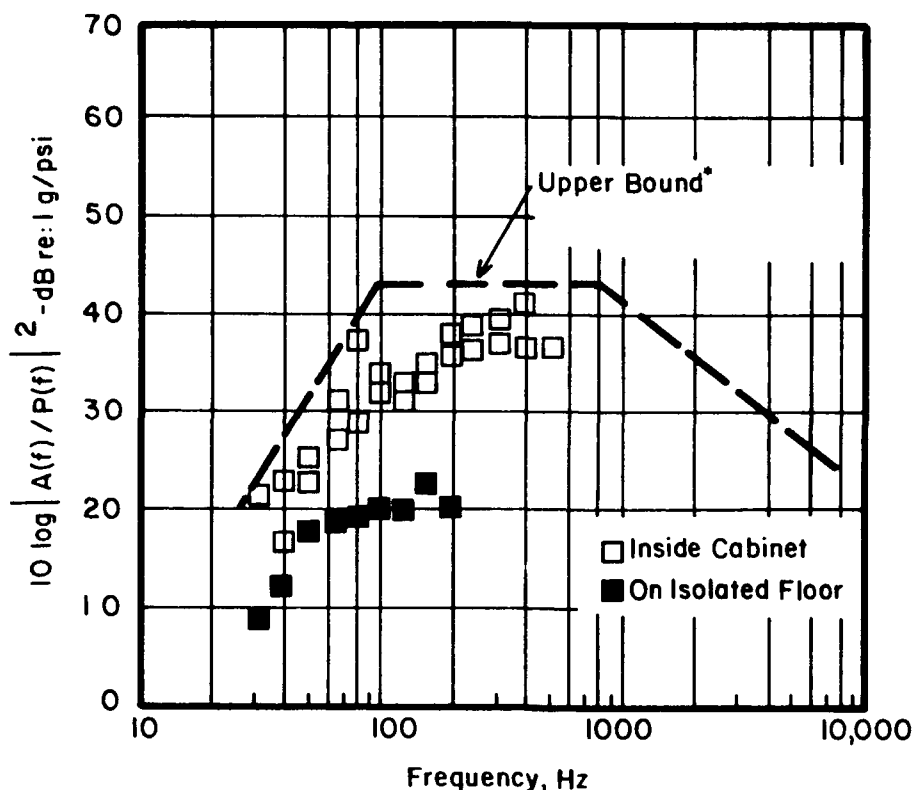
Figure 34. Design envelope for acoustic mobility of baffled flat panel with mounted equipment.

comparable experimental data on the measured vibration spectrum of a large electronic equipment cabinet exposed to acoustic excitation. The equipment was mounted on a vibration-isolated floor. Thus, the internal vibration response of the equipment cabinet was due primarily to acoustic excitation of the cabinet sidewalls and not from structure-borne vibration from the base of the cabinet.

The acceleration response spectrum, measured in one-third octave bands at various locations on the cabinet, has been normalized by the corresponding sound pressure level in each band. A predicted acceleration response is also shown for this case based on Figure 34. For this prediction, it was assumed that the total cabinet weight (1800 lb) was evenly distributed over the entire surface area of the 34 x 36 x 80 in. cabinet to give a value for the average surface density (w) of 0.132 lb/sq in. One important result from these data is that the acceleration response of the equipment cabinet is higher inside the cabinet than at points near its mounting on the vibration-isolated floor.

General Criteria for Threshold of Equipment Malfunction from Acoustic Environments

Based on available test data, tentative criteria outlined in this section may be used as a guide for estimating the noise level threshold for malfunction of sensitive equipment due to the acoustic environments inside the AMD. It must be emphasized, however, that these data are more than 20 years old (Sutherland 1968; Sugamele 1966) and do not necessarily reflect the acoustic fragility or sensitivity of current technology, which will often be lighter, smaller, and more rugged.



*Estimated from Figure 29 of Sutherland 1968.

(Source: Sutherland 1968)

Figure 35. Maximum acoustical mobility of equipment cabinets measured in one-third octave bands in direction normal to cabinet walls from acoustic test of ground computer system.

The following breakdown of equipment has been found useful for determining criteria for vibro-acoustic response of equipment:

- Component Types

- | | | |
|--------|---|---|
| Type A | — | Components whose function involves motion of flexible parts (i.e., relays, pressure switches, mechanical signal commutators) |
| Type B | — | Components that are nominally stationary but contain structural parts that are relatively flexible (i.e., vacuum tubes, accelerometers, etc.) |
| Type C | — | Components with relatively rigid parts and support structure (i.e., solid state items, capacitors, resistors, inductors, etc.). |

- Equipment Types

- | | | |
|----------|---|---|
| Type I | — | Equipment containing types A, B, and C components |
| Type II | — | Equipment packages containing only types B and C components |
| Type III | — | Equipment employing type C components only. |

The categories indicated are used here to examine available data from acoustic environment tests of equipment for tentative acoustic criteria for possible thresholds of malfunction. These data are summarized in Table 14. As expected, the data show considerable scatter.

A further analysis of these and other data from the same source, encompassing over 65 tests of electrical components (without vacuum tubes), pneumatic and hydraulic components showed that the most sensitive types of equipment had, as shown in Table 15, the following log-normal distribution in malfunction rate as a function of the average one-third octave band sound level from 250 to 2000 Hz.

It must be emphasized again that the above data reflect the sensitivity of 1960s-era equipment. A more rugged group of equipment from these same data showed approximately the same rate of increase of malfunction with level, but at an average sound level about 22 dB higher than indicated by the above trend.

Based on the above information, an estimated threshold for acoustically induced malfunction (at the 5 percent rate) of current state-of-the-art equipment probably falls at one-third octave band levels of not less than 125 dB. This potential threshold for malfunction of sensitive equipment is 5 to 15 dB below the maximum design levels for the AMD, indicating the potential for malfunction of lightweight equipment that may be sensitive to the vibro-acoustic excitation inside the AMD. However, a major qualifier

Table 14
Trend in Threshold Levels for Malfunction of
Equipment Exposed to Acoustic Environments*

Component	Typical Examples	One-Third Octave Band Levels (dB) 500-2000 Hz
Type A	Relays, Pressure Switches, Potentiometers	123 - 150
Type B	Vacuum Tubes, Inductors	115 - 145
Type C	Capacitors, Alone Mounted on Circuit Board Resistors Cables	>165** 115 - 145** 145 - 185** 145 - 155**
<u>Equipment</u>		
Type I	with Type A, B, and C Components	123 - 137
Type II	with Type B and C Components	145
Type III	with Type C Components	125

*Source: Sugamele 1966.

**Sound level, in dB re 20 microPascals, required to produce 1 millivolt electrical signal output.

Table 15

Estimated Acoustically Induced Malfunction Rate of Sensitive Equipment Manufactured in the 1960's
as a Function of Average One-Third Octave Sound Level

Malfunction Rate (%)	5	10	50	90
Avg. 1/3rd OBL* (dB) (250-2000 Hz)	115	120	130	140

*1/3rd OBL = one third octave band level

must be placed on this pessimistic view. Equipment inside the AMD that must be explosion-proof and, hence, housed in a heavy-duty case, will tend to be much less susceptible to acoustically induced malfunction than the same equipment not housed in an explosion-proof container. Thus, acoustic qualification tests may only be required for some very sensitive items for which there are inadequate measured or predicted vibro-acoustic sensitivity data to assure no significant malfunction during operations in the AMD. This case-by-case examination may be required of equipment items for which adequate acoustic or vibration fragility data or analyses are not currently available.

Response of Equipment to Random Vibration Environments

Two types of response to environmental vibration can occur for equipment: (1) rigid body vibration at frequencies well below any structural resonance frequencies for the equipment and its components and (2) the usual complex vibration response of the equipment at frequencies equal to and above the lowest fundamental resonance. This section briefly reviews the characteristics and significance of each of these forms of response.

Rigid-Body Response to Vibration

For low-frequency sinusoidal vibration tests, such as those required in MIL-STD 810D to simulate transportation environments, the peak acceleration of all parts of an equipment package, which can be considered as a rigid body, is simply equal to the peak input acceleration. There is no dynamic amplification.

For random vibration under the same conditions (i.e., rigid-body response), the only difference is that the peak acceleration response of the equipment can only be defined statistically. If the responding system is assumed to be a linear single-degree-of-freedom system and the input is Gaussian random vibration, then the cumulative probability that the *envelope* of peak acceleration response (a_p) will exceed a value, Y , times the rms acceleration response (\bar{a}) is defined by a Rayleigh distribution given by (Sutherland 1968):

$$\text{Cum}(a_p > Y \times \bar{a}) = \exp\left(-\frac{Y^2}{2}\right) \quad [\text{Eq 20}]$$

These values as a function of Y are shown in Table 16.

Analysis of structural fatigue from random vibration or of rattle space required around a package undergoing random vibration is ordinarily based on the cumulative distribution of the envelope of peak responses. Thus, adopting a 10 percent exceedance limit for design purposes, a peak rigid body

Table 16

Cumulative Probability of a_p Exceeding $Y \times \bar{a}$

Cum Prob ($a_p > Y \times \bar{a}$) (%)	20	10	5	2.5	1
$Y = a_p / \bar{a}$	1.79	2.15	2.45	2.72	3.03

acceleration of 2.15 times the rms value should be used to define a maximum predicted acceleration (or limit load) for a rigid-body response to a random vibration excitation.

Vibration Response of Nonrigid Equipment

An equipment item exposed to environmental vibration will vibrate in one or more normal modes at, and above, the lowest structural resonance frequency. Each such mode can be treated as a single-degree-of-freedom system. A detailed discussion of this complex type of response is not called for here since the analytical background in this area is well documented in any standard text on mechanical vibration. (See review in Chapter 2 of Sutherland 1968.)

The most important aspect of the flexible-body response to vibration is the dynamic magnification in response (i.e., acceleration or stress) that takes place at each structural resonance. The following design equations are applicable, in this case, to predict the peak acceleration response (a_p), in g's:

For sinusoidal excitation,

$$a_p = a_{in} \times Q$$

For random excitation,

$$a_p = 2.15 \sqrt{\frac{\pi}{2} a_f^2 \times f \times Q} \quad [\text{Eq 21}]$$

where a_{in} = The peak amplitude of a sinusoidal acceleration input

a_f^2 = The acceleration power spectral density for a random excitation, g^2/Hz

Q = Dynamic magnification factor

f = Resonance frequency, Hz.

The second equation, based on the "Miles equation" (see Appendix D), uses the peak to rms factor of 2.15 for 10 percent exceedance limits of the random vibration *envelope* as outlined above.

As discussed earlier in this chapter, empirical statistical models for the variation in the dynamic magnification factor indicates that in 10 percent of equipment measurement locations, a value of $Q = 13$ would be exceeded. Thus, for estimation of maximum (limit) accelerations exceeded 10 percent of the

time at approximately 10 percent of equipment positions, the peak (or limit) acceleration response for a *single resonant vibration mode* can be obtained from Eq 22 by using a Q value of 13.

For N modes, assuming no correlation between modal response, the total peak acceleration response (a_{pt}) for random excitation will be approximately equal to the square root of the sum of the squared peak acceleration values (a_{pi}) for each *i*th mode, or

$$a_{pt} = \sqrt{\sum_{i=1}^N (a_{pi})^2} \quad [\text{Eq 22}]$$

General Criteria for Equipment Malfunction from Vibration Environments

The variety of responses of all types of equipment to environmental vibration is too vast to define any rigid quantitative guidelines for fragility limits. However, some qualitative guidance is provided by the information in Table 17.

Table 17

**Failure Modes and Fragilities of Some Electronic
Components from Vibration and Shock Environments***

Item	Vibration Failure Modes	Shock Failure Modes	Fragility
<i>Type A Components**</i>			
Choppers	Increase in phase angle and dwell time	Contacts open; change in phase angle and dwell time	
Circuit Breakers	Premature activation	Premature close or open	Circuit breakers are generally rugged and stand up in severe dynamic environments. Shock and vibration failures often are the fault of poor bracket and hold-down design rather than of the element itself
Clutches, magnetic	Creep	Intermittent operation	
Potentiometers	Increased noise; change in torque and linearity; wiper brush bounce; open circuit	Increased noise; change in torque linearity, and resistance; open circuit	
Relays	Contact chatter	Contact opening or closing	Relays often chatter and ultimately fail when subjected to more than about 10 g vibration above about 500 Hz. Special relays can take up to 100 g. Plunger and rotary types are most rugged; clapper types are relatively fragile
Switches	Contact chatter	Contact opening	
<i>Type B Components</i>			
Diodes	Open circuit	Open circuit	
Coils	Loss of sensitivity; detuning; breaking of parts, leads, and connectors	Lead breakage; detuning; loss of sensitivity	
Transformers	Shorts; opens; modulation of output	Shorts; opens; modulation of output	Transformers are generally rugged and stand up in severe dynamic environments, shock and vibration failures of ten are the fault of poor bracket and hold-down design rather than the element itself

* Source: Sugamele 1966 and Lawrence 1961.

** Type A — Components whose function involves motion of flexible parts (i.e., relays, pressure switches, mechanical signal commutators); Type B — Components which are nominally stationary but containing structural parts which are relatively flexible (i.e., vacuum tubes, accelerometers, etc.); Type C — Components with relatively rigid parts and support structure (i.e., solid state items, capacitors, resistors, transistors, integrated circuits, etc.).

Table 17 (Cont'd)

Item	Vibration Failure Modes	Shock Failure Modes	Fragility
<i>Type C Components</i>			
Ceramic capacitors	Increase lead breakage; piezoelectric effect; body and seal breakage	Lead breakage; piezoelectric effect; body and seal breakage	Transistors, capacitors, and resistors have low mass and good rigidity. Correctly supported and anchored, they withstand as much as 15 g
Electrolytic capacitors	Increased lead breakage; seal damage; current surges	Lead breakage; seal damage; current surges	Capacitors and resistors in particular usually fail from lead flexure rather than structural breakdown
Mica capacitors	Lead breakage	Lead breakage	
Paper capacitors	Increase in opens and shorts; lead breakage	Opens; increased dielectric breakdown shorts; lead breakage	
Tantalum capacitors	Opens; shorts; current surges; lead breakage	Opens; lead breakage; shorts; current surges	
Connectors, standard	Separation plugs and receptacle; opening of contacts	Opening of contacts	Electric cables and connectors need to be well anchored especially for high-impedance coaxial leads to prevent flexure, abrasion, and noise voltage due to flexing
Resistors	Lead breakage; cracking	Cracking; opens	
Transistors	Opens; functional disintegration	Opens; seal breakage	
Insulators	Cracking; elongation	Cracking	
Joints, solder	Cracking; opens	Cracking; opens	
Motors	Brinelling of bearings; loosening of hardware		
Thermistors	Lead breakage; case cracking; open circuit	Lead breakage; case cracking; open circuit	
Resolvers	Intermittent, brush operation; brinelling of bearings; cracking of terminal board; loosening of hardware	Intermittent brush operation; cracking of terminal board; loosening of hardware	
Servos	Brinelling of bearings; loosening of hardware; cracking of terminal board	Loosening of hardware; cracking of terminal board	
Blowers	Brinelling of bearings		

6 RECOMMENDED VIBRO-ACOUSTIC ENVIRONMENT DESIGN PRACTICES FOR AMD COMPONENTS

This chapter comprises a list of design recommendations to minimize the effects of the vibro-acoustic environment within the AMD.*

1. Under no circumstances shall any physical component (hardware, conduit, electrical panels/switches, etc.) be attached directly to any wall or roof panel within the high bay area. Exterior wall panels should be specified to have *external fasteners* to allow visual inspection of their structural integrity.

2. Maximum spacing between internal support points for the front and back interior door panels is not expected to be as critical as was first thought. Decreasing support spacing increases the resonance frequency and hence decreases panel deflection. However, the acoustic pressure also increases with frequency in the range of concern to effectively nullify selection of an optimum spacing. More important will be the degree of vibration damping provided by the door construction and the avoidance of stress-concentration points. Damping of the door panels will be enhanced by ensuring that the thermal insulation inside the door cavities is packed densely enough to exert some positive force on the interior panels. Good engineering practice should be followed for fatigue-resistant steel construction, such as that reprinted in Appendix F of this report.

3. Supports for piping and conduit should be attached to wall girts away from their center points or near column supports if not directly to column supports. Components hung from roof joists should be located near the ends of the joists, if possible.

4. Some items supported by hangers or brackets require vibration isolation as specified in Chapter 8. Ductwork will receive loading from the acoustic field and its supports will be subject to fatigue, similar to the exterior wall panels. For ductwork, reliance solely on sheet metal screws to maintain joints should be avoided. For rough design guidance, ductwork joints should withstand equivalent static pressures of about 40 times the rms acoustic pressure specified in Table 3. More details are included in Chapter 7.

5. HV equipment, even though it may have significant mass, can be affected by vibro-acoustic loads due to the fact that its exterior is made up of large metal panels that may be subject to the same loading effects as the exterior building wall panels. Care should be taken by the manufacturer to provide adequate means for fastening panels and that no small components are directly attached to the centers of the panels.

6. All external fasteners must be captivated. The use of "loc-tite" two-part epoxies, jet-fuel-resistant coatings, or other means may be acceptable; however, the captivation material selected must remain flexible with time. The type of captivation used will depend on the item being secured: if an item requires periodic maintenance, a removable type of coating must be specified. The fasteners should also be accessible for visual inspection. All washers and panel clips should be of good quality to prevent sharp edges that produce stress concentrations.

7. Components located close together should be mounted with sufficient "rattle space" to avoid vibration-induced contact with each other and, hence, development of high internal shock loads on the equipment. "Adequate" rattle space can be assumed to be about three times the peak displacement (at mounting resonance frequency) of either item.

*This material includes contributions from USACE Omaha District.

8. Cantilevered or pendulum-type mounting brackets or designs should be avoided because they are very prone to vibration-induced fatigue failure. Chapter 43 of R.V. Waterhouse (Waterhouse 1955) illustrates typical problems and solutions for the mounting of inherently flexible components.

9. Any equipment located on ceiling or roof structure should be mounted in a fail-safe manner as a backup for possible vibration-induced loosening of primary mounting fasteners.

10. As an additional precaution, the installation of a foreign object damage (FOD) net over the engine areas should be considered, to prevent the ingestion of falling objects into the engines.

11. Greater care and attention to vibration-resistant design should be exercised for components at any location within the middle two-thirds of each AMD high bay area (i.e., within about ± 72 ft of the AMD centerline). This general region will experience the most severe vibro-acoustic environment.

7 BUILDING COMPONENT RESPONSE AND STRENGTHENING RECOMMENDATIONS

Additional recommendations to ensure the integrity of structural and nonstructural building components in the AMD are categorized as either primarily strengthening or primarily isolating measures. This chapter presents both individual component response as well as strengthening and stiffening recommendations. (Component isolation recommendations are presented in Chapter 8. Recommendations that were presented in earlier chapters are not repeated.)

Hangar Door Panels

Both the larger west side hangar doors on the front of the building, and the smaller east side hangar doors on the back of the building will be open during the maximum operating periods of the vehicle. The west doors will not be exposed to the large acoustic loads because they roll into door pockets, out of the range of acoustic pressures. The east doors however, when open, roll into the building and rest against the back wall of the facility.* This places them in a position that will receive high acoustic loading.

Individual door panels will be vibrating out of phase with each other, so that the overall loading on the door frame and supports will not be highly significant. The door frame and supports will not need to be checked for acoustic loading. The wind load (30 psf) when the doors are closed, then, will control the design of the door frame and supports.

Individual door panels have been analyzed for the worst-case acoustic environment as summarized in Table 3. This analysis assumed the individual panels, which are welded to the door frame, are simply supported at all four edges. This analysis uses the procedure presented in Appendix H and the spreadsheet extract reproduced in Table H8. The procedure combines the vibration response of the panel vibrating in several modes at the same time. Only those modes with frequencies less than 1000 Hz are included in this analysis because vibration at higher frequencies will have a negligible effect on the overall panel response. The panels were analyzed for several support spacing (panel size) and panel thickness (t) conditions, because these design details were left for the contractors to decide. A conservative value of 30 was used for the dynamic magnification factor (Q). This worst-case condition assumes the thermal insulation in the door cavity is poorly packed. However, good construction practice requires the cavity to be densely packed. Table 18 presents the results of this analysis, defining the peak deflection (X_{pk}), load factor (LF), peak stress (σ_{pk}), equivalent static pressure (P_s), long side maximum and average reaction, short side maximum and average reaction, and recommended interior door panel gage (Ga) for each panel size analyzed. The recommended gage is based on displacement considerations and a deflection comparison with $L/120$. The calculated peak deflection (X_{pk}) normally exceeds $L/120$, but because of the low stresses this is acceptable as long as no equipment is attached to these panels. Other panel sizes may be evaluated by interpolating between the panel sizes listed in the table. The interpolation should be based on the smaller dimension of the panel. The panel connections to the door frame should be checked for their capacity to carry the maximum reactions listed in this table. If bolts rather than welds were used for these connections, the load per fastener equals the maximum reaction per foot times the spacing between fasteners (in feet). The door frame should be checked against the average reaction acting on the frame along both sides of the panel. When two adjacent panels are supported by the same frame member, the load acting on the frame is twice the average reaction load listed in the table.

*Architectural Drawings No. 4, 5, 6, 9, and 26 for the AMD.

Table 18
Hangar Door Panel Loading (Q=30)*

Panel Size	Rec** Ga.	t (in.)	f ₁ *** (Hz)	L/120 (in.)	X _{pk} (in.)	LF† (g)	σ _{pk} (psi)	P _s (psf)	Short Side Reactions		Long Side Reactions	
									Max	Avg	Max	Avg
108 x 72 in.	9	0.1495	3.96	0.60	0.46	1.9	2500	3.2	6.0	1.3	14.0	2.5
	10	0.1345	3.56	0.60	0.56	1.8	2800	2.9	5.3	1.2	11.7	2.1
	11 [§]	0.1196	3.17	0.60	0.71	1.9	3100	2.5	4.8	1.2	10.3	1.9
72 x 48 in.	11	0.1196	7.13	0.40	0.32	3.0	3200	5.8	5.2	1.3	13.2	0.8
	12	0.1046	6.23	0.40	0.41	3.1	3600	5.1	4.7	1.2	11.7	2.4
	13	0.0897	5.35	0.40	0.56	3.3	4200	4.4	4.1	1.1	9.7	2.0
	14 [§]	0.0747	4.45	0.40	0.81	3.3	5000	3.6	3.6	0.9	7.9	1.6
72 x 36 in.	11	0.1196	10.97	0.30	0.23	3.7	3900	10.7	4.9	1.3	14.0	3.1
	12	0.1046	9.59	0.30	0.27	4.0	4100	8.1	4.5	1.2	12.9	2.7
	13	0.0897	8.23	0.30	0.37	3.6	4800	6.9	3.7	1.1	9.6	2.1
	14 [§]	0.0747	6.85	0.30	0.53	4.4	5700	5.7	3.6	0.9	9.6	2.0
	15	0.0673	6.17	0.30	0.63	4.5	6300	5.2	3.3	0.9	8.1	1.7
	16	0.0598	5.48	0.30	0.82	4.4	7000	4.6	2.9	0.8	6.9	1.5
72 x 24 in.	11	0.1196	21.93	0.20	0.13	6.4	4400	11.4	7.6	1.9	24.1	6.1
	12	0.1046	19.18	0.20	0.16	6.5	4900	9.6	6.9	1.7	21.3	5.2
	13	0.0897	16.45	0.20	0.22	6.7	5400	7.9	6.1	1.5	18.7	4.4
	14 [§]	0.0747	13.70	0.20	0.31	6.7	6300	6.4	5.2	1.3	15.2	3.6
	15	0.0673	12.34	0.20	0.38	6.0	6900	5.7	4.5	1.2	12.7	3.1
	16	0.0598	10.97	0.20	0.47	6.6	7800	5.0	4.3	1.1	11.5	2.8
48 x 16 in.	14	0.0747	30.82	0.13	0.15	8.4	7700	34.0	3.2	1.1	10.4	2.8
	15	0.0673	27.77	0.13	0.18	8.8	8400	30.1	3.1	1.1	9.9	2.5
	16 [§]	0.0598	24.68	0.13	0.23	8.7	9300	26.2	2.8	0.9	8.8	2.3
	17	0.0538	22.20	0.13	0.28	9.1	10100	23.2	2.7	0.9	8.3	2.0
	18	0.0478	19.72	0.13	0.35	9.3	11200	20.3	2.4	0.8	7.5	1.9

* A peak-to-random ratio (F_p) of 2.15 was used in calculating the peak response, and a fatigue reduction factor (F_f) of 0.75 were used for calculating the peak deflection (X_{pk}), peak stress (σ_{pk}), equivalent static pressure (P_s) and reactions.

** The section symbol (§) designates the gage (Ga) recommended by USACERL for the particular panel size. The other gage panels illustrate the impact of thickness on panel response.

*** Frequency (f₁) of the panel fundamental mode of vibration.

† The load factor (LF) contains only the peak-to-rms ratio (F_p) of 2.15.

Personnel Door

The personnel doors measure 3 ft x 7 ft. They are 1.75 in. thick hollow metal with pressed metal frames.* The doors, door frames, and fasteners should be designed for an equivalent static pressure equal to that applied to the wall panels. This is a conservative design requirement, and the value, ± 32 ps, is taken from Table 5. If the doors are rated for sound control, this requirement should not be a problem.

* Architectural Drawing No. 10 for the AMD.

Roof Deck

The dynamic behavior of the roof truss/deck system is needed for two reasons: (1) to evaluate the overall dynamic response of the roof system and (2) to evaluate the support conditions for the HV unit.

Dynamic Response of the Roof System

A finite element modal analysis of roof truss 4 was conducted to evaluate the overall dynamic response of the roof system. Truss 4 spans from the front to the back of the building.* The vertical flexural modes of vibration of this truss should be representative of the overall building roof. The surface density of roofing is (steel deck) 2.2 psf plus (insulation plus EPDM membrane) 3.5 psf plus (fire protection piping) 0.2 psf, which equals 5.9 psf. The distributed weight of the bar joists, spaced at 5.7 ft, vary from 0.9 psf to 1.7 psf (as explained in Table H4). These together result in a dead load of 6.8 to 7.6 psf. Additional dead load comes from the hot-water-heating pipe, steam and condensate pipes, ductwork, exhaust fans, light fixtures, roof trusses spanning north to south, truss bracing, horizontal wind braces, and vertical support and monorail system. Trusses 4, 5, and 6 should have reasonably similar natural frequencies, even though trusses 5 and 6 have heavier members and, thus, a stiffer system (because they support the additional mass of the draft curtain). With these additional loads, the minimum total dead load is estimated to be 8 psf; the maximum dead load is 15 psf.

Table 19 shows the natural frequencies of truss 4 for the truss by itself and with roof dead loads of 8 and 15 psf. For both the 8 and 15 psf dead loads, the weight of the truss itself is also included. Figure 36 illustrates the displaced shape of roof truss 4 vibrating in the modes indicated.

Table H4 indicates that individual roof panels have a fundamental natural frequency of about 10 Hz. Mode 8 in Figure 36 and Table 19 has the shape that would correspond to a mode that could be excited through the vibration of an individual roof panel. Table 19 indicates that this mode has natural frequencies of 69.2 Hz for the truss alone, 36.5 Hz for the 8 psf dead load, and 28.3 Hz for the 15 psf dead load. This indicates that the roof truss system is too stiff to be excited in a resonant condition through vibration of the roof panels. Building motions will only be generated through exciting elements with large lightweight surface areas, such as the roof panels or wall panels. Thus these results demonstrate that the overall building will not be excited, but rather individual roof panels and the supporting truss members will be excited to a limited degree, as indicated in Tables 6 and H6.

HV Unit Dynamic Behavior

An additional finite element modal analysis was conducted on roof truss C to determine the modal response of the roof truss system supporting the HV unit. Truss C spans north to south on the west side of the HV unit.** Truss D also spans north to south, but on the east side of the HV unit. Two W8 x 28 beams span between trusses C and D to support both the HV unit and its maintenance catwalk. This finite element model includes only the two bays near the HV units, as only this portion of the truss is needed to define the dynamic response of the roof truss in the region of the HV unit. Figure 37 shows the finite element model for this analysis. The natural frequencies of this roof truss system in the vertical flexural modes are shown in Table 20. These results were used in the analysis of the HV unit support system in Appendix H.

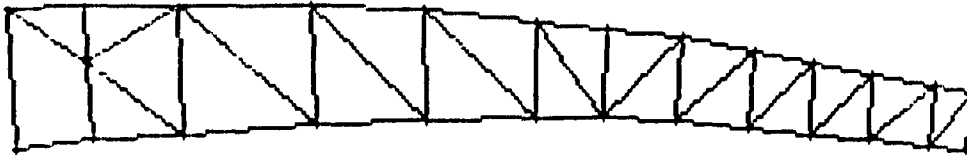
* Structural Drawing No. 14 for the AMD.

** Structural Drawing No. 12 for the AMD.

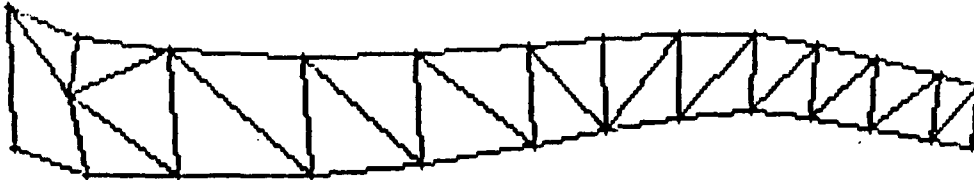
Table 19

Truss 4 Natural Frequencies (Hz)

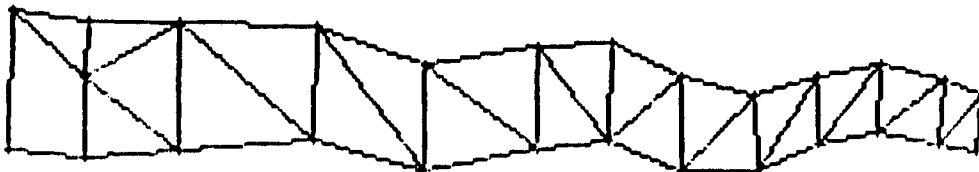
Mode No.	Truss Alone	8 psf	15 psf
1	8.1	3.9	3.1
2	19.1	10.0	8.0
3	21.1	15.0	11.8
4	30.4	18.9	16.1
5	42.1	20.9	19.1
6	55.9	27.6	22.1
7	61.3	31.2	24.6
8	69.2	36.5	28.3
9	78.0	39.0	30.1
10	87.9	46.6	36.7
11	92.9	55.6	43.3
12	95.9	59.6	57.5



Mode 1, 8.09998D+00 Hz.

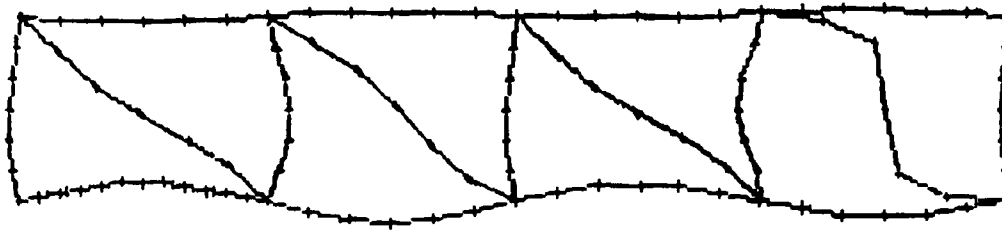


Mode 3, 2.10681D+01 Hz.



Mode 8, 6.92070D+01 Hz.

Figure 36. Modal vibration of roof truss 4.



Mode 6, 3.17453D+01 Hz.

Figure 37. Modal vibration of roof truss C.

Table 20

Natural Frequencies for Roof Truss C

Mode Number	Frequency
1	24.6 Hz
2	32.0 Hz
3	55.4 Hz
4	72.1 Hz

Ductwork

Both the north and south sides of the maintenance bays have an HV unit and ductwork system.* The air intakes are on the north and south walls in the roof truss area, and HV unit rests on two W8 x 28 support beams about 6 ft in from the wall. Each HV unit has a 36 x 36 in. duct that runs horizontally from this unit in the roof truss area and branches out to smaller ducts. Each of the smaller ducts lead to the building walls, where they drop down to air diffusers about 9 ft above the facility floor. Other ducts pull air from an exhaust grille near the floor, up the walls to the roof, and out an exhaust fan on the roof. Still other ducts ventilate trenches and fuel vaults in the floor with a duct that runs up the wall to an exhaust fan on the roof. The horizontal ducts in the roof truss area are supported by the bar joists, and the vertical ducts are supported by the wall girts. The horizontal ducts will be supported off of every other bar joist at approximately 133 in. on center, and the vertical ducts will be supported by every wall girt at a maximum of 90 in. on center.

*Mechanical Drawings No. 1,3,10,11,25,26,27,28, and 29 for the AMD.

Duct Gage Thickness

Standard duct gage thickness according to National Fire Protection Association (NFPA) Standard 91 (NFPA 1990, par. 3-3.3) is as follows:

- Up to 8 in. — 24 gage
- 8 to 18 in. — 22 gage
- 18 to 30 in. — 20 gage
- Over 30 in. — 18 gage.

Table 10 presents the vibro-acoustic response of several sizes of 18 gage ductwork, including the effects of diffracted sound propagation to the back side of the duct and sound transmission through the duct (see Appendix H). Those ducts shown in Table 10 are only for 18 gage duct skin.

An additional analysis for the response of duct panels was conducted for vertical ducts up against an exterior wall and horizontal ducts in the roof truss area where diffraction will have an impact, because the sound wave is free to load the duct from the back side. (See Appendix H for a discussion on diffracted sound wave propagation.) Therefore, the vertical duct analysis does not include the effect of diffraction, but diffraction is included for the horizontal ducts. This analysis combines the response of the panel vibrating in several modes at the same time. Only those modes with frequencies less than 1000 Hz are included in this analysis because vibration at higher frequencies will have a negligible effect on the overall panel response. This analysis also considers the response of ducts with wall thicknesses (t) other than 18 gage. Table 21 (a and b) summarizes this analysis in a similar manner as Tables 10 and H12. The table provides the peak displacement (X_{pk}), load factors (LF), peak stress (σ_{pk}), equivalent static pressure (P_s) and support reactions, for ductwork at various gages. The load acting on the duct-support frame is twice the average reaction load where two adjacent ducts are supported by the same frame member.

Duct Connection Details

Even with the recommended increase in duct thickness, the peak deflections still exceed the normally accepted deflection of the panel width divided by 120. The high deflections indicate the potential for fatigue damage at points of stress concentrations. For the ducts, the most vulnerable location will be at the joints. With this concern in mind, the following joint detail is recommended to both strengthen the joints and provide some damping.

Ductwork joints should be reinforced and attached with the following procedure:

1. A five in. wide reinforcing collar S-strap of at least twice the thickness of the duct base metal, preattached by spot welding, should be put in place around the entire outside perimeter of one edge of the two ducts being joined together.
2. In the field, apply three beads of silicon caulking around the perimeter on the surface of this strap.
3. The adjoining ductwork, with its ends slightly flared out, are then brought over the reinforced end of the other duct, creating a lap joint of five in.
4. Wired sheet metal screws should be used to fasten together all three thicknesses of sheet metal in the lap joint area.

Figure 38 illustrates this duct connection recommendation.

Table 21

Ductwork Loading and Motion

a. Horizontal (Q=30)*

Panel Size										Support Reactions (lb/ft) [‡]	
Duct Size (in.)	W (in.)	L** (in.)	Ga***	(f ₁) [†] (Hz)	W/120 (in.)	X _{pk} [‡] (in.)	LF ^{1†} (g)	σ _{pk} [‡] (psi)	Ps [‡] (psf)	Along the Long Duct Edge	Along the Duct Support
22 x 20	20	133	16	14.5	0.167	0.40	17.4	13300	23.0	68	156
			18 [§]	11.6		0.52	23.7	15900	17.0	80	171
			20	8.7		0.77	24.0	27500	17.0	74	128
22 x 20 24 x 22	22	133	16	12.1	0.183	0.42	18.8	12900	18.0	85	169
			18 [§]	9.6		0.49	16.9	11200	10.0	74	121
			20	7.2		0.66	23.4	13000	6.7	84	127
24 x 22 24 x 24	24	133	14	12.1	0.200	0.34	13.9	10000	19.0	86	155
			16 [§]	10.2		0.43	16.0	10400	12.0	89	144
			18	8.1		0.50	17.8	10100	8.0	98	128
30 x 30	30	133	14	8.3	0.250	0.33	10.3	6200	8.0	99	116
			16 [§]	6.6		0.42	11.6	7100	6.0	100	104
			18	5.3		0.53	13.5	8200	4.0	103	97
36 x 36	36	133	14	5.9	0.300	0.35	7.9	5100	4.0	110	89
			16 [§]	4.7		0.45	9.5	6300	3.0	114	85
			18	3.8		0.57	9.5	7700	3.0	101	68
14 x 8	8	90	16	89.5	0.067	0.07	14.7	10500	111.9	13.	90.
			18 [§]	71.6		0.11	19.0	13700	93.5	14.	93.
			20	53.7		0.19	29.0	19900	76.5	17.	106.
16 x 10	10	90	16	57.6	0.083	0.11	16.9	11500	79.1	20.	103.
			18 [§]	46.0		0.17	21.7	15300	66.7	22.	106.
			20	34.6		0.29	27.3	20200	49.9	25.	100.
16 x 12	12	90	16	40.2	0.100	0.15	16.8	12100	57.6	28.	102.
			18 [§]	32.1		0.23	20.4	15000	45.8	29.	99.
			20	24.1		0.40	26.8	19700	33.8	33.	98.

* The dynamic magnification factor (Q) for all ductwork panel response calculations is conservatively taken as 30.

** All horizontal duct calculations are for 133 in. spacing between supports and, thus, a 133 in. length for the panel response calculations.

*** The gage recommended by USACERL for the particular duct panel width is designated by a section symbol (§). The other gage ducts illustrate the impact of panel thickness on the response. The last duct gage for each panel width is the gage required by NFPA 91, paragraph 3-3.3; thus, USACERL is recommending an increase in panel thickness for each duct.

† Frequency (f₁) of the panel fundamental mode of vibration.

‡ A peak-to-rms ratio (F_p) of 2.15 and a fatigue reduction factor (F_f) of 0.75 were used for calculating the peak displacement (X_{pk}), peak stress (σ_{pk}), equivalent static pressure (P_s), and support reactions.

1† A peak-to-rms ratio (F_p) of 2.15 was used in calculating the load factor (LF).

Table 21 (Cont'd)

b. Vertical (Q=30)*

Duct Size (in.)	Panel Size W L** (in.) (in.)		Ga***	(f ₁)† (Hz)	W/120	X _{pk} ‡ (in.)	LF ^{1†} (g)	σ_{pk} ‡ (psi)	Ps‡ (psf)	Reactions (lb/ft)‡	
										Along the Long Duct edge	Along the Duct Support
14 x 8	14	90	16	29.7	0.117	0.20	16.2	11900	41.6	34.	99.
			18§	29.7		0.25	20.3	14900	33.3	34.	103.
			20	17.8		0.51	23.0	18000	22.7	39.	84.
16 x 12	16	90	16	29.7	0.133	0.20	16.2	11800	31.7	38.	99.
			18§	18.3		0.38	17.5	13500	23.2	43.	85.
			20	13.8		0.65	19.2	16500	16.0	42.	70.
24 x 24	24	90	11	13.2	0.200	0.32	8.7	7500	14.3	56.	66.
			14§	10.6		0.49	9.4	9000	10.9	56.	57.
			16	8.5		0.68	10.3	10300	8.0	54.	50.
42 x 16	42	90	11	7.8	0.350	0.29	3.7	3700	6.7	77.	45.
			14§	4.9		0.73	4.1	5800	4.2	61.	31.
			16	3.9		1.15	4.7	7200	3.3	63.	29.
50 x 16	50	90	11	6.0	0.417	0.38	2.7	3400	4.9	67.	33.
			14§	3.7		0.97	4.4	5100	2.9	106.	34.
			16	3.0		1.60	4.5	10700	3.8	72.	27.
36 x 12	36	90	11	10.2	0.300	0.25	4.4	4200	9.7	72.	54.
			14§	6.4		0.57	4.4	6000	5.6	46.	33.
			16	5.1		0.89	4.9	7600	4.4	40.	30.
54 x 12	54	90	11	5.3	0.450	0.42	2.7	3300	4.4	77.	33.
			14§	3.3		1.09	3.7	5300	2.7	75.	28.
			16	2.7		1.70	4.2	6600	2.2	75.	26.
72 x 12	72	90	11	3.6	0.600	0.63	2.4	2900	2.9	91.	29.
			14§	2.2		1.68	2.4	9600	3.8	12.	18.
			16	1.8		2.50	3.7	5700	1.4	70.	22.

* The dynamic magnification factor (Q) for all ductwork panel response calculations is conservatively taken as 30.

** All horizontal duct calculations are for 133 in. spacing between supports and, thus, a 133 in. length for the panel response calculations.

*** The gage recommended by USACERL for the particular duct panel width is designated by a section symbol (§). The other gage ducts illustrate the impact of panel thickness on the response. The last duct gage for each panel width is the gage required by NFPA 91, paragraph 3-3.3; thus, USACERL is recommending an increase in panel thickness for each duct.

† Frequency (f₁) of the panel fundamental mode of vibration.‡ A peak-to-rms ratio (F_p) of 2.15 and a fatigue reduction factor (F_f) of 0.75 were used for calculating the peak displacement (X_{pk}), peak stress (σ_{pk}), equivalent static pressure (P_s), and support reactions.^{1†} A peak-to-rms ratio (F_p) of 2.15 was used in calculating the load factor (LF).

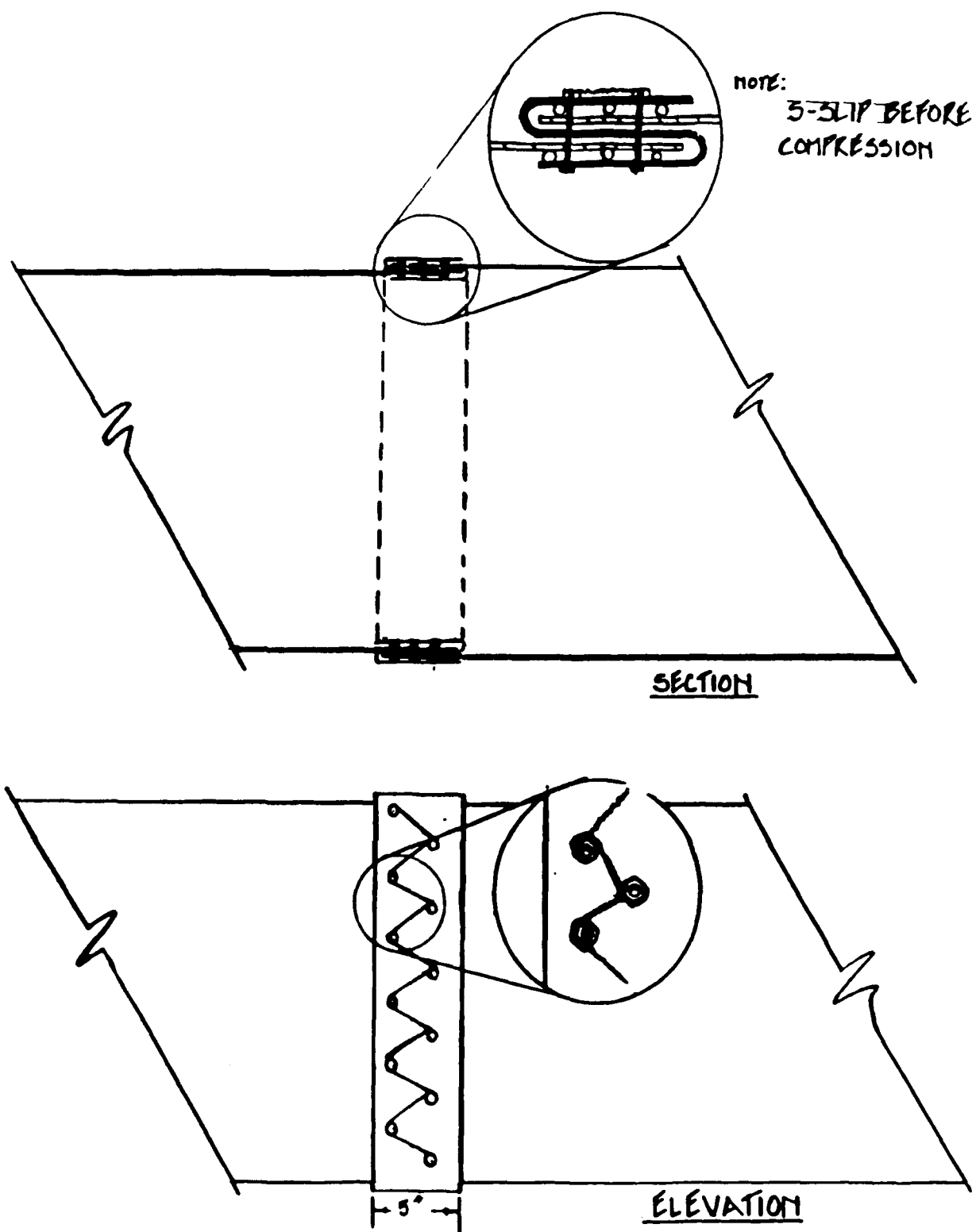


Figure 38. Duct connection detail.

Longitudinal Duct Seams. The longitudinal seams should be constructed of heavy-duty interlocking lap seams.

Flexible Joint Between HV Unit and Ductwork. The joint between HV unit and ductwork should include a flexible connection to isolate the movement of the two systems from each other.

Control Panels

The maintenance bays of the AMDs will contain control panels for the consolidated aircraft support structure (CASS), gaseous nitrogen remote panels, receptacle cabinets, contactor control cabinets, and power panels. These panels may be contained in explosion-proof boxes, which would protect sensitive items from the acoustic environment. They should be mounted on a frame supported directly by the floor, independent of the walls, and at a height from which a person can operate them.

USACERL recommends that these panels, their supports, and connections be conservatively designed for an equivalent static load of 32 psf applied over the face of the panels. This is the same load as given for the wall panels in Table 5.

Fire Protection Oscillating Monitor Nozzles

The fire protection monitor nozzles will be mounted to the floor in the maintenance bays. The nozzles themselves should be designed for vibrations due to changes in water pressure, which would be much greater than those produced from the acoustic environment. Therefore, the only concern for this system is for the mounting supports. If the nozzles are mounted to the floor there will be no problem. However, if they are attached to a wall, the supports must be designed for the appropriate load factor at the location they are to be attached. For example, if attached to a column on the back wall, the acoustic horizontal reaction loads (R_h), using Table 6, become:

$$R_h = \text{Nozzle Weight} \times 5.4 \left(\frac{5035 \text{ lb}}{5035 \text{ lb} + \text{Nozzle Weight}} \right) \quad [\text{Eq 23}]$$

Also the supports must be designed for potential eccentric loading that would cause bending moment or torsional loads in the support members.

Louvers and Dampers

A number of louvers and dampers are located above both the front and back AMD doors.* The back door has the larger louver and dampers. Each 36 ft wide wall section supports three 72 by 48 in. louvers and one 60 by 48 in. louver. The total louver and damper system weight including the framing is taken as 10.5 psf,** which results in louver and panel weights of 252 lb and 210 lb, for the 72 by 48 in. and 60 by 48 in. panels respectively. The louver and damper supports will frame into the wall girts. The units and their supporting elements must be designed for the wall girt load factor (8 g from Table 6) times the component weight. A mass loading reduction for the weight of the louvers, minus the weight of the removed wall panel, will reduce the load factor. The 30 by 72 in. wall panel weighs 52 lb, so the

* Mechanical Drawings No. 1 and 3 (including Note 1) for the AMD.

** From telephone conversation with Mr. Kevin Howe, USACE Omaha District Special Projects Branch, in April 1989.

removed wall panel weights are 83 lb and 69 lb for the 72 by 48 in. and 60 by 48 in. panels, respectively. The effective weight of the wall panel above the back door increase from the 715 lb (in Table 6) to 1662 lb. This increase is due to the presence of two W10 x 33 wall girts for a single wall section, and the increased span of the wall girts from 25 to 36 ft. Thus the total horizontal reaction (R_H) normal to the wall, for a single 72 by 48 in. louver and damper, becomes:

$$R_H = 252 \text{ lb} \times 8 \times \left[\frac{1662 \text{ lb}}{1662 \text{ lb} + 3 \times (252 \text{ lb} - 83 \text{ lb}) + 210 \text{ lb} - 69 \text{ lb}} \right] = 1450 \text{ lb} \quad [\text{Eq 24}]$$

Wall Mounted Emergency Shower and Eye Wash

Emergency showers and eye wash are attached to the side walls of each bay in the AMD.* The supports and pipe connections should be designed for the load factor (Table 6) and peak deflection (Table 5) of the structural member to which it is attached. For example, if the shower is attached to the girts on the side wall, the support members and connections should be designed for the following horizontal load (R_H):

$$R_H = 8 \times \text{Shower Weight}$$

The supports and connections must also be designed for any eccentric loading. The showers should be attached to structural members. However, if they are attached to the wall panels themselves, not only must they be designed for the increased load factor, but must also be flexible enough to accommodate the peak wall panel deflection given in Table 5.

Carbon Monoxide/Carbon Dioxide Detector Sensors

Carbon monoxide/carbon dioxide detector (CO/CO_2) sensors are located below the roof deck approximately 6 ft inside the corners of the draft curtain. The supports for these units must withstand the 5.2 g load factor listed in Table 6 for the roof panel/bar joist. Conduit and other connection details should follow the recommendations presented in Chapter 8. These sensors should also pass the acoustic and vibration test environment described in Chapter 4. The appropriate acceleration power spectral density (APSD) plot for these sensors is for the roof deck/bar joist location, and is defined in Figure 30a.

Thermostats and Other Small Controls

Thermostats and other small controls are attached to the wall panels in many locations of the AMD. These items and their connections must withstand the loads of their self weight multiplied by the appropriate load factor taken from Table 6. Items attached directly to the wall panels should be designed for a load normal to the panel surface of their self weight multiplied by a load factor of 17. The load for motion in the plane of the panel will be one half the load normal to the panel. In addition, these controls must withstand the environment described in Chapter 4 for the acoustic and vibration test specifications. Conduits and connections should follow the recommendations provided below in the section "Conduit, Connectors, Fittings, and Mineral-Insulated Cable."

* Mechanical Drawings No. 5, 6 and 7 for the AMD.

Miscellaneous Detectors, Switches and Other Electrical Equipment

Ultraviolet/infrared (UV/IR) detectors, heat detectors, pull stations, abort stations, receptacles, disconnect switches, and miscellaneous switches for lights, alarm bells, horns, and lights are located at the AMD trusses, roof deck, and walls. These items should be designed for the appropriate load factor given in Table 6a, and the environment described in Chapter 4 for acoustic and vibration test specifications.

Conduit, Connectors, Fittings, and Mineral-Insulated Cable

On the exterior of the building, mechanical equipment is attached by conduit to control panels on the building interior. The panels on the interior are framed into the wall girts at 7 ft, 6 in. and the floor at the base. The conduit of concern will pass through the wall panel at 7 ft above the floor. The spacing between the wall panel and connection to the unit outside the building will be at least 2 ft. The wall panels and girt will vibrate horizontally normal to the direction of the pipe, thus driving the control panel and in return forcing compression and tension loading on the conduit.

A flexible connection between the conduit and mechanical equipment outside the buildings should be provided, which will allow at least 1/4 in. of axial motion. A sleeve for the wall panel should be provided where conduit passes through to mechanical equipment that will allow the conduit to move freely at least 1/4 in. axially. The conduit should first run parallel to the wall with a 90-degree bend before penetrating the wall. Figure 39 illustrates this recommendation.

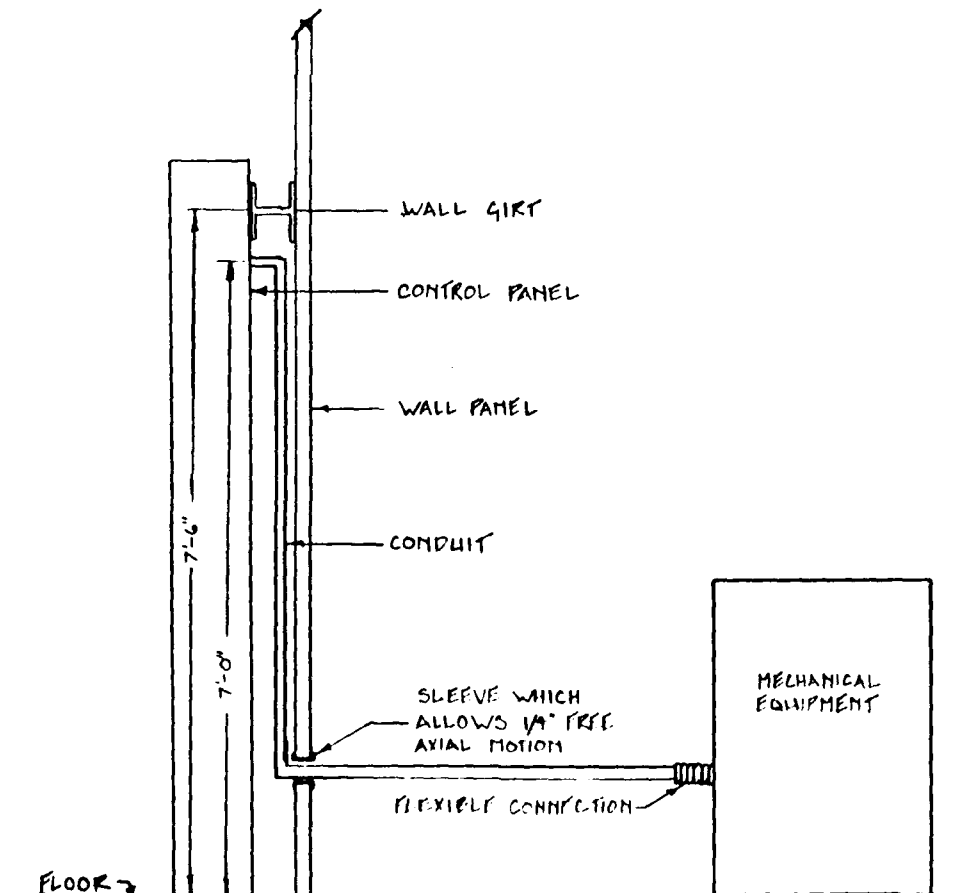


Figure 39. Detail for attaching conduit to mechanical equipment.

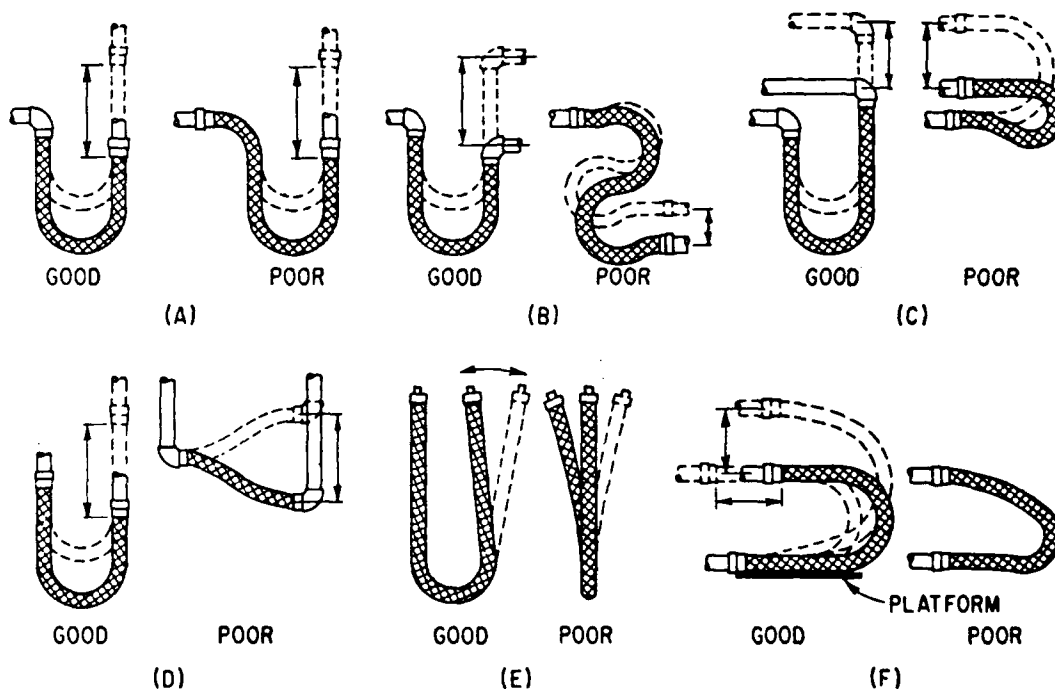
Numerous other conduit, connectors, fittings, and cables are located in the roof truss area and attached to the walls. This conduit should generally run along primary structural members and rest on these members to provide continuous support, such as against the fillet of a column or girt. Conduit should never run right up to a light fixture, sensor controls, or other electrical units, but should instead provide a short piece of flexible cable to allow some differential movement. Conduit attachments should never be near bends in the conduit (elbows or tees). The following spacing between bends and attachments are recommended:

- 3/4 in. - 1 1/4 in. conduit — 2 ft spacing
- 1 1/2 in. - 2 1/2 in. conduit — 4 ft spacing

Conduit and cable attachments should be capable of carrying the weight of the cable multiplied by the appropriate load factor of that member to which it is attached. Figure 40 provides examples of good and poor flexible cable connection detailing.

Combustible Vapor Sensors

Combustible vapor sensors will be located in the front trench drain, rear trench drain, wing tip trench drain, and fuel vault. Acoustical vibration in the trench drains will be negligible, but these sensors should still be qualified according to the acoustic test specification described in Chapter 4.



(Source: Geiger 1953.)

Figure 40. Examples of good and poor flexible cable connection details.

*Mechanical Drawings No. 1 and 3 (Note 2) for the Aircraft Maintenance Dock.

8 BUILDING COMPONENT VIBRATION ISOLATION RECOMMENDATIONS

Several components should be isolated, both to protect the equipment being isolated and reduce the loads on the building. This chapter provides isolation recommendations and supporting analysis for these components. Table 22 provides a overall summary of the vibration isolation recommendations. The dynamic response of every item shown in Table 22 incorporates the effects of mass loading, as discussed in Chapter 4. Mass loading reduces the supporting member motion by the ratio of $W_m/(W_e + W_m)$. W_e is the total weight of equipment being attached to the supporting member including the item being isolated, and W_m is the effective weight of the mounting structure, as defined in Table 6 and Appendix H. The following sections give the necessary background to support these recommendations. A detailed description for the roof truss brace supports is given in the first section, and this same procedure is repeated for other isolated items. The sections for these other items will include only summarizing information and details that are unique to them. The isolated items in Table 22 are grouped into those items supported by the roof bar joists, those items supported by the wall girts, and, lastly, those items supported by the roof truss.

The vibration isolation recommendations are based on the understanding that the support points will vibrate at well understood minimum frequencies based on the lowest natural frequency of the supporting system that is being driven by acoustical loading. For example, most of the items being isolated are supported at either the roof bar joists or wall girts, where these members will have a lowest mode of vibration at those frequencies defined by the roof panel/bar joist or wall panel/wall girt dynamic response (as defined in Appendix H). One of the most important factors for properly designing the vibration isolation system is the minimum weight of the system. This is especially true when isolators with very low damping are used, such as those recommended here. For most of the items, a good idea of the minimum load was clear. However close attention should be paid to the minimum weight values given in Table 22a through 22c, or the minimum length of ducts and pipes defined in the following sections. One unfamiliar with vibration isolation may think that, if unsure, provide an extra support. However, it may be better to overload an isolator rather than underload it. If underloaded, the isolation benefits will diminish, and in the extreme condition, the intended isolation system could actually resonate at the natural frequency of the support motion.

Appendix J provides the background and discussion for the qualification of alternate isolators that exceed the maximum stiffness requirements presented in this chapter and summarized in Table 22.

Horizontal Wind Braces

The bottom cord of the roof truss system is braced with several crossing double angle members.* The angle members are intended to transfer the windload through the truss system at the bottom cord level. These are very slender members and are only designed for tensile load, so buckling is not a concern. These members are not stiff enough vertically to carry their own load without excessive deflections. As an example of such excessive deflections, the braces crossing between roof truss 4 and 5, and C and D, would deflect 7 in. under their own dead weight, assuming pinned connections to the bottom cords of these trusses. Because of these excessive deflections, a pipe support will be installed from the crossing point of the braces up to the roof bar joist above.

*Structural Drawings No. 8 (including Note 1), 9, and 44 for the AMD.

Table 22

Support Condition Specifications

a. Items Supported at Roof Bar Joists

Item	W _{min} (lb)	W _{max} (lb)	T	f _d (Hz)	f _n (Hz)	k _{max} (lb/in.)	ξ	a _{eff} (g)	V _{max} (lb)	H _{max} (lb)	Iso Type
Horizontal Wind Truss Support (single isolator)											
One bar joist (BJ)	482	1009	0.2	9.85	4.02	797	0.005	0.269	1280	271	E
Three BJ	482	1009	0.2	9.85	4.02	797	0.005	0.395	1408	399	E
Three BJ	482	1009	0.23	9.85	4.26	894	0.005	0.396	1409	400	E
Horizontal Ductwork (two isolators per support location)											
One BJ	35	140	0.27	9.85	4.54	74	0.005	0.459	204	64	F
Two BJ	35	140	0.27	9.85	4.54	74	0.005	0.488	208	68	F
Three BJ	35	140	0.27	9.85	4.54	74	0.005	0.498	210	70	F
One BJ	110	320	0.244	9.85	4.36	214	0.005	0.365	437	117	G
Two BJ	110	320	0.244	9.85	4.36	214	0.005	0.429	457	137	G
Three BJ	110	320	0.244	9.85	4.36	214	0.005	0.455	466	146	G
Exhaust Horizontal Ductwork (two isolators per (BJ at each support location)											
for EF-3,4,9,10,13,14,19,20,31,32	25	50	0.27	9.85	4.54	53	0.005	0.475	74	24	J
for EF-5,6,7,8,9,15,16,17,18,19	45	130	0.39	9.85	5.22	125	0.005	0.450	189	59	I
EF-6 Only	105	130	0.39	9.85	5.22	292	0.005	0.376	179	49	H
Exhaust Fans and Attached Ductwork (4 iso./unit)											
EF-1,2,11,12	200	238	0.23	9.85	4.26	371	0.005	0.293	307	70	P
EF-3,4,13,14	26	30	0.244	9.85	4.36	51	0.005	0.472	44	14	J
EF-5,6,7,8,15, & 16,17,18	90	100	0.2	9.85	4.02	149	0.005	0.385	138	38	I
EF-9,19,31,32	25	30	0.27	9.85	4.54	53	0.005	0.475	44	14	J
EF-10,20	7	26	0.68	9.85	6.27	28	0.005	0.541	40	14	S
Steam and Condensate Pipe Vertical Supports											
One B.J.	360	850	0.244	9.85	4.36	701	0.005	0.307	1111	261	L
Two B.J.	360	850	0.244	9.85	4.36	701	0.005	0.386	1178	328	L
Horizontal Steam Supply and Condensate Return Pipe attached to BJ w/ two isolators per support											
4" Steam Sup.	45	70	0.2	9.85	4.02	74	0.005	0.441	101	31	J
4" Steam Sup.	45	70	0.39	9.85	5.22	125	0.005	0.450	102	32	M
2" Cond. Ret.	20	35	0.39	9.85	5.22	56	0.005	0.490	52	17	J
Hot Water and Heating Pipes (two isolators per support)											
6"	125	195	0.27	9.85	4.54	264	0.005	0.420	277	82	O
4"	65	105	0.27	9.85	4.54	137	0.005	0.463	154	49	M
Overhead Sprinkler Fire Protection Pipes (two isolators per support)											
Full 6 in.	150	200	0.27	9.85	4.54	316	0.005	0.404	281	81	N
Empty 6 in.	80	125	0.23	9.85	4.26	148	0.005	0.450	181	56	M
(90 lb) 4 in.	40	60	0.2	9.85	4.02	66	0.005	0.481	89	29	J
(60 lb) 3 in.	30	45	0.2	9.85	4.02	50	0.005	0.490	67	22	J
(45 lb) 2.5 in.	25	35	0.27	9.85	4.54	53	0.005	0.497	52	17	J

Table 22 (cont'd)

b. Items Supported by Wall Girts

Item	W_{min}	W_{max}	T	f_d	f_n	k_{max}	ξ	a_{eff}	V_{max}	H_{max}	Iso
	(lb)	(lb)		(Hz)	(Hz)	(lb/in.)		(g)	(lb)	(lb)	Type
Vertical Ductwork (two isolators per support location)											
	110	160	0.225	11	4.71	250	0.005	0.607	257	97	H
	40	135	0.34	11	5.54	126	0.005	0.766	238	103	I
	17	50	0.31	11	5.35	50	0.005	0.827	91	41	J
Vertical Steam Supply and Condensate Return Pipe attached to BJ w/two isolators per support											
4" Steam Sup.	22	40	0.225	11	4.71	50	0.005	0.801	72	32	J
Hot Water and Heating Pipes (two isolators per support)											
Vertical 6"	95	125	0.2	11	4.49	196	0.005	0.631	204	79	M
4"	50	70	0.31	11	5.35	146	0.005	0.736	122	52	I
(Full Weight) Overhead Sprinkler Fire Protection Pipe											
(170 lb) 6"	40	110	0.4	11	5.88	141	0.005	0.775	195	85	M
Oscillating Monitor Fire Protection Pipes											
Horiz. 6"	170	240	0.2	11	4.49	351	0.005	0.813	435	195	N
Horiz. 4"	65	125	0.2	11	4.49	134	0.005	0.846	231	106	I
Horiz. 4"	85	125	0.4	11	5.88	301	0.005	0.869	234	109	N
Vertical 6"	70	130	0.2	11	4.49	144	0.005	0.726	224	94	M
(Actual Weight) FP Lighting (single isolator)											
Strobe (10 lb)	8	12	0.31	11	5.35	23	0.005	0.869	22	10	C
Beacon (9 lb)	7	11	0.36	11	5.66	23	0.005	0.878	21	10	C
Beacon (9 lb)	7	11	0.4	11	5.88	25	0.005	0.886	21	10	C
(Actual Weight) Emergency Exit Lights attached to the rear hangar door frame and side wall girts											
Type 650 (15 lb)	12	18	0.2	11	4.49	25	0.005	0.848	33	15	C

c. Items Supported by Roof Truss

HV Unit	654	700	0.2055	5	2.06	285	0.005	0.627	1139	439	R
	654	700	0.341	5	2.52	425	0.005	1.183	1528	828	V
Steam and Condensate Pipe Guided Supports											
4 Iso.	130	200	0.24	9.85	4.33	250	0.005	0.281	256	56	K
Horizontal Steam Supply attached to catwalk (two isolators per support)											
Empty 4"	55	75	0.26	5	2.27	29	0.005	0.447	109	34	T
Hot Water and Heating Pipes attached to catwalk (two isolators per support)											
Full 4"	70	90	0.65	5	3.14	71	0.005	1.098	189	99	U
Oscillating Monitor Fire Protection Pipes - Supported by Wind Truss 2											
Horiz. 6"	115	200	0.272	11	5.09	304	0.005	0.566	313	113	N
(Actual Weight) HID Lighting (single isolator)											
(55 lb)	50	60	0.26	9.85	4.47	102	0.005	0.300	78	18	A
(43 lb)	40	50	0.344	9.85	4.98	102	0.005	0.306	65	15	A

The dynamic behavior of the cross bracing and support structure was evaluated to determine the effective load transferred to the bar joists at these locations. The roof brace is much more flexible than the roof panel/bar joist system. For example, the fundamental natural frequency of the braces crossing between roof trusses 4 and 5 and C and D without a support is 1.21 Hz. The calculations for this value are provided in Appendix I. The fundamental natural frequency of the roof panel/bar joist system directly above the cross braces specified above is 9.85 Hz. This panel is supported by a 16K6 bar joist, and the roof panel calculations are shown in Table H5. The supporting pipe or threaded rod joining the braces and bar joist will transfer the load axially. Thus it will be very stiff and will act as a rigid link. The braces will, therefore, only be excited at their higher modes by roof motion, so the increase in load on the roof due to the dynamic response of the braces will be very small. The roof panel/bar joist and roof truss brace system will respond dynamically, as the roof panel/bar joist system by itself, but with the additional lumped mass of the braces at the center. The roof panel/bar joist and roof truss brace system will respond dynamically, as the roof panel/bar joist system by itself, but with the additional mass of the braces at the center. The braces will not be excited by the roof motion because they comprise a much softer system.

The mass loading from the weight of the brace will reduce the load on the roof to a degree, but the load will still be quite large because of the acceleration levels at the roof. Therefore, USACERL recommends that a vibration isolator be installed at the top of each pipe support for these braces to reduce the additional load on the bar joist. The minimum weight (W_{min}) and maximum weight (W_{max}) supported by an isolator was calculated for each brace location, as shown in Table I1 of Appendix I. The minimum weight is taken as half the total weight of the braces, and the maximum weight is five-eighths of the total brace weight. The overall minimum and maximum weights for all the braces are 482 lb and 1009 lb, respectively. These values were used in selecting the appropriate isolator and calculating the final effective dynamic load applied to the bar joist through the isolator.

Table 22a shows these calculations in a spreadsheet program that models this support as a single degree of freedom system. Isolating the braces from the roof motion will reduce the dynamic load on the roof bar joist and also reduces the vibration of the brace itself. The transmissibility (T) is ratio of dynamic output to dynamic input. A reasonable goal is to isolate the brace with a spring soft enough to limit the transmissibility through itself to 0.2. The transmissibility at a particular driving frequency (f_d) of a single-degree-of-freedom oscillator with a natural frequency, f_n , is given by the following equation (Thomson 1981, p 65):

$$T = \frac{\sqrt{1 + (2\xi \frac{f_d}{f_n})^2}}{\sqrt{[1 - (\frac{f_d}{f_n})^2]^2 + [2\xi \frac{f_d}{f_n}]^2}} \quad [\text{Eq 25}]$$

In this case spring steel isolators are used, and the damping coefficient (ξ) for these is 0.005, which causes the damping coefficient to be negligible and the transmissibility equation simplifies to:

$$T = \frac{1}{(\frac{f_d}{f_n})^2 - 1} \quad [\text{Eq 26}]$$

The transmissibility is set to 0.2 and the equation is solved for the resulting maximum natural frequency (f_n) of the isolated system. This value, along with the minimum load of the single-degree-of-freedom

system, is used to calculate the maximum acceptable stiffness of the isolator that will keep the transmissibility to 0.2. The maximum stiffness (k_{max}) is given by the following equation:

$$k_{max} = 2\pi f_n \left(\frac{W_{min}}{g} \right) \quad [Eq 27]$$

From this maximum stiffness, an isolator is selected. The stiffness of this isolator is used to calculate the actual natural frequency of the isolated system. The isolated acceleration of the bracing system is then calculated from the motion at the roof. The peak acceleration (a_{pk}) for each mode of vibration of the roof panel system with the 16K6 bar joist was calculated in Table H5. Those values are listed in Table I2. For each mode, the transmissibility was calculated using Eq 25. For all but the first mode, the transmissibility is less than 0.1. However, it is known that some motion will pass through even at the higher modes and the minimum transmissibility is set to 0.1 for each mode. The effective acceleration (a_{eff}) is then calculated as the square root of the sum of the squares of the peak acceleration for each mode multiplied by its transmissibility factor, all multiplied by a reduction for the mass loading reduction of the roof panel motion. For the roof panel system with a 16K6 bar joist, the effective weight (W_m) is taken from Table 6 and has a value of 520 lb. Table I2 illustrates the calculation of the transmissibility, and the peak acceleration times the transmissibility squared. The following equation illustrates the calculation of the effective acceleration:

$$a_{eff} = \sqrt{\sum [(a_{(f_i)}) \times (T_{(f_i)})]^2} \times \left(\frac{W_m}{W_e + W_m} \right) \quad [Eq 28]$$

The effective acceleration (plus one for gravity) times the maximum weight of the item being isolated gives the maximum vertical isolated load (V_{max}). The maximum horizontal isolated load (H_{max}) is the effective acceleration times the maximum weight of the item being isolated. These results are shown in Table 22. The same procedure is repeated assuming the load for the support is spread out over three bar joists. The purpose of this is to reduce the load on each bar joist by transferring part of it to the two adjacent bar joists. This will increase the total isolated vertical load because the mass loading benefits are reduced. The last column in Table 22 lists the isolator (Iso) type selected. The isolator selected for the roof truss brace support is Type E, and it must have a maximum capacity greater than the maximum vertical load. Table 23 identifies specific isolators or equals that meet the requirement of each isolator type. For the roof truss brace support, the capacity is 1500 lb, which exceeds even the applied load of 1408 lb (if the load were supported by three bar joists). Figure 41 illustrates the roof truss cross brace support condition.

Heating and Ventilating Units

An HV unit is located in the roof truss area near both side walls in each maintenance dock high bay area. The HV unit will be serviced with a catwalk accessible by a ladder from the building exterior. The initial design of the HV unit required that this unit be supported by the roof bar joists above. This would result in fairly high vibration load factors and high support reactions and loads to the roof truss members supporting these units. Also, bar joists are not designed for concentrated loads, and a load of this magnitude could be better accommodated by framing into the main building structure.

Table 23
Isolator Characteristics

Type	K_{max} (lb/in.)	V_{max} (lb)	H_{max} (lb)	Peabody Model Number	Amber/Booth Model Number
A	102	78	18	SH-1-120	BSA-1-100
C	23	33	15	SH-1-35	
	25	33	15		BSA-1-25
E	797	1408	399	SH-2-1500	
	894	1409	400		BSA-2-1600
F	74	210	70	FDS-3-215	SW-3A-200
G	214	466	146	FDS-3-640	SW-3A-600
H K & O	250	277	97	FDS-2-500B	SW-2-500
					SW-2-400
					SW-1-250
I	125	238	106	FDS-2-250B	SW-2-250
J	50	101	41	FDS-2-100B	SW-3A-150
L	701	1178	328	SH-2-1400	BSA-2-1300
M	137	224	94	FDS-1-750B	
	125	224	94		SW-2-250
N	304	435	195	FDS-1-450B	
	301	435	195		SW-1-300
P	371	307	70	FDS-1-370B	SW-1-350
R	285	1139	439	FDS-4-1140	SW-4.5A-1250
S	28	40	14	FDS-3-85	SW-3A-75
T	29	109	34	FDS-4-115	
U	71	189	99	FDS-4-285	
V	425	1528	828	FDS-4-1700	

Early in this project a recommendation was made to support the HV unit and catwalk with two W8 x 28 members that frame into roof truss C and D.* A vibro-acoustic response analysis for this unit and the catwalk was conducted as described in Appendix H. The support motion defined through this analysis also provides a peak acceleration spectrum as shown in Table 19a. This environment is not too severe for the HV unit but vibration isolation is still recommended as good engineering practice to reduce the structure-borne noise radiation and also minimize the dynamic load on the W8 x 28 support members. The HV unit weighs 2700 lb, and this unit should be supported by four isolators resulting in an estimated 654 to 700 lb per isolator. The HV unit should be supported with an R isolator at each corner. The maximum effective load per isolator, then, becomes 1139 lb, as indicated in Table 22c. Figure 42 illustrates the isolation detail for the HV unit supported at the roof truss by W8 x 28 members.

The catwalk is located very close to roof truss D, and it should not be isolated. The vibration load factor at this location is taken as 60 percent of the 2.3 g load factor for the HV unit without vibration isolation (see Chapter 5 and Appendix H). As indicated in Appendix H, the weight of the portion of the catwalk carried by the W8 x 28 beams is 1500 lb. Thus, the total effective load (P_c) applied to both W8 x 28 beams from the catwalk is:

$$P_c = 0.6 \times 2.3 \text{ g} \times 1500 \text{ lb} = 2070 \text{ lb.}$$

*Structural Drawings No. 5, 7, 8, 9, and 35; Mechanical Drawings No. 1, 2, 3, 25, 26, and 27 for the AMD.

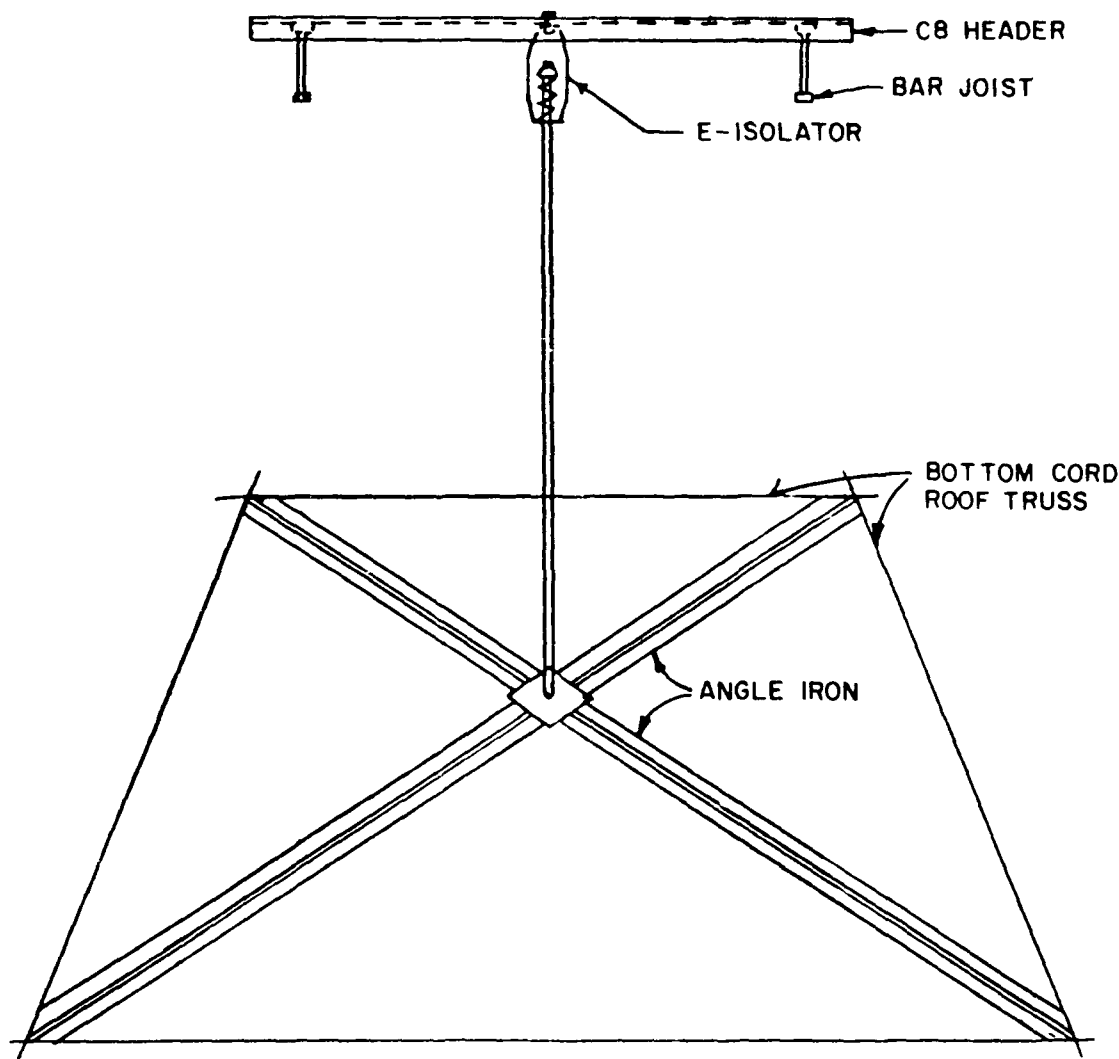


Figure 41. Horizontal wind truss support.

Ductwork

HV ductwork runs through the roof truss system on the north and south ends of the building, and down the walls as described in Chapter 7. Other ducts run from the facility floor, up the walls, and out the exhaust fans on the roof.

The natural frequency of each duct was calculated assuming it was simply supported at every support location. This analysis considers only the overall duct flexural modes assuming the entire duct behaves as a box beam. This is the motion that could be excited through support motion. Tables 24a and 24b summarize the lowest natural frequency of each of the ducts for the size and support spacing indicated. It can be seen that the duct natural frequency is much higher than the primary frequency of the support motions, especially if the ducts are vibration isolated. Thus, overall flexural motion will not be excited in the duct. The natural frequency of individual duct panels is much lower, as seen in Chapter 7. However this type of vibration will not be excited by the support motion, but significant panel motion can be expected from direct acoustical loading on the panels (as was seen in Chapter 7).

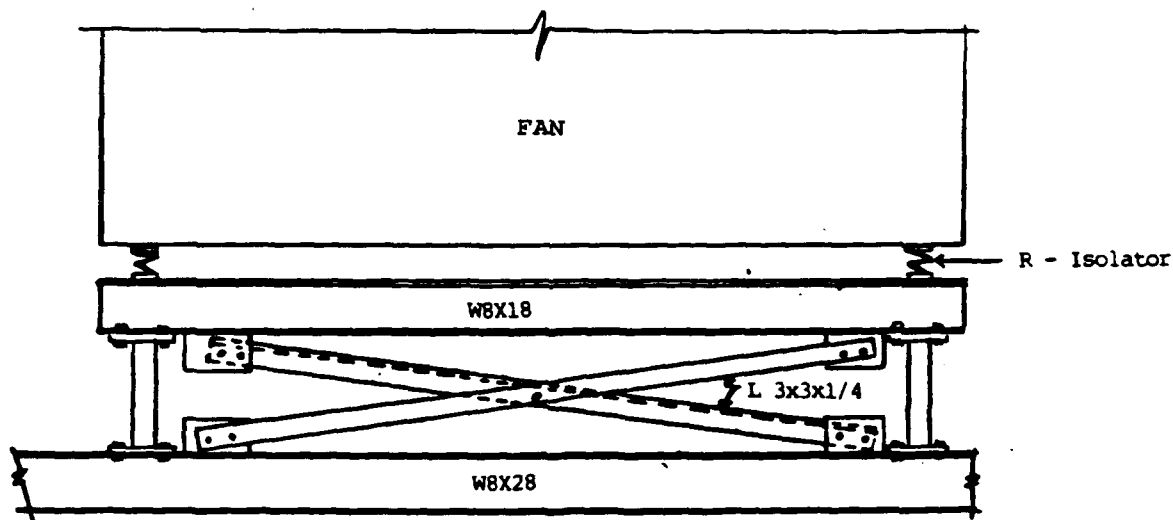


Figure 42. HV unit isolation.

Each of these ducts is to be isolated from the building motion to reduce the load on the roof bar joists. Table I3 presents detailed spreadsheet calculations for the weight supported at every isolator. These dead-load calculations assume that each support carries the weight of the duct tributary area around the support. The weights at each support were grouped together in a way that the fewest number of isolator types could be used for the isolator supports. One isolator was used to support the range of weights for each group. Through an iterative process the maximum and minimum dead weights were established for each group. The maximum and minimum weights given in Table 22a and 22b provide a wider range than required from the calculations in Table I3 to allow for variation of how the load will be distributed. Table I3 shows how the weights were assigned to a particular isolator. The same series of calculations to select the appropriate isolator was performed here, as for the roof truss bracing supports, explained in more detail previously. Table 22a illustrates these spreadsheet calculations for the horizontal ducts supported at the bar joists. The horizontal ductwork calculations allowed the transmissibility to increase to values of 0.243 up to 0.39 in the worst case. This increases the effective acceleration and maximum vertical isolated load shown in Table 22a. As seen in Tables I3a, I3b, and 22a, all the HV horizontal ductwork should be supported with either the F or G isolators. The exhaust fan horizontal ductwork should be supported by I or J isolators, as indicated in Tables I3c through I3k and 18a. Figure 43 shows a plan view of the HV horizontal ductwork isolator locations. Figure 44 illustrates a horizontal ductwork support detail.

The calculations assume the roof is supported with 16K6 bar joists, with a roof panel/bar joist system natural frequency of 9.85 Hz. In many instances, however, a 16K4 bar joist will be used. This will reduce the natural frequency to 9.04 Hz, as shown in Table H4, which, in turn, will increase transmissibility slightly. However, the decrease in natural frequency of the roof panel system will reduce the acceleration level at which this system vibrates, which, in turn, will reduce the load transmitted through the isolators. It is known that the peak acceleration for the first mode of vibration will decrease when the panel frequency decreases. The peak acceleration levels for the remaining modes will have a minimal influence, because the transmissibility for these modes is very small—conservatively taken to be 0.1. For example, a value of 9.04 Hz for the roof panel system natural frequency was substituted into the spreadsheet calculations for the exhaust fan horizontal ducts, where the transmissibility is already at 0.39. This

Table 24
Lowest Natural Frequency of Ductwork

a. Horizontal

ga	Duct Size W H		t (in.)	I (in. ⁴)	Wgt (lb/ft)	L (in.)	K (k/in.)	Mass (lb/in.)	Freq (Hz)	End React (lb)
16*	36	36	0.0598	1851	30.5	133	1133	0.547	229.	338
16*	30	30	0.0589	1070	25.6	133	655	0.460	190.	284
16*	24	24	0.0598	547	20.8	133	335	0.372	151.	230
16*	22	24	0.0598	513	19.9	133	314	0.357	149.	221
18*	20	22	0.0478	314	14.6	133	192	0.262	136.	162

b. Vertical

14*	72	12	0.0747	403	44.2	90	796	0.537	194	332
14*	54	12	0.0747	308	35.1	90	608	0.426	190	263
14*	36	12	0.0747	212	25.9	90	419	0.351	184	194
14*	50	16	0.0747	523	35.1	90	1034	0.426	248	263
14*	42	16	0.0747	447	31.0	90	884	0.376	244	233
18*	16	12	0.0478	68	10.1	90	134	0.122	167	76
18*	16	10	0.0478	46	9.4	90	90	0.114	141	71
18*	12	12	0.0478	54	8.8	90	107	0.107	160	66
18*	12	10	0.0478	36	8.1	90	71	0.099	136	61
18*	14	8	0.0478	25	8.1	90	50	0.099	113	61
18*	10	8	0.0478	19	6.8	90	38	0.083	107	51
18*	8	8	0.0478	16	6.2	90	32	0.075	103	46
16	38	38	0.0598	2177	32.2	30	116100	0.130	4757	80
18	20	20	0.0478	253	14.0	30	13500	0.057	2459	35
18	18	18	0.0478	184	12.7	30	9830	0.051	2203	32
18	14	14	0.0478	87	10.1	30	4620	0.041	1693	25

* Indicates the duct gage recommended by USACERL, as noted in Tables 21a and 21b.

substitution does increase the transmissibility for the first mode to 0.50, but with conservatively leaving the peak acceleration levels as they were for the 16K6 bar joists, the effective acceleration transmitted through the isolator only increases by 2 percent. Therefore, the 16K6 bar joists will be assumed for the remaining calculations for equipment supported by the roof panel/bar joist system.

Most of the ductwork attached to the walls is supported at the north and south walls, where the wall girts are W8 x 21 members. These wall girts will also vibrate at the highest acceleration levels, as seen in Table 6a. Therefore, these peak acceleration levels will be used for all the vertical duct and pipe isolation calculations. The wall girt motion is defined in terms of peak acceleration versus frequency for the wall panel and W8 x 21 girt system motion. These levels are defined in Table I4, along with the isolator transmissibility, in the same way as the 16K6 bar joist motion. The effective weight (W_m) is taken as 505 lb (from Table 6a) for the mass loading calculations.

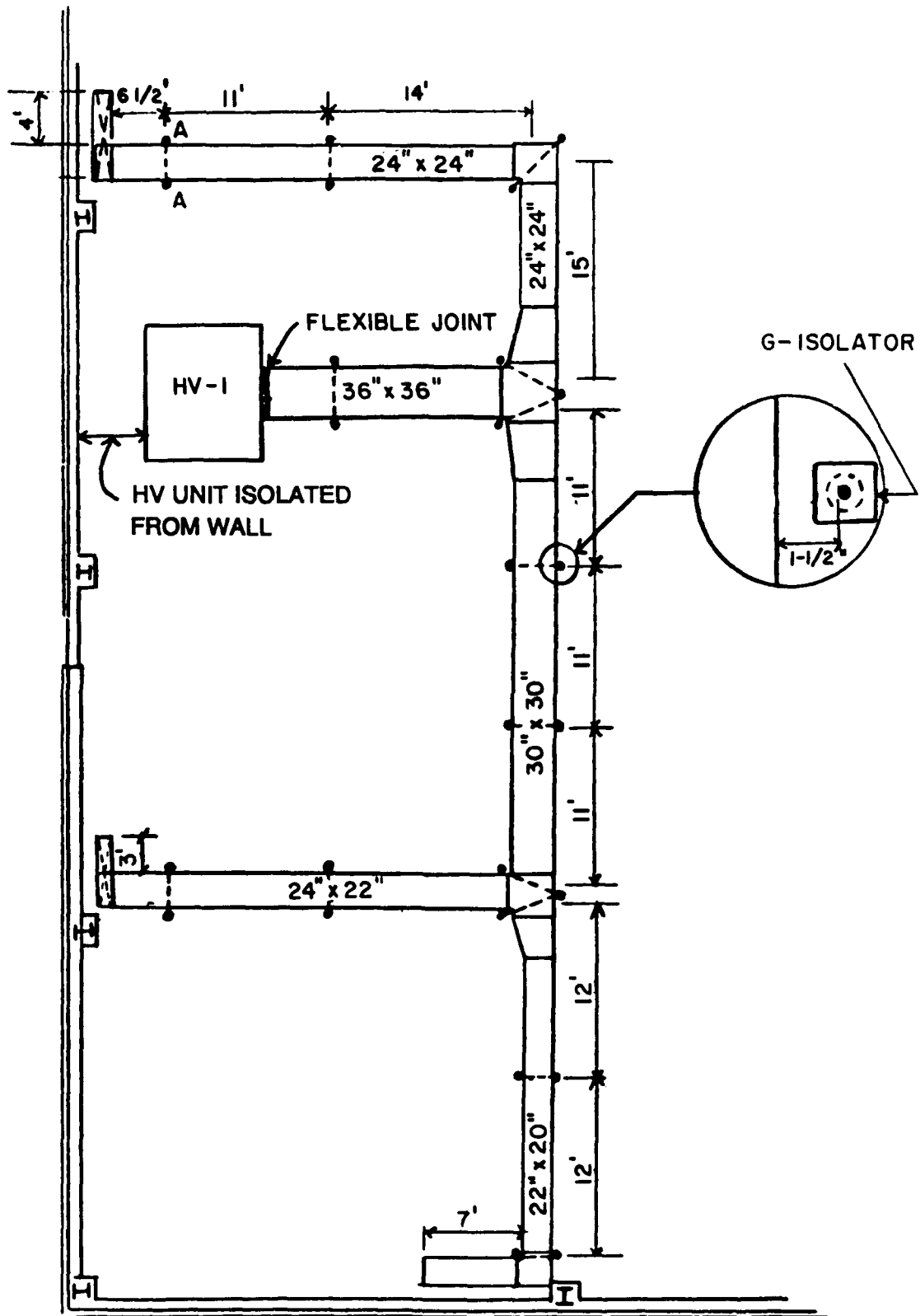


Figure 43. HV horizontal ductwork isolator locations.

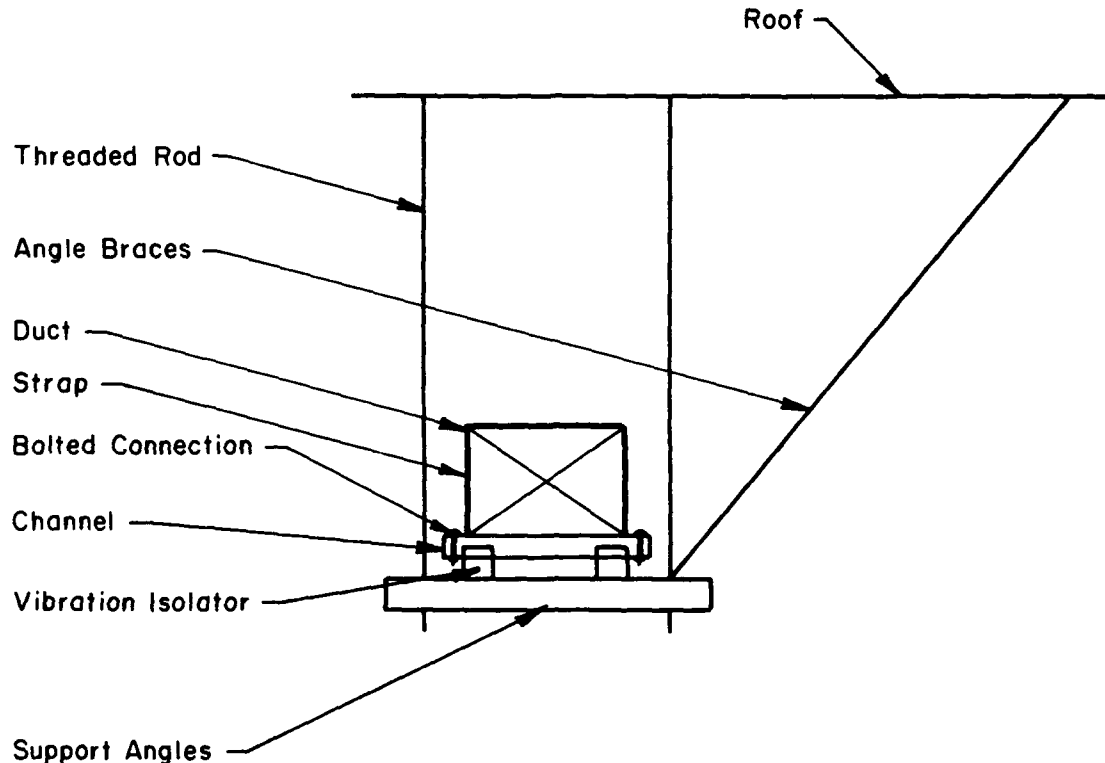


Figure 44. Horizontal duct vibration isolation support.

At the wall girt supports the minimum and maximum weights for a particular isolator type were determined, as shown in Tables I3a through Table I3l. Table 22b illustrates the spreadsheet calculations for the vertical ducts supported at the wall girts. The HV vertical ductwork should be supported at the wall girts with H, I, or J isolators, as indicated in Tables I3a, I3b, and 22b. The exhaust fan vertical ductwork should be supported by I and J isolators, as indicated in Tables I3c through I3l and 22b. Figure 45 illustrates the isolation of a typical vertical duct.

Exhaust Fans

Several exhaust fans are located on the roof of the maintenance dock high bay. All these fans must be explosion-proof, which will ensure that they will not be damaged by the vibration of the AMD. The largest fan exhausts the area enclosed by the draft curtain above the auxiliary power units (APU). The total weight of these APU exhaust fans will be 925 lb. The other fans range in weight from 28 lb (for exhaust fan [EF] 10 and 20) up to 400 lb for EF 5, 6, 7, 8, 15, 16, 17, and 18. All of the fans will be supported at the roof deck, and the load will be carried by the roof panel/bar joist system.

All of these fans should be isolated from the roof to reduce the load on the roof. Each fan will be isolated with four isolators—one at each corner. Tables I3c through I3k provide a range of weight that will be supported by each isolator for each fan. These weights were used in the spreadsheet calculations of Table 22a to determine the appropriate isolator and effective load acting on the roof through each isolator. The exhaust fans will be supported by I, J, S, and P isolators, as indicated in Table 22a. Figure 46 illustrates a typical exhaust fan isolation detail.

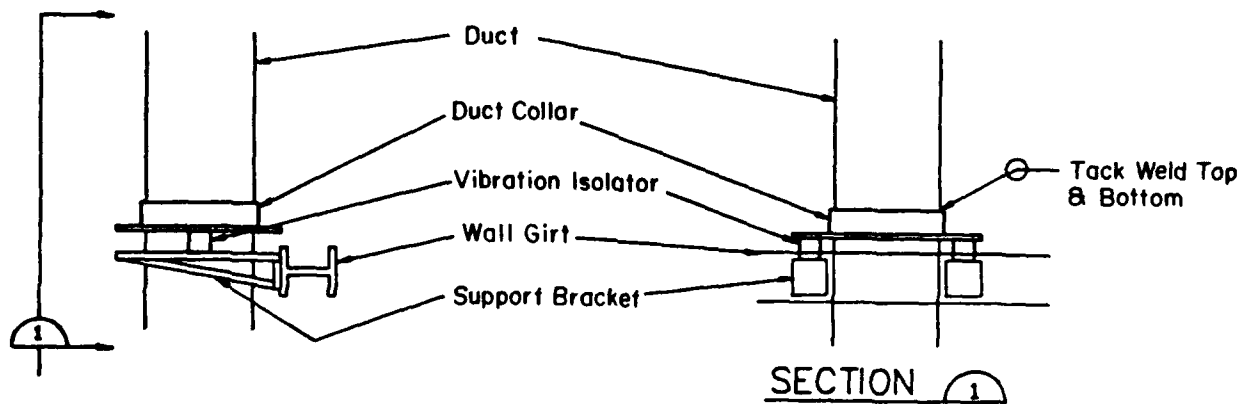


Figure 45. Vertical ductwork vibration isolation support.

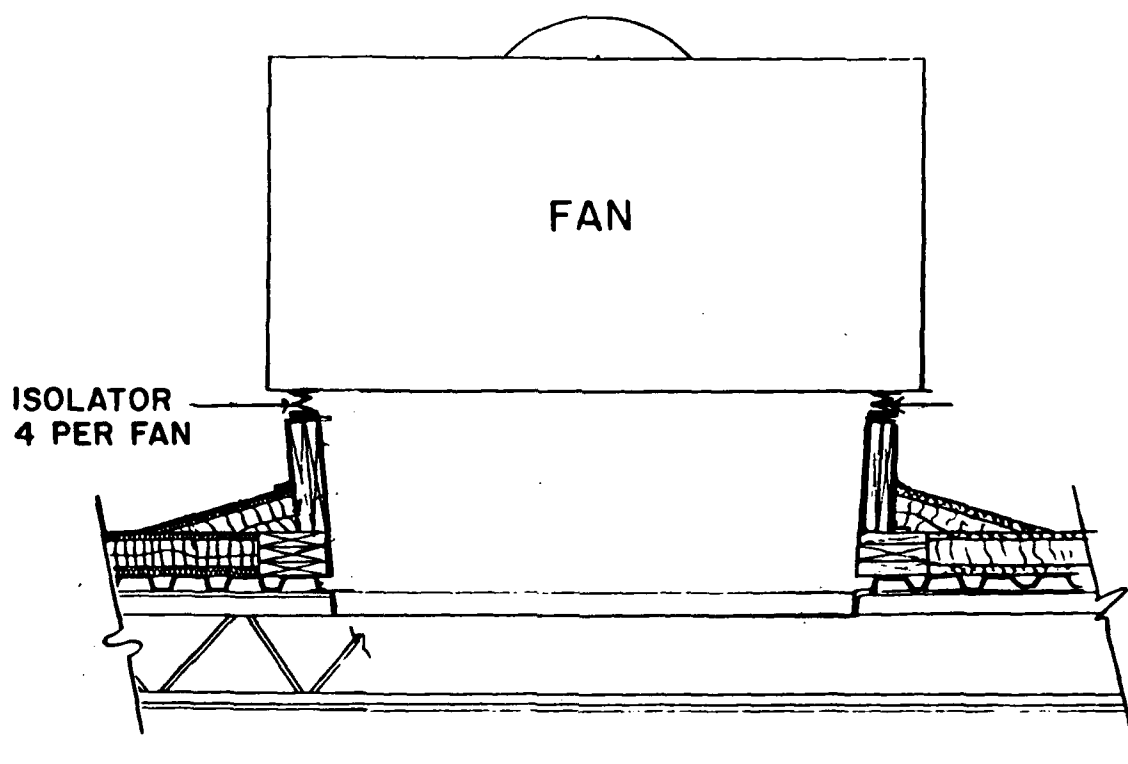


Figure 46. Exhaust fan isolation support.

Pipe Systems

The AMD contains three piping systems: the steam and condensate pipes, the hot water and heating pipes, and the fire protection pipes. The pipes will not be significantly excited by the direct acoustic environment inside the AMD because they offer a relatively low surface area on which the acoustic pressure can act. Another reason is that the relatively small cross section of the pipe will cause the loading essentially to equalize all around a pipe at any given time, resulting in a negligible net load. However the pipes will experience some movement from vibration at their support locations. Those pipes that will be most significantly shaken will be the ones supported by the roof bar joists and wall girts, because these locations are subject to the greatest accelerations. If the pipes are allowed to move significantly, the additional loading on the bar joists will also be significant. It is also possible that, if the pipes were driven to severely, the pipe joints could fatigue and fail. The following sections provide recommendations for isolating pipes larger than 2 in. in diameter from the building motions.

Steam and Condensate Pipes

The steam and condensate pipes must be free to expand and contract. These pipes are supported by vertical, guided, and anchor supports.* The vertical supports allow free motion in both horizontal directions, and provide support vertically. The guided supports allow free horizontal movement along the axis of the pipe. Where these pipes pass through trusses 2 and 13, an anchor support provides restraint for motion in all three directions. The vertical supports are attached either to a single bar joist or a joist header, and distribute the load to two bar joists.** All the guided pipe supports and anchor support attach to the roof truss system near the front of the building.***

The steam pipe is a 10 in. diameter, Schedule 40 pipe, and the condensate pipe is a 6 in. diameter, Schedule 80 pipe. The condensate pipe is the only Schedule 80 pipe in the facility—all others are the standard Schedule 40. The calculations for the maximum and minimum weights at each type of support, for the steam and condensate pipes are shown in Table I5a and Table I5b, respectively. The steam and condensate pipe vertical supports must provide vibration isolation from motion at the roof. A single hanging isolator is used at each vertical support. The same procedure for selecting the isolator and calculating the pipe effective acceleration and total vertical load is repeated here and summarized in Table 22a. The isolator type selected here will reduce the maximum vertical load (including gravity) to 1178 lb. Figure 47 illustrates the vertical steam and condensate pipe isolation detail.

The guided supports are located near the front of the building, supported by the roof trusses. The minimum and maximum weights per isolator are 130 lb and 200 lb respectively, as calculated in Table I5. The roof truss will be driven by the roof panel/bar joist system vibro-acoustic response. The roof truss can conservatively be assumed to vibrate at the same modes as the roof bar joist, but at reduced acceleration levels. The peak acceleration and frequency data used to calculate the isolator response are taken from the bar joist response in Table H5 or I2 and multiplied by the ratio of the truss load factor over the bar joist load factor. The calculations for the peak acceleration and transmissibility at the roof truss are shown in Table I7a. This pipe should be supported using K isolators, and the maximum effective load per isolator becomes 256 lb, as indicated in Table 22c. Figure 48 illustrates the isolation detail for a guided steam or condensate pipe supported by the roof truss.

* Mechanical Drawings No. 1, 3, 15, 16, 25, 26, 27, and 28 for the AMD.

** Mechanical Drawings No. 25, 26, and 28 for the AMD.

*** Mechanical Drawings No. 16, 25, and 26 for the AMD.

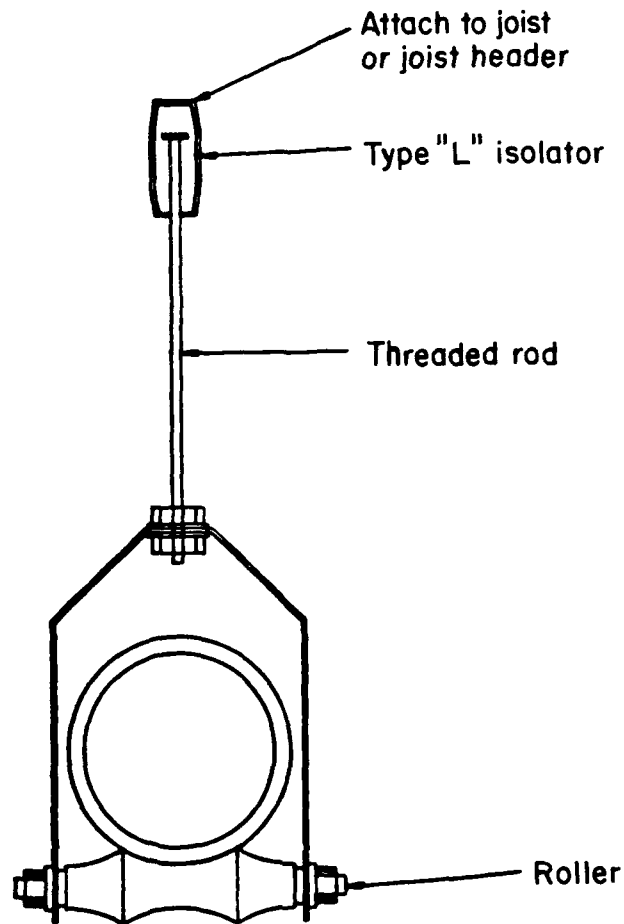


Figure 47. Vertical support for steam and condensate pipes.

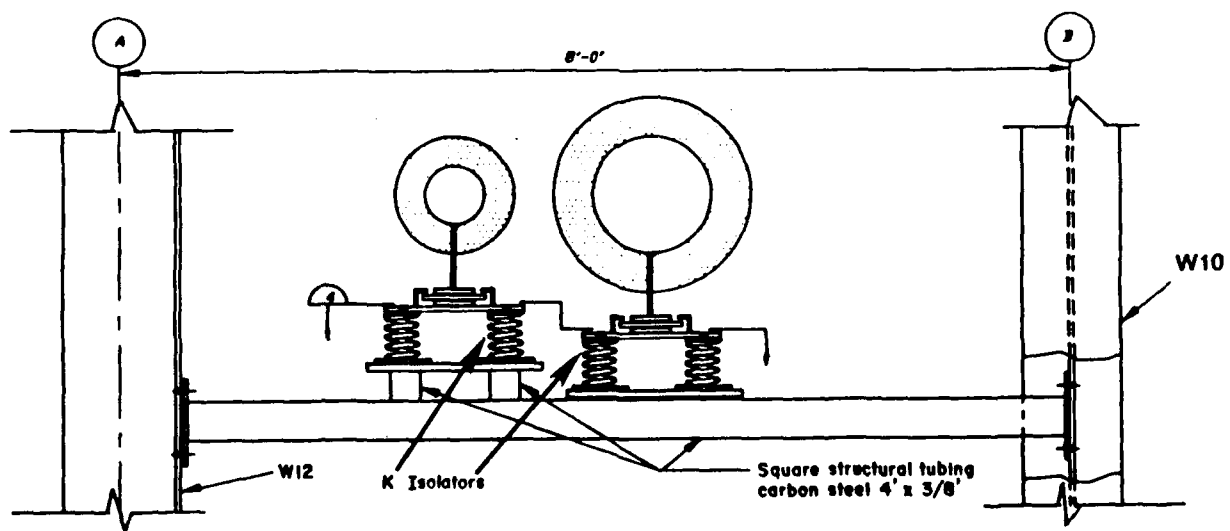


Figure 48. Guided support for steam and condensate pipe.

There is only one anchor support in the Southwest door pockets of both Areas A and C, at trusses 2 and 13 respectively. These locations will experience low vibro-acoustical loading. Therefore, no vibration isolation is needed at the anchor supports, and these supports can provide the needed rigid restraint for the steam and condensate piping system.

The steam pipe is connected to a 4 in. steam supply pipe at the front of the high bay at column line 9. This pipe runs toward the rear of the building near the side wall, and is supported by pipe hangers to the roof bar joists. Then it drops down the wall of the building to a point where it penetrates the wall entering area B.* The vertical section that drops down along the wall is supported by the wall girts. This pipe must be isolated from the motion of both the bar joists and the wall girts to which it is attached. Two isolators should be used on the pipe at each support location.

The horizontal portion of the steam supply pipe is supported by the roof bar joists. The weight per isolator for this essentially empty pipe ranges from 45 to 70 lb. These weights were calculated based on the weight per foot of the pipe multiplied by the length of pipe that will be supported at each location. Table I6 provides the weight calculations and determines the natural frequency of simply supported pipes with the support spacing indicated. The fundamental mode of vibration of the pipes should have a natural frequency well above the frequency of the isolated systems (given in Tables 22a through 22c). The weights used in Table 22 are the minimum and maximum for the given range of support spacing. These weights also include a small additional weight for the pipe connections. This pipe should be supported using J isolators. The maximum effective load per isolator becomes 101 lb, as indicated in Table 22a. Figure 49 illustrates a typical isolation detail for a pipe supported by a bar joist.

The 4 in. steam supply pipe is supported under the catwalk at one location. The support motion defined for the HV unit is also used here because it is part of the same system analyzed in Appendix H. The catwalk, however, will vibrate at less severe levels because it is located near the supporting truss D. The peak acceleration levels used here are the HV unit levels multiplied by 0.6 to account for the less severe environment near the supports. The calculations for the peak acceleration spectrum are shown in Table I9b. An 11 ft long section of pipe is supported at this location, so the total weight per isolator is 55 to 75 lb. This pipe should be supported with a T isolator, for which the maximum effective load per isolator would be 109 lb, as indicated in Table 22c.

The vertical portion of the steam supply pipe is supported by the wall girts. The weight range per isolator is 22 to 40 lb. This pipe should be supported using J isolators, for which the maximum effective load per isolator is 72 lb (as indicated in Table 22b). Figure 50 illustrates a typical isolation detail for a vertical pipe supported by a wall girt.

The condensate return pipe is 2 in. in diameter, and all pipes 2 in. in diameter and smaller may be attached directly to the supporting pipe hanger. The support locations should be at least 4 ft from both the connection to the main condensate pipe and the nearest elbow in the pipe. This will allow the pipe to move freely with the supporting structure without stressing the pipes significantly. The pipe connections and attachments must be designed for the forces of the load factor for the particular support location (see Table 6a) times the pipe weight in addition to the gravity load.

Hot Water and Heating Pipes

The hot water and heating pipes run through the roof truss area, between the heating and ventilating units.** Two of these pipes are 4 in. and the other is 6 in. The pipes in the roof truss area will be

* Mechanical Drawings No. 25 and 27 for the AMD.

** Mechanical Drawings No. 1, 3, 25, 26, and 28 for the AMD.

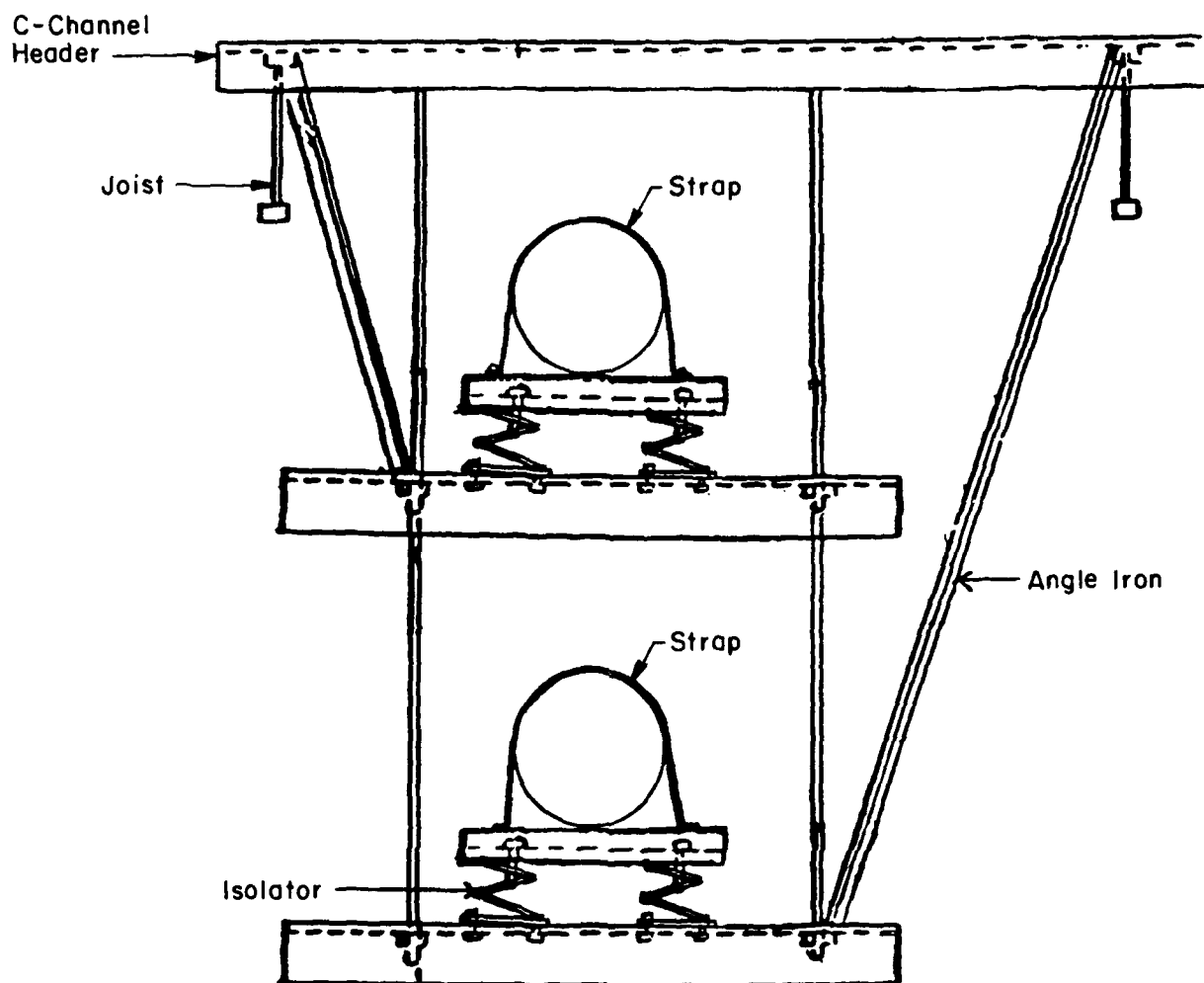


Figure 49. Horizontal pipes supported by bar joists.

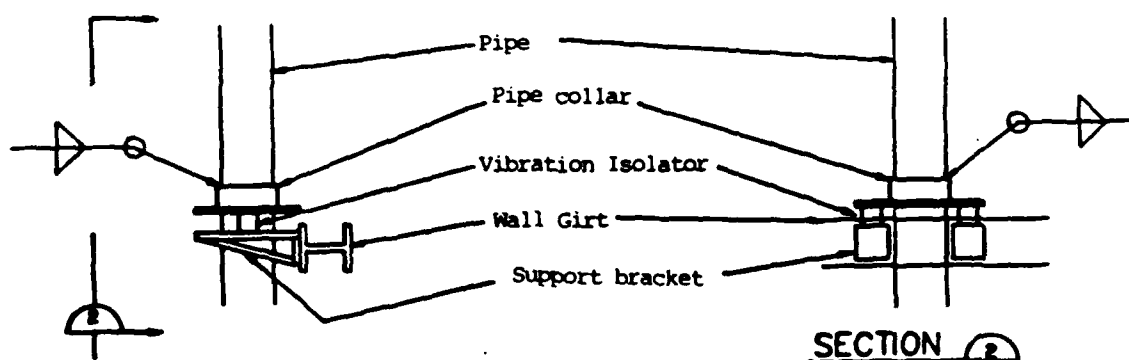


Figure 50. Vertical pipe support and isolation.

supported by hangers attached to the roof bar joists. Other pipes to supply the HV unit are attached to the wall girts. For the purposes of weight and vibration isolation calculations, the pipes will always be filled with water.

For those pipes in the roof truss area, supported by the bar joists, the support spacing range is 96 to 144 in. The weight per isolator for the 6 in. pipe varies from 125 to 195 lb, and 65 to 105 lb for the 4 in. pipe. The 6 in. pipe should be supported with O isolators, for which the maximum load per isolator is 277 lb (as indicated in Table 22a). The 4 in. pipe should be supported with M isolators, for which the maximum load per isolator is 154 lb (Table 22a).

The 4 in. hot water and heating pipe is supported under the catwalk at one location. The support motion defined for the HV unit is also used here because it is part of the same system analyzed in Appendix H. The catwalk, however, will vibrate at less severe levels because it is located near the supporting truss D. The peak acceleration levels used here are the HV unit levels multiplied by 0.6 to account for the less severe environment near the supports. The calculations for the peak acceleration spectrum are shown in Table 19c. A 9 ft long section of pipe is supported at this location, for which the total weight per isolator is 70 to 90 lb. This pipe should be supported with a U isolator, for which the maximum effective load per isolator is 189 lb (Table 22c).

The hot water supply and return pipes will be supported by the wall girts. The minimum support spacing for these pipes is 72 in. and the maximum is 90 in.* The weight per isolator for the 6 in. pipe varies from 95 to 125 lb, and 50 to 70 lb for the 4 in. pipe. The 6 in. pipe should be supported by M isolators, for which the maximum load per isolator is 204 lb (Table 22b). The 4 in. pipe should be supported with I-isolators, for which the maximum load per isolator is 121 lb (Table 22b).

Fire Protection Pipes

The fire protection piping consist of two independent systems: the first supplies overhead sprinklers and the second supplies oscillation monitor nozzles. The first system is a group of three 6 in. pipes that comes through the wall from the mechanical room, runs up the walls to the roof truss area, and branches out in a network to cover the entire roof truss area.** Each of the main three pipes branch out to progressively smaller pipes in the roof truss area, all the way down to 3/4 in. column sprinkler pipes, which are attached to each column. (See Fire Protection Drawing No. 2 for the AMD, for a detailed illustration of this pipe network.) The pipes along the wall will be supported by the wall girts, and the pipes in the roof truss area will be supported by the bar joists.

Overhead Sprinkler Pipes. All of these pipes that are larger than 2 in. in diameter must be isolated from the motion of their respective supports to reduce the dynamic loading on these members. The connections for the smaller pipes must be designed for their own weight multiplied by the appropriate load factor at their support (see Table 6a for load factors) plus the gravity load.

The fire protection pipes that lead to overhead sprinklers will normally be empty. In the event of a fire, the aircraft will not be operated, so there should never be an acoustic load on the pipes when they are full of water. Therefore, the vibration isolation recommendations assume the pipes are empty. However, even if an emergency situation caused the pipes to fill while acoustical loading was still applied, the maximum load applied to the isolator would not exceed the additional minimum overload capacity of 50 percent.

* Mechanical Drawings No. 27 and 28 for the AMD.

** Mechanical Drawings No. 25, 26, 27, and 28; and Fire Protection Drawing No. 2 for the AMD.

The three 6 in. pipes are supported by the wall girts. The minimum and maximum lengths of pipe per support are 48 and 120 in. All the pipe weights per support were calculated as shown in Table 16. Each support will have two isolators, for which the minimum and maximum weights per isolator are 40 and 110 lb, respectively. The transmissibility becomes 0.38, as seen in Table 14e. The recommended isolator for these pipes is an M isolator, for which the maximum dynamic load per isolator is 195 lb (Table 22b). The maximum static load that must be carried by an isolator when the pipes are full is 170 lb, which is well within the 250 lb capacity of these isolators.

The 6 in. pipe supported by the bar joist has a range of support spacing from 133 to 144 in. The minimum length of pipe supported at an isolator location is taken as 96 in. and the maximum is 144 in. This results in a range of weight per isolator of 80 to 125 lb. Each pipe is supported by a hanger that distributes the load between two bar joists, but at every pipe support location at least two pipes of the same size are being supported, so the minimal mass loading benefit for these pipes is when two bar joists are supporting two pipes. For this 6 in. pipe an M isolator was selected, for which the maximum dynamic load per isolator is 180 lb, as indicated in Table 22a. The maximum static load that must be carried by an isolator when the pipes are full is 200 lb, which, again, is within the 250 lb capacity of these isolators. If the pipe were acoustically loaded while full, as in the emergency situation suggested above, the maximum dynamic load would reach 280 lb, which is well within 50 percent overload capacity of the isolator. For the remaining pipes this emergency condition will not be considered, but each pipe isolator does have the same 50 percent overload capacity, if needed.

Each 6 in. pipe branches off at a Tee into two 4 in. pipes. The supports for each 4 in. pipe are 120 in. apart. Half the load supported by the 4 in. pipe hanger will be carried by the nearest bar joist, and the remaining load will be carried by the top cord of the nearby roof truss. The weight per isolator, accounting for the transitions to pipes of other sizes, is a minimum of 40 lb and a maximum of 60 lb. The J isolator is recommended for this pipe, for which the maximum dynamic load is 89 lb (Table 22a). The maximum static load that must be carried by an isolator when the pipes are full is 90 lb, which is within the 100 lb capacity of these isolators.

The 4 in. pipes branch off into several pipes that are 2 in. or smaller, and these lead to sprinkler heads. The 4 in. pipe also transitions to a 3 in. pipe, then to either a 2.5 in. or 2 in. pipe, and finally to smaller ones. The smaller pipes eventually attach to sprinkler heads either near the roof or down the columns. Again, only the pipes larger than 2 in. should be isolated: the smaller pipes should be hard mounted. The 3 in. and 2.5 in. pipes will also be supported every 120 in. The weight will vary from 30 to 45 lb per isolator for the 3 in. pipe. The J isolator is recommended for supporting this pipe, for which the maximum dynamic load is 67 lb (Table 22a). The maximum static load that must be carried by an isolator when the pipes are full is 60 lb, which is within the 100 lb capacity of these isolators.

The weight will vary from 25 to 35 lb per isolator for the 2.5 in. pipe. The J isolator is recommended for supporting this pipe, for which the maximum dynamic load is 52 lb (Table 22a). Here the maximum static load is only 45 lb, which is obviously well within the 100 lb capacity of these isolators.

Oscillating Monitor Pipes. The second pipe system supplies four oscillating monitor nozzles in each maintenance bay.* This system consists of an 8 in. pipe that penetrates the wall from the mechanical room at about 11 ft above the floor. This pipe immediately drops down to 8 ft above the floor, and tees off to 4 in. and 6 in. pipes that run along the maintenance bay walls. Both the 4 and 6 in. pipes are supported by a structural tubing member that is supported by either every column or by the wall girt at

* Fire Protection Drawings No. 1 and 3; Mechanical Drawings No. 25, 26, 27, and 28 for the AMD.

an intermediate position between the columns.* All pipes in this system will be filled with water at all times. The 4 in. pipe runs along the side wall to near the front of the building, where it drops down to a monitor nozzle.

The 6 in. pipe runs along the side wall at 8 ft above the floor to the back wall, and then along the back wall to a point just before the position of the open rear hangar door.** At this point, a 4 in. pipe branches off and drops down to the rear door monitor nozzle. This 4 in. section of pipe can be supported directly by the maintenance bay floor with no isolation. The 6 in. pipe also branches off into another 6 in. pipe that runs up along the back wall to the roof truss, and then across the back door opening, supported by the wind truss. At the end of the open hangar door this same pipe drops down along the wall to 8 ft above the floor. The vertical section of pipe is supported at every wall girt. The horizontal section of pipe above the rear hangar door is supported at the W6 x 9 "post" member of the wind truss above the rear hangar door. The 6 in. pipe, now again at 8 ft above the floor just past the position of the open rear hangar door, branches into a 4 in. pipe that again drops down to another rear door monitor nozzle. This 6 in. pipe also branches off to another 4 in. pipe that runs horizontally along the side wall, at 8 ft above the floor to the side wall, and then runs all the way up to the oscillating monitor nozzle near the front of the building. Again this 4 in. pipe is supported at every column and at an intermediate point to the wall girt with a structural tubing member.

The minimum pipe length per support, for the 6 in. horizontal pipe attached to the columns and wall girts, is 132 in. and the maximum is 168 in. The minimum weight per isolator is 170 lb and the maximum is 240 lb. The peak acceleration levels used for the support motion will be lower at the wall columns than for the wall girt. These levels will decrease by the ratio of their load factors as given in Table 6. The frequency at which these peaks occur will be approximately the same because both the columns and girts are being driven by the wall panel/wall girt motion. However, since the pipe is being supported by both wall columns and wall girts, the vibration isolation design will be based on the more severe wall girt motion. The mass loading benefits, when supporting at the column, are minimal because the mass of the isolated pipe is very small relative to the mass of the column system (5035 lb for the back wall, as given in Table 6a). Thus, the effective acceleration values are quite large. The N isolator is recommended for supporting this pipe, for which the maximum dynamic load is 435 lb (as indicated in Table 22b).

The minimum pipe length per support for the 4 in. pipe is 93 in. at the point where the pipe drops down to the monitor nozzle, and the maximum length is 168 in. The minimum weight per isolator is 65 lb and the maximum is 125 lb. The 65 lb minimum weight includes a small contribution from the pipe elbow where the pipe drops down to the monitor nozzle. As for the 6 in. pipe, the wall girt motion will be used for defining the support motion of the 4 in. pipe. The I isolator is recommended for supporting this pipe, for which the maximum dynamic load is 231 lb (Table 22b).

The minimum pipe length per support for the 6 in. vertical pipe is 54 in. and the maximum length is 90 in. The minimum weight per isolator is 70 lb and the maximum is 130 lb. The M isolator is recommended for supporting this pipe, for which the maximum dynamic load is 224 lb (Table 22b).

For the 6 in. horizontal pipe supported by the wind truss over the rear hangar door, the minimum pipe length per support is 90 in. and the maximum length is 144 in. The minimum weight per isolator is 115 lb and the maximum is 200 lb. The support motion for this location is determined by the motion of both the wall panels and roof panels. The wall panel/wall girt motion is more severe than that of the roof panel/bar joist motion, as seen by comparing the peak acceleration values in Tables 12a and 14d. The

* Mechanical Drawings No. 25, 26, and 28 for the AMD.

** Mechanical Drawings No. 25 (Note 6), 26, 27, and 28; Fire Protection Drawing No. 1 for the AMD.

wind truss will be driven by the wall panel/wall girt system vibro-acoustic response, through the back wall columns. The wind truss can conservatively be assumed to vibrate at the same modes as the wall girts, but at reduced acceleration levels. The peak acceleration and frequency data used to calculate the isolator response are the same data taken from the wall girt response in Table 14 multiplied by the ratio of the back wall column load factor over the back wall girt load factor. These load factors are taken from Table 6a. The calculations for the peak acceleration and transmissibility at the wind truss are shown in Table 18. The N isolator is recommended for supporting this pipe, and the maximum dynamic load is 313 lb (Table 22c).

General Recommendations for Pipe Systems

The following general recommendations concern all AMD pipe systems.

Care must be exercised with pipe valves because they may input some eccentric loading on the pipes. A separate support may be needed for large pipe valves.

If possible, supports should be located near large pipe fittings. However the minimum support spacing or weight per isolator must not be violated for the isolated pipe. (These values were given in Tables 16 and 22.)

The 1 in. fire protection pipe that follows the columns from the roof should not be attached near the 90 degree corner as it comes down the column. A minimum spacing to either a wall or roof member should be at least 2 ft from the corner, to allow adequate flexibility in the pipe.

Lighting Fixtures

The high bay area of the AMD contains a number of lighting systems. The high-intensity discharge (HID) lights provide the primary overhead lighting for the high bay area. Fire protection strobe and beacon lights are attached to the walls in the high bay area, and emergency exit lights are located above personnel doors. Most of these lighting fixtures will need to be isolated from the building motions as described in the following sections.

HID Lights

The original HID lighting fixture support structure consisted of an additional structural frame to support the lights at the optimum locations. This light grid was to be supported by the main roof truss system. However, preliminary analysis indicated that the light grid would vibrate at a level significantly amplified from the motion of the primary roof truss system. This would cause vibration loads to the lighting grid, both from the weight of the grid members and the weight of the lighting fixtures. The size of the grid members would have been significantly increased to accommodate these loads, thus adding significant weight to the entire roof truss system. Therefore, a modification was made to remove the light grid system completely and support the lighting fixtures from the bottom cord of the trusses.*

The total weight of the overhead HID lighting fixtures is 55 lb for the primary fixtures and 43 lb for smaller fixtures. These fixtures should be isolated to protect them from the motion of the roof truss and reduce the additional load on the roof truss. The peak acceleration levels at roof truss are based on the roof panel/bar joist system vibro-acoustic response. The roof truss can conservatively be assumed to

* Electrical Drawings No. 1, 3, and 5; Specifications for Construction 16415.31, for the AMD.

vibrate at the same modes as the roof bar joist, but at reduced acceleration levels. The peak acceleration and frequency data used to calculate the isolator response are the same data taken from the bar joist response in Table H5 or I2 multiplied by the ratio of the truss load factor over the bar joist load factor. The calculations for the peak acceleration and transmissibility at the roof truss are shown in Table I7b. Each light fixture should be supported with a single isolator. The minimum and maximum weights for the 55 lb light fixture are taken as 50 and 60 lb respectively. This fixture should be supported with an A isolator. The maximum dynamic load is 78 lb, as indicated in Table 22c.

The minimum and maximum weights for the 43 lb light fixture are taken as 40 and 50 lb respectively. The transmissibility and peak acceleration levels have been calculated as shown in Table I7c. This fixture should also be supported with an A isolator. The maximum dynamic load is 65 lb, as indicated in Table 22c. Figure 51 illustrates the isolation detail for a typical HID light fixture supported at the bottom cord of the roof truss.

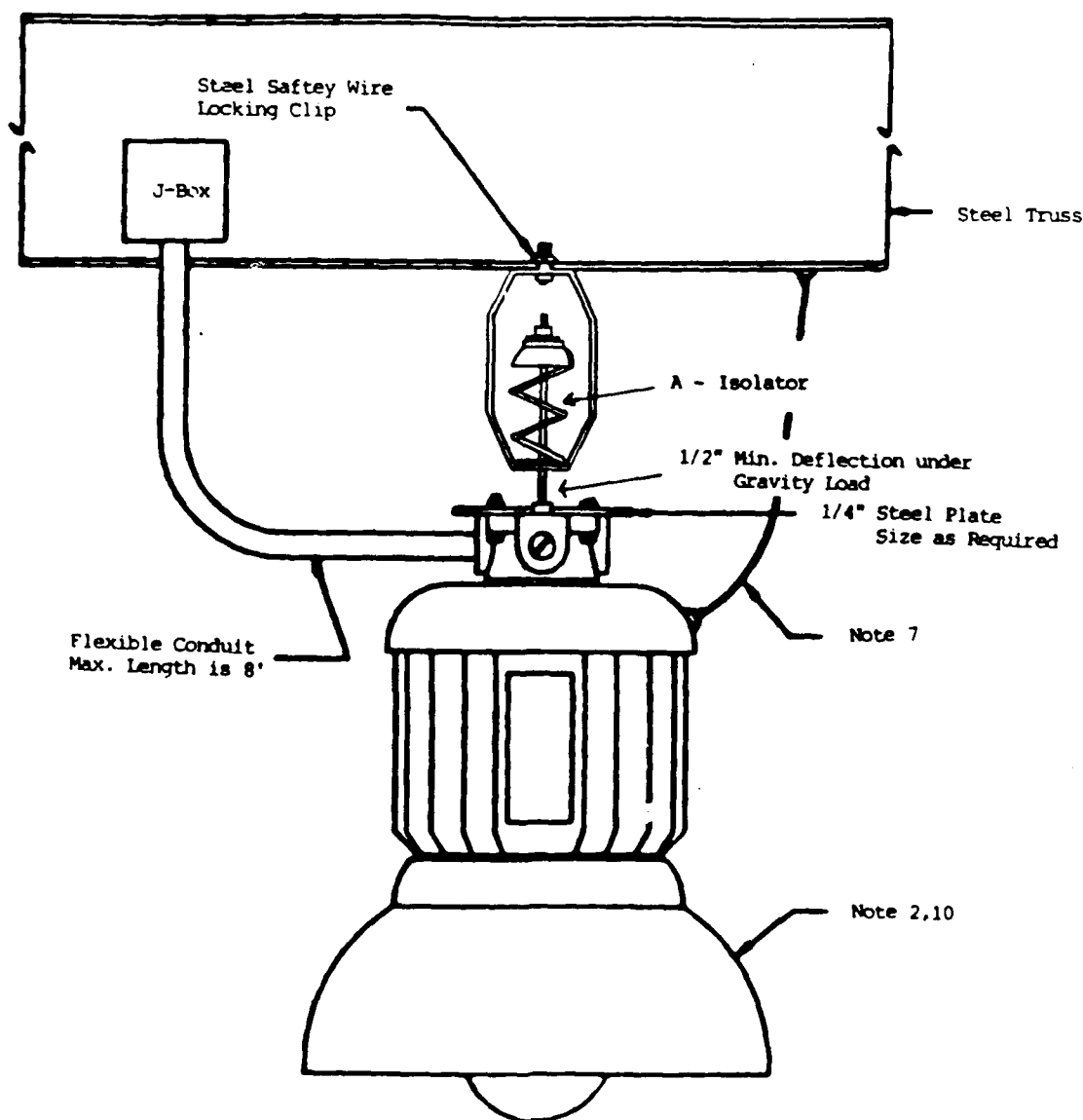


Figure 51. HID light fixture support detail.

Fire Protection Strobe and Beacon Lights

Fire protection strobe and beacon lighting will be attached to the wall girts inside the maintenance dock bays. These fixtures should also be isolated to protect them from the high acceleration levels of the wall girts. The weight of the strobe light fixture is 10 lb, and minimum and maximum weights of 8 and 12 lb respectively are used for the calculations. This fixture should be supported with a C isolator, for which the maximum dynamic load becomes 22 lb as indicated in Table 22b. The weight of the beacon light fixture is 9 lb, and minimum and maximum weights of 7 and 11 lb respectively are used for the calculations. This fixture should also be supported with a C isolator, for which the maximum dynamic load becomes 21 lb (Table 22b). Figure 52 illustrates the isolation detail for a typical fire protection lighting fixture supported at a wall girt.

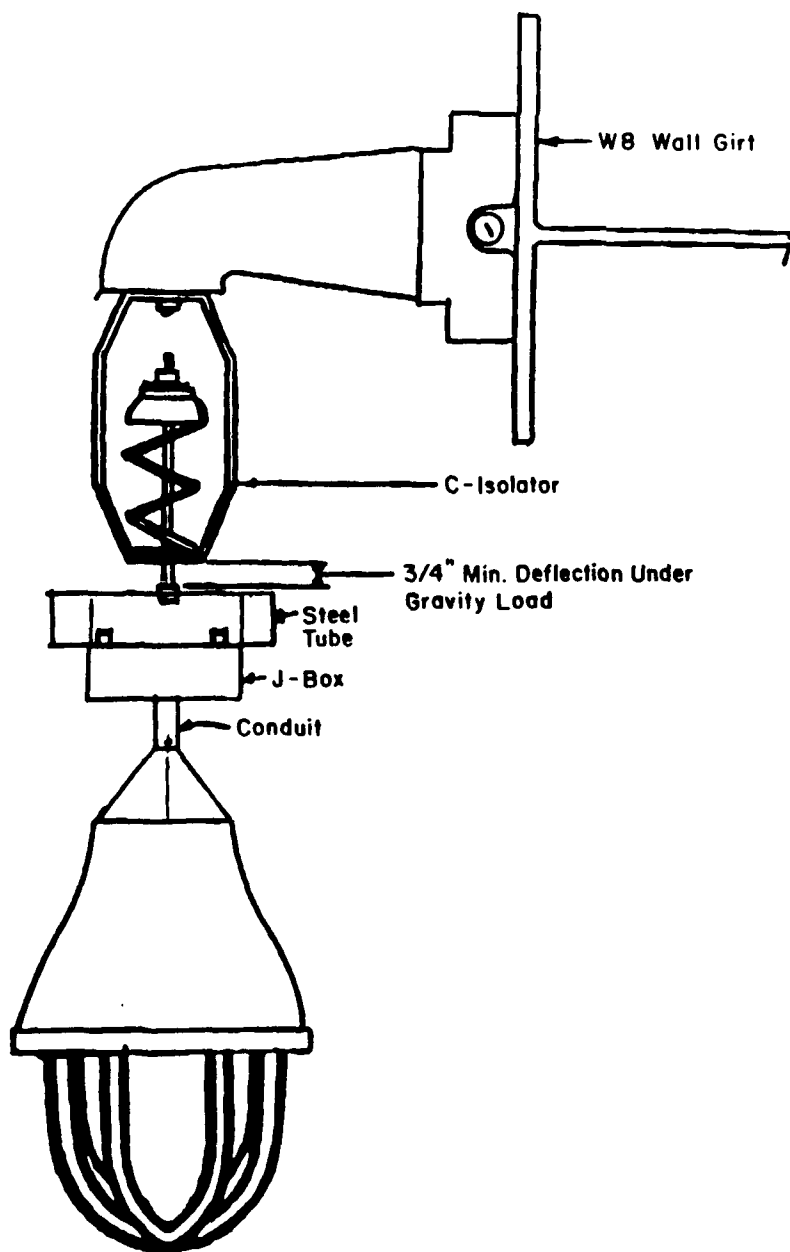


Figure 52. Strobe light fixture support detail.

Emergency Exit Lights

Emergency exit lights will be located above personnel doors. They will be attached to the frame of both the front and rear hangar doors, the concrete masonry unit (CMU) side wall, and a girt on the opposite side wall. The light attached to the front door and CMU wall will experience little vibration because the front hangar door will be protected in the door pocket when the building is being acoustically loaded and the CMU wall will not respond significantly to the acoustic loads. However, the light attached to the rear hangar door and the wall girt will experience significant vibration. The individual wall panels of the rear door will vibrate at a similar fundamental frequency (11 Hz for the panel size and gage indicated in Table H8) as the wall girts, but lower acceleration levels (5.7 g versus 8 g for the wall girt as indicated in Table 6a). Therefore, the acceleration levels used to calculate the response of this system will conservatively use the same levels as for the beacon light, which is attached to the wall girt. These are shown in Table I4f. The weight of the Type 650 emergency exit light is 15 lb, and minimum and maximum weights of 12 and 18 lb respectively are used for the calculations. The fixture attached to the wall girt and rear hangar door frame should be supported with a C isolator. The maximum dynamic load is 33 lb, as indicated in Table 22b. The emergency exit light attached to the wall girt will be very similar to the strobe light support shown in Figure 52. The attachment of the emergency exit light to the rear hangar door frame, using a C isolator, is illustrated in Figure 53.

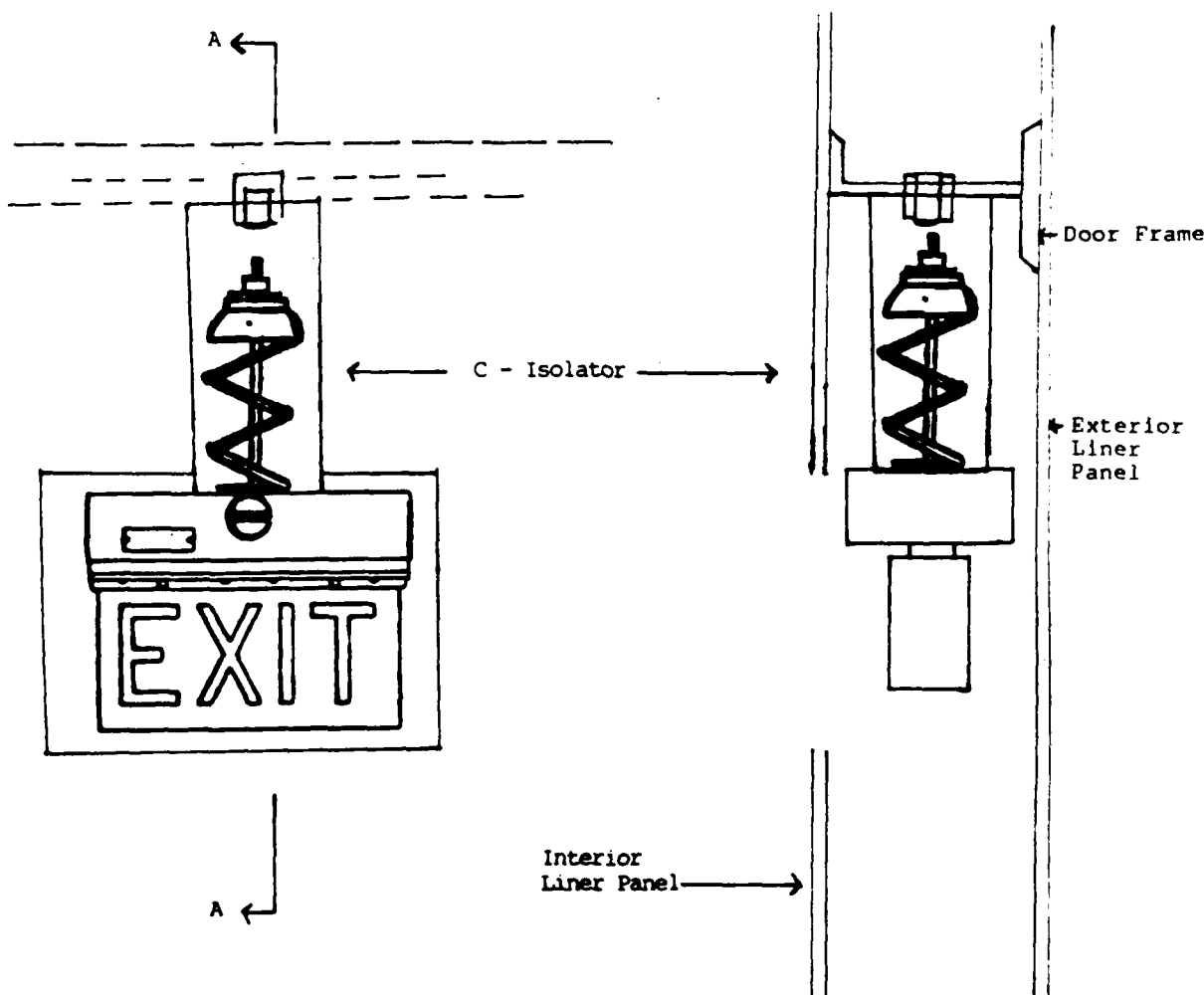


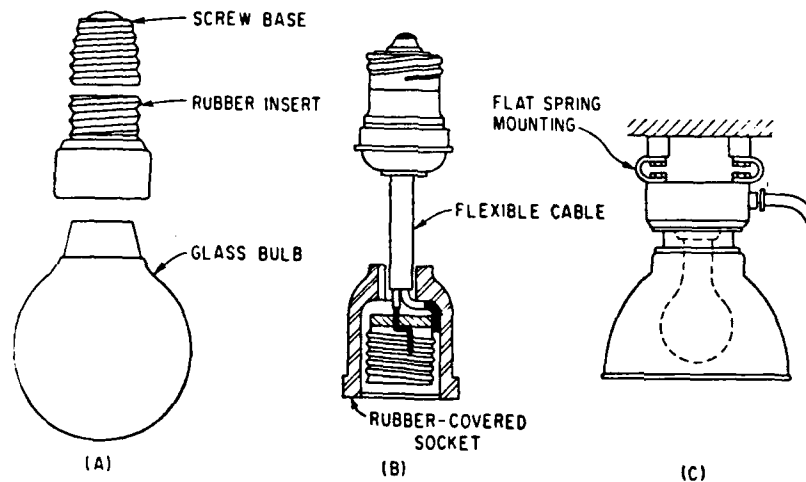
Figure 53. Emergency exit light fixture.

General Recommendations for Lighting Fixtures

The following general recommendations should be followed to assure that the lights do not become a hazard:

1. Each lighting fixture should have a shield to prevent the bulb from falling.
2. Use steel safety wire locking for the bolted connection of the HID lighting fixture.
3. Provide a fail-safe backup for HID light supports, such as a snug cable draped over the bottom cord of the roof trusses. This cable must not hinder free deflection of the isolator.
4. Do not run rigid conduit into lighting fixtures; provide for flexible cables.

Figure 54 illustrates examples of shockproof designs for lights. These do not represent USACERL recommendations, but the supplier responsible for providing qualified lights may find these diagrams helpful.



(Source: C.M. Harris, *Shock and Vibration Handbook*, 3rd ed. [1988], Fig. 43.29.
Reproduced with the permission of McGraw-Hill, Inc.)

- (A) Rubber insert between screw base and glass bulb
(B) Rubber-covered socket and flexible cable
(C) Flexible U-shaped flat spring mounting.

Figure 54. Shockproof designs for lights.

9 CONCLUSIONS AND RECOMMENDATIONS

Conclusions

An evaluation of the acoustic environment estimated for the high bay portions of the AMD and its effects on structure and equipment indicates the following:

The middle two-thirds of the AMD will receive the highest acoustic exposure for various positions of the main engine. However, due to the effects of acoustic reverberations, high sound levels will exist throughout the facility.

The acoustic environment from operations at 6820 rpm, the maximum level evaluated in detail in this study, would be expected to cause some secondary structural failures or equipment malfunction if the design loads developed in this report are not considered. Only secondary structures, i.e., walls and ceiling panels (primarily at fastener locations), would be at risk in the absence of proper design. However, if the operational condition for the main engines is increased to 8060 rpm, failures of some secondary structure and equipment mounting are probable unless the design loads defined herein are increased by about 320 percent. Operation of the main engines at an idle rpm of 3220 rpm is not expected to cause structural failures or equipment malfunctions under any conditions.

Maximum static pressure design loads equivalent to the acoustic environment will be as high as ± 32 psf on the back wall. These loads are comparable to, or exceed in magnitude, the maximum static pressure loads from wind or snow, but they should be within the design capability of presently envisioned wall panels if care is taken on panel fastener details.

It should not be necessary to combine the equivalent acoustic loads with the other static design loads, except for snow loads on the roof. However, in this case, as snow load builds up, the response to acoustic loading will decrease, so the combined loads will not add linearly.

Dynamic load factors due to acoustically induced vibration will vary, depending on mounting location and equipment mass. For equipment not mounted on panels or the surface of the draft curtain, vibration load factors are estimated to be no greater than 8 g.

Some cost benefit may be achieved by adding acoustic absorption inside the AMD, but the data needed for analyzing cost tradeoffs in detail were not available at this point in the research. Part of the reason for a possible benefit could be associated with limitations on noise exposure time for personnel inside the AMD during low-level maintenance operations.

Recommendations

It is recommended that numerous strengthening and vibration-isolation measures, as developed in Chapters 7 and 8, be taken to ensure the integrity of this facility.

Cost savings in the form of relaxed design requirements may be appropriate. If so, it is recommended that:

1. Limited vibro-acoustic response data be collected in a similar high bay building to confirm the predictions developed in this study

2. An acoustic test on one or more prototype wall panel design concepts should be conducted to validate their structural integrity and fastener design concepts long before construction is completed.

It is recommended that every effort be made to use currently available resources of information on fragility levels of proposed equipment, to allow prequalification by example, test data, or design analysis of as much of the vibration-sensitive equipment in the AMD as possible.

REFERENCES

- Abramovitz, M., and I.A. Stegun, *Handbook of Mathematical Functions*, Applied Mathematics Series 55 (National Bureau of Standards, June 1964).
- Air Force Regulation (AFR) 161-35, *Hazardous Noise Exposure*, Change 2 (Headquarters, U.S. Air Force, December 1976).
- American National Standards Institute (ANSI) Standard S1.26-1978, *Method for the Calculation of the Absorption of Sound by the Atmosphere*.
- ANSI S1.4-1983, *Specification for Sound Level Meters*.
- ANSI S1.11-1986, *Specification for Octave-Band and Fractional-Octave-Band Analog and Digital Filter*.
- ANSI S1.26-1978, *Method for the Calculation of the Absorption of Sound by the Atmosphere* (Acoustical Society of America, 1978).
- Beranek, L.L., *Noise and Vibration Control* (McGraw-Hill, New York, 1971).
- Cremer, L., M. Heckl, E.E. Ungar, *Structure-Borne Sound* (Springer-Verlag, New York, 1973).
- Geiger, P.H., *Noise Reduction Manual* (University of Michigan Press, 1953).
- Harris, C.M., *Shock and Vibration Handbook*, 3rd ed. (McGraw-Hill, New York, 1988).
- Hunt, F.V., "Velocity-Strain Ratio for Vibrating Elastic Bodies," *Journal of the Acoustical Society of America*, Vol 32 (September 1960), pp 1123-28.
- Lawrence, H.C., "Shock and Vibration Design," *Space/Aeronautics* (December 1961), pp 49-53.
- Lipson, C., and R.C. Juvinall, "Application of Stress Analysis to Design and Metallurgy," *Handbook of Stress and Strength* (MacMillan Press, 1963).
- Lyon, R. H., *Statistical Energy Analysis of Dynamical Systems: Theory and Applications*, The MIT Press, Cambridge, MA, 1975.
- Maintenance Dock Hydrant Fuel System Aircraft Apron/Taxiway*, vol. II FY 90/91 (USACE, Omaha District, April 1991).
- Manual of Steel Construction*, 8th ed. (American Institute of Construction [AISC], Chicago, 1980).
- Miner, M.A., "Cumulative Damage in Fatigue," *Journal of Applied Mechanics*, Vol 12, No. 3 (American Society of Mechanical Engineers, 1945), A159-A164.
- NFPA 91-1990, *Blower and Exhaust System for Dust, Stock, and Vapor Removal or Conveying* (NFPA, 1990), par 3-3.3.
- Powell, Alan, *Random Vibration* (MIT Press, 1958), Chapter 8.
- Richards, R.J., and D.J. Mead, eds, *Noise and Acoustic Fatigue in Aeronautics* (John Wiley & Sons, 1968).

REFERENCES (Cont'd)

- Roark, R.J., *Formulae for Stress and Strain* (McGraw-Hill, New York, 1954).
- Sugamele, J., "Evaluation of Acoustic Environmental Effects on Flight Electronic Equipment" *The Shock and Vibration Bulletin*, Bulletin 35, Part 3 (The Shock and Vibration Information Center, U.S. Naval Research Library, Washington D.C., January 1966), pp 259-279.
- Sutherland, L., (ed.), *Sonic and Vibration Environments for Ground Facilities--A Design Manual* Wyle Report (WR) 68-2 for NASA Marshall Space Flight Center (Wyle Laboratories, 1968).
- Thomson, W.T., *Theory of Vibration with Applications*, 2nd ed (Prentice Hall, 1981), p 65.
- Waterhouse, R.V., "Interference Patterns in Reverberant Sound Fields," *Journal of the Acoustical Society of America*, Vol 27 (1955), pp 247-258.
- Waterhouse, R.V., and R.K. Cook, "Interference Patterns in Reverberant Sound Fields II," *Journal of the Acoustical Society of America*, Vol 37, No. 3 (1965), pp 424-428.
- White, R.W., *Predicted Vibration Responses of Apollo Structure and Effects of Pressure Correlation Length on Response*, WR 67-4 (Wyle Laboratories, March 1967).

APPENDIX A: List of AMD Components and Initial Indication of Potential Sensitivity to Vibro-Acoustic Loads

Items Marked May be Sensitive Components

Description	Qty	Wt.	S	Location	Reference*
Structural					
Columns	14			Perimeter	S-4
Roof Truss Type 1	1			Roof	S-8 A-8
Truss Type 2	5			Roof	S-7 A-8
Truss Member Connections	--		S	Truss	
Roof Joist	30			Roof	S-5 A-8
Joist Connections	--		S	Roof Joists	
Misc. Bracing				Roof Framing	S-5 S-7
Bracing Connectors			S	Misc. Bracing	
Vertical Bracing				Perimeter	S-9 to S-12
Wall Girts				Perimeter	S-13 to S-15
Girt Connections			S	Girts	
Truss Bracing				Lower Chord	S-7
Bracing Connectors			S	Lower Chord	
Monorail				Below L.C.	S-7
Monorail Connectors			S	Monorail/L.C.	
Trolleys	4		S	Monorail	Design 2-21
Roof Deck					
1-1/2" 20GA 6' Span		2.2 psf	S	Roof	S-22
Insulation		0.8 psf	S	Roof	
EPDM Membrane		0.2 psf		Over Roof Deck	A-9
(Not Exposed to Noise)					
Floor					
Trench Drains					
Cover - West	200L'			Parallel to Hangar Doors	S2
Cover - East	72L'			Parallel to Hangar Doors	S2
Cover - North	3L'			At Personnel Door	S-2
Cover - South	3L'			At Personnel Door	S-2
Utility Pits				Center Bay	S-2
Pit Covers				Center Bay	S-2

* Drawings, Design Analysis

Items Marked May be Sensitive Components

Description	Qty	Wt.	S	Location	Reference*
Catwalk Platform	2			Lower Chord	S-5
Catwalk Railings				Lower Chord	
Catwalk Supports			S	Lower Chord	
Support Connectors			S	Lower Chord	
Draft Curtain				Roof Truss	S-5 A-4
3" 20GA					DA 2-25
14' Avg. Height			S		
Draft Curtain Connectors			S		
Hangar Doors - East	2			East Wall	A-5 A-4 A-12 A-9
Hangar Doors - West	6			West Wall	A-6 A-4 A-12 A-9
• 16 GA Liner Panel					
On Interior Face			S		
• Liner Panel					
Attachment			S		
•					
Wall Panels 30" x 2-1/2"				Perimeter	07415-4
• Face Panel 24 GA			S		
• Liner Panel 24 GA					
• Foam Core					
• Panel Connectors			S		
(Panel Span 5' 6" and 7' 6")					
Louvers, Wall	8			East, Above Doors	A-5 M-3
Louvers, Wall	2			West, Above Doors	A-6 M-3
Louvers, Wall	4			EA, End Wall	A-7 M-3
Doors, Personnel	5				A-2

* Drawings, Design Analysis, or Specifications

Items Marked May be Sensitive Components

Description	Qty	Wt.	S	Location	Reference*
Ventilation Equipment					
H.V. (Heat & Vent)			S	East and West	M-1 M-3 M-9
E.V. (Exhaust Vent)	2		S	On Roof and Misc.	M-1 M-3 M-9
HV Supports	10		S		
Ductwork		14 plf	S	Above L.C.	M-1 M-3 15804-16
Duct Supports			S	Above L.C.	15200-3/5
Steam Piping		23 plf	S	Above L.C.	M-1 M-3
Pipe Supports			S	Above L.C.	
Detection Sensors	10		S	Floor and Roof	M-1
Misc. Control Switches			S	East and West Wall	M-1
Electrical					
Hid Lights	56		S	Lower Chord	E-1 E-3 16415-31
Incandescent Lights	10		S	Lower Chord	E-1 E-3 16415-31
Fixture Supports	66		S	Truss Space	
Conduit				Truss Space	
Conduit Hangers			S	Truss Space	
Connectors and Fittings			S	Truss Space	E-7
Misc. Switches			S	Walls	

* Drawings or Specifications

APPENDIX B: Calculation of the Acoustic Environment Inside the AMD

Calculation of the acoustic environment of the AMD has been carried out as detailed in this appendix. This has involved determination of the reverberant field sound levels from the auxiliary power sources (auxiliary power units) and primary noise sources (main engines), and the direct field sound levels from these same noise sources. (The direct sound field from the auxiliary power sources is not significant.) The overall acoustic levels on the AMD structure are then found from an energy sum of these reverberant and direct components of the sound field. In all cases, the effective sound levels on the AMD have been corrected to account for the effect of reflection at the boundaries.

SOUND POWER LEVELS

The starting point for development of the reverberant sound levels was the determination of the sound power output for each source. The sound power levels of the auxiliary power sources and primary noise sources were calculated from sound pressure level data supplied by the U.S. Air Force.

Sound Power Level of Auxiliary Power Sources

The sound power level of the auxiliary noise source, L_w , is calculated from measured near field one-third octave band sound pressure level spectra. This measured level, \bar{L}_p at each frequency was assumed to be a space-averaged value. This level was used to compute the sound power level as follows (Beranek 1971):

$$L_w = \bar{L}_p + 10 \log A - 0.1, \text{ dB re } 10^{-12} \text{ watts} \quad [\text{Eq B1}]$$

where A equals the radiation area in square meters. Microphone position M13 of the auxiliary power source acoustic test report was located 2.5 ft (0.762 m) from the center of the auxiliary power source which was assumed to be nondirectional. Therefore the radiation area A (assuming spherical radiation), would be:

$$A = 4\pi r^2 = 7.30 \text{ m}^2 \quad [\text{Eq B2}]$$

For example, the measured level at the 2.5 ft radius was 99 dB for the 200 Hz one-third octave band. The sound power level of the auxiliary power source at this frequency would be (note that throughout this report, log denotes logarithm to the base 10):

$$\begin{aligned} L_w &= 99 + 10 \log (7.30) - 0.10 \text{ dB} \\ &= 107.5 \text{ dB re } 10^{-12} \text{ watts} \end{aligned}$$

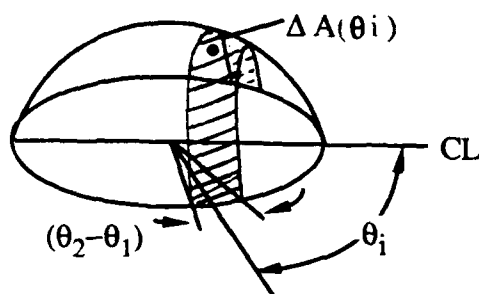
Sound Power Level of Primary Noise Sources

Calculation of sound power levels of the four primary noise sources was carried out in a different fashion, since these noise sources are very directional. The total power is calculated from average sound intensities over axisymmetric segments over the sphere of radiation. For these sources, measured free field data were given in 10 degree increments on a 150 ft (45.7 m) arc from 20° to 160° (the sound field of this source is axisymmetric about the 0-180° axis). The sound levels were actually measured with a

ground plane microphone, however, the tabulated 150 ft sound level data provided to Wyle had been corrected to spherical (free field) conditions by subtracting 6 dB.

Refer to the sketch below, which shows, for simplicity, only half of the spherical radiation area. For the i th angle θ_i , relative to the axis of symmetry of the source a spherical area segment $\Delta A(\theta_i)$ can be defined. It is assumed, by standard conversion for this type of noise source, that the sound pressure level (or more precisely, sound power per unit area) is constant over this segment, i.e., the source directionality pattern is axisymmetric.

By integration, the area of the full spherical segment is given by:



$$\begin{aligned}\Delta A(\theta_i) &= 2 \int_{\theta_2}^{\theta_1} (\pi r \sin \theta) (r d\theta) \\ &= 2\pi r^2 [\cos \theta_1 - \cos \theta_2]\end{aligned}\quad [\text{Eq B3}]$$

where

$$\theta_1 = \begin{cases} \theta_i - 5^\circ & \text{for } \theta_i = 30^\circ \text{ to } 160^\circ \\ 0 & \theta_i = 20^\circ \end{cases}$$

$$\theta_2 = \begin{cases} \theta_i + 5^\circ & \text{for } \theta_i = 20^\circ \text{ to } 150^\circ \\ 180^\circ & \theta_i = 160^\circ \end{cases}$$

Then, applying Eq [B1], the element $L_w(\theta_i, f)$ of total sound power passing through this area segment is, for each one-third octave band frequency,

$$L_w(\theta_i, f) = L_p(\theta_i, f) + 10 \log [\Delta A(\theta_i)] - 0.1, \text{ dB re } 10^{-12} \text{ watts} \quad [\text{Eq B4}]$$

where $L_p(\theta_i, f)$ is the one-third octave band sound pressure level at frequency f .

The overall sound power $L_w(f)$ at this frequency is then given by the energy sum:

$$L_w(f) = 10 \log \sum_i 10^{\frac{L_w(\theta_i, f)}{10}} \text{ dB re } 10^{-12} \text{ watts} \quad [\text{Eq B5}]$$

Repeating this process for each frequency provides the complete sound power spectrum needed to define the reverberant sound field.

Table B1 provides a sample calculation of the one-third octave band sound power level for one of the primary noise sources for the case of 6820 rpm at the peak frequency of the spectrum, 200 Hz.

Table B1

Sample Calculation of One-Third Octave Band Sound Power Level at 200 Hz
(Input Data Provided by Main Engine Manufacturer)

θ_i (degrees)	$L_p(\theta_i, f)$ dB	$\Delta A_i(\theta_i)$ m^2	$10L_w(\theta_i, f)/10$ Rel. Sound Power
20	88.7	1231	9×10^{11}
30	89.3	1145	10×10^{11}
40	90.0	1472	14×10^{11}
50	90.9	1754	21×10^{11}
60	90.0	1983	19×10^{11}
70	91.1	2151	27×10^{11}
80	92.6	2255	40×10^{11}
90	94.9	2289	69×10^{11}
100	96.4	2255	96×10^{11}
110	99.2	2151	175×10^{11}
120	103.0	1983	387×10^{11}
130	109.5	1754	1528×10^{11}
140	114.1	1472	3697×10^{11}
150	114.2	1145	2943×10^{11}
160	114.5	1231	3390×10^{11}
			Total = $12,430 \times 10^{11}$

Note: Total $L_w(f) = 10 \log (12,430 \times 10^{11}) = 150.9 \text{ dB re } 10^{-12} \text{ watts.}$

REVERBERANT SOUND PRESSURE LEVELS

For an ideal diffuse (reverberant) sound field, the sound pressure level at positions well removed from any boundaries is given by Beranek (1971):

$$L_r = L_w - 10 \log \left[\frac{S \bar{\alpha}_t}{4(1 - \bar{\alpha}_t)} \right] + 0.1, \text{ dB} \quad [\text{Eq B6}]$$

where S = Interior surface area, m^2
 $\bar{\alpha}_t$ = Mean acoustic absorption coefficient

$$= \frac{\sum \bar{\alpha}_i S_i + 4mV}{\sum S_i}$$

$\bar{\alpha}_i, S_i$ = Acoustic absorption coefficient and area for i th surface

m = Atmospheric absorption coefficient, m^{-1}

V = Room volume, m^3

Interior Surface Absorption

Based on the geometry of one high-bay area of the AMD shown in Figure B1, the values assumed, for design purposes, for the acoustic absorption for each internal surface are listed in Table B2. Note that for the sake of conservative design, a value of $\alpha = 0$ is used for absorption at the walls and roof instead of a more typical value of $\alpha = 0.1$. This assumption increases the reverberant sound level by 2.2 dB within the margin of error of the environmental estimates. Furthermore, as will be shown later, maximum sound levels inside the AMD are dominated by the direct field and the net increase in maximum sound levels due to this assumption is only 0.2 dB.

One additional conservative assumption should be pointed out. An area of approximately 51 sq. ft on the back wall above the door opening consists of louvers for ventilation purposes. The surface absorption coefficient of this louvered area can be expected to fall between about 0.5 and 0.9. Assuming a value of 0.7, the added acoustic absorption area is 36 m², or less than 5 percent of the total absorption provided by the open doors. The effective reverberant or direct sound levels on these louvers will be somewhat lower than for adjacent wall areas due to a reduced reflection effect but the more flexible nature of these louvers and their potential susceptibility to acoustically-induced vibration dictates that the design acoustic load on these louvered areas not be reduced below that for solid wall areas.

Interior Volume Absorption

Volume absorption inside the AMD will occur due to: (a) atmospheric absorption, and (b) absorption by the internal equipment and test systems. The latter source of acoustic absorption is expected to be a small part of the total and was neglected for this report. The absorption due to atmospheric absorption in the air inside the AMD is defined by the quantity $4mV$ where V is the interior volume m³, and m is the intensity loss coefficient due to atmospheric absorption and equal to:

$$m = \frac{a}{1000 \log(e)}, m^{-1} \quad [\text{Eq B7}]$$

where a equals the atmospheric attenuation coefficient in dB/100m (ANSI S1.26-1978). Based on the dimensions in Figure B1, V equals 28,113 m³ so that:

$$4mV = \frac{(4)(28,113)}{[1000 \times \log(e)]} \times a = 259 \times a, m^2$$

Assuming a standard day of 20°C, 70 percent RH, and defining a , dB/100 m from ANSI S1.26-1978 for these conditions, Table B3 defines the frequency-dependent values for the volume absorption term $4mV$, along with the remaining quantities required to define the total reverberant sound level according to Eq B6, given the total sound powers for the four primary sources or the two auxiliary power sources.

Reverberant Sound Pressure Levels on AMD Structures

The reverberant sound level L_r defined by Eq B6 is the free field value for positions well removed from any surface. The effective reverberant levels on the AMD structure must account for the effect of reflection at the surface of the structure. As shown in Waterhouse (1955), at all wall surfaces, a correction of +3 dB must be added to values of L_r from Eq 6 to define effective reverberant field sound levels on the surface. At a wall-roof or wall-floor edge, the correction is +6 dB, and +9 dB at a 3 plane corner.

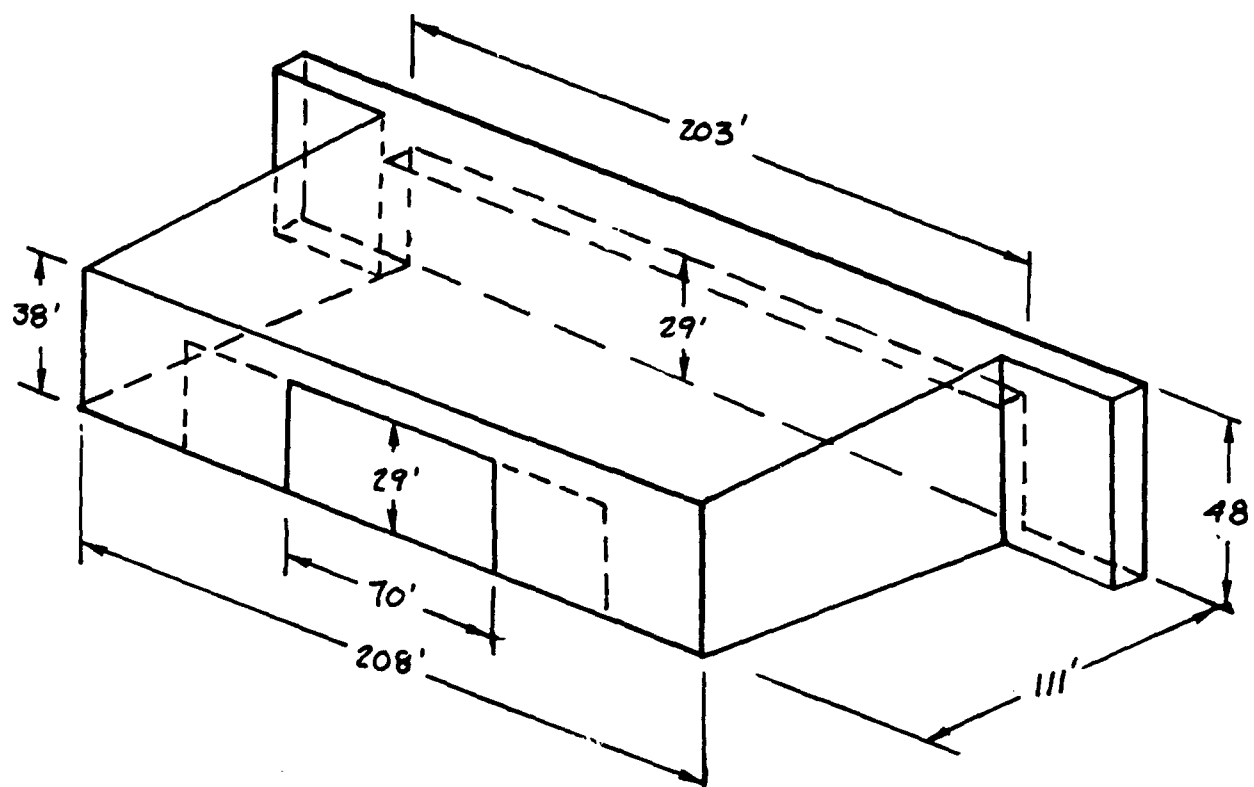


Figure B1. Rear view of one high bay area of AMD (approximate interior dimensions in feet).

Table B2

Interior Surface Acoustic Absorption for AMD

Surface Element	Area (S_i)		(α_i)	Absorption	
	ft ²	m ²		Base** m ²	Design*** m ²
Sides	9,546	887	0.2	89	0
Floor	23,088	2,145	0	0	0
Roof	23,181	2,154	0.2	215	0
Back Wall†	5,874	546	0.2	55	0
Front Wall	4,097	381	0.2	38	0
Back Door	2,030	189	1.0	189	189
Front Door	<u>5,887</u>	<u>547</u>	<u>1.0</u>	<u>547</u>	<u>547</u>
TOTAL AREA	73,703	6,849	$\Sigma(\alpha_i S_i) = 1,133$		736

* Range of absorption coefficients evaluated for walls and roof.

** Baseline values for absorption using $\alpha = 0.1$ for walls and roof.

*** Design values for absorption using $\alpha = 0$ for walls and roof.

† Including inside surface of opened back door located along back wall.

Table B3

Summary of Calculation of Reverberant Sound Pressure Levels

Design Case, α (Walls, Roof) = 0

1/3rd o.b. Freq Hz	Alpha [*] db/100m	4mV m ²	$\bar{\alpha}_1$ ^{**}	Lr-Lw dB	-----Lw ^{***} -----		-----Lr†-----	
					Main Engines dB	APU dB	Main Engines dB	APU dB
12.5	0.0004	0.09	0.107	-23.0	126.0		106.0	
16	0.0006	0.15	0.107	-23.0	128.8		108.8	
20	0.0009	0.24	0.107	-23.0	132.6	83.5	112.6	63.5
25	0.0014	0.37	0.108	-23.0	135.8	94.5	115.8	74.5
31.5	0.0023	0.59	0.108	-23.0	139.6	93.5	119.6	73.5
40	0.0036	0.94	0.108	-23.0	142.4	95.0	122.4	75.0
50	0.006	1.47	0.108	-23.1	145.3	96.5	125.2	76.5
63	0.009	2.32	0.108	-23.1	147.3	100.5	127.2	80.5
80	0.014	3.69	0.108	-23.1	149.7	105.5	129.6	85.5
100	0.022	5.68	0.108	-23.1	151.9	106.5	131.8	86.5
125	0.034	8.67	0.109	-23.1	153.7	106.5	133.6	86.4
160	0.053	13.6	0.109	-23.1	155.1	109.0	135.0	88.9
200	0.078	20.2	0.110	-23.2	157.0	110.5	136.8	90.4
250	0.112	29.1	0.112	-23.2	158.4	113.5	138.2	93.3
315	0.159	41.1	0.113	-23.3	155.7	110.6	135.4	90.3
400	0.217	56.3	0.116	-23.4	154.4	113.9	134.0	93.5
500	0.279	72.3	0.118	-23.5	153.3	110.5	132.8	90.0
630	0.348	90.0	0.121	-23.6	151.9	111.5	131.3	90.9
800	0.422	109	0.123	-23.7	150.5	119.0	129.8	98.3
1000	0.498	129	0.126	-23.8	149.6	108.4	128.8	87.6
1250	0.589	153	0.130	-24.0	148.3	113.4	127.3	92.5
1600	0.725	188	0.135	-24.2	147.0	113.4	125.8	92.3
2000	0.905	234	0.142	-24.4	145.5	113.5	124.1	92.1
2500	1.174	304	0.152	-24.8	143.9	113.9	122.1	92.2
3150	1.606	416	0.168	-25.3	143.0	116.5	120.7	94.2
4000	2.312	599	0.195	-26.1	145.2	117.0	122.1	94.0
5000	3.351	867	0.234	-27.1	141.6	118.1	117.5	94.1
6300	5.031	1303	0.298	-28.5	134.6	118.7	109.1	93.2
8000	7.778	2014	0.401	-30.5	131.1	119.8	103.6	92.3
10000	11.774	3048	0.553	-33.2	127.8	124.5	97.6	94.4

* Attenuation coefficient due to atmospheric absorption from ANSI S1.26-1978 for temperature = 20 °C, relative humidity = 70 percent.

** Total absorption coefficient for sum [$\bar{\alpha}_i \times S = 736 \text{ m}^2$] for design case; see Eq B6.

*** Total sound power level in dB re: $10^{(-12)}$ watts for 4 main engines and 2 APU's

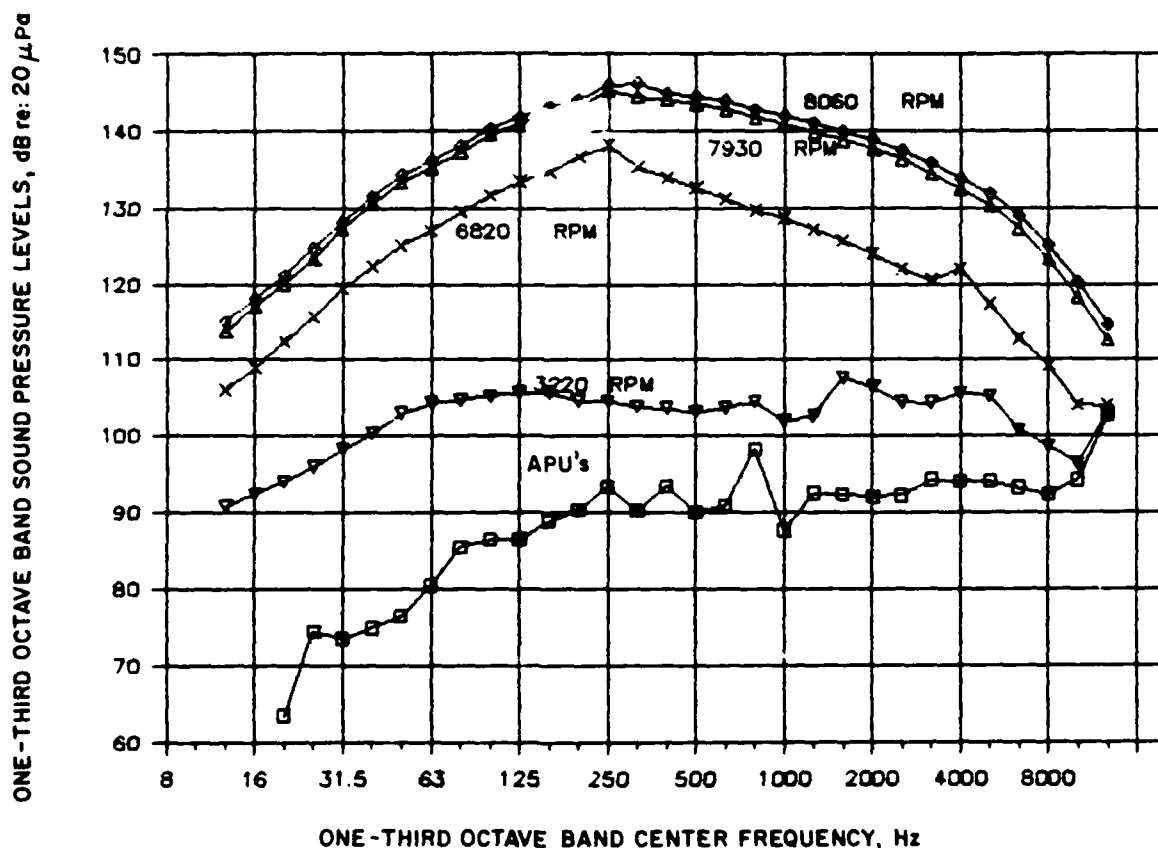
† Resultant total sound pressure level on inside of AMD walls (Add 3 dB at edge or 6 dB at corner).

The last two columns in Table B3 list these resultant reverberant one-third octave band sound pressure levels, including the +3 dB correction to account for the reflection effect at the AMD interior wall and roof surfaces.

Figure B2 shows the estimated one-third octave band reverberation sound pressure level spectra at any interior surface of the AMD, not close to an interior edge or corner. The figure shows this spectra computed according to the preceding methods for four different power (rpm) settings of the primary source and for a maintenance power setting for the auxiliary power units. The levels labeled with an rpm are the composite values for four main engines and two auxiliary power units operating simultaneously.

DIRECT SOUND FIELD

The direct sound field for the auxiliary power units was calculated from measured near field data, assuming a nondirectional point source. For the main engine, sound level contours measured in the near field of one engine was used to estimate the direct sound field for four such engines operating simultaneously.



(Source at reference position, 40 ft from back wall, absorption coefficient for walls and roof = 0.)

Figure B2. Composite reverberant sound level spectra on walls of AMD facility for various power settings (rpm) of main engines or for auxiliary power units operating at maintenance power.

Direct Field Sound Pressure Levels from Auxiliary Power Units

The direct sound field for the auxiliary power unit can be defined from the measured near field levels for this assumed nondirectional source. The applicable expression for the one-third octave band sound pressure level L_p of this source is:

$$L_p = L_p(\text{ref}) + 10 \log \left(\frac{R}{2.5} \right)^2, \text{ dB re } 20 \mu\text{Pa} \quad [\text{Eq B8}]$$

where

$L_p(\text{ref})$ = The measured one-third octave band sound pressure level at 2.5 ft, dB

R = Distance from the center of the auxiliary power units to the desired location where the direct field level is to be defined, ft

Figure B3 shows the one-third octave band sound pressure level data provided to USACERL which was measured at a 2.5 ft radius for one auxiliary power unit at a normal maintenance power setting and at MES power setting. The latter condition is associated with initial operation of the main engines. The levels for the two conditions are essentially identical. The reference positions of the two auxiliary power units are:

- Fore and Aft - 73.5 ft forward of back wall
- Lateral ± 18.5 ft on either side of AMD centerline
- Vertical 14 ft above floor.

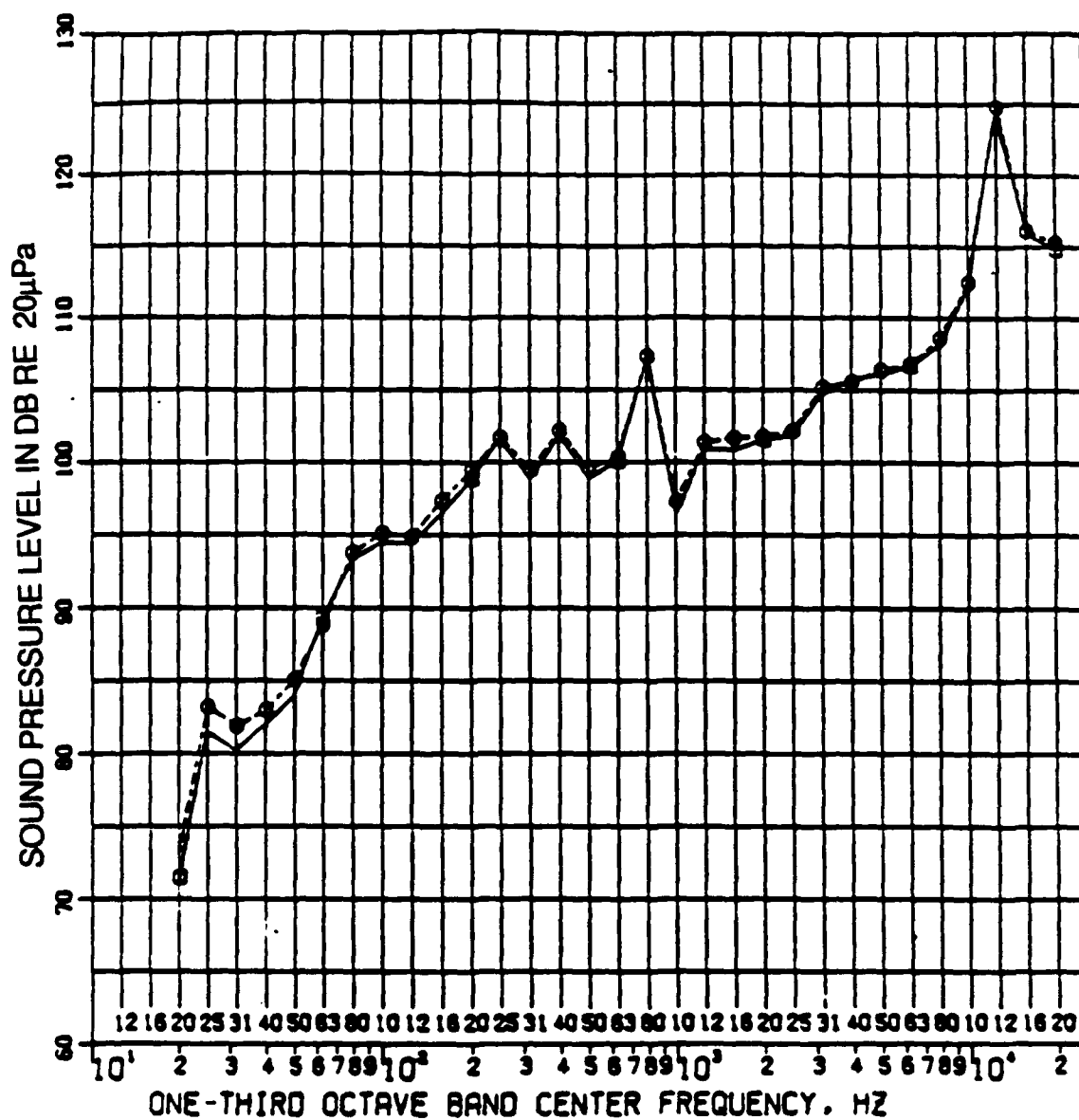
Based on Eq B8, the maximum one-third octave band level at frequencies significant for structural response (below 1000 Hz) will be less than about 91 dB of the bottom of the draft curtain ($R = 16$ ft) the closest AMD structure to the auxiliary power units. Such levels will not generate significant structural vibration response at the draft curtain structure or any adjacent structure-mounted equipment, and can be ignored.

Direct Field Sound Pressure Levels from Main Engines

As indicated earlier, near field noise contours of one-third octave band levels for the main engine were provided to USACERL in the main engine manufacturer's test report. Figure B4 shows a typical example of such contours for the 200 Hz one-third octave band and for a power setting corresponding to 6820 rpm. Also shown on the figure are elevation and plan views of the positions that the roof and back wall respectively would occupy for the nominal reference position of one of the main engines. Both of the views can be shown in this figure since the noise contours can be rotated, without change, about the axis of symmetry of the engine.

The reference positions of the exit planes of the four main engines are:

- Fore and aft 40 ft forward of back wall
- Lateral ± 10.4 and ± 15.1 ft on either side of AMD centerline
- Vertical 13 ft above floor.

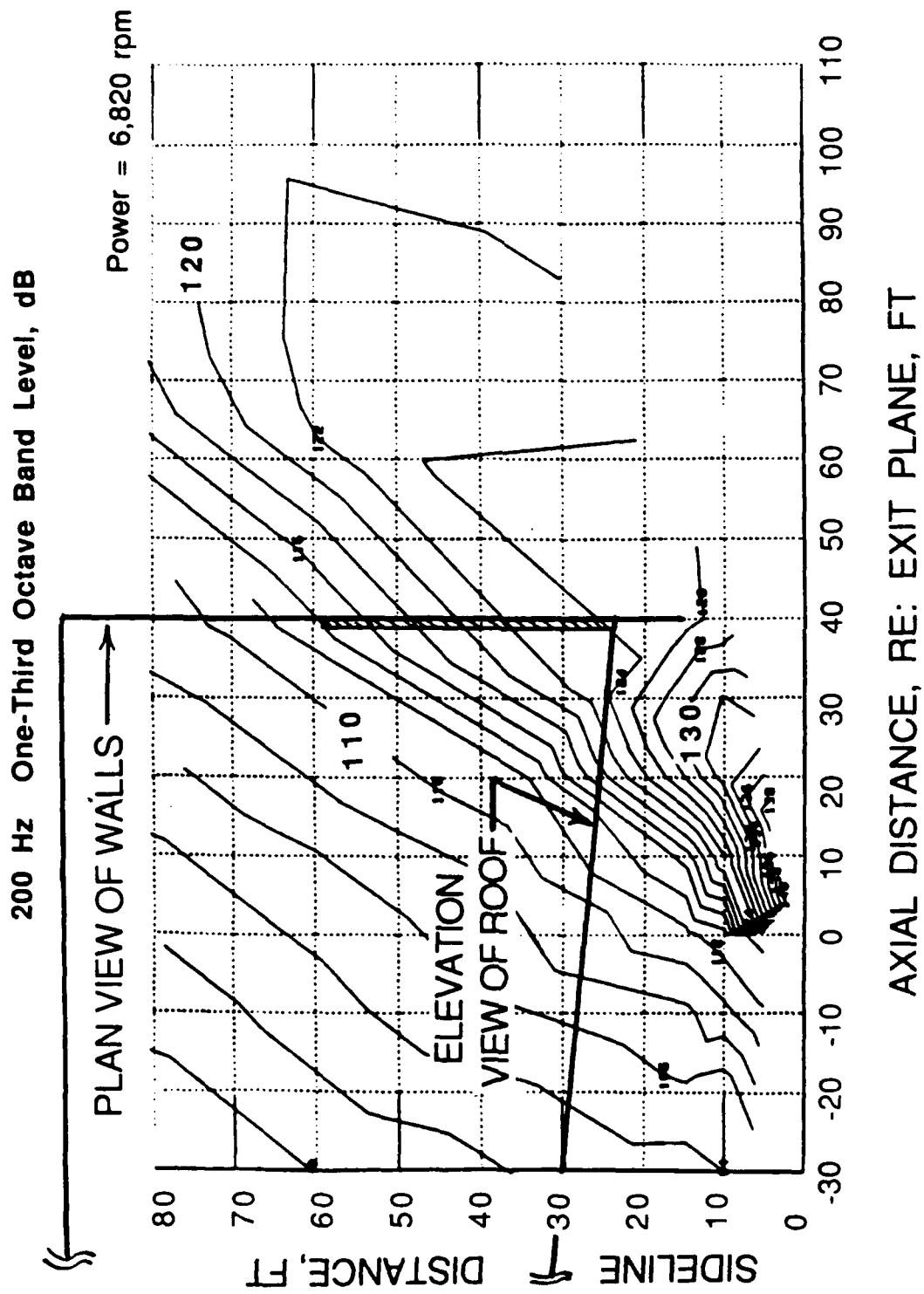


□ - Maintenance power setting

○ - MES power setting

(Data from auxiliary power source manufacturer.)

Figure B3. One-third octave band sound pressure levels at radius of 2.5 ft from center of auxiliary power unit.



(Source: main engine test data.)

Figure B4. Near field sound pressure level contours for one of four main engines.

Development of the direct field sound levels on the AMD structure for the main engines involved use of the type of overlay on noise contours illustrated in Figure B4 and, using interpolation where necessary, establishing the near field levels at positions of interest on the AMD structure. For each of the main engines this process was carried out for each set of the contours provided for one-third octave band sound levels, at octave band frequency intervals, from 50 to 6300 Hz. This process was repeated for each of the four main engines and the total direct field sound pressure levels determined by an energy summation.

The process was also repeated for representative (worst case) locations along the AMD roof centerline for alternate (further forward) positions of the primary noise sources.

TABULATED RESULTS

Following the procedures outlined in the preceding section, composite (energy sum) reverberant plus direct sound pressure levels have been determined for all four main engines operating at 6820 rpm or idle (3215 rpm) and for the two auxiliary power units operating at maintenance power. These composite levels have been computed for the sources in their reference positions, as specified in Chapter 2, or at alternate engine positions 20 ft and 40 ft forward and at the positions on the AMD structure indicated by the dashed lines or filled squares shown in Figure B5. These results are provided in Tables B4 through B12, in terms of one-third octave band sound pressure levels at octave frequency intervals from 50 to 6300 Hz.

<u>Table</u>	<u>Location</u>
B4	Roof ($y = 0$ to 110.4 ft, $z = 37.25$ -47.25 ft)
a.	$x = 103.7$ ft, centerline of roof
b.	$x = 91$ ft, midway between two main engines
c.	$x = 81$ ft
d.	$x = 71$ ft
e.	$x = 61$ ft
B5	Back Wall ($y = 0$, $x = 0$ to 103.7 ft)
a.	$z = 37.25$ ft, upper edge of back wall
b.	$z = 29$ ft, at height of back door
c.	$z = 20$ ft, halfway between (b) and (d)
d.	$z = 11$ ft, 2 ft below height of main engines
e.	$z = 0$ ft, lower edge of back wall
B6	Across bottom edge of draft curtain ($x = 67.7$ to 103.7 ft, $y = 55$ ft, $z = 30$ ft)
B7	Up from center of back door and then along centerline of roof
a.	Main engines at 40 ft, 6820 rpm
b.	Main engines at 60 ft, 6820 rpm
c.	Main engines at 80 ft, 6820 rpm
B8	Same as Table B6 except main engines at idle power
B9	Lower midpoint of draft curtain for three positions of main engines ($y = 40$, 60 and 80 ft)
a.	6820 rpm
b.	Idle rpm.

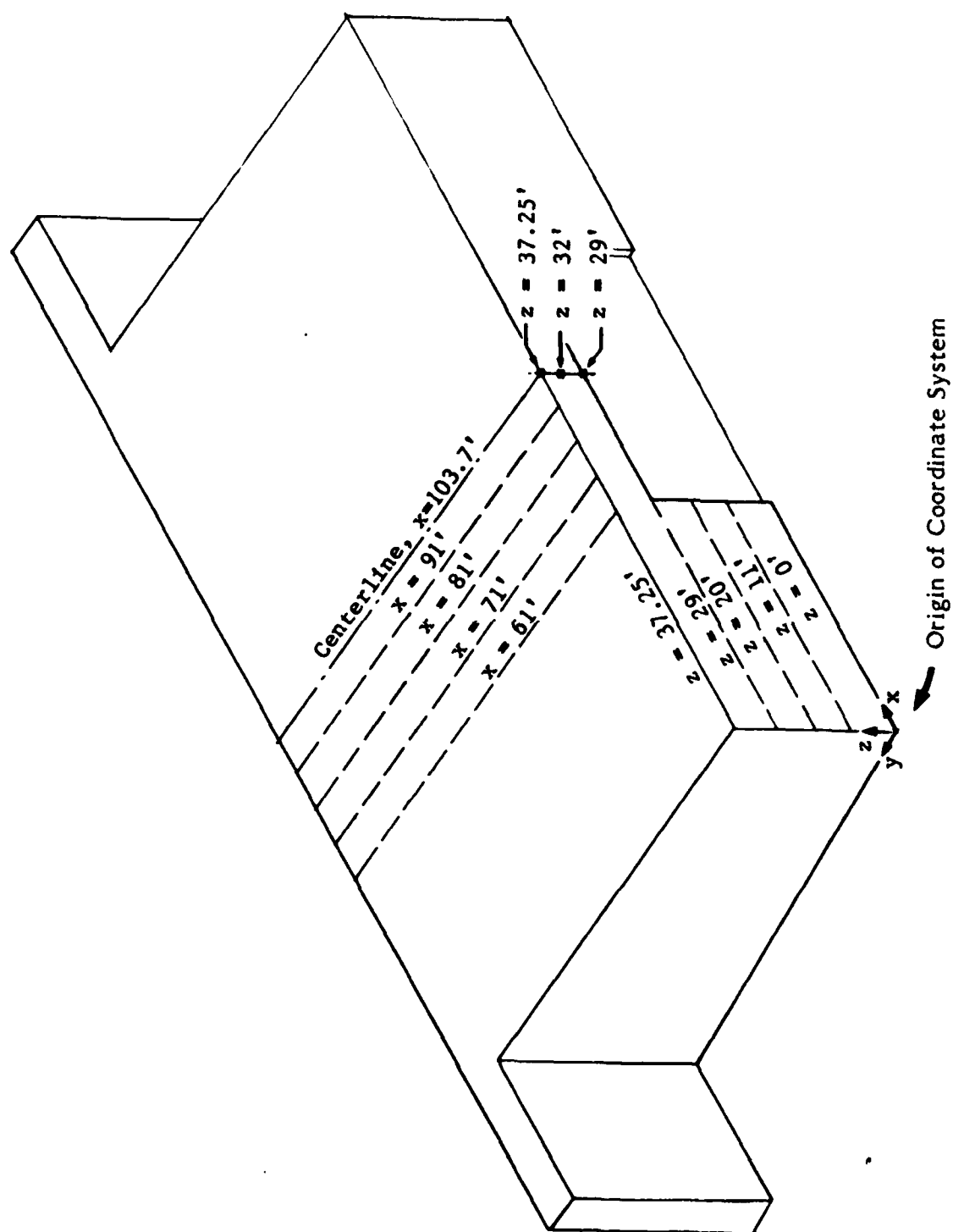


Figure B5. Location of positions where sound levels on the inside of the AMD structure are tabulated.

**Composite Reverberant Plus Direct One-Third Octave Band Sound Pressure Levels on Roof
(Main Engines at Y = 40 ft, 6820 rpm)**

[illegible][illegible]

Page 11

[illegible]

c) ACROSS THE ROOF 1" OUT FROM MIDWAY BETWEEN SOURCES 1a AND 1b,

[illegible]

(p) ACROSS THE ROOF 20 OUT FROM MIDWAY BETWEEN SOURCES 10 AND 10

[illegible]

(2e) ACROSS THE ROOF 30' OUT FROM MIDWAY BETWEEN SOURCES 1a AND 1b

[illegible]

Table B5

Composite Reverberant Plus Direct One-Third Octave Band Sound Pressure Levels on Back Wall
(Main Engines at Y = 40 ft, 6820 rpm)

a) UPPER END OF BACK WALL

Pos., ft	9	3.7	13.7	23.7	33.7	43.7	49.7	53.7	58.7	63.7	68.7	73.7	78.7	83.7	88.7	93.7	98.7	103.7
x	0	0	0	0	0	0	0	0	0	0	0	0	0	0	0	0	0	0
y	0	0	0	0	0	0	0	0	0	0	0	0	0	0	0	0	0	0
z	37.25	37.25	37.25	37.25	37.25	37.25	37.25	37.25	37.25	37.25	37.25	37.25	37.25	37.25	37.25	37.25	37.25	37.25
Freq.																		
Hz	50	131.2	128.3	128.3	128.3	128.3	128.3	128.4	128.4	128.4	128.5	128.5	128.6	128.7	128.7	128.8	128.8	128.8
100	137.8	134.8	134.8	134.8	134.9	134.9	134.9	135.0	135.0	135.1	135.2	135.3	135.3	135.4	135.4	135.5	135.5	135.5
200	142.8	139.8	139.8	139.9	139.9	140.0	140.0	140.1	140.3	140.4	140.5	140.6	140.6	140.9	141.0	141.1	141.2	141.2
400	146.1	137.1	137.1	137.1	137.2	137.2	137.3	137.4	137.6	137.7	138.0	138.2	138.4	138.6	138.7	138.9	139.0	139.0
800	135.8	132.9	133.0	133.1	133.2	133.4	133.5	133.7	133.9	134.1	134.2	134.4	134.4	134.5	134.6	134.7	134.8	134.6
1600	131.4	128.8	128.9	129.0	129.2	129.4	129.5	129.6	129.7	129.9	130.1	130.1	130.1	130.1	130.2	130.3	130.1	130.1
3150	126.7	123.9	124.0	124.1	124.3	124.4	124.5	124.7	124.8	125.0	125.1	125.1	125.1	125.2	125.3	125.3	125.1	125.1
6300	117.7	117.2	117.4	117.6	117.9	118.2	118.3	118.4	118.6	118.8	118.8	118.9	118.9	118.8	118.9	118.8	118.7	118.7

b) BACK WALL AT HEIGHT OF TOP OF BACK DOOR

Pos., ft	0	3.7	13.7	23.7	33.7	43.7	48.7	53.7	58.7	63.7	68.7	73.7	78.7	83.7	88.7	93.7	98.7	103.7
x	0	0	0	0	2	2	2	2	2	2	2	2	2	2	2	2	2	2
y	0	0	0	0	2	2	2	2	2	2	2	2	2	2	2	2	2	2
z	29	29	29	29	29	29	29	29	29	29	29	29	29	29	29	29	29	29
Freq.																		
Hz	50	128.3	125.3	125.3	125.3	125.4	125.4	125.5	125.6	125.7	125.8	126.2	126.5	126.9	127.1	127.2	127.1	127.1
100	134.8	131.9	131.9	131.9	132.0	132.1	132.2	132.4	132.4	132.6	133.0	133.5	134.0	135.0	135.3	135.3	135.4	135.2
200	139.8	136.9	136.9	136.9	137.0	137.2	137.3	137.5	137.8	138.1	138.3	138.7	139.0	139.3	139.4	139.6	139.7	139.7
400	137.1	134.1	134.2	134.2	134.3	134.5	134.7	135.0	135.4	135.8	136.3	136.7	137.0	137.3	137.5	137.8	137.9	138.2
800	132.9	130.1	130.3	130.5	130.7	131.2	131.5	131.6	132.2	132.5	132.7	132.9	132.9	133.0	133.0	133.0	132.9	132.9
1600	128.8	126.1	126.3	126.5	126.8	127.2	127.4	127.6	128.3	128.5	128.6	128.6	128.6	128.1	128.1	128.0	127.7	127.4
3150	123.9	121.3	121.5	121.7	122.0	122.3	122.5	122.8	123.1	123.3	123.3	123.4	123.6	123.6	123.6	122.9	122.8	122.6
6300	117.1	115.0	115.5	115.8	116.6	116.9	117.2	117.3	117.4	117.6	117.7	117.1	117.1	117.1	117.1	116.9	116.7	116.7

c) BACK WALL AT HEIGHT BETWEEN TOP OF BACK DOOR AND HEIGHT OF SOURCES 1a-2b,

Pos., ft	0	3.7	13.7	23.7	33.7	43.7	48.7	53.7	58.7	63.7	68.7							
x	0	0	0	0	2	2	2	2	2	2	2							
y	0	0	0	0	2	2	2	2	2	2	2							
z	20	20	20	20	20	20	20	20	20	20	20							
Freq.																		
Hz	50	128.3	125.3	125.3	125.3	125.4	125.5	125.5	125.6	125.8	126.1							
100	134.8	131.9	131.9	131.9	132.1	132.1	132.2	132.4	132.7	133.4	134.1							
200	139.8	136.9	136.9	137.0	137.2	137.4	137.5	137.7	138.1	138.4	138.6							
400	137.1	134.1	134.2	134.2	134.3	134.6	134.8	135.1	135.7	136.2	136.7							
800	132.9	130.1	130.3	130.5	130.9	131.5	131.6	132.2	132.5	132.7	132.8							
1600	128.8	126.2	126.3	126.5	126.8	127.4	127.7	128.0	128.3	128.4	128.3							
3150	123.9	121.3	121.5	121.7	122.0	122.4	122.7	123.0	123.2	123.3	123.3							
6300	117.2	115.1	115.5	115.8	116.6	116.9	117.2	117.3	117.4	117.4	117.3							

Table B5 (Cont'd)

d) BACK WALL AT HEIGHT OF SOURCES 1a-2b, $z = 13$ ft

Pos., ft											
x	0	3.7	13.7	23.7	33.7	43.7	48.7	53.7	58.7	63.7	68.7
y	0	0	0	0	2	2	2	2	2	2	2
Freq.											
Hz											
50	128.3	125.3	125.3	125.3	125.4	125.4	125.5	125.6	125.7	125.8	126.1
100	134.8	131.9	131.9	131.9	131.9	132.1	132.2	132.4	132.9	133.4	134.5
200	139.8	136.9	136.9	137.0	137.0	137.2	137.5	137.7	138.1	138.4	138.6
400	137.1	134.1	134.2	134.2	134.3	134.6	134.9	135.4	135.8	136.2	136.7
800	132.9	130.2	130.3	130.5	130.9	131.5	131.8	132.2	132.5	132.7	132.7
1600	128.8	126.2	126.3	126.6	126.8	127.4	127.8	128.2	128.3	128.1	128.0
3150	123.9	121.3	121.5	121.7	122.2	122.4	122.7	123.0	123.3	123.2	123.1
6300	117.2	115.1	115.5	115.9	116.6	116.9	117.2	117.3	117.4	117.4	117.3

e) FLOOR EDGE OF BACK WALL, $z = 0$ ft

Pos., ft											
x	0	3.7	13.7	23.7	33.7	43.7	48.7	53.7	58.7	63.7	68.7
y	0	0	0	0	2	2	2	2	2	2	2
Freq.											
Hz											
50	131.2	128.3	128.3	128.3	128.3	128.3	128.4	128.4	128.4	128.5	128.6
100	137.8	134.8	134.8	134.8	134.9	134.9	135.0	135.1	135.3	135.5	135.9
200	142.8	139.8	139.9	139.9	139.9	140.0	140.1	140.3	140.5	140.6	140.7
400	140.1	137.1	137.1	137.1	137.2	137.3	137.5	137.6	137.9	138.2	138.5
800	135.8	132.9	133.0	133.1	133.3	133.7	133.9	134.0	134.3	134.4	134.5
1600	131.6	128.8	128.9	129.0	129.2	129.5	129.7	129.9	130.1	130.2	130.0
3150	126.7	123.9	124.0	124.1	124.3	124.6	124.7	124.9	125.0	125.1	125.1
6300	119.8	117.3	117.5	117.7	118.2	118.5	118.7	118.8	118.8	118.9	118.9

Table B6

Composite Reverberant Plus One-Third Octave Band Sound Pressure Levels
Across Bottom Edge of Draft Curtain
(Main Engines at Y = 40 ft, 6820 rpm)

Pos., ft									
x	67.7	73.7	78.7	83.7	88.7	93.7	98.7	103.7	
y	55	55	55	55	55	55	55	55	
z	30	30	30	30	30	30	30	30	
Freq.									
Hz									
50	125.3	125.3	125.3	125.3	125.3	125.3	125.3	125.3	
100	131.8	131.9	131.9	131.9	131.9	131.9	131.9	131.9	
200	136.9	136.9	136.9	136.9	136.9	136.9	136.9	136.9	
400	134.1	134.1	134.2	134.2	134.2	134.2	134.2	134.2	
800	130.8	130.8	130.8	130.8	130.1	130.1	130.1	130.1	
1600	126.8	126.8	126.1	126.2	126.2	126.2	126.2	126.2	
3150	121.4	121.5	121.6	121.6	121.6	121.7	121.7	121.7	
6300	115.4	115.6	115.8	115.8	115.8	115.9	116.0	116.0	

**Composite Reverberant Plus Direct One-Third Octave Band Sound Pressure Levels
Along Line from Center of Back Door Opening Up to Roof and Then Along Roof Centerline
(for three different positions of source: 40 ft, 60 ft, and 80 ft, all at 6820 rpm)**

UP FROM TOP CENTER OF FACT DOOR, THEN
ACROSS THE ROOF AT THE CENTER LINE, SOURCES AT
Y=40

[illegible]

UP FROM TOP CENTER OF BACK DOOR, THEN
ACROSS THE ROOF AT THE CENTER LINE, SOURCES AT Y=60

[illegible]

UP FROM TOP CENTER OF RACK DOOR, THEN
ACROSS THE ROOF AT THE CENTER LINE, SOURCES AT Y=80

[illegible]

**Composite Reverberant Plus Direct One-Third Octave Band Sound Pressure Levels
Along Line from Center of Back Door Opening Up to Roof and Then Along Roof Centerline
(for three different positions of source: 40 ft, 60 ft, and 80 ft. all at idle power [3215 rpm])**

[illegible]

(C) UP FROM TOP CENTER OF THE BACK DOOR, THEN ACROSS THE ROOF AT THE CENTER LINE, SOURCES AT Y=40

[illegible]

c) UP FROM TOP CENTER OF THE BACK DOOR, THEN ACROSS THE ROOF AT THE CENTER LINE, SOURCES AT $v=80$

[illegible]

Table B9

Composite Reverberant Plus Direct One-Third Octave Band Sound Pressure Levels At Lower Midpoint of Back Side at Draft Curtain

Note: Data for three different positions of main engine:

Y = 40 ft, 60 ft and 80 ft

(a) for 6820 rpm, and (b) for idle rpm

(a) 6820 rpm

Position	----- Source at -----		
ft	40	60	80
X	103.7	103.7	103.7
Y	55	55	55
Z	30	30	30
Freq.			
Hz			
50	125.3	125.4	126.3
100	131.9	132.0	133.9
200	136.9	137.0	139.5
400	134.2	134.6	138.0
800	130.2	131.4	134.1
1600	126.4	128.2	130.4
3150	121.8	125.1	125.4
6300	115.8	123.0	120.4

(b) Idle rpm

ft	----- Source at -----		
ft	40	60	80
X	103.7	103.7	103.7
Y	55	55	55
Z	30	30	30
Freq.			
Hz			
50	103.2	103.9	104.4
100	105.7	106.7	108.7
200	105.6	107.0	107.7
400	104.8	106.9	106.6
800	106.0	107.9	106.4
1600	108.5	109.2	108.3
3150	105.4	106.9	105.3
6300	103.6	108.5	105.3

Table B10

**Effect of Changing Absorption Coefficient for Walls and Roof From
0 (Hard) to 0.1 (Soft) On Sound Levels On the Roof Centerline, 5 ft Forward**
(Main engines at 40 ft. 6820 rpm)

Position	---- a(walls) ----	
ft	0	0.1
X	103.7	103.7
Y	5	5
Z	37.7	37.7
Freq.		
Hz		
50	126.0	124.3
100	133.8	132.6
200	138.8	137.6
400	137.3	136.5
800	134.0	133.4
1600	129.3	128.7
3150	124.3	123.8
6300	118.6	118.2

Table B11

**Effect of Closing Doors with Only APUs Operating on Level
at Bottom Center of Back of Draft Curtain**
(Units at 40 ft, main engines off)

Position	Doors	Doors
ft	Open	Closed
X	103.7	103.7
Y	55	55
Z	30	30
Freq.		
Hz		
50	77.1	79.9
100	87.1	89.9
200	91.0	93.8
400	94.3	96.8
800	99.3	101.5
100	93.5	95.4
3150	96.2	97.7
6300	97.4	98.2

Table B12

**Change in Level for Operation at Idle, 6820, and 8060 rpm
(Main engines at 40 ft)**

(a) On the roof centerline, 5 ft forward.

Position			
ft	Idle	6820	8060
X	103.7	103.7	103.7
Y	5	5	5
Z	37.7	37.7	37.7
Freq.			
Hz			
50	104.1	125.6	135.0
100	107.3	136.5	141.9
200	106.4	144.1	147.1
400	105.5	146.8	148.9
800	105.7	145.0	147.0
1600	107.8	142.0	144.0
3150	104.7	138.3	140.2
6300	103.3	135.0	136.1

(b) Between the top of the back door and the roof, at the center.

Position			
ft	Idle	6820	8060
X	103.7	103.7	103.7
Y	0	0	0
Z	32	32	32
Freq.			
Hz			
50	104.6	129.8	135.8
100	107.5	140.8	143.7
200	106.3	146.4	148.4
400	104.9	147.1	149.2
800	105.2	143.8	146.3
1600	107.6	139.4	142.6
3150	104.6	136.2	139.0
6300	102.5	132.5	134.3

(c) To the side of the back door at the height of the sources.

Position			
ft	Idle	6820	8060
X	68.7	68.7	68.7
Y	2	2	2
Z	13	13	13
Freq.			
Hz			
50	104.1	127.7	135.3
100	107.1	138.7	142.7
200	106.1	144.2	147.1
400	104.8	145.3	148.1
800	105.5	142.7	145.7
1600	107.7	139.3	142.5
3150	104.7	136.1	139.0
6300	102.9	132.8	134.4

The results of additional cases studied are also tabulated as follows:

<u>Table</u>	<u>Condition/Location</u>
B10	Effect of changing absorption coefficient for walls and roof from 0 (hard) to 0.1 (soft), 5 ft forward at back wall on roof centerline (engines at 40 ft, 6820 rpm)
B11	Effect of closing doors with only auxiliary power units operating on level at bottom center of back of draft curtain. (Units at 40 ft, maintenance power for auxiliary power units)
B12	Change in level for operation at idle (3215 rpm), 6820 rpm and 8060 rpm (sources at 40 ft)
a.	At 5 ft forward of back wall on roof centerline (x,y,z = 103.7, 5, 37.7 ft)
b.	At center of back wall between roof and top of back door (x,y,z = 103.7, 0, 32 ft)
c.	On back door and 2 ft below height of sources (x,y,z = 68.7, 2, 11 ft).

A full discussion of the significance of these tabulated results is presented in Chapter 3 of the main body of this report.

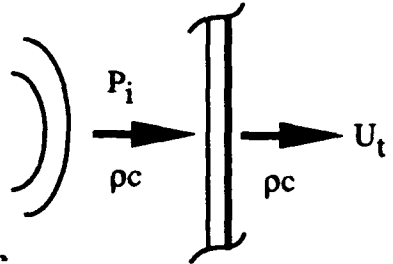
Finally, a brief investigation was made to ensure that the predicted sound levels would not be sensitive to changes in temperature, humidity, or pressure altitude. For changes in temperature from 15° F to 25° F, relative humidity from 20 to 70 percent, and pressure altitude from sea level to 5000 ft, the change in sound level was negligible (less than 0.5 dB).

APPENDIX C: Near Field and Approximate Angle of Incidence Effects on Acoustic Loads on Walls and Roof of AMD

This appendix considers additional details concerning the acoustic loads on AMD surfaces from the direct sound field. It is shown that it is not necessary to consider near field effects (i.e., curvature of the wave front) in evaluating panel responses. Furthermore, it is shown that the effective sound pressure on the panel can be assumed to be equal to twice the incident pressure, regardless of the angle of incidence of the direct field. However, angle of incidence effects, per se, require the more sophisticated analysis presented in Appendix D.

EFFECTIVE DIRECT SOUND PRESSURES IN NEAR FIELD

For a plane wave of sound normally incident on a flexible wall, it can be shown that the rms vibration velocity U_t of the panel due to the incident sound field is given by:



$$U_t = \frac{2P_i}{Z_w + 2\rho c} \quad [\text{Eq C1}]$$

where: P_i = rms sound pressure of incident sound wave

Z_w = specific transmission impedance of wall

ρc = specific acoustic impedance of air on both sides of wall (product of density ρ and speed of sound c)

This expression makes clear one basic point about defining the acoustic load on a wall; the effective driving pressure is $2 P_i$, which is the "pressure doubled" value that would be measured on a rigid wall.

If the source of the incident sound field is at a distance from the wall and is considered, for a first approximation, to be a point source, the amplitudes of the incident, reflected, and transmitted sound waves can be defined in complex form as follows, where $k = 2\pi f/c$, the wave number, f = frequency, c = speed of sound, and $j = (-1)^{1/2}$

Incident wave

$$\frac{P_i}{U_i} = \frac{\rho c}{1 - \frac{j}{kr}} \quad [\text{Eq C2}]$$

Reflected wave

$$\frac{P_r}{U_r} = \frac{-\rho c}{1 - \frac{j}{kr}} \quad [\text{Eq C3}]$$

Transmitted wave

$$\frac{P_t}{U_t} = \rho c \quad [\text{Eq C4}]$$

The first two expressions define the relationships between incident (direct sound) and reflected (image source) spherical waves for a plane reflector while the last expression assumes that the transmitted wave radiated by the flexible reflecting surface (wall) is a plane wave radiated normally to wall.

Including the boundary conditions:

- Total pressure on source side of wall = $P = P_i + P_r$
- Wall velocity $U_t = U_i + U_r$
- $Z_w = (P - P_t)/U_t$

and solving for U_t ,

$$U_t = \frac{P - P_t}{Z_w} = \frac{P_i + P_r + P_t}{Z_w} \quad [\text{Eq C5}]$$

it can be shown that the absolute value of U_t is:

$$U_t = \frac{2P_i}{\sqrt{(Z_w + 2\rho c)^2 + \left(\frac{Z_w + \rho c}{kr}\right)^2}} \quad [\text{Eq C6}]$$

Comparing this to Eq C1, the ratio of the amplitudes of the panel velocity in the near field ($r \rightarrow 0$) of a point source to the velocity for excitation by a plane wave ($r \rightarrow \infty$) with the same incident sound pressure, P_i , is:

$$\frac{U_t(r \rightarrow 0)}{U_t(r \rightarrow \infty)} = \frac{Z_w + 2\rho c}{\sqrt{(Z_w + 2\rho c)^2 + \left(\frac{Z_w + \rho c}{kr}\right)^2}} = \frac{1}{\sqrt{1 + \left[\frac{Z_w + \rho c}{kr(Z_w + 2\rho c)}\right]^2}} \quad [\text{Eq C7}]$$

The maximum panel velocity response will tend to occur at the fundamental resonance frequency (f_0) of the panel. At this frequency, Z_w can be approximated by a pure resistance equal to:

$$Z_w \equiv \frac{2\pi f_0 \frac{\bar{M}}{A}}{Q} \quad [\text{Eq C8}]$$

where \bar{M} = Generalized mass of panel (equal to 1/4 panel weight/g for simply supported edges)

g = Acceleration of gravity

A = Panel area

Q = Dynamic magnification factor of resonant response of panel

For a typical wall panel for the Aircraft Maintenance Dock,
Panel Weight/Area $\equiv 2.5 \text{ lb/ft}^2$ (0.0174 psi)

For $g = 386 \text{ in/sec}^2$, and assuming that $f_0 = 20 \text{ Hz}$ and $Q = 10$,

$Z_w = 0.000141 \text{ lb sec/in}^3$ at resonance,

$$\rho c = \frac{(0.076474)(1116)(12)}{(12)^3(386)} \text{ lb sec/in}^3$$

$$= 0.00153 \text{ lb sec/in}^3 @ 15^\circ \text{ C/sea level}$$

$$Z_w < \rho c$$

Therefore, to a first approximation, from Eq C7, the relative fundamental mode panel vibration response in the near field of the source relative to its response in the far field, for the same pressure, is:

$$\frac{U_t(r \rightarrow 0)}{U_t(r \rightarrow \infty)} \equiv \frac{1}{\sqrt{1 + \left(\frac{1}{2kr}\right)^2}} \quad [\text{Eq C9}]$$

Thus, provided that the non-dimensional parameter kr ($= 2\pi r/c$) is greater than about 1.6, the change in panel response due to curvature of the sound wave front in the near field will be less than 5 percent. For the typical panel resonance frequency of 20 Hz assumed above, this criteria (e.g., $kr > 1.6$) reduces to a requirement that the source-to-panel distance r be greater than 14 ft. In all cases, the distance between any position of the primary noise sources and the nearby wall or roof surfaces is greater than 14 ft, so that near field effects on panel acoustic loading can be ignored.

FIRST APPROXIMATION FOR ANGLE OF INCIDENCE EFFECTS

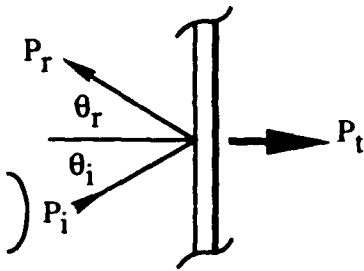
Consider the effective acoustic loads on the wall and roof panels due to a non-normal angle of incidence of the direct field.

Applying the first two boundary conditions used earlier for Eq C5:

1. Continuity of pressure (a scalar quantity) at the surface of a panel, and
2. Continuity of particle velocity (a vector quantity) normal to this surface.

From 1, $P_i + P_r = P_t$, the total sound pressure on source-side of panel.

From 2, $U_i \cos \theta_i - U_r \cos \theta_r = U_t \cos \theta_t$



But for each wave, the particle velocity $U = P/(\text{Wave Impedance})$ which can be expressed as:

$$U_i = \frac{P_i}{\rho c}, \quad U_r = -\frac{P_r}{\rho c} \quad [\text{Eq C10a}]$$

and for the panel velocity, U_t (equal to the particle velocity of the transmitted sound wave), two expressions apply:

- (1) the panel velocity is equal to the net pressure differential across the panel divided by the specific mechanical impedance Z_w of the panel, and

$$U_t = \frac{P - P_t}{Z_w} \quad [\text{Eq C10b}]$$

- (2) the panel velocity, U_t , is equal to the particle velocity of the transmitted wave given by:

$$U_t = \frac{P_t}{\rho c} \quad [\text{Eq C10c}]$$

where it is assumed, for simplicity, that the transmitted sound wave radiates as a plane wave normal to the panel (i.e., $\theta_t = 0$).

Combining the above to solve for the panel velocity in terms of the incident pressure P_i gives:

$$U_t = \frac{P - U_t \rho c}{Z_w} \quad \text{or} \quad U_t = \frac{P}{Z_w + \rho c} = \frac{P_i + P_r}{Z_w + \rho c}$$

or

$$U_t = \frac{2P_i}{Z_w + \rho c \left(1 + \frac{1}{\cos \theta}\right)} \quad [\text{Eq C11}]$$

Comparing this with Eq C1, the effective load on the panel for other than normal incidence is still twice the incident pressure. Based on this conclusion, the effective acoustic loads for the direct field for all locations, regardless of the incidence angle is defined by doubling the incident sound pressure (i.e., adding 6 dB to the free field contours). Although this simplified model also indicates that the panel response reduces to zero for grazing incidence, this is not true, and the response for grazing incidence requires the more general analysis of the response of a flexible panel to an incident sound field that is carried out in Appendix D.

APPENDIX D: Review of Structural Response for Wide Band Random Noise Field

GENERAL RESPONSE RELATIONSHIP

For a single mode of a uniform panel with a generalized mass M_{mn} , area A , length a , width b and thickness t , exposed to a wide band noise with a pressure spectral density $P^2(f)$, the acceleration spectral density of the response, $W_a(f)$ of the panel in its m th vibration mode, at a frequency f and at a general panel coordinate Y is (Sutherland 1968):

$$W_a(Y, f) = \frac{\ddot{X}^2(f)}{g^2} = \frac{P^2(f) A^2 J_{mn}^2(f) \left(\frac{f}{f_{mn}}\right)^4 |H_{mn}(f)|^2 \phi_{mn}^2(Y)}{M_{mn}^2 g^2} \quad [\text{Eq D1}]$$

where

$J_{mn}^2(f)$ = Joint acceptance squared for m, n th mode at frequency f

f_{mn} = m th resonance frequency

$H_{mn}(f)$ = Dynamic response function for m th resonance frequency, or

$$|H_{mn}(f)| = \frac{1}{\sqrt{\left(1 - \left(\frac{f}{f_{mn}}\right)^2\right)^2 + \left(\frac{f}{f_{mn} Q_{mn}}\right)^2}}$$

$\phi_{mn}(f)$ = Mode shape of m th mode

M_{mn} = Generalized mass in m th mode

g = Acceleration of gravity

The rms acceleration of the m th mode is obtained by integrating Eq D1 over frequency. Within a frequency range of about $f_{mn}/2$ to $2 f_{mn}$, for a nominally constant pressure spectral density input, this integration gives an approximate value for the rms response equal to:

$$\ddot{a}_{mn}(Y) = \sqrt{W_a(Y, f_{mn}) \Delta f_c} \quad [\text{Eq D2}]$$

where

$$\Delta f_e = \frac{\pi f_{mn}}{2 Q_{mn}}$$

which is the effective bandwidth for response of the SDOF system to the random input

Q_{mn} = Dynamic magnification factor (Q) for the mnth mode

$W_a(Y, f_{mn})$ = The maximum acceleration spectral density of the response which occurs at the resonance frequency f_{mn} (i.e., $f = f_{mn}$)

For $f = f_{mn}$, the value of $H_{mn}(f)$ is simply Q, so that from Eqs D1 and D2 at the position Y on the plate, the rms acceleration for this mnth mode is:

$$\ddot{a}_{mn}(Y) = \left[\frac{\pi P^2(f_{mn}) J_{mn}^2(f_{mn}) Q^2 \phi_{mn}^2(Y) f_{mn}}{e_{mn}^2 \left(\frac{W}{A}\right)^2} \right] \quad [\text{Eq D3}]$$

where e_{mn} equals the ratio of generalized mass M_{mn} to total mass W/g where W is the panel weight.

Two values for the response are desired: (a) the spatial average rms, and (b) the maximum rms value. Consider, then, the specific case of a simply supported plate for which:

$$e_{mn} = (1/4)$$

$$\phi_{mn}(Y) = \sin \frac{\pi m Y_1}{a} \sin \frac{\pi n Y_2}{b}$$

where Y_1 and Y_2 are panel coordinates in the directions along sides a and b respectively.

The rms spatial average response will be found by obtaining the rms average of the mode shape $\tilde{\phi}_{mn}(Y)$ or

$$\tilde{\phi}_{mn}(Y) = \frac{1}{ab} \int_0^a \int_0^b \sin^2 \frac{\pi m Y_1}{a} \sin^2 \frac{\pi n Y_2}{b} dY_1 dY_2 \quad [\text{Eq D4}]$$

$$= \frac{1}{ab} \left[\frac{a}{2} - \frac{\sin(2\pi m)}{4\pi m} \right] \left[\frac{b}{2} - \frac{\sin(2\pi n)}{4\pi n} \right] = \frac{1}{4} \quad [\text{Eq D5}]$$

since the $\sin(2\pi m)$ terms are zero for all integer values of m.

Substituting Eqs D4 and D5 into D3, the rms spatial average response \bar{a}_{mn} is

$$\bar{a}_{mn} = \sqrt{\frac{\pi}{2} \frac{P^2(f_{mn}) J_{mn}^2(f_{mn}) Q f_{mn}}{w^2}}, g's \quad [\text{Eq D6}]$$

where $w = W/A =$ the surface weight.

The maximum response will occur at values of Y_1, Y_2 for which the mode shape $\phi_{mn}(Y) = 1$. This will be at the center of the plate for all odd modes (i.e., m, n odd). The *spatial maximum* (temporally rms) response $\bar{a}_{mn}(\text{max})$ will be, for a simply supported plate, equal to four times the spatial average response, or

$$\bar{a}_{mn}(\text{max}) = \frac{\bar{a}_{mn}}{\phi_{mn}} = 4\bar{a}_{mn} \quad [\text{Eq D7}]$$

Eqs D6 and D7 provide the general forms of the response equations of concern. Consider now the special case of an acoustic plane wave field normally incident on a simply supported panel vibrating in its fundamental (1,1) mode. In this case (Sutherland 1968, pp 8-21):

$$J_{1,1}^2(f_{1,1}) = \left(\frac{2}{\pi}\right)^4$$

Thus, the two forms of the response for this case are, where $m, n = 1$:

rms spatial average

$$\bar{a}_{1,1} = \sqrt{\left(\frac{2}{\pi}\right)^3 \frac{P^2(f_{mn}) Q f_{mn}}{w^2}} \quad [\text{Eq D8}]$$

rms maximum

$$\bar{a}_{1,1}(\text{max}) = \sqrt{\left(\frac{2^7}{\pi^3}\right) \frac{P^2(f_{mn}) Q f_{mn}}{w^2}} \quad [\text{Eq D9}]$$

The rms spatial average response is used to estimate dynamic load factors on structure and the rms maximum response to estimate structural stress levels.

In either case, one more modification of Eq D6 is desired to allow use of mean square pressures in a one-third octave band, $P_b^2(f_{mn})$ centered on the resonance frequency, f_{mn} , of concern. In this case,

$$P^2(f) = \frac{P_b^2(f)}{\Delta f_b} \quad [\text{Eq D10}]$$

where $\Delta f_b = (2^{1/6} - 2^{-1/6})f = 0.2316f$.

Thus, the corresponding expressions from Eqs. (D6) and (D8) for the rms spatial average response are:

$$\tilde{a}_{m,n} = \sqrt{\frac{\pi}{2} \frac{P_b^2(f_{mn}) J_{mn}^2(f_{mn}) Q}{(0.2316) w^2}} \quad [\text{Eq D11}]$$

or, for $m,n = 1,1$

$$\tilde{a}_{1,1} = \sqrt{\left(\frac{2}{\pi}\right)^3 \frac{P_b^2(f_{1,1}) Q}{(0.2316) w^2}} = 1.06 \frac{\tilde{P}_b \sqrt{Q}}{w} \quad [\text{Eq D12}]$$

In the case of the AMD, acceleration responses were computed for areas near the back wall due to exposure from both a reverberant (diffuse) and a direct sound field. This distinction is necessary due to the differences in the joint acceptances for each type of sound field. In this case, the overall spatial average rms response was equal to the square root of the sum of the mean square responses for each component of the sound field. That is,

$$\tilde{a}_{mn}(\text{total}) = \sqrt{\tilde{a}_{mn}^2(\text{diffuse}) + \tilde{a}_{mn}^2(\text{direct})} \quad [\text{Eq D13}]$$

where $\tilde{a}_{mn}(\text{diffuse})$ and $\tilde{a}_{mn}(\text{direct})$ differ due to the difference in the joint acceptances for each type of sound field and due to their different sound levels. The same approach was used to define the maximum rms response levels.

JOINT ACCEPTANCE FOR STRUCTURAL RESPONSE TO WIDE BAND RANDOM NOISE

As reviewed in detail in Sutherland (1968), the joint acceptance $J_{mn}^2(f)$ for response of a panel vibrating in its m th mode to acoustic excitation is normally specified as the product of joint acceptances

for acoustic loading on two orthogonal beams corresponding to the m th and n th orthogonal modes of the panel respectively. That is, as illustrated in the sketch:

$$J_{m,n}^2 \left(\begin{array}{c} \text{rectangle} \\ \text{width } a, \text{ height } b \end{array} \right) = J_m^2 \left(\begin{array}{c} \text{rectangle} \\ \text{width } a \end{array} \right) \cdot J_n^2 \left(\begin{array}{c} \text{rectangle} \\ \text{width } b \end{array} \right)$$

The following defines the applicable expressions utilized for this report to define joint acceptances for each type of noise field. The expressions apply only to the case of simply supported beams (and hence simply supported plates).

$J_n^2(f)$ for Simply Supported Beams in a Diffuse Sound Field

For a diffuse (or reverberant) sound field, $J_n^2(f)$ depends only on one non-dimensional frequency parameter $x = fL/c$ where f =frequency, L =length of beam, and c =speed of sound. The expression for $J_n^2(f)$ for a simply supported beam vibrating in its n th mode under excitation by a diffuse sound field is (Sutherland 1968; White 1967):

$$\begin{aligned} J_n^2(f) = & \left[\frac{1}{(2\pi m)^2 x} \right] \{ C_{in}[\pi(n+2x)] - C_{in}[\pi|n-2x|] \} \\ & + \frac{1}{4\pi x} \{ S_i(n+2x) - S_i[\pi(n-2x)] \} \\ & + \left(\frac{1}{n\pi} \right)^2 \frac{1 - \cos(n\pi)\cos(2\pi x)}{1 - \left(\frac{2x}{n} \right)^2} \end{aligned} \quad [\text{Eq D14}]$$

where

$$C_{in}(z) = \int_0^z \frac{1 - \cos t}{t} dt, \text{ the cosine integral}$$

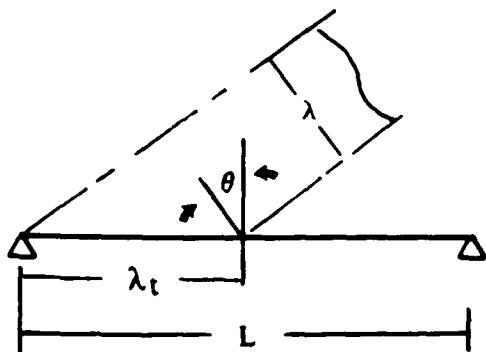
$$S_i(z) = \int_0^z \frac{\sin t}{t} dt, \text{ the sine integral.}$$

These functions were computed using asymptotic expressions and rational fraction numerical approximations given in Abramovitz (1964).

$J_n^2(f)$ for Simply Supported Beam in a Direct Sound Field

In this case, $J_n^2(f)$ depends on two parameters; the same nondimensional frequency $x = fL/c$, and the angle of incidence θ of the direct sound field. However, these two parameters can be expressed in terms of one revised non-dimensional frequency, $x' = fL \sin \theta / c$ where θ is the angle between the incident sound ray and a normal to the panel. As indicated in the sketch, this quantity is actually equal to the ratio

L/λ_t of the beam length L to the trace wavelength $\lambda_t = c/f \sin \theta$ of the incident sound field whose wavelength $\lambda = c/f$. For this case (Sutherland 1968; Powell 1958, Chapter 8),



$$J_n^2(f) = \frac{2}{(n\pi)^2} \frac{1 - \cos(n\pi) \cos(2\pi x')}{1 - (\frac{2x'}{n})^2} \quad [\text{Eq D15}]$$

where $x' = fL \sin \theta / c$.

For the fundamental mode of a simply supported panel, when x or $x' < 0.3$, the two values of $J_n^2(f)$ have the same maximum value equal to:

$$J_1^2(\text{Diffuse}) = J_1^2(\text{Direct}) = \left(\frac{2}{\pi}\right)^2 \quad [\text{Eq D16}]$$

In the case of J_1^2 (Direct), $x < 0.2$ means that the ratio of the beam length to trace wavelength is less than 0.2. This includes the case of a normally incident direct sound field (which is of primary interest for back wall panels). In this case, the trace wavelength, $\lambda_t = \lambda / \sin \theta$ approaches infinity as θ approaches zero.

Figure D1 shows the values of $J_n^2(f)$ for a reverberant sound field for the first ten modes of a simply supported beam. The figure represents a corrected version of an earlier figure presented in the draft report and in Sutherland (1968). This earlier version was in error for mode numbers greater than one, for values of the abscissa parameter $L/\lambda < 1$. For purposes of this study, only the joint acceptance for a diffuse field, as illustrated in Figure D1, was necessary since it turned out that the acoustic design environment could be conservatively defined by just the diffuse sound field.

EQUIVALENT STATIC PRESSURE

Now use the preceding analyses to estimate an equivalent static pressure load on a panel which would produce the same effective stress (for a one time load) as provided by the actual repeated random acoustic loading. First, define the stress due to acoustic loading.

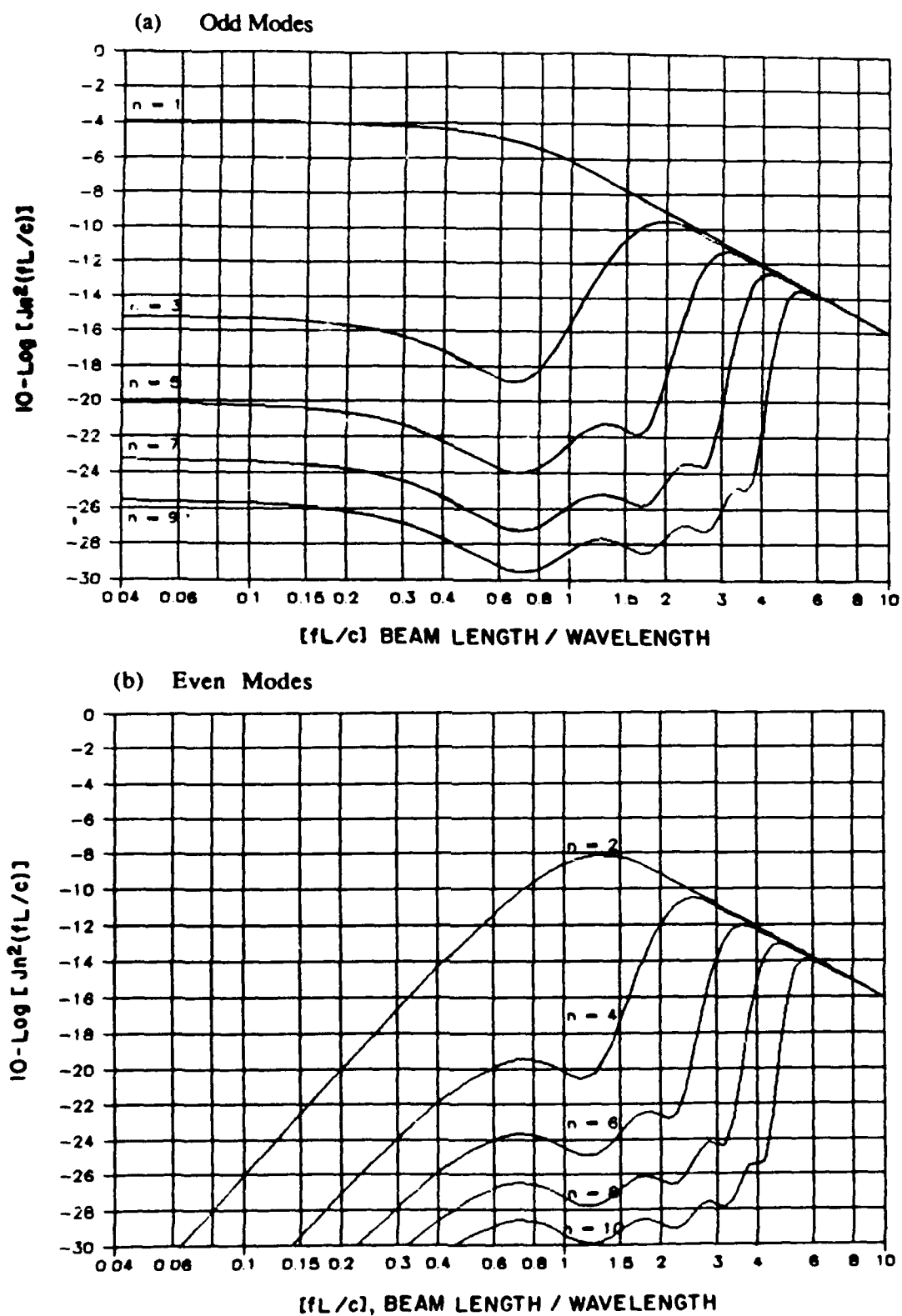


Figure D1. Comparison of joint acceptance for the first ten (a) odd and (b) even modes of a simply supported beam in a diffuse sound field.

Maximum rms Panel Stress Due to Acoustic Loading

Hunt (1960) has shown that the maximum rms stress in a uniform plate vibrating in an orthogonal mode may be estimated by:

$$\bar{\sigma}_{\max} = K_s \sqrt{3} E \frac{\bar{X}_{\max}}{C_L} = K_s \sqrt{3} \rho C_L \bar{X}_{\max} \quad [\text{Eq D17}]$$

where

K_s = Shape constant depending on panel edge constraints and aspect ratio.

E = Modules of elasticity, psi

\bar{X}_{\max} = Maximum rms velocity of panel, in/sec

C_L = longitudinal speed of sound in plate material

$$C_L = \sqrt{\frac{E}{\rho}} \quad , \quad \text{in/sec}$$

ρ = Mass density of plate material, lb sec²/in⁴

For a simply supported panel, the constant K_s is (Hunt 1960):

$$K_s = (1-\mu^2)^{-1/2} \frac{[1+\mu(\frac{a/m}{b/n})^2]}{[1+(\frac{a/m}{b/n})^2]} \quad [\text{Eq D18}]$$

where

μ = Poisson's ratio (0.3 for metals)

a, b = Panel dimensions where $a < b$

m, n = Mode numbers in directions of a, b respectively.

For example, for one section of a wall panel, with $a, b = 30", 90"$, $K_s = 0.975$.

Thus, since the maximum rms velocity of the panel is given by

$$\tilde{X} = \frac{\tilde{X}_{\max}}{2\pi f} = \frac{\tilde{a}_{\max} g}{2\pi f} \quad [\text{Eq D19}]$$

Eqs D6, D7, D17, and D19 can be combined to estimate the maximum rms stress in a panel vibrating in its m,nth mode. The resulting expression, for the case of the first mode of a simply supported panel driven by a normally incident sound field is:

$$\sigma_{1,1\max} = K_s \sqrt{3} E \frac{\tilde{X}}{C_L} = K_s \sqrt{3} E \tilde{a}_{1,1\max} \frac{g}{2\pi f C_L} \quad [\text{Eq D20a}]$$

or

$$\sigma_{1,1\max} = \left[\sqrt{\frac{3\pi}{2(0.2316)}} \frac{8}{\pi^3} \right] \frac{K_s E g \tilde{P}_b}{f_{1,1} C_L w} \sqrt{Q} \quad [\text{Eq D20b}]$$

where $K_s =$ Constant given by Eq D18

$P_b =$ Rms pressure in one-third octave band centered at fundamental resonance frequency, $f_{1,1}$, psi

$g =$ Acceleration of gravity, 386 in/sec².

The other parameters are specified under Eq D17 and the term in brackets is equal to 1.16.

The preceding expressions define the maximum rms stress in a simply supported panel vibrating in its fundamental mode under the type of acoustic excitation defined. Stress concentration factors are not considered, since it is assumed that they would apply equally to dynamic (i.e., acoustic) or static loads. Also, linearity of panel response is assumed.

Peak Stress Due to Random Acoustic Loads

The acoustic excitation is random gaussian noise, so the peak stress σ_p can be defined statistically by a Rayleigh Probability Distribution (Powell 1958, Chapter 8):

$$P(\sigma_p > Y \times \sigma) = e^{(-1/2 Y^2)} \quad [\text{Eq D21}]$$

That is, the probability that the peak stress, σ_p , will exceed Y times the RMS stress σ is given by the exponential function $\exp(-1/2 Y^2)$.

For design purposes, a probability of percent exceedance was chosen to find a peak dynamic stress that will be equated to a static stress and equivalent static pressure load. In this case, if $P(\sigma_p Y \cdot \bar{\sigma}) = 0.1$, then

$$Y = 2.146 \cong 2.15 \quad [\text{Eq D22}]$$

or

$$\sigma_p = 2.15 \times \bar{\sigma} \quad \text{for 10\% of the time}$$

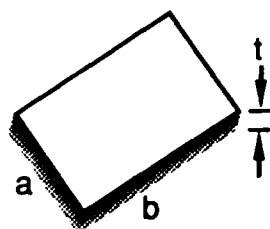
This peak factor will be identified by the symbol F_p . Thus, for the fundamental mode of a simply supported plate loaded by a random acoustic noise, the peak stress σ_p will be:

$$\sigma_p = F_p \times \bar{\sigma}_{1,1\max} \quad [\text{Eq D23}]$$

where the maximum rms stress $\bar{\sigma}_{1,1\max}$ is given by Eq D20a or D20b.

Panel Stress Under Static Load

Now, to find an equivalent static load, the maximum stress in a homogeneous plate under uniform load may be expressed in the following form (Roark 1954):



$$\sigma_s = K P_s \left(\frac{a}{t}\right)^2 \quad [\text{Eq D24}]$$

where

σ_s = Maximum principal axis fiber stress, lb/in²

P_s = Uniform static load, lb/in²

t = Actual thickness of plate, in

a = Short side of plate, in

b = Long side of plate, in

K = Function of the ratio of a/b and edge constraints on the panel (Roark 1954)

To equate the damage of a random dynamic load on the panel to an equivalent static load, let the maximum stress of the static load σ_s be related to the peak dynamic stress σ_p by a factor $F_f < 1$. Thus,

$$\sigma_p = F_f \times \sigma_s \quad [\text{Eq D25}]$$

This factor is used to account approximately for the greater damage due to fatigue effects of the dynamic load.

Equivalent Static Pressure for Response in Fundamental Mode

Combining Eqs D20b, D23, and D24 by Eq D25

$$F_p \times \sigma_{\max} = F_f \times \sigma_s \quad [\text{Eq D26}]$$

or, solving for the equivalent static load,

$$P_s = \left[\sqrt{\frac{3\pi}{2(0.2316)}} \frac{8}{\pi^3} \right] \frac{K_s F_p E g P_b \sqrt{Q}}{K F_f f_{1,1} C_1 w} \left(\frac{t}{a}\right)^2 \quad [\text{Eq D27}]$$

A simplification of this result is possible by including the expression for the fundamental resonance frequency, $f_{1,1}$ for a simply supported plate.

$$f_{1,1} = \frac{\pi}{2} \sqrt{\frac{D}{\rho t_m} \left(\frac{1}{a^2} + \frac{1}{b^2} \right)}, \text{Hz} \quad [\text{Eq D28}]$$

where

D = Stiffness for a uniform plate, or

$$D = \frac{Et_d^3}{12} \sqrt{1-\mu^2}, \text{ lb in}$$

ρt_m = Surface mass density = w/g , $\text{lb sec}^2/\text{in}^3$

a, b = Plate length and width, in

t_d = Dynamically-equivalent thickness of plate, in

t_m = Mass-equivalent thickness of plate, in

Substituting Eq D28 into D27, the equivalent static pressure load which produces the same effective stress (allowing for fatigue) as the actual random acoustic load is given by (setting $w = p t_m g$):

$$P_s = \left[\sqrt{\frac{\pi(1-\mu)^2}{2(0.2316)}} \right] \frac{48}{\pi^4} \left(\frac{t^2}{t_d^{3/2} t_m^{1/2}} \right) \frac{K_s F_p \bar{P}_b \sqrt{Q}}{K F_f} \left[\frac{2}{1 + (\frac{a}{b})^2} \right] \quad [\text{Eq D29}]$$

The first (numerical) term in brackets, for $\mu = 0.3$, is equal to 1.224.

Adapting, for design purposes, $F_p = 2.15$ (10 percent peak exceedances) and $F_f = 0.75$ for the relative material strength under fatigue loading (over 2×10^6 cycles of stress reversals are expected), then the equivalent static pressure to produce the same effective stress as that experienced by the panel vibrating in the first mode is, for a homogeneous panel (i.e., $t = t_m = t_d$):

$$P_s \equiv 3.51 \frac{K_s}{K} P_b \sqrt{Q} \left[\frac{2}{1 + (\frac{a}{b})^2} \right] \quad [\text{Eq D30}]$$

The "constants" K_s and K both vary with the aspect ratio a/b . The variation of K with a/b is given by the following double infinite series (Sutherland 1968):

$$K = \frac{16}{\pi^6} \left[\sum_{m=1}^{\infty} \sum_{n=1}^{\infty} \frac{\sin \frac{m\pi}{2} \sin \frac{n\pi}{2}}{mn(m^2 + (\frac{na}{b})^2)^2} \right], m, n \text{ are odd} \quad [\text{Eq D31}]$$

Thus, the equivalent static pressure can be expressed as:

$$P_s = K' \bar{P}_b \sqrt{Q} \quad [\text{Eq D32}]$$

where

$$K' = 3.51 \frac{K_s}{K} \frac{2}{1 + (\frac{a}{b})^2}$$

However, as indicated by Table D1, the value of K' , computed from the above definition of K' , Eq D31 and Eq D18, is nearly independent of the panel aspect ratio a/b for $1 < a/b < 0.3$ and has an average value of about 8.3 over this range of a/b .

Table D1

Variation in Constant K' in Eq D32 with Panel Aspect Ratio a/b

a/b	1.0	0.9	0.8	0.7	0.6	0.5	0.4	0.3	0.2	0.1
Ks	0.6814	0.7199	0.7619	0.8070	0.8540	0.9015	0.9471	0.9877	1.020	1.041
K	0.2873	0.3378	0.3966	0.4633	0.5359	0.6101	0.6776	0.7267	0.7478	0.7502
K'	8.32	8.26	8.22	8.20	8.22	8.30	8.46	8.75	9.20	9.64

Thus Eq D32, with K' approximately equal to 8.3, provides a simple expression for estimating the equivalent static pressure which will produce the same effective maximum (bending) stress as occurs in a simply supported panel vibrating at its fundamental frequency under excitation by a random noise with an rms pressure P_b in the third octave band centered at this frequency.

Equivalent Static Pressure for Response in All Modes

A more general expression is desirable to define the equivalent static pressure which would produce the same effective maximum stress a panel experiences when responding in all of its resonant modes to a broadband acoustic excitation.

For this case, ignoring any coupling between modes, one can simply use Eqs D17 through D19 and D26 to define this equivalent static pressure.

First, find the overall rms stress in the panel due to acoustic loading by summing over all the significant modes,

$$\sigma_{\max} = \sqrt{\sum_{m=1}^M \sum_{n=1}^N \sigma_{mn}^2(\max)} \quad [\text{Eq D33}]$$

where $\sigma_{mn}(\max)$ is the maximum rms stress in the mnth mode found using Eqs D17 through D19 and Eqs D11 and D7. The "significant" modes will normally include all modes up to about 20 to 40 times the fundamental mode. At higher frequencies, values of the joint acceptance or the acoustic pressures spectrum decrease significantly.

Next, use Eq D26 to define the equivalent stress σ_s under a static load as given by:

$$\sigma_s = F_p \frac{\sigma_{\max}}{F_f} \quad [\text{Eq D34}]$$

Finally, use Eq D24 to define the static load which will produce this same effective stress, or

$$P_s = \frac{F_p}{F_t K} \left(\frac{t}{a}\right)^2 \bar{\sigma}_{max} \quad [\text{Eq D35}]$$

where $\bar{\sigma}_{max}$ is the overall maximum rms stress found from the summation in Eq D33. This is the expression which was used to estimate effective values of a static load, for design purposes, to represent the overall acoustic loads on the AMD roof and draft curtain panels, and for equipment enclosure panels. For the AMD insulated wall panels, the combined analytical/experimental approach described in Chapter 4 of the main body of the text was utilized to define an equivalent static pressure for design purposes. This approach utilized actual measured dynamic response data on a representative sample of such a wall panel to predict panel stiffness for comparison with manufacturers' rated static pressure (wind load) tolerances.

APPENDIX E: Experimental Measurement and Analysis of Typical Pre-Insulated Wall Panel Structural Characteristics

EXPERIMENTAL DATA

A test was performed at Wyle Research to determine the response characteristics of a section of a preinsulated wall panel typical of the type proposed for use in the AMD. The test specimen was approximately 66 in. long by 30 in. wide by 2 in. thick, composed of two outer 26 gage steel panels filled in the 2 in. space with polyurethane foam. (The panels for the AMD are expected to have 24 gage skins.) The surface on one side was lightly dimpled and the other side was corrugated. The panel is designed to be interleaved with adjacent panel sections on either side as illustrated in Figure 4 in Chapter 2 of the main body of this report.

Figures E1(a) and E1(b) show the panel mounted on a large table of an electrodynamic shaker which was used to vibrate the test panel. The panel ends were clamped between two angle-iron supports as shown in Figure E1(b), simulating a simple support. Three accelerometers were mounted on the upper panel surface, at the center and halfway between the center and each side (i.e., quarter span). The photograph in Figure E1(a) shows the accelerometers on the panel.

The test panel was vibrated in a sine sweep test in a direction normal to the panel surface over the frequency range of 5 Hz to 500 Hz. An accelerometer mounted on the shaker head was utilized to maintain a constant input acceleration of 0.1 g during the sine sweep tests. Figure E2 illustrates the vibration response of the panel measured at two of the accelerometer positions. The data plotted in the figure show the panel response relative to the input acceleration; the plots clearly show the fundamental frequency at 31 Hz. Other modal frequencies are also observable in this figure.

The estimated and experimentally observed modes shapes of the panel are illustrated in Figure E3 for several panel modes. Shown with the measured data are the measurement locations on the panel.

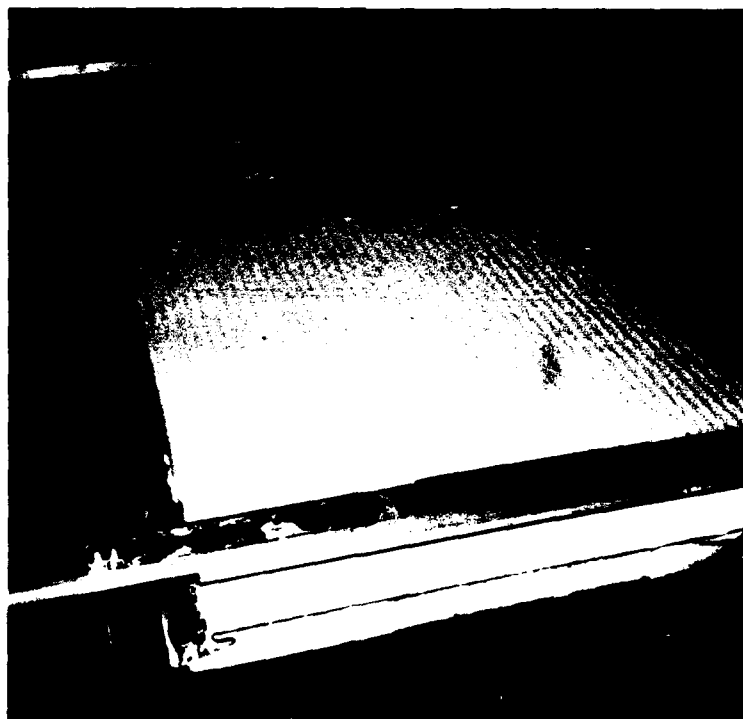
As discussed in the next section of this appendix, the measured fundamental frequency made it possible to establish an effective stiffness for this composite panel.

Some, but not all, of the first few higher modal frequencies agreed closely with expected values based on a plate with simple supports along the short edges and free along the long edges. This corresponded to the test configurations. Table E1 shows the observed and predicted values.

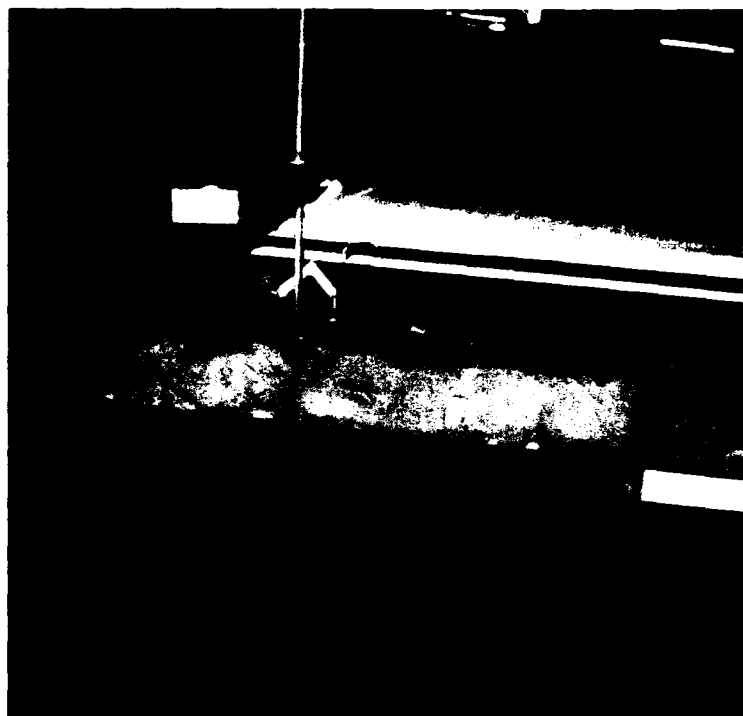
In the subsequent vibration design analysis, developed in detail in Appendix H, a value of $Q = 25$ was used for the first (1,0) mode of wall panels, and a root mean square average value over all the observed modes of 14.7 rounded to 15 was used for all other modes.

ANALYSIS OF WALL PANEL CHARACTERISTICS

On the basis of the above data, the following analysis was made of the basic static and dynamic characteristics of the test wall panel and of the anticipated 7.5 ft panel design for the AMD.



a.



b.

Figure E1. Photographs of vibration test setup on representative 2 in. wall panel.

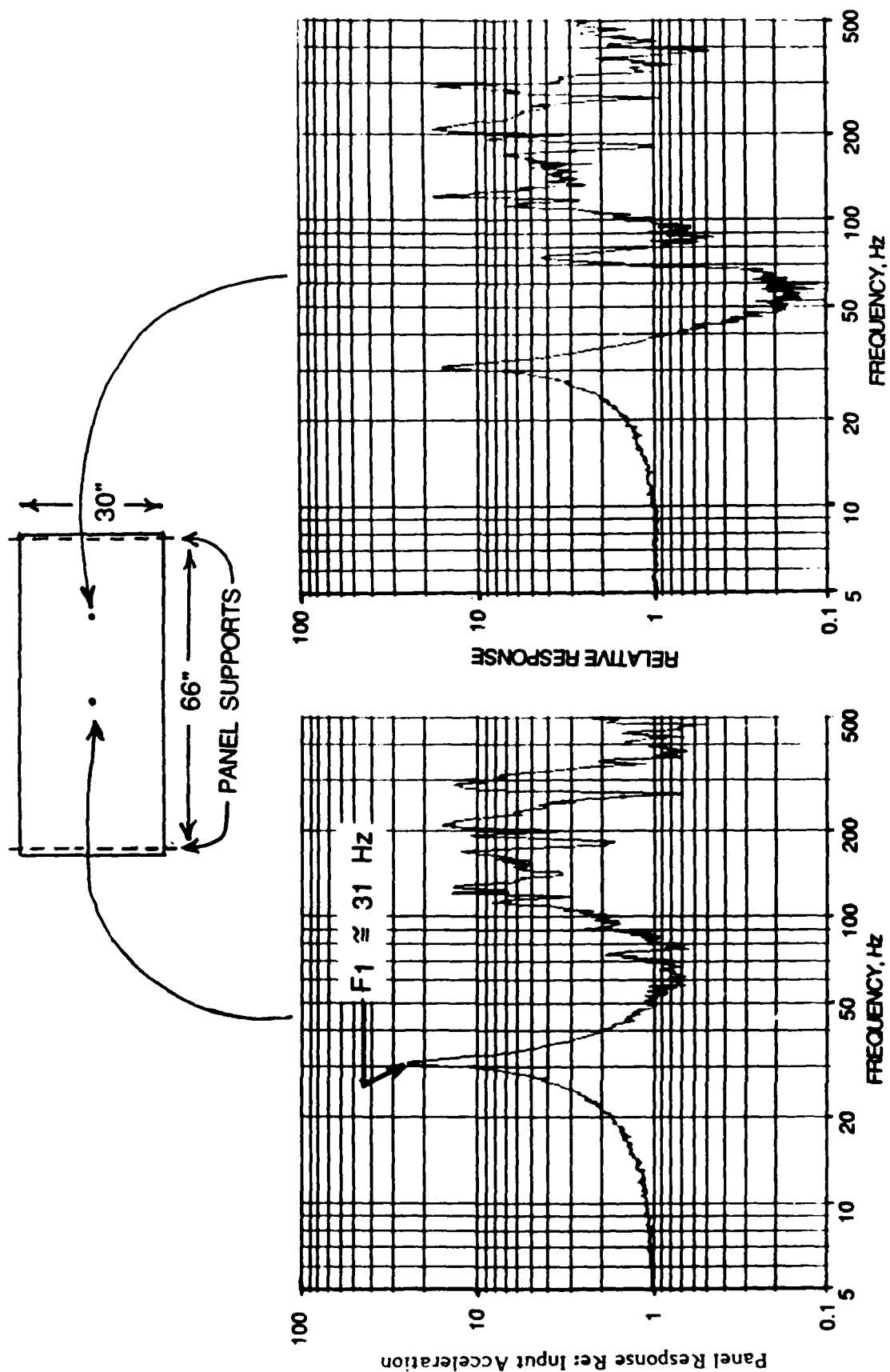


Figure E2. Vibration response of test panel.

AMPLITUDE, ARBITRARY SCALE

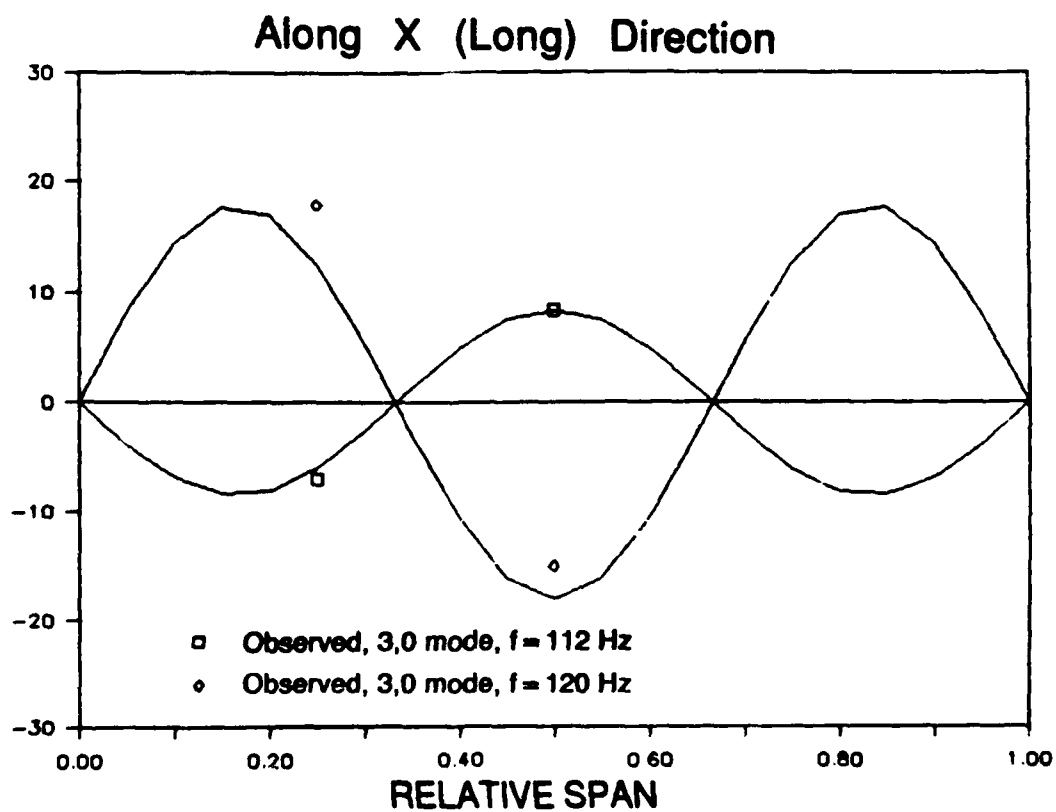
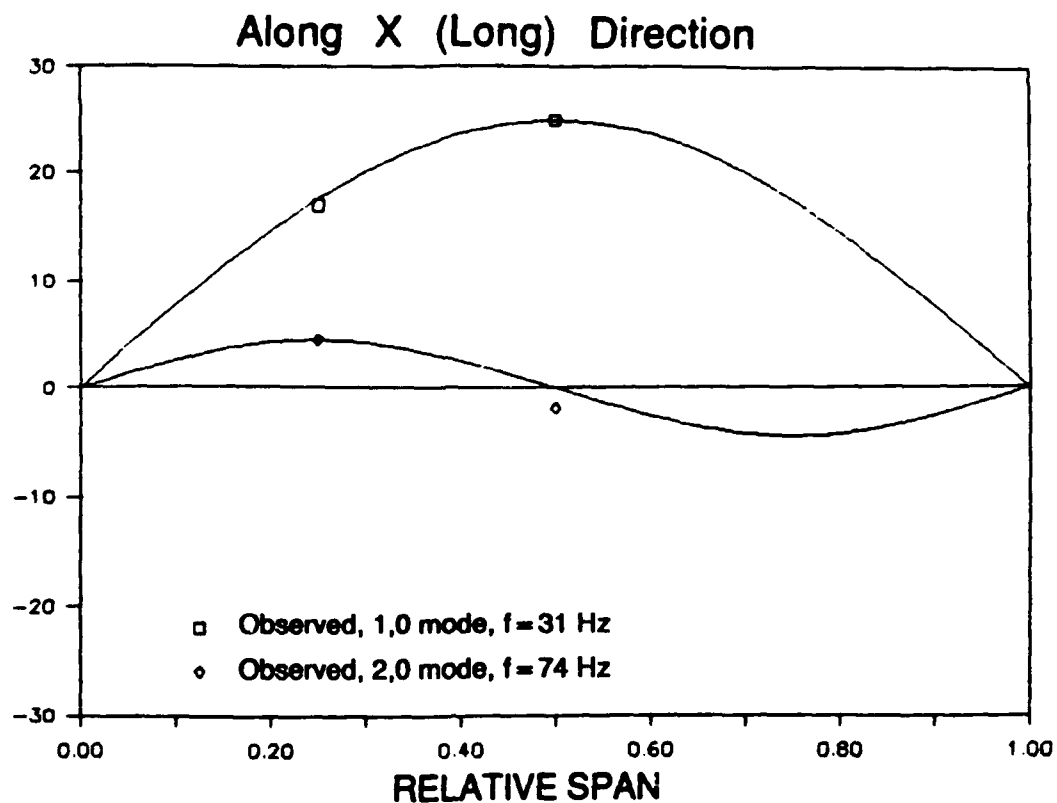


Figure E3. Vibration mode shapes of test panel.

Table E1

Observed and Predicted Modal Frequencies

Mode No. p [*] q [*]		Frequency, Hz Measured Predicted ^{**}		Q
0	2	31	29.8	25
		74		4.5
1	2	91	89.4	2
		112		8.5
0	3	120	119.2	18
		168		12
		191		11
1	3	205	203.8	18
		282		14
		291		18

* Number of mode lines perpendicular to sides a and b respectively where side a is the short, simply supported side and b is the long free side. The p, q = 0,2 and 0,3 modes correspond to the first and second beam modes of the plate.

** Predicted resonant frequencies according to the analysis at the end of this Appendix.

	<u>Test Panel</u>	<u>AMD Panel</u>
<u>Surface Density</u>		
Panel Only, psi		0.0193
+Girts (W8x18)	18/(7.5 x 144)	0.0167
+Columns (W12x31)	31/(25 x 144)	0.0086
Total Panel + Girts, psi		0.0360
+ Columns, psi		0.0446
<u>Allowable Deflection</u> , in.	0.40	0.50
$Y_{max} = \text{Span}/180$		

Deflection Under Uniform Load

$$Y_{max} = [5L^4a/(384EI) + L^2/(8dG_c)] \times P_s$$

where L = Span, in.
 a = Panel width, in.
 d = Panel thickness, in.
 EI = Stiffness of skin, lb sq in
 G_c = Shear Modules of core, psi
 P_s = Static pressure Load, psi

Allowable Pressure Load (Single Span)

$$P_s = (L/180)/[5L^4a/(384EI) + L^2/(8dG_c)]$$

	<u>Units</u>	<u>Test Panel</u>	<u>AMD Panel</u>
for L	in.	66*	90
a	in.	30	30
d	in.	2	2
t	in.	0.0179	0.0239
E	psi	30×10^6	30×10^6
$I = ad^2t/2$	in ⁴	1.074	1.434
Gc	psi **	400	400
P _s	psi	0.403	0.269

* Effective length for vibration test

** Gc per H.H. Robertson Co.

AMD Panel

Allowable Pressure Load (Triple Span)

Based on manufacturer's Specification data for 530-20 24/24 Panel
Empirical fit to Span vs Wind Load (See Figure E4) gives:

$$\begin{aligned} \text{or } P_s (\text{psf}) &= 16,056/L^{1.317} (\text{in}) \\ P_s (\text{psi}) &= 111.5/L^{1.317} (\text{in}) \end{aligned}$$

$$\text{therefore, } P_s = 111.5/(90)^{1.317} = 0.298 \text{ psi}$$

Effective Stiffness of Equivalent Homogeneous Plate

For such a plate, $Y_{\max} = [5L^4a/(384 \times (EI)_{\text{eff}})] \times P_s = L/180$

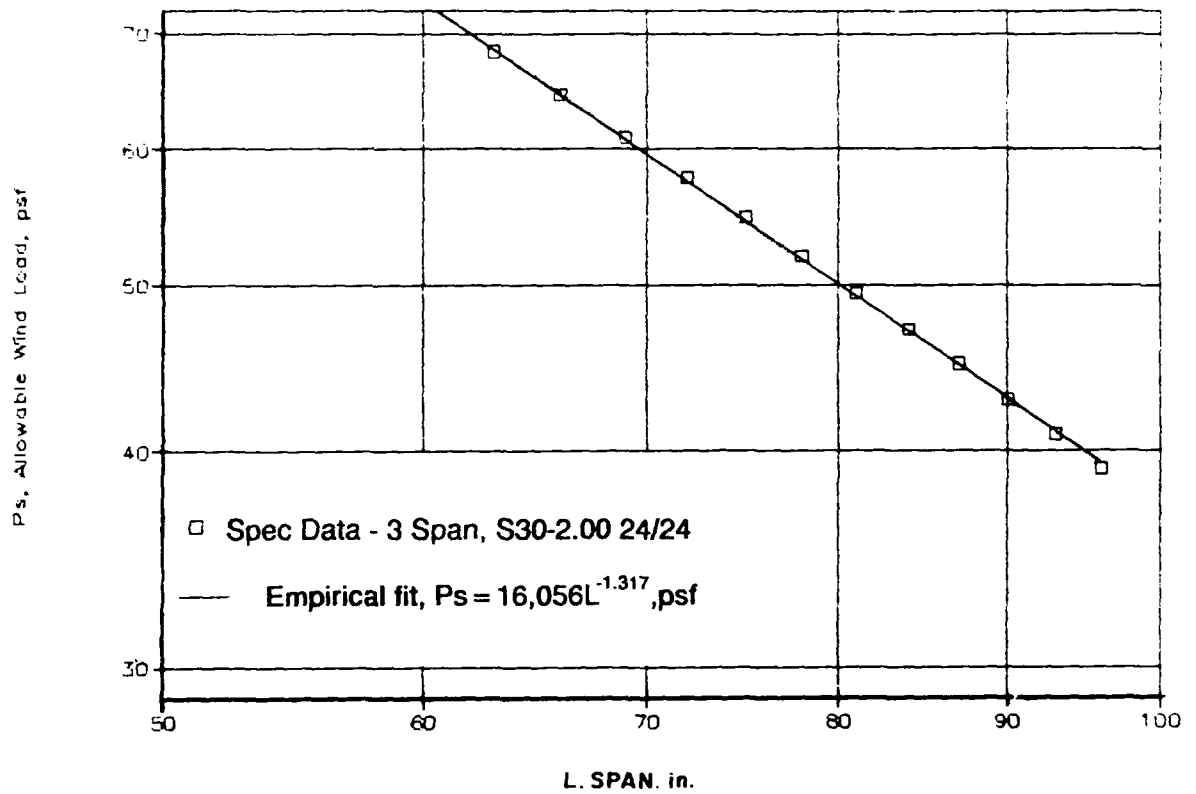
	<u>Units</u>	<u>Test Panel</u>	<u>AMD Panel</u>
P _s	psi	0.403	0.298 (3 Span)
L	in.	66	90
a	in.	30	30
Y _{max}	in. (L/180)	0.367	0.50
EI _{eff}	lb sq in.	8.15×10^6	15.3×10^6

Resonance Frequency of Equivalent Homogeneous Plate

For a beam,

$$f_1 = \frac{\pi}{2L^2} \sqrt{\frac{(EI)_{\text{eff}} \times Lg}{W}}$$

L	in	66	90
W/Lg	lb x (sec/in) ²	0.00119	0.00150
f ₁	Hz (Predicted)	29.8	19.6
f ₁	Hz (Measured)	31	



(Data from H.H. Robertson, Inc., for Type 530-2.00 24/24 panel.)

Figure E4. Allowable wind load for typical preinsulated panel versus span based on maximum deflection \approx span/180.

APPENDIX F: Extract From AISC Code for Steel Building Construction Fatigue*

SECTION 1.7 MEMBERS AND CONNECTIONS SUBJECT TO REPEATED VARIATION OF STRESS (FATIGUE)

1.7.1 General

Fatigue, as used in this Specification, is defined as the damage that may result in fracture after a sufficient number of fluctuations of stress. Stress range is defined as the magnitude of these fluctuations. In the case of a stress reversal, stress range shall be computed as the numerical sum of maximum repeated tensile and compressive stresses or the sum of maximum shearing stresses of opposite direction at a given point, resulting from differing arrangements of live load.

Few members or connections in conventional buildings need to be designed for fatigue, since most load changes in such structures occur only a small number of times or produce only minor stress fluctuations. The occurrence of full design wind or earthquake loads is too infrequent to warrant consideration in fatigue design. However, crane runways and supporting structures for machinery and equipment are often subject to fatigue loading conditions.

1.7.2 Design for Fatigue

Members and their connections subject to fatigue loading shall be proportioned in accordance with the provisions of Appendix B.

*Reprinted with permission from *Manual of Steel Construction*, 8th ed (American Institute of Steel Construction [AISC], 1980), pp 5-28, 5-29, and 5-86 to 5-91.

SECTION B1 LOADING CONDITIONS; TYPE AND LOCATION OF MATERIAL

In the design of members and connections subject to repeated variation of live load stress, consideration shall be given to the number of stress cycles, the expected range of stress, and the type and location of member or detail.

Loading conditions shall be classified as in Table B1.

The type and location of material shall be categorized as in Table B2.

SECTION B2 ALLOWABLE STRESSES

The maximum stress shall not exceed the basic allowable stress provided in Sects. 1.5 and 1.6 of this Specification, and the maximum range of stress shall not exceed that given in Table B3.

SECTION B3 PROVISIONS FOR MECHANICAL FASTENERS

B3.1 Range in tensile stress in properly tightened A325 or A490 bolts need not be considered, but the maximum computed stress, including prying action, shall not exceed the values given in Table 1.5.2.1, subject to the following stipulations:

1. Connections subject to more than 20,000 cycles, but not more than 500,000 cycles, of direct tension may be designed for the stress produced by the sum of applied and prying loads if the prying load does not exceed 10 percent of the externally applied load. If the prying force exceeds 10 percent, the allowable tensile stress given in Table 1.5.2.1 shall be reduced 40 percent, applicable to the external load alone.
2. Connections subject to more than 500,000 cycles of direct tension may be designed for the stress produced by the sum of applied and prying loads if the prying load does not exceed 5 percent of the externally applied load. If the prying force exceeds 5 percent, the allowable tensile stress given in Table 1.5.2.1 shall be reduced 50 percent, applicable to the external load alone.

B3.2 The use of other bolts and threaded parts subjected to tensile fatigue loading is not recommended.

B3.3 Rivets, bolts, and threaded parts subjected to cyclic loading in shear may be designed for the bearing-type shear stresses given in Table 1.5.2.1 insofar as the fatigue strength of the fasteners themselves is concerned.

TABLE B1
NUMBER OF LOADING CYCLES

Loading Condition	From	To
1	20,000 ^a	100,000 ^b
2	100,000	500,000 ^c
4	500,000	2,000,000 ^d
^a Approximately equivalent to two applications every day for 25 years. ^b Approximately equivalent to ten applications every day for 25 years. ^c Approximately equivalent to fifty applications every day for 25 years. ^d Approximately equivalent to two hundred applications every day for 25 years.		

TABLE B2

General Condition	Situation	Kind of Stress ^a	Stress Category. (See Table B3)	Illustrative Example Nos. (See Fig. B1) ^b
Plain material	Base metal with rolled or cleaned surfaces.	T or Rev.	A	1,2
	Base metal and weld metal in members, without attachments, built-up of plates or shapes connected by continuous full- or partial-penetration groove welds or continuous fillet welds parallel to the direction of applied stress.	T or Rev.	B	3,4,5,6
	Calculated flexural stress, f_b , in base metal at toe of welds on girder webs or flanges adjacent to welded transverse stiffeners.	T or Rev.	C	7
Built-up members	Base metal at end of partial-length welded cover plates having square or tapered ends, with or without welds across the ends.	T or Rev.	E	5
	Base metal at gross section of high-strength-bolted friction-type connections, except connections subject to stress reversal and axially loaded joints which induce out-of-plane bending in connected material.	T or Rev.	B	8
	Base metal at net section of other mechanically fastened joints.	T or Rev.	D	8,9
Mechanically fastened connections	Base metal at net section of high-strength bolted bearing connections.	T or Rev.	B	8,9
	Base metal at intermittent fillet welds.	T or Rev.	E	
	Base metal at junction of axially loaded members with fillet welded end connections. Welds shall be disposed about the axis of the member so as to balance weld stresses.	T or Rev.	E	17,18,20
Fillet welded connections	Weld metal of continuous or intermittent longitudinal or transverse fillet welds.	S	F	5,17,18,21

^a "T" signifies range in tensile stress only; "Rev." signifies a range involving reversal of tensile or compressive stress; "S" signifies range in shear including shear stress reversal.

^b These examples are provided as guidelines and are not intended to exclude other reasonably similar situations.

TABLE B2 (continued)

General Condition	Situation	Kind of Stress ^a	Stress Category (See Table B3)	Illustrative Example Nos. (See Fig. B1) ^b
Groove welds	Base metal and weld metal at full-penetration groove welded splices of parts of similar cross section ground flush, with grinding in the direction of applied stress and with weld soundness established by radiographic or ultrasonic inspection in accordance with the requirements of Table 9.25.3 of AWS D1.1-77.	T or Rev.	B	10
	Base metal and weld metal at full-penetration groove welded splices at transitions in width or thickness, with welds ground to provide slopes no steeper than 1 to 2½, with grinding in the direction of applied stress, and with weld soundness established by radiographic or ultrasonic inspection in accordance with the requirements of Table 9.25.3 of AWS D1.1-77.	T or Rev.	B	12,13
	Base metal and weld metal at full-penetration groove welded splices, with or without transitions having slopes no greater than 1 to 2½, when reinforcement is not removed and/or weld soundness is not established by radiographic or ultrasonic inspection in accordance with the requirements of Table 9.25.3 of AWS D1.1-77.	T or Rev.	C	10,11,12,13
Plug or Slot Welds	Weld metal of partial-penetration transverse groove welds, based on effective throat area of the weld or welds.	T or Rev.	F	16
	Base metal at plug or slot welds.	T or Rev.	E	27
	Shear on plug or slot welds.	S	F	27
Attachments	Base metal at detail of any length attached by groove welds subject to transverse and/or longitudinal loading, when the detail embodies a transition radius, R , 2 inches or greater, with the weld termination ground smooth: $R \geq 24$ in. 24 in. $> R \geq 6$ in. 6 in. $> R \geq 2$ in.	T or Rev. T or Rev. T or Rev.	B C D	14 14 14

TABLE B2 (continued)

General Condition	Situation	Kind of Stress ^a	Stress Category (See Table B3)	Illustrative Example Nos. (See Fig. B1) ^b
Attachments (cont'd)	Base metal at detail attached by groove welds or fillet welds subject to longitudinal loading, with transition radius, if any, less than 2 inches: 2 in. $< a \leq 12b$ or 4 in. $a > 12b$ or 4 in. where a = detail dimension parallel to the direction of stress b = detail dimension normal to the direction of stress and the surface of the base metal	T or Rev. T or Rev.	D E	15 15,23,24, 25,26
	Base metal at a detail of any length attached by fillet welds or partial-penetration groove welds in the direction parallel to the stress, when the detail embodies a transition radius, R , 2 inches or greater, with weld termination ground smooth: $R \geq 24$ in. 24 in. $> R \geq 6$ in. 6 in. $> R \geq 2$ in.	T or Rev. T or Rev. T or Rev.	B C D	19 19 19
	Base metal at a detail attached by groove welds or fillet welds, where the detail dimension parallel to the direction of stress, a , is less than 2 in.	T or Rev.	C	23,24,25
	Base metal at a stud-type shear connector attached by fillet weld.	T or Rev.	C	22
	Shear stress on nominal area of stud-type shear connectors.	S	F	22

TABLE B3
ALLOWABLE RANGE OF STRESS (F_u), KSI

Category (From Table B2)	Loading Condition 1 F_{u1}	Loading Condition 2 F_{u2}	Loading Condition 3 F_{u3}	Loading Condition 4 F_{u4}
A	60	36	24	24
B	45	27.5	18	16
C	32	19	13	10*
D	27	16	10	7
E	21	12.5	8	5
F	15	12	9	8

* Flexural stress range of 12 ksi permitted at toe of stiffener welds on webs or flanges.

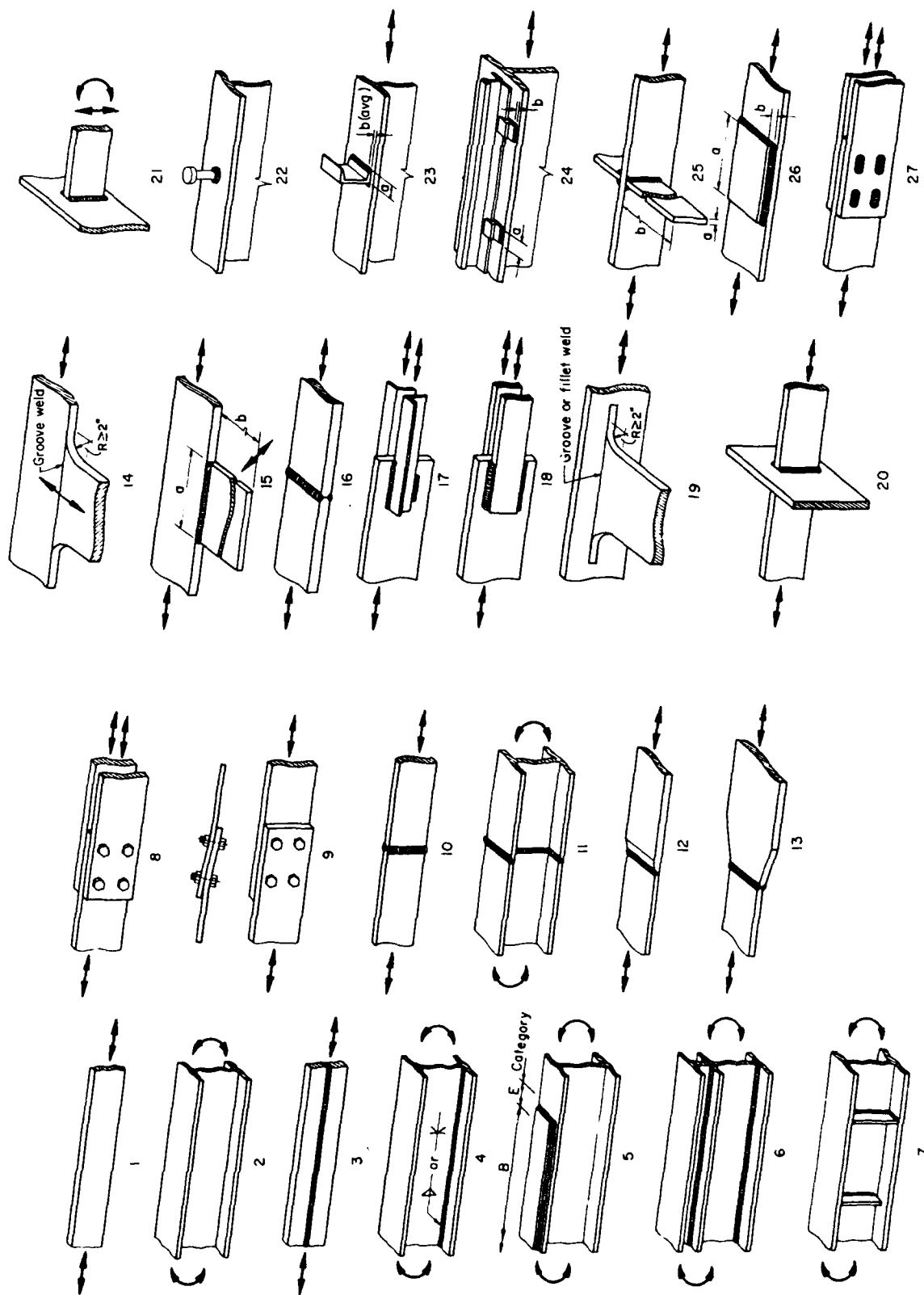


Fig. B1. Illustrative examples

Fig. B1. Illustrative examples (continued)

APPENDIX G: Reaction Loads on Supporting Structures for Beams and Plates Subject to Vibration*

3.3.6.5 Reaction Forces at Boundaries of Beams and Plates

For the analysis of vibration transmission through structures, it is desirable to define the forces developed at support points of vibrating beams and plates due to external loads or local vibratory forces located on the member.

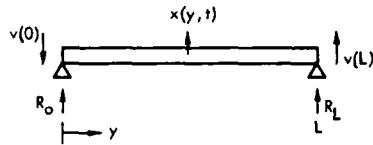


FIGURE 3.107 Reaction Forces Developed at Support Points of Vibrating Beam

The basic method for defining the reaction forces at support points may be demonstrated by considering the case illustrated in Figure 3.107. As shown in Table 3.5, the vertical shear $V(y, t)$ at any section of the beam of stiffness EI and deflection $x(y, t)$ is

$$V(y, t) = -EI x'''(y, t)$$

This is the shear force as viewed, for example, from the left end of the beam so that the reaction forces which oppose this shear at each end are

$$\text{Left Reaction Force } R_O(t) = +EI x'''(0, t)$$

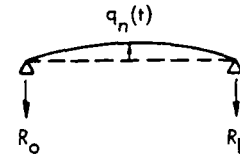
$$\text{Right Reaction Force } R_L(t) = -EI x'''(L, t)$$

Using a normal mode expansion for the deflection, the reaction force at the left end can be given by

$$R_O(t) = +EI \sum_n q_n(t) \phi_n'''(0) \quad (3.389)$$

where $\phi_n'''(0)$ is the third derivative of the mode shape with respect to y at $y = 0$. This general form for the reaction force at $y = 0$ can be applied to any beam whose motion is described in terms of normal modes. Based on the expressions developed in Section 3.3.6.2 for the forced response of simply-supported beams, the following expressions for the reaction load at the ends of a simply-supported beam can be derived. In all cases, the mode shape $\phi_n(y)$ is assumed to be $\sin(n\pi y/L)$. Sinusoidal loads or motions are specified in a general form i.e., $P(t)$, omitting the usual $\cos(2\pi ft)$ term. The resulting expressions relate the reaction loads to the excitation force or an equivalent inertial force.

• General Vibratory Motion of Beam



$$R_O(t) = -W_b \sum_n \left(\frac{1}{\pi n} \right) \frac{1}{g} \ddot{q}_n(t) \quad (3.390a)$$

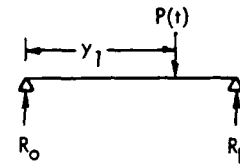
$$R_L(t) = R_O(t) [-(-1)^n], n = 1, 2, 3, \text{ etc.}$$

where W_b = weight of beam

$q_n(t)$ = modal acceleration in n th mode

g = acceleration of gravity

• Point Sinusoidal Force at y_1

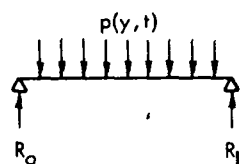


$$R_O(t) = +P(t) \sum_n \left(\frac{2}{\pi n} \right) \sin(n\pi y_1/L) |H_n(f)| \quad (3.390b)$$

$$R_L(t) = R_O(t) [-(-1)^n], n = 1, 2, 3, (y_1 \neq L/2)$$

*Reprinted with permission from L.C. Sutherland, ed, *Sonic and Vibration Environment for Ground Facilities - A Design Manual*, Report WR 68-2 (Wyle Laboratories, 1968), pp 3-155 to 3-156.

• Uniform Sinusoidal Force per Unit Length



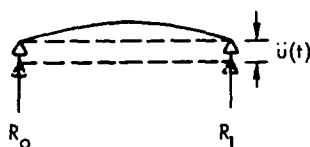
$$R_O(t) = p(y, t) L \sum_n \left(\frac{2}{\pi n}\right)^2 |H_n(f)|_{n=\text{odd}} \quad (3.390c)$$

$$R_L(t) = R_O(t)$$

where

$$|H_n(f)| = 1 / \left[\left(1 - (f/f_n)^2\right)^2 + (2 \delta_n f/f_n)^2 \right]^{1/2}$$

• Uniform Vertical Acceleration of Pinned-Supports



$$R_O(t) = W_b \frac{\ddot{u}(t)}{g} \left[\sum_n \left(\frac{2}{\pi n}\right)^2 |H_n(f)| - 1 \right]_{n=\text{odd}} \quad (3.390d)$$

$$R_L(t) = R_O(t)$$

For the first two cases illustrated above, both odd and even modes are possible. For even modes, the two reaction forces are 180 degrees out of phase. For the last two cases, the assumed symmetrical loading suppresses any even modes.

Reaction Forces at the Boundaries of Vibrating Plates

A similar concept can be used to determine reaction forces at the boundaries of plates. The total reaction forces are defined by more complex expressions which account for the vertical forces due to vertical shear and twisting moments along the edges of the plate (Reference 3.66).

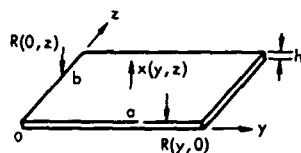


FIGURE 3.108 Vertical Reaction Forces (per Unit Length) Along Edges of Vibrating Plates

Based on the coordinate system illustrated in Figure 3.108, the vertical reaction force per unit length $R(y, 0)$ along side (a), for a lateral deflection $x = x(y, z)$, can be expressed as

$$R(y, 0) = + D \left[\frac{\partial}{\partial z} \left(\frac{\partial^2 x}{\partial y^2} + \frac{\partial^2 x}{\partial z^2} \right) + (1 - \nu) \frac{\partial^3 x}{\partial z \partial y^2} \right] \quad (3.391a)$$

where D , ν = plate stiffness and Poisson's ratio, respectively.

Along side (b), the reaction force $R(0, z)$ is

$$R(0, z) = + D \left[\frac{\partial}{\partial y} \left(\frac{\partial^2 x}{\partial y^2} + \frac{\partial^2 x}{\partial z^2} \right) + (1 - \nu) \frac{\partial^3 x}{\partial y \partial z^2} \right] \quad (3.391b)$$

(Note that the internal force acting on the edge of the plate has the opposite sign.)

A general evaluation of reaction loads for plates is not practical here. For example, the reaction forces at the corners of a rectangular plate are not considered (Reference 3.66). It is sufficient to illustrate the general trend by considering the reaction forces at the edge of a simply-supported plate with a stiffness D , thickness h , mass density ρ , which is vibrating in the m th normal mode with a deflection given by

$$x_{mn}(y, z, t) = q_{mn}(t) \left[\sin\left(m \frac{\pi y}{a}\right) \sin\left(n \frac{\pi z}{b}\right) \right]$$

The frequency for this mode is given by

$$2\pi f_{mn} = \omega_{mn} = \pi^2 \sqrt{\frac{D}{\rho h}} \left[\left(\frac{m}{a}\right)^2 + \left(\frac{n}{b}\right)^2 \right]$$

Using these expressions in Equation 3.391a, it can be shown that the amplitude of the reaction force per unit length along side (a) is

$$R(y, 0) = - \frac{W_p}{a} \sum_m \sum_n \frac{1}{\pi n} \frac{\bar{q}_{mn}}{g} \frac{\left[1 + (2 - \nu) \left(\frac{m/a}{n/b}\right)^2 \right]}{\left[1 + \left(\frac{m/a}{n/b}\right)^2 \right]^2} \sin\left(m \frac{\pi y}{a}\right) \quad (3.392)$$

where

$$W_p/a = \text{weight of plate per length of side (a)}$$

$$\bar{q}_{mn} = \text{peak amplitude of } m\text{th mode at center of plate.}$$

The similarity is clear when this equation is compared with Equation 3.390a for the beam. For example, for a square plate vibrating in its 1,1 mode, setting $\nu = 0.3$, the reaction force along side (a) per unit length would be

$$R(y, 0) = - \frac{W_p}{a} \frac{1}{\pi} \frac{\bar{q}_1}{g} \frac{[2.7]}{[4]} \sin\left(\pi \frac{y}{a}\right)$$

Replacing $\sin \pi y/a$ by $2/\pi$, the average reaction force per unit length will be $(2.7) (\pi/2)/4$. This is 0.43 times as great as an equivalent beam with the same weight per unit width W_p/a and the same peak acceleration in g's at the center.

APPENDIX H: Detailed Data on Vibro-Acoustic Loads on Specific AMD Elements

Detailed data are provided in this Appendix on vibro-acoustic loads on the major secondary structural elements and critical equipment inside the AMD. These data have already been summarized in Chapter 4 of the main body of this report. The data illustrate most of the range of sensitivity and parameter studies carried out or provide more detailed information on the vibratory loads.

DETAILED VIBRO-ACOUSTIC LOADS FOR AMD STRUCTURAL SYSTEMS

The analyses carried out in this appendix are based, to a large extent, on the detailed theory in Appendix D on response of structure to acoustic excitation. In all cases, the analysis of panel responses is carried out over a frequency range extending from the panel fundamental frequency up to 1000 Hz, and assumes simply supported edges.

Wall System Vibration Loads

Details of typical panel dimensions and measured and computed dynamic properties of the wall panels are given in Appendix F. Based on the measured data for a prototype wall panel, the dynamic magnification factor, Q , for the wall panel fundamental mode was assumed to be 25, and 15 for all other modes.

The upper part of Table H1 summarizes the wall panel response parameters, including all modes up to 1000 Hz. The left side lists the space average rms acceleration and spatial maximum rms velocity, stress (from Eq D17 and displacement along with static properties of the panel. The right side of the upper part of Table H1 summarizes the equivalent static pressure, Load Factor and reaction loads.

The lower part of Table H1 lists the computed response at each modal response frequency from the fundamental frequency (19.6 Hz) to an arbitrary cutoff point, for the sake of brevity, of 250 Hz. Starting from the left, the table lists mode numbers, frequency, the spatial average mean square acceleration in gravities and in decibels re: 1g, the spatial maximum mean square velocity, stress, and displacement, the peak acceleration in gravities, the joint acceptances in decibels for each mode, the maximum and average reaction load per foot (see Appendix G) for the short and long sides of the panel, and the estimated total reaction load at each panel/girt joint (see Figure 4, page 19, for illustration of a typical panel/girt fastener detail at such a joint).

Reaction Loads - Wall Panel/Girt Connections

The reaction loads at panel/girt joints were estimated by two different methods. The first, based on the theory presented in Appendix G, is summarized as follows. Referring to the sketch below, reaction

Table H1

Summary of Calculation of Vibro-Acoustic Response of Wall Panels

A) SUMMARY OF WALL PANEL RESPONSE MODES, (106 Modes from 20 to 996 Hz).

SUMMARY OF RESPONSE PARAMETERS							
			Ps/h	0.596	= Static Pressure/Deflection, psi/in		
Space Avg rms Accel. =	7.89 g's		K	0.7116	= Static Stress/[Ps·(a/h) ²], Polynomial Approx.		
Maximum rms Velocity =	19.27 in/sec.		Fp	2.15	= Peak/rms factor for random noise (10% exceedance)		
Maximum rms Stress =	5,116 psi		Ff	0.75	= Reduced strength due to fatigue		
Maximum rms Displ. =	0.132 in.						
Surface Density =	0.0193 psi		EQUIV.STATIC PRESSURE		----- REACTION LOADS , lb./ft. -----		
a/b =	0.3333		32 psf		Along 30' side : Along 90° Side		
h =	0.1946 in.		-----		Max. Avg. : Max. Avg.		
Fundamental Freq. =	19.6 Hz		LOAD FACTOR		19.1 14.1 : 32.8 14.2		
Q for 1,0 mode =	25		17 g s		-----		
For m>0, Qm =	15				Load per Panel/Girt Joint = 172 lb.		

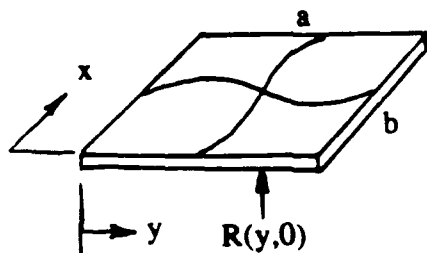
B) FREQUENCY SPECTRUM OF PANEL RESPONSE CHARACTERISTICS [First 25 modes from 19.6 Hz to 242 Hz]

MODAL PARAMETERS			AVG. M.S. ACCEL.		-- MAXIMUM M.S. VALUE -----									
-- Mode No --			Value		La		Velocit		Stress		Stress		Displ.	
Length	Width	Freq(mn)	g ²	dB re:1g	(in/s) ²	(in/sec (psi) ²	(in) ²	g's	10-Log(J ²)	10-Log(J ²)	10-Log(J ²)	10-Log(J ²)	10-Log(J ²)	10-Log(J ²)
m	n	Hz.												
1	0	19.6	1.39	1.45	219.1	272 1.6E+07	1.4E-02	2.54	-3.97	0.00	2.80	2.80	1.87	1.87
1	1	22.8	0.47	-3.25	54.8	245 3.3E+06	2.7E-03	1.48	-3.98	-3.93	0.61	0.39	2.42	1.54
1	2	29.7	0.00	-26.48	0.2	189 5.5E+03	4.4E-06	0.10	-4.03	-29.65	0.06	0.04	0.19	0.00
1	3	41.1	0.12	-9.11	4.4	136 8.1E+04	6.6E-05	0.75	-4.12	-15.33	0.41	0.26	1.22	0.26
1	4	57.1	0.01	-21.68	0.1	98 1.2E+03	9.8E-07	0.18	-4.30	-30.89	0.08	0.05	0.22	0.00
1	5	77.6	0.14	-8.66	1.4	72 7.1E+03	5.7E-06	0.79	-4.61	-20.52	0.32	0.21	0.75	0.10
2	0	78.4	2.86	4.56	28.1	272 2.1E+06	1.2E-04	3.64	-12.01	0.00	2.01	2.01	1.34	1.34
2	1	84.5	1.40	1.46	11.8	265 8.3E+05	4.2E-05	2.54	-11.81	-4.02	0.30	0.00	1.56	1.00
2	2	91.3	0.05	-13.21	0.3	245 2.1E+04	1.0E-06	0.47	-11.27	-19.98	0.10	0.00	0.38	0.00
1	6	102.8	0.03	-15.86	0.1	54 4.4E+02	3.6E-07	0.35	-5.08	-29.90	0.12	0.08	0.25	0.00
2	3	102.8	0.19	-7.27	1.1	218 5.1E+04	2.6E-06	0.93	-10.50	-15.88	0.24	0.00	0.86	0.18
2	4	118.7	0.04	-14.37	0.2	189 5.6E+03	2.8E-07	0.41	-9.65	-24.90	0.12	0.00	0.39	0.00
1	7	132.4	0.12	-9.17	0.4	42 7.4E+02	6.0E-07	0.75	-5.74	-24.42	0.23	0.15	0.42	0.04
2	5	139.3	0.13	-8.90	0.4	161 1.0E+04	5.2E-07	0.77	-8.88	-21.39	0.22	0.00	0.69	0.09
2	6	164.4	0.06	-12.19	0.1	136 2.5E+03	1.3E-07	0.53	-8.31	-26.46	0.14	0.00	0.43	0.00
1	8	166.7	0.05	-12.93	0.1	34 1.2E+02	1.0E-07	0.49	-6.54	-29.07	0.13	0.08	0.21	0.00
3	0	176.4	11.43	10.58	22.2	272 1.6E+06	1.8E-05	7.27	-12.52	0.00	2.68	2.68	1.78	1.78
3	1	187.2	5.10	7.07	8.8	269 6.4E+05	6.3E-06	4.85	-12.09	-4.38	0.26	0.05	1.73	1.10
2	7	194.1	0.10	-9.88	0.2	115 2.2E+03	1.1E-07	0.69	-8.08	-25.61	0.18	0.00	0.50	0.05
3	2	194.1	0.72	-1.45	1.1	260 7.7E+04	7.7E-07	1.82	-11.45	-13.80	0.18	0.04	0.84	0.00
1	9	205.5	0.07	-11.64	0.1	27 7.3E+01	5.9E-08	0.56	-7.41	-28.16	0.14	0.09	0.20	0.01
3	3	205.5	0.36	-4.49	0.5	245 3.1E+04	3.0E-07	1.28	-10.74	-17.68	0.18	0.04	0.70	0.15
3	4	221.5	0.18	-7.54	0.2	227 1.1E+04	1.1E-07	0.90	-10.49	-20.71	0.15	0.03	0.54	0.00
2	8	228.3	0.06	-12.14	0.1	98 6.8E+02	3.4E-08	0.53	-8.37	-27.33	0.13	0.00	0.33	0.00
3	5	242.0	0.10	-9.95	0.1	208 4.5E+03	4.5E-08	0.68	-9.93	-23.38	0.12	0.03	0.43	0.05

loads alongside a simply supported plate can be defined as follows. For any position y along side a , the reaction load, $R(y,0)$ is:

$$R(y,0) = -\frac{W_p}{a} \sum_m \sum_n \frac{1}{\pi m n} a_{mn} F(m,n,a,b) \sin \frac{m\pi y}{a} \cdot \frac{lb}{ft} \quad [\text{Eq H1}]$$

where W_p = weight of plate, lbs
 a,b = length of sides of plate, ft
 m,n = m,n th mode number along sides a and b respectively
 a_{mn} = maximum amplitude of panel acceleration in m,n th mode, gravities
 $F(m,n,a,b)$ = the function of mode numbers m,n and lengths a and b given by the terms in brackets in Eq (3.392) in Appendix G.



The maximum value of this reaction load along side a , $R(y,0)_{\max}$ is given by Eq H1 for any value of y for which the sine function is 1. The first position (i.e., smallest value of y) for this maximum will occur at $y = a/2m$ (e.g., at midspan for the first mode where $m = 1$).

The average reaction load \bar{R} along side a is obtained by integrating Eq H1 over the length of side a . The result is:

$$\bar{R}(a/2,0) = \frac{2}{\pi m} R(y,0)_{\max}, \quad m = \text{odd} \quad [\text{Eq H2}]$$

$$= 0, \quad m = \text{even}$$

Applying this first method, it is assumed that the average vibration reaction load per unit length along the long 7.5 ft section of the panel (14.2 lb/ft) multiplied by 7.5 ft and by 2 for the two 7.5 ft sides of the panel gives the total reaction load per 2.5 ft x 7.5 ft panel section. This load must be carried by the panel/girt fasteners. However, for an average full floor to ceiling height of about 45 ft for these panels, over a 25 ft wide bay between columns, there will be $(45/7.5 \times (25/2.5))$ or $6 \times 10 = 60$ panel sections per bay and $(6+1) \times (10+1) = 77$ panel/girt joints (i.e., one joint at each corner of each panel which carries the load for four panel/girt corners). On this basis, the total vibration reaction load R_{PG} at each panel/girt joint, would be:

$$R_{PG} = 14.2 \times 7.5 \times 2 \times \frac{60}{77} = 166 \text{ lb}$$

The second method simply assumes that the total reaction load per panel section is equal to the *spatial average* vibration load factor, 17 g times the generalized weight of each panel section, $1/4 (2.78)(7.5)(2.5)$.

Applying the same correction of 60 panel sections for 77 joints, the estimated total reaction load at each panel/girt joint, R_{PG} , would be

$$R_{PG} = 17 \times \frac{1}{4} \times 2.78 \times 7.5 \times 2.5 \times \frac{60}{77} = 173 \text{ lb}$$

These two different estimates are in very close agreement and the higher value (173 lb) is adopted for design purposes for the panel/girt fasteners. Note that this is actually the alternating (\pm) peak tension/compression load which includes the correction factors for random peak/rms (2.15) amplitude and fatigue effects (1/.75) but does *not* include any correction for stress concentration. However, prudent design for the panel/girt fasteners would dictate that an additional multiplier of this basic design load of 173 lb be included to allow for this. Assuming a value of 3.5 for such a multiplier, the final recommended design tension/compression load for each panel/girt joint is 610 lb (rounded to 2 significant figures).

Assuming the vibratory in-plane load is one-half of the above value, allowing for the dead weight load (52 lb) of the panels, the estimated peak shear load V_{PG} downward on each panel/girt joint would be (including a multiplier of 3.5 for stress concentration):

$$V_{PG} = -\left(\frac{1}{2} \times 173 + 52 \times \frac{60}{77}\right) (3.5) = -440 \text{ lb}$$

Reaction Loads - Girt/Column Connections

The girt/column reaction loads due to vibration were also computed by two methods.

- (1) For the first method, according to Table H1, the average reaction load along the 30 in. span of each panel is 14.1 lb/ft. Thus, over a 25 ft girt span, allowing for two panel sections per girt (above and below each girt), and two ends to each girt, a baseline peak vibratory load at each girt/column joint, normal to the panel surface, would be $25 \times 14.1 \times 2 \times (1/2) = \pm 352 \text{ lb}$. Allowing for a stress concentration factor of 3.5, a design vibration reaction load would be $\pm 1235 \text{ lb}$.
- (2) For the second method, assume the 610 lb design load per panel/girt joint times 11 joints per 25 ft girt span is carried by both ends of a girt but that each 610 lb panel load is randomly phased with the others. On this basis, the net vibratory reaction load at each girt/column joint would be:

$$\sqrt{\sum_{i=1}^{11} (610)^2} \times \frac{1}{2} = \sqrt{(610)^2 \times 11} \times \frac{1}{2} = 1010 \text{ lb}$$

The higher estimate (1235 lb) from Method No. 1 is recommended for a tension-compression design load for the girt/column joint to account for vibration.

The corresponding shear at a girt/column connection including the average static weight of the panels and girts, is estimated as follows:

1/2 Basic Vibration Reaction Load Normal to Wall	$1/2 \times 352$	$= \pm 176 \text{ lb}$	
Static Weight of 10 Panel Sections/Girt	10×52	$= 520 \text{ lb}$	
Static Weight of 1 Girt	25×24	$= \underline{600 \text{ lb}}^*$	
Total Baseline Shear Load		$= +1,296$	$= 1300 \text{ lb}$

* Based on average weight per foot of the various size girts on all four walls.

Thus, a minimum shear load for a typical girt/column connection, which includes the effect of vibration, would be 1,300 lb. This does not include any additional static load associated with the weight of equipment mounted to a girt. This baseline vertical shear load also does not include any allowance for stress concentration. Note that the vibratory portion of this shear load is less than 14 percent of the total so that, unlike the horizontal reaction loads, static loads will dominate the vertical shear loads at girt/column connections.

To summarize so far, the wall panels should be designed to withstand an alternating pressure load of ± 32 psf for acoustic loading. The recommended design tension/compression load for each panel/girt joint is 610 lb and the corresponding shear load is 440 lb. These latter two recommended design loads include a multiplier of 3.5 to allow for stress concentration. The recommended tension/compression reaction load at girt/column joints is 1235 lb, including a multiplier of 3.5 for stress concentration. The vibration reaction load in shear for girt/column joints is only 14 percent of the basic static weight load.

Vibration Load Factors - Wall Mounted Equipment

Attachments of equipment components to the panel surface should be avoided but, if necessary, must be designed to withstand a vibratory load, developed in Table H1, of ± 17 g in the direction perpendicular to the panel. In the plane of the panel, the load factor is reduced by a factor of 2 to 8.5 g's.

Vibration load factors on girt or column-mounted equipment are estimated by reducing the baseline vibration load factors by the relative increase in average surface weight of the structure, as shown in Table H2.

The design load factors in the right-hand column of Table H2 are baseline values in the absence of any additional mass loading by equipment. The baseline load factor of 8.0 g for girt-mounted equipment was computed as follows.

- The basic load factor of 17 g at the center of a wall panel was obtained in Table H1 from the analysis of wall panel response to the design acoustic input.
- The combined surface weight of a girt and section of supported wall panel is, on the front wall for example, $2.78 + 18/7.5 = 5.18$ psf.

Table H2

Load Factors for Equipment Mounted on Wall Panels, Girts and Columns

Location	Element	Size ft	Spacing ft	w* psf	Σw** g	LF g	Design LF g
Wall	Panel	2.5 x 7.5	-	2.78	2.78	17	17
Girt	Back wall	W10 x 33/39	7.5	4.80	7.58	6.23	8.0
Girt	Side wall	W8 x 21	7.5	2.80	5.58	8.47	8.0
Girt	Front wall	W8 x 18	7.5	2.40	5.18	9.12	8.0
Column	Back wall	W12 x 65	25	2.60	10.24	4.62	5.4
	Side wall	W12 x 53	25	2.12	7.70	6.14	5.4

* Average surface weight for panels, girts or columns: $w = (wt/ft)/spacing$

** Cumulative surface weight (e.g., panel + girt, or panel + girt + column)

- Thus, to a first approximation, using the higher combined surface weight of panel plus girt, the estimated baseline girt load factor is equal to the baseline load factor, 17 g, for the panel alone, which is based on a space-average acceleration, times the ratio of the panel surface weight to the panel plus girt surface weight or $17 \times 2.78/5.18 = 9.12$ g.
- The same process is carried out for each type of girt and the results averaged to give a design baseline load factor for girt-mounted equipment of 7.94, rounded to 8 g.

A similar process is carried out to define an average baseline load factor for column-mounted equipment of 5.4 g.

Reduction in Vibration Load Factors Due to Mass Loading Effects

The baseline vibration load factors specified in Table H2 will begin to decrease significantly for equipment which has a weight greater than about 10 percent of the basic weight of the mounting structure. A highly simplified method is used to account for this effect which is based on concepts similar to that employed above in computing baseline load factors for girt- or column-mounted equipment.

This process was illustrated in the main body of the text in the Mass Loading Effects section (p 54). The net result is that an effective vibration load factor LF_{eff} for an equipment item with a weight W_e mounted on a structure with a weight W_m is given by:

$$LF_{eff} = LF \left[\frac{W_m}{W_m + W_e} \right] \quad [Eq H3]$$

where LF is the baseline load factor.

For application of Eq H3, it is important to note that the dynamically effective weight of the mounting structure W_m is less than the true weight. For example, consider a simply supported beam with a point (equipment) mass load in the middle of the beam. It can be shown, by equating the fundamental resonance frequency of the beam to that of an equivalent lumped mass-spring system with the same stiffness, as measured at the center of the beam, that the dynamically equivalent weight of the beam at this point is equal to $48/\pi^4 = 0.493$ times the true weight. This is rounded to a factor of 0.5 for design purposes. This reduced dynamically equivalent weight would be higher for a mounting location nearer the end of a beam. However, response levels would also be lower, so, for simplicity, the dynamically equivalent values for W_m are considered applicable at any location on a particular structure. Applying this refinement tends to reduce the effective load factor.

It should also be noted that the value of W_m includes both the basic mounting structure, such as a girt and that portion of the secondary structure (e.g., wall panel) supported by the structure (girt). Including this correction increases the effective structural mounting weight W_m and hence increases the effective load factor.

The net results of these two refinements to the evaluation of the effective structural mounting weight W_m are summarized in Table H3 for wall-mounted equipment.

Finally, a conservative method for applying Eq H3 would dictate that the value for the equipment weight W_e should be the actual weight divided by the number of different structural elements on which it is mounted. For example, for an equipment package weighing 400 lb mounted between two girts, on

Table H3
Effective Structural Weights for Wall-Mounted Equipment

Mounting Structure	Size	Length ft	W_m lb
Wall Panel Section	2.5' x 7.5'	-	26*
Girt - Back Wall	W10 x 39	25	750**
Girt - Back Wall	W10 x 33	25	675**
Girt - Side Wall	W8 x 21	25	525**
Girt - Front Wall	W8 x 18	25	485**
Column - Back Wall	W12 x 65	38	5,035***
Column - Side Wall	W12 x 53	43 ±5	4,150***
Column - Front Wall	W12 x 53	48	4,375***

* Effective weight for one 2.5 ft section of wall panel

** Includes effective weight (one-half of true weight) of panel carried by girt, e.g., for back wall, $W_m = 10 \times 26 + 1/2 \times 39 \times 25 = 750$ lb

*** Includes effective weight of wall panels and girts between columns, e.g., for back wall, $W_m = (38/7.5) \times 750 + (1/2) \times 65 \times 38 = 5,035$ lb

the side wall, $W_m = 525$ lb, $W_e = 400/2 = 200$ lb and, from Table H2 with a baseline $LF = 8$ g for equipment mounted on girts, the effective load factor at each girt/equipment mounting point would be:

$$LF_{eff} = 8g \left[\frac{525}{525 + 200} \right] = 5.8g$$

In summary, baseline vibration load factors for wall mounted equipment are specified in Table H2. These baseline values should be reduced by the correction defined in Eq H3 using the values of W_m in Table H3.

Roof and Ceiling Mounted Systems

The same basic process carried out above for wall structure and wall mounted equipment is repeated here, without detailed elaboration, for the roof structure and roof/ceiling mounted equipment. The dynamic magnification factor, Q , was assumed to be 15 for all modes of the roof deck/bar joist system.

Alternate Bar Joists

Table H4 summarizes the vibro-acoustic parameters for the roof for alternative bar joist configurations. The last three columns list the key vibration loads data in terms of baseline load factors, LF , equivalent static pressures, P_s , and vertical vibration reaction loads R/b per unit width of roof panel.

For the analysis carried out to develop vibration loads for the roof shown in Table H4, each section of the roof between bar joists of the roof/bar joist system was treated as a beam with a weight per unit length equal to the weight of a 5.7 ft span of a roof deck/bar joist combination. The remaining roof vibration loads are based on the 16K6 bar joist.

Vibration Reaction Loads for Roof System

The reaction loads for the roof system are defined first for each bar joist/roof truss joint as follows.

The magnitude of the reaction load R at either end of a simply supported vibrating beam (the dynamic model for a bar joist/roof deck section) is given by (see Appendix G):

$$R = W \sum_n \left(\frac{1}{\pi n} \right) \times a_m \quad [\text{Eq H4}]$$

where W = total weight of beam

a_m = peak acceleration of beam in $m+h$ mode

For a 25 ft 16K6 bar joist ($W/L = 8.1$ lb/ft) supporting an average 5.7 ft span of roof deck with a surface weight of 5.9 psf, W is equal to $8.1 \times 25 + 5.7 \times 5.9 = 1043$ lb.

Table H4

Roof Vibro-Acoustic Loads for Alternative Bar Joists

Bar Joist	Span(L) ft	I in ⁴	W/L lb/ft	w _{BJ} [*] psf	w _{ROOF} ^{**} psf	w _{TOT} psf	f ₁ [†] Hz	LF g	Ps psf	R/b [‡] lb/ft
8K1	8	6.6	5.1	0.89	5.9	6.79	26.2	4.52	63.4	447
14K6	25	70	7.7	1.35	5.9	7.25	8.47	5.34	23.4	384
16K4	25	78.4	7.0	1.23	5.9	7.13	9.04	5.37	24.9	389
16K5	25	88	7.5	1.32	5.9	7.22	9.51	5.23	26.1	394
16K6	25	95.6	8.1	1.42	5.9	7.32	9.85	5.15	27.0	397
16K7	25	106	8.6	1.51	5.9	7.41	10.31	5.04	29.7	406
16K9	25	125	10.0	1.75	5.9	7.65	11.0	4.86	31.6	413
22K5	25	172	8.8	1.54	5.9	7.44	13.1	4.85	36.9	425

* Average surface density of bar joist over average spacing, b, of 5.7 ft.

** Surface density of roofing (steel deck, 2.2 psf; + insulation + EPDM, 3.5 psf; + fire protection piping, 0.2 psf) = 5.9 psf.

*** w_{TOT} = w_{BJ} + w_{ROOF}.

† Fundamental frequency =

$$f_1 = \frac{\pi}{2L^2} \sqrt{\frac{EI}{(\rho A)_{\text{eff}}}}$$

where

$$(\rho A)_{\text{eff}} = \frac{W}{Lg} = \left[\frac{w_{\text{TOT}}(\text{psf})}{144} \right] \left[\frac{b(\text{in})L}{Lg} \right] = \frac{(w_{\text{TOT}}(\text{psf}))(b(\text{ft}))}{12g}, \text{ lb sec}^2/\text{in.}^2$$

where

b = panel width in feet

L = panel length in inches

‡ Reaction load per foot width (b) of roof panel.

As shown in the analysis worksheet in Table H5, the total vibratory reaction load R is 1131 lb at each end for 11 modes of a bar joist/roof deck beam between a fundamental mode of 9.85 Hz (see Table H4) and 1000 Hz. Thus, the peak vertical reaction load at each bar joist/roof truss joint will be, allowing for the static load and a stress concentration factor of 3.5:

$$R_{\text{vib}} = \pm 1131 \text{ lb} \times 3.5 = \pm 3960 \text{ lb}$$

$$R_{\text{wt}} = -1043 \text{ lb} \times 3.5 = -3650 \text{ lb}$$

Bar Joist/Roof Truss Joint	R _{TOTAL}	= -7610 lb down = + 310 lb up
----------------------------	--------------------	----------------------------------

Table H5

Summary of Calculations of Vibro-Acoustic Response of Roof

A.) SUMMARY OF ROOF DECK RESPONSE MODES, (11 Modes from 9.85 to 1192 Hz)

Bar Joist = 16K6, W/L =	8.10 lb/ft	Ps/K =	NA	= Static Pressure/Deflection when available
Sp. Avg. rms Accel. =	2.394 g's	K =	0.7607	= Static Stress/[Ps·(a/h) ²], Polynomial Approx.
Maximum rms Velocity =	5.725 in/sec.	Fp =	2.15	= Peak/rms factor for random noise (10% exceedance)
Maximum rms Stress =	1,559 psi	Ff =	0.75	= Reduced strength due to fatigue
Maximum Peak Displ. =	0.1266 in.			
Surface Density =	0.0508 psf	Equiv. Static Pressure		Vibration Reaction Load on Bar Joist/
a/b =	0.0000	Ps =	27.0 psf	Roof Deck Connection = 90.5 lb/ft.
h =	9.775 in.			
Fundamental Freq. =	9.85 Hz	Load Factor =	5.15 g's	Vibration Reaction Load at each
Dyn. Magnif. Factor =	15			Bar Joist/Truss Joint = 1131 lb.

B.) FREQUENCY SPECTRUM OF ROOF DECK RESPONSE CHARACTERISTICS

long. & lateral Value	AVG. M.S. ACCEL. J ² m,n	La	Velocity (in/s) ²	Stress (psi) ²	Displ. (in) ²	Freq. Hz.	Peak Accel. g's	10·Log(J ²) Jm ² Jn ²	REACTION LOAD lb. (0 end)	La	Peak Accel. g's			
		dB re:1g	(in/s) ²	(in/sec) (psi) ²	(in) ²									
		-40												
	0.39	0.02	-16.89	12.75	272.36	9.46E+05	3.33E-03	9.85	0.31	-4.050	0	102.2	-15.90	0.345
	0.12	0.17	-7.63	6.71	272.36	4.98E+05	1.10E-04	39.40	0.89	-9.139	0	148.3	-6.40	1.029
	0.11	0.96	-0.17	7.39	272.36	5.48E+05	2.38E-05	88.65	2.11	-9.505	0	233.3	-0.14	2.116
	0.07	1.67	2.23	4.06	272.36	3.01E+05	4.14E-06	157.60	2.78	-11.61	0	230.6	2.20	2.770
	0.04	1.38	1.39	1.37	272.36	1.02E+05	5.73E-07	246.25	2.52	-13.48	0	167.6	2.19	2.766
	0.03	0.72	-1.42	0.35	272.36	2.57E+04	6.97E-08	354.60	1.83	-15.03	0	101.0	-1.29	1.852
	0.02	0.37	-4.26	0.10	272.36	7.20E+03	1.06E-08	482.65	1.32	-16.36	0	62.4	-4.24	1.320
	0.02	0.20	-6.97	0.03	272.36	2.26E+03	1.94E-09	630.40	0.96	-17.51	0	40.0	-6.79	0.984
	0.01	0.12	-9.37	0.01	272.36	8.14E+02	4.37E-10	797.85	0.73	-18.52	0	27.0	-9.04	0.759
	0.01	0.07	-11.51	0.00	272.36	3.26E+02	1.15E-10	985.00	0.57	-19.43	0	19.0	-11.06	0.602
	0.01	0.05	-13.45	0.00	272.36	1.43E+02	3.43E-11	1191.85	0.46	-20.26	0	13.8	-12.88	0.488

* Combined surface weight in psi of roof deck (5.9/144 psi) and 16K6 bar joist (8.1/(5.7·144) psi) when the later are spaced an average of 5.7 ft apart.

The corresponding shear load, V, assuming a 50 percent in-plane reduction of vibration loads, is:

$$\text{Bar Joist/Roof Truss Joint} \quad V = \pm 1/2 \times 3960 \text{ lb} = \pm 1980 \text{ lb}$$

The vertical reaction load along the roof deck/bar joist connections will be assumed to simply be the total reaction loads at both ends of a bar joist distributed over the length of the bar joist. Including a stress concentration factor of 3.5, these roof deck/bar joist connection loads are:

Roof Deck/Bar Joist

$$\text{Vertical Load } R_{\text{TOTAL}} \begin{cases} + 310 \text{ lb} \times 2/25 \text{ ft} & = + 25 \text{ lb/ft} \\ -7610 \text{ lb} \times 2/25 \text{ ft} & = -610 \text{ lb/ft} \end{cases}$$

$$\text{Horizontal Load } V = \pm 1980 \text{ lb} \times 2/25 \text{ ft} = \pm 160 \text{ lb/ft}$$

Load Factors for Roof Truss-Mounted Equipment

Estimates of vibration load factors for any equipment to be supported directly on, or hung from, the bar joists or roof truss system were generated by using the same type of mass loading algorithm used earlier to define reduced load factors on wall girts and columns. For example, for equipment to be mounted on a roof truss, the load factor was assumed equal to the baseline load factor for the adjacent roof deck (equal to 5.15 g for the 16K6 bar joist) multiplied by the ratio of the average surface weight of this combination (7.32 psf according to Table H4) to the average surface weight of the roof deck, bar joist and roof truss combination *in the vicinity of the mounting location*. This process required that: (a) the weight of all basic structural elements of the roof structure be developed, (b) average surface densities defined, and (c) load factors established accordingly for each section of the roof truss system. The result of this process is summarized schematically in the three parts (A, B and C) of Table H6. For example, in Table H6A, the total weight of that part of the total weight of the roof truss between columns A and B is 797 lb, 2121 lb between trusses B and C, 2270 lb between trusses C and B, etc. The weight of the side to side roof truss (including the average weight of light fixtures mounted on this truss of 5.5 lb/ft) is 4608 lb between roof trusses 3 and 4 on column line B, 4374 lb on column line C, 3432 lb on column line D, etc. The sums of the table columns and rows thus represent the total base weight of the roof structure plus light fixtures over one-half of the AMD roof.

Table H6B presents in each cell the surface weights of the basic roof deck/bar joist structure (7.32 psf) and the average surface weight of the entire roof structure for each segment of roof truss (e.g., 17.9 psf is the value for the segment of roof supported by the roof truss on column line B between roof trusses 3 and 4).

Table H6C presents the resulting vertical (bidirectional) vibrational load factors for the roof deck (± 5.2 g) and for each segment of the roof trusses. The latter vary from a minimum of ± 1.6 g for the segment on column line F between trusses 5 and 6 to a maximum of ± 3.9 g. The average, excluding

Table H6

Schematic Diagram of Analysis of Vibro-Acoustic Load Factors on Truss-Mounted Equipment

TABLE H-6A. TOTAL WEIGHT OF STRUCTURAL ELEMENTS, lb.

FRONT TO BACK \\	33.25 ft.			FRNT/BK TRUSS	33.25 ft.			FRNT/BK TRUSS	36 ft.			FRNT/BK TRUSS	CENTER- LINE SUB-TOTAL
	ROOF DECK	LIGHT FIXTURES	BRACES		ROOF DECK	LIGHT FIXTURES	BRACES		ROOF DECK	LIGHT FIXTURES	BRACES		
A >>		5,477 (5)				4,495 (5)				4,950 (5)			14,922
B ft.	1,947 (4)		808	797 (1)	1,947		703	1,112	2,108		703	872	10,997
B >>		4,608 (1,2)				3,626				4,169			12,403
25 ft.	6,085		1,614 (3)	2,121	6,085		965	3,531	6,588		1,165	2,888	31,042
C >>		4,374				3,840				4,556			12,770
25 ft.	6,085			2,270	6,085		1,032	3,591	6,588			2,333	27,984
D >>		3,432				3,276				3,815			10,523
25 ft.	6,085			2,075	6,085		1,065	3,360	6,588			2,212	27,470
E >>		2,881				2,787				3,748			9,416
25 ft.	6,085		1,373	2,017	6,085		1,675	3,238	6,588		2,102	1,610	30,773
F >>		3,150				5,246				6,293			14,689
TOTAL >>	26,286	23,922	3,795	9,280	26,286	23,270	5,440	14,832	28,460	27,531	3,970	9,915	202,986 lb. (5)

(1) Mt. of TRUSS Section + Light fixtures

(2) Avg. Mt./ft of Light Fixtures on roof trusses is

5.5 lb/ft.

(3) Mt. of Cross Braces and Horizontal Wind Trusses

(4) Based on Average Surface Mt of Roof Deck/Bar Joist Combined = 7.32 psf

(5) Includes weight of additional bracing for wind truss

(5) Overall TOTAL Mt.
From TRUSS 3 to 6,
excluding TRUSS 3TABLE H-6B. AVERAGE SURFACE WEIGHTS, psf
(as distributed over roof surface)

TABLE II.32. AVERAGE SURFACE WEIGHTS, psf (as distributed over roof surface)							CENTER- LINE
FRONT TO BACK \\	Area per Cell(1) 831.3 sq.ft.	FRNT/BK TRUSS 4	Area per Cell(1) 831.3 sq.ft.	FRNT/BK TRUSS 5	Area per Cell(1) 900 sq.ft.	FRNT/BK TRUSS 6	
A >>	51.5		43.8		44.1		
	7.32	13.2 (2)	7.32	13.9	7.32	12.8	
B >>	17.9 (2)		15.4		15.9		
	7.32	11.4	7.32	12.6	7.32	11.8	
C >>	13.6		13.1		19.7		
	7.32	10.7	7.32	12.1	7.32	9.9	
D >>	11.4		12.5		17.5		
	7.32	10.5	7.32	11.8	7.32	9.8	
E >>	11.6		12.3		19.2		
	7.32	11.6	7.32	13.2	7.32	11.4	
F >>	16.6		22.0		23.6		

(1) Except Area between Truss A and B

(2) "Surface Mt." of Total Roof Structure over 1/2 of Roof
Area on each side of TRUSS section.

Table H6 (Cont'd)

TABLE H-6C. LOAD FACTORS ON ROOF, g's (3)
 [Based on Table H-6B. and Load Factor for Roof Deck = 5.15 g's]

SIDE TO SIDE TRUSS \\ /	FRNT/BK TRUSS 4	FRNT/BK TRUSS 5	CENTER- LINE FRNT/BK TRUSS 6
A >>	0.7	0.9	0.9
	5.2 (1)	2.9 (2)	2.9
B >>	2.1 (2)	2.4	2.4
	5.2	3.3	3.2
C >>	2.8	2.9	1.9
	5.2	3.5	3.8
D >>	3.3	3.0	2.2
	5.2	3.6	3.9
E >>	3.2	3.1	2.0
	5.2	3.3	3.3
F >>	2.3	1.7	1.6

(1) Load factor for Roof Deck.

(2) Load Factor for Equipment mounted on this section of Roof Truss.

(3) This load factor is applicable in both the up and down directions.

It is in addition to the downward load due to gravity so that, for example, the total load factor in the vertical direction on the roof deck is 4.2 g up and 6.2 g s down.

In a horizontal plane, the total load factor can be taken as plus or minus

1/2 the values shown above at all locations on the roof system.

(4) Average Load Factor on Trusses ± 1 SD = 3.1 ± 0.5 g's

(Excluding truss sections on column line A and between column lines A and B).

values on the roof truss on column line A and between column line A and B, is 3.1 ± 0.5 g. Thus baseline vibration load factors for roof-mounted equipment will be:

Vertical Direction	- - - - Location - - - -	
	Roof Deck or Bar Joists	Roof Trusses*
Up	+4.2 g	+ 2.1 g
Down	- 6.2 g	- 4.1 g
Lateral Direction	± 2.6 g	± 1.6 g

* Average

Mass Loading Effects for Roof-Mounted Equipment

The values of effective structural mounting weights, W_m , to employ with Eq H3 for computing reduced load factors due to mass loading are as follows.

- For Equipment Mounted on One Bar Joist

$$W_m = \left(\frac{\text{Effective Mass}}{\text{Actual Mass}} \right) (\text{Span}) (\text{Avg Spacing}) (\text{Surface Wt})$$

$$= 1/2 \times 25 \text{ ft} \times 5.7 \text{ ft} \times 7.32 \text{ psf} = 520 \text{ lb}$$

When equipment is supported from more than one bar joist, then the equipment weight W_e to use in Eq H3 should be taken as that portion of the total equipment weight supported by one bar joist.

- For Equipment Mounted on Roof Trusses

The appropriate values for W_m for each section of roof truss (in both directions) were developed in the same way as above. The results are listed in Table H7. For example, for a 650 lb equipment item mounted to roof truss No. 4 between column lines A and B, the effective load factor LF_{eff} would be $LF_{\text{eff}} = \text{Baseline Value of } 2.9 \text{ g} \times [1750/(1750 + 650)] = 2.1 \text{ g}$.

Table H7

Effective Weights of Roof Truss Mounting Structure, lbs

TABLE H-7. EFFECTIVE WEIGHTS OF ROOF TRUSS MOUNTING STRUCTURE, lbs.

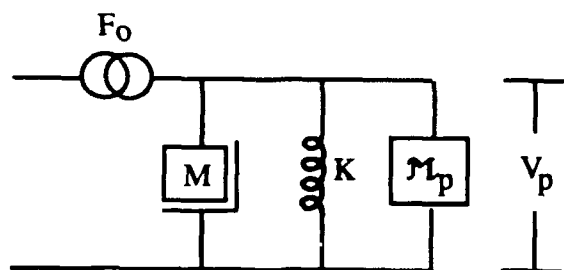
FRONT TO BACK \\ /	33.25 ft.	FRNT/BK TRUSS	33.25 ft.	FRNT/BK TRUSS	36 ft.	FRNT/BK TRUSS
A >>	3,427		2,910		3,178	
B ft.		1,750		1,921		1,842
B >>	4,917		4,238		4,725	
25 ft.		4,748		5,466		5,321
C >>	5,633		5,462		5,863	
25 ft.		4,435		5,222		4,461
D >>	4,758		5,205		5,201	
25 ft.		4,346		5,114		4,400
E >>	4,826		5,121		5,693	
25 ft.		4,813		5,731		5,150
F >>	3,439		4,563		5,319	

Average $W_m \pm 1$ SD = 5017.0 \pm 464 lbs.

(Excluding truss sections on column line A and between column lines A and B).

Vibration Load Factors for Pipe Hangers Supported from Bar Joists

An additional evaluation was made of the vibration loads on pipe hangers supporting cooling system pipes hung from the bar joists. The vibration response of the pipes was evaluated by a lumped parameter mechanical mobility analog "circuit" illustrated in the sketch below, where:



Mobility Model of Pipes Hung from Roof

F_o is the acoustic driving force, M is the mass of the roof deck/bar joist system, K is the spring rate of this system that corresponds to the fundamental frequency (9.85 Hz) of the roof deck/bar joist equivalent beam, M_p is the mechanical mobility of the pipe system as seen at one pipe hanger, and V_p is the velocity response of the roof/pipe hanger combination.

Note that a mobility analog model has the desirable feature that a force is analogous to a current and just as mechanical forces acting on a point must sum to zero, "currents" in a mobility analog circuit sum to zero at any junction. Similarly, the velocity response in a mobility analog circuit is like a voltage the motion with respect to a fixed ground location being analogous to the voltage with respect to an electrical ground. The mobility of a mechanical element is the ratio of velocity response to applied force. Thus, the mobility of a mass M is equal to $V/F = \dot{x}/j\omega F = 1/j\omega M$. The mobility of a spring with stiffness K is $V/F = j\omega x/F = j\omega/K$.

Based on these concepts, the sum of the forces (currents) at the top of the circuit is found by applying the mobility analog equivalent of Ohms law (i.e., current = voltage/resistance) to give:

$$F_o = \frac{V_p}{\frac{1}{j\omega M}} + \frac{V_p}{\frac{j\omega}{K}} + \frac{V_p}{M_p} \quad [\text{Eq H5}]$$

where $1/j\omega M_1$ and $j\omega K_1$ are the mobilities of the mass and spring respectively, $\omega = 2\pi f$, and $j = (-1)^{1/2}$.

Damping is included by using a complex spring constant, $K = K_o(1+j/Q)$ where Q is the dynamic magnification factor of the roof deck resonance and K_o is the actual spring rate corresponding to the stiffness of the roof deck for the fundamental mode.

Without the pipe hanger (i.e., for the pipe mobility becoming infinite) the unloaded velocity response of the roof deck/bar joist V_o will be

$$V_o = F_o \left[\frac{1}{j\omega M + \frac{1}{j\omega K}} \right]$$

$$= \frac{F_o j\omega}{K_o - \omega^2 M + \frac{jK_o}{Q}} \quad [\text{Eq H6}]$$

The maximum response (in the fundamental vibration mode) occurs at the resonance frequency

$$f_0 = \frac{1}{2\pi} \sqrt{\frac{K_o}{M}}$$

Setting $\omega = \omega_c = 2\pi f_0$ in Eq H6, the maximum unloaded response becomes:

$$V_{o\max} = F_o \omega_o \frac{Q}{K_o} = F_o \frac{Qg}{\omega_o W} \quad [\text{Eq H7}]$$

where $W = Mg$, the effective weight of the roof deck/bar joist.

The added load of the pipe is represented by the mobility M_p which is conveniently represented by the mobility of an infinite pipe (beam) driven at a point. This can be given by (Beranek 1971):

$$M_p = \frac{g}{[2 w C_B (1+j)]} \quad [\text{Eq H8}]$$

where g = acceleration of gravity, 386 in/sec²

w = weight per in. of pipe beam

C_B = bending wave velocity in pipe beam, in/sec

$$= \left[\frac{EI \omega^2 g}{w(1-v^2)} \right]^{1/4}$$

EI = bending stiffness of pipe beam, lb-in²

$\omega = 2\pi f$

v = Poisson's ratio = 0.3 for steel

For a Schedule 80 6.625 in. outside diameter (OD) pipe with wall thickness of 0.432 in., the empty weight is 28.57 lb/ft or 2.38 lb/in and, when full of water, $w = 3.32$ lb/in; $EI = 1.22 \times 10^9$ lb-in².

At the resonance frequency f_0 of the roof deck/bar joist of 9.85 Hz, the addition of the pipe load does not reduce the fundamental resonance frequency more than about 23 percent and changes the higher roof deck/bar joist beam modes by much less, so these changes in resonance frequency with loading by the pipe are neglected. Thus, the value for C_{Bo} at $f = f_0$ or

$$C_{Bo} = \left[\frac{1.22 \times 10^9 \times (2\pi \times 9.85)^2 \times 386}{3.32 \times (1-.3^2)} \right]^{1/4} = \frac{4940 \text{ in.}}{\text{sec}}$$

For the n th roof deck/bar joist mode, the resonance frequency f_n increases as n^2 and the corresponding value for C_B increases as $n^{1/2}$.

From Eqs H5 through H7 it can be shown that, at the n th resonance frequency, $\omega_n = 2\pi f_n$, the ratio of the maximum acceleration response with the pipe, $a_{pmax}(f_n)$, to the response without the pipe, $a_{omax}(f_n)$, (neglecting the change in resonance frequency due to pipe loading) is given by:

$$\frac{a_{pmax}(f_n)}{a_{omax}(f_n)} = \frac{V_p}{V_o} \Big|_{f=f_n} = \frac{\frac{\omega_0^2 n^2 W}{Qg}}{R_n + \frac{\omega_0^2 n^2 W}{Qg}} \quad [\text{Eq H9}]$$

where W = the effective weight associated with one section of roof deck/bar joist (520 lb as indicated earlier)

R_n = the mechanical "resistance" of the infinite pipe at angular frequency $\omega = \omega_n$, or

$$R_n = \frac{2wC_{Bo}\sqrt{n}}{g}$$

The above values were substituted into Eq H9, and a resonance amplification factor, Q , of 10 was assumed since the effect of adding the pipe is expected to appreciably increase the damping of the roof deck/bar joist vibration.

The peak input acceleration $a_{omax}(f_n)$ without the pipe, derived from Table H5, was then used with Eq H9 to define peak acceleration levels at each mode with the pipe. The result, shown in Figure H1, indicates that the vibration load factor at the pipe hanger reduces from 5.15 gravities without the pipe to 1.85 g with the pipe.

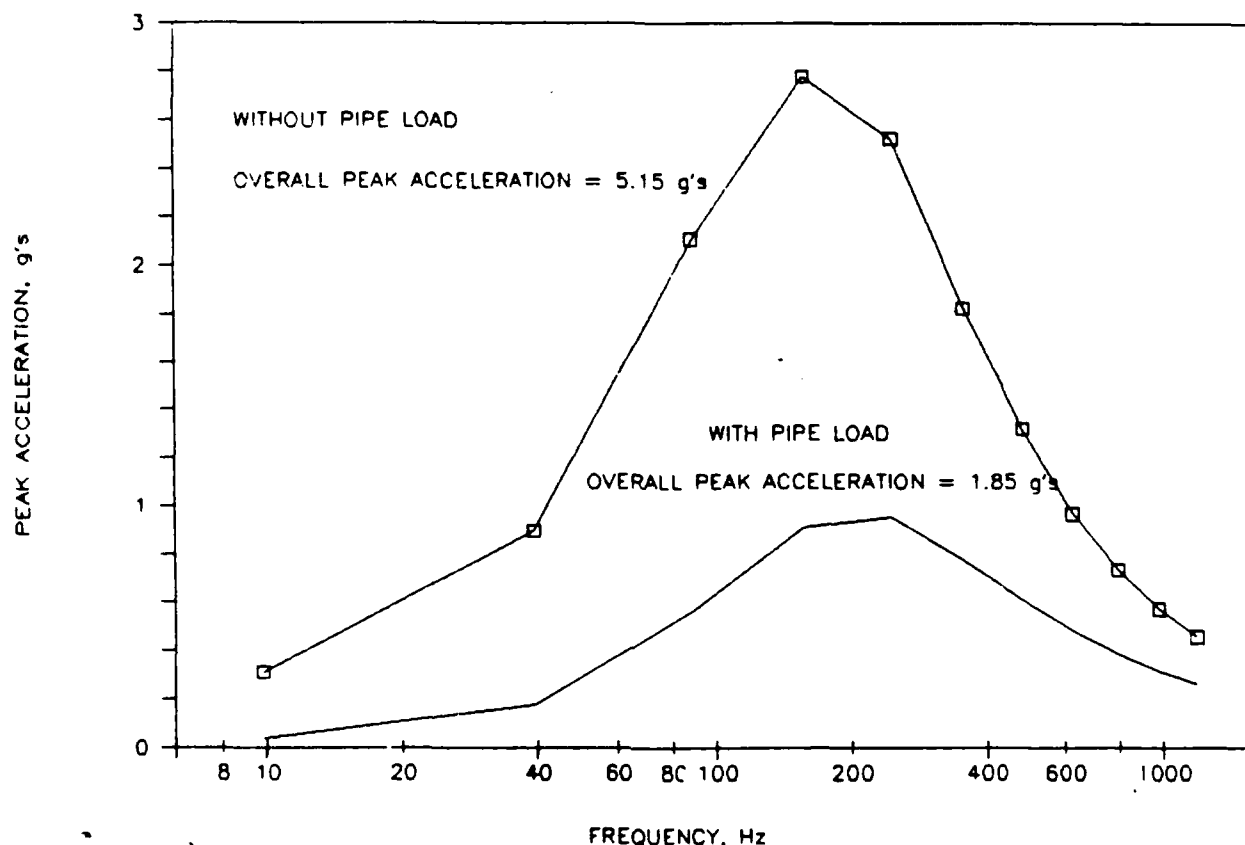


Figure H1. Spectrum of acceleration response of roof deck/bar joist with and without loading by 6 in. diameter, Schedule 80 pipe.

For a comparison, apply the mass loading approximation of Eq H3 and assume that the equipment weight, W_e would be equal to the effective weight (one-half of the weight) for a 5.7 ft section of pipe (recall that the bar joists are spaced an average of 5.7 ft apart). Thus, $W_e = 1/2 \times 3.32 \times 12 \times 5.7 = 114$ lb. On this basis, the reduced load factor LF_{eff} from Eq H3 is given by:

$$LF_{eff} = 5.15g \left(\frac{520}{114 + 520} \right) = 4.22g$$

These two estimates of the pipe hanger vibration loads (1.85 g and 4.22 g) differ substantially. The average load factor, 3.0 g can be used for preliminary design. Chapter 8 presents the application of the second method with the addition of vibration isolation to the pipe supports.

Rear Door Panel

A detailed design for the rear door of the AMD was not available, so the analysis of vibration loads on the door panels assumed a design such as illustrated earlier of a 16 gage interior skin panel over a steel door frame with 2 ft x 6 ft spacing of interior frame members. The outside skin would be similar to the building wall panels but is not of concern since it will not be directly exposed to the interior noise levels.

The interior space will be filled with fiberglass insulation providing considerable vibration damping (in addition to the thermal insulation intended by its use). For conservatism, a value of $Q = 15$ was selected for the dynamic magnification factor, even though a lower value may occur due to the damping provided by the fiberglass padding behind the door panels. Table H8 provides a summary of the response analysis for one 2 ft x 6 ft panel of the inner door surface. The upper part of the table summarizes the overall response parameters for 220 modes from 11 to 1005 Hz. The lower part presents a summary of the response characteristics for the first 36 modes.

Vibration Reaction Loads at the Top and Bottom of the Door

Due to the acoustically induced vibration of the door panels, the top and bottom rollers and retainers will be subject to a horizontal vibratory load. Assuming, conservatively, that the 72 in. panel dimension is horizontal, the magnitude of these reaction loads is estimated to be no more than the average load per foot along each 72 in. side (1.1 lb/ft) times the number of such 72 x 24 in. panels over the 15 ft vertical height of the door vertically times one-half for the split between top and bottom. This is a conservative value which assumes that all of the panels will vibrate in phase. Allowing for a stress concentration factor of 3.5, the net result is:

$$R_{\text{vib}} = \left(\frac{1}{2}\right) \times (1.1) \left(15 \times \frac{12}{24}\right)(3.5) = 14 \text{ lb/ft}$$

Load Factors for Equipment Mounted on Inside Door Panels

It is recommended that the baseline vibration load factor of $\pm 5.7 \text{ g}$ be used in the direction normal to the door surface and $\pm 2.9 \text{ g}$ be used in the other two in-plane directions for any equipment mounted on the inside door. No allowance is provided for mass loading effects since it is assumed that only relatively lightweight equipment would be mounted on the inner door surface. Any such mounting (i.e., wire clamps, etc.) should be made, whenever possible, at positions on the inner door panel directly over one of the door frame mountings. However, for conservative design, since the inside door panels will be exposed to the most severe acoustic environment, the same load factor, $\pm 5.7 \text{ g}$, should be used in the direction normal to the door for any equipment mounting location on the doors.

Chapter 7 provides additional inner door panel response calculations for panels of other sizes and gauges. These calculations are summarized in Table 15. This information should be used by the construction contractor for evaluating the variation of response for panels of different sizes and gauge.

Draft Curtain

The draft curtain forms vertical walls of an open box with 58 ft front to back walls along roof trusses 5 and 7 between column lines A and D, and a 66.5 ft back wall along the roof truss on column line D between roof trusses 5 and 7.

The preliminary design concepts for the draft curtain walls consisted of 3 in. deep 20 gage corrugated panels supported on a 3 in. channel at the bottom tied to a W16 x 45 in. girder which was the bottom member of the roof truss (see Figure 6). The walls of the draft curtain were treated as a non-homogeneous corrugated beam. However, tabulated values of the area moment of inertia, I , per unit width and surface weight (listed later), made it possible to predict the resonance frequencies for such a structure by treating the corrugated panels in terms of equivalent uniform beams. A Q of 25 was assumed for all draft curtain vibration modes reflecting the lack of any significant damping mechanisms for these corrugated panels.

Summary of Vibro-Acoustic Response Calculations of Door Panels

Gage = 16	Pn/X = 7777 = Static Pressure/Deflection, psi/in
Sp. Avg. rms Accel. = 2.52 g's	K = 0.7116 = Static Stress/[Pn · (a/h) ²], Polynomial Approx.
Maximum rms Velocity = 9.059 in/sec.	Fp = 2.15 = Peak/rms factor for random noise (10% exceedance)
Maximum rms Stress = 2.136 psi	Ff = 0.75 = Reduced strength due to fatigue
Maximum rms Displ. = 0.116 in.	
Surface Density = 0.0169 psi	
a/b = 0.3333	
b = 0.0598 in.	
Fundamental Freq. = 10.97 Hz	
Dyn. Magnif. Factor = 15	

Equiv. Static Pressure	----- REACTION LOADS -----	
Pn, psf = 7.7 psf	Along 24" side	Along 72" Side
	lb/ft.	lb/ft.
	Maximum 1.7	Maximum 5.2
	Average 0.5	Average 1.1

	LOAD FACTOR
	5.4 g's

Long. #	AVG. M.S. ACCEL.	Lat	MAXIMUM Velocity	M.S. VALUE Strg/Vel	Stress	Displ.	Freq.	Peak Accel.	10-Log(J ²)	REACTION LOADS, lb./ft.				
J'm.m	g's	dB re: 1g	(in/s)	(in/sec)	(psi)	(in)	Hz.	g's	Jn'	Jn'	24" Side	72" Side		
											Max.	Avg.	Max.	Avg.
		-40												
0.16	0.12	-9.13	61.30	245.12	3.68E+06	1.29E-02	10.97	0.75	-3.931	-3.923	0.11	0.07	0.43	0.27
0.00	0.00	-40.82	0.03	188.56	9.15E+02	3.21E-06	14.26	0.02	-3.937	-37.93	0.00	0.00	0.01	0.00
0.01	0.03	-14.80	5.13	136.18	9.52E+04	3.34E-04	19.74	0.39	-3.952	-15.24	0.08	0.05	0.22	0.05
0.00	0.00	-35.53	0.02	98.05	2.16E+02	7.58E-07	27.42	0.04	-3.979	-39.11	0.01	0.00	0.02	0.00
0.00	0.04	-13.68	1.86	72.10	9.68E+03	3.39E-05	37.29	0.45	-4.028	-20.18	0.06	0.04	0.15	0.02
0.00	0.06	-12.03	2.30	265.00	1.61E+05	3.54E-05	40.58	0.54	-19.44	-3.936	0.02	0.00	0.12	0.07
0.00	0.00	-34.89	0.01	245.12	6.12E+02	1.34E-01	43.87	0.04	-18.78	-28.20	0.00	0.00	0.01	0.00
0.00	0.01	-19.88	0.25	217.89	1.21E+04	2.65E-06	49.35	0.22	-17.79	-15.32	0.02	0.00	0.07	0.02
0.00	0.00	-28.73	0.03	54.47	9.85E+01	3.45E-07	49.35	0.08	-4.107	-37.86	0.01	0.01	0.02	0.00
0.00	0.00	-34.76	0.01	188.56	2.20E+02	4.83E-08	57.03	0.04	-16.59	-32.79	0.00	0.00	0.01	0.00
0.00	0.06	-11.97	0.95	42.26	1.69E+03	5.93E-06	63.61	0.54	-4.227	-23.43	0.06	0.04	0.11	0.01
0.00	0.01	-19.44	0.15	160.74	3.97E+03	8.69E-07	66.90	0.23	-15.29	-20.31	0.02	0.00	0.07	0.01
0.00	0.00	-30.09	0.01	136.18	1.76E+02	3.86E-08	78.96	0.07	-13.98	-33.87	0.01	0.00	0.02	0.00
0.00	0.01	-22.91	0.05	33.58	5.43E+01	1.90E-07	80.06	0.15	-4.399	-36.41	0.01	0.01	0.02	0.00
0.01	0.52	-2.95	3.87	269.04	2.80E+05	1.21E-05	89.93	1.55	-17.88	-3.991	0.03	0.01	0.19	0.12
0.00	0.01	-20.38	0.06	259.54	4.29E+03	1.86E-07	93.22	0.21	-18.04	-21.70	0.01	0.00	0.03	0.00
0.00	0.02	-16.98	0.14	115.35	1.85E+03	4.06E-07	93.22	0.30	-12.72	-23.63	0.03	0.00	0.08	0.01
0.00	0.04	-13.98	0.25	245.12	1.49E+04	6.45E-07	98.70	0.43	-18.29	-15.61	0.02	0.00	0.08	0.02
0.00	0.09	-10.70	0.53	27.24	3.92E+02	1.37E-06	98.70	0.63	-4.634	-25.98	0.05	0.03	0.08	0.01
0.00	0.00	-25.64	0.01	227.43	7.53E+02	3.26E-08	106.38	0.11	-18.59	-27.55	0.01	0.00	0.02	0.00
0.00	0.00	-24.65	0.02	98.05	1.65E+02	3.63E-08	109.67	0.13	-11.55	-33.82	0.01	0.00	0.03	0.00
0.00	0.01	-18.40	0.06	208.12	2.80E+03	1.21E-07	116.25	0.26	-18.86	-20.69	0.02	0.00	0.06	0.01
0.00	0.01	-18.76	0.06	22.49	2.84E+01	9.97E-08	119.54	0.25	-4.941	-35.18	0.02	0.01	0.03	0.00
0.00	0.00	-26.96	0.01	188.56	2.63E+02	1.14E-08	128.31	0.10	-18.94	-29.90	0.01	0.00	0.02	

Table H9 presents a summary of the response analysis for the "panel" response of a section of the draft curtain walls consisting of an 18 gage, 16 ft long panel. For this structure, as explained in the *Equivalent Static Pressures for Other AMD Structural Panels* section in the main body of the text, the acoustic excitation was modified to account for the diffraction of sound around both sides of the draft curtain. This decreased the net acoustic load at frequencies below about 30 Hz and increased it at higher frequencies.

Reaction Loads

Vibration reaction loads on the draft curtain support structure are listed later in Table H10 for different gages and lengths of the draft curtain. The average value, in the direction normal to the draft curtain, is 207 lb/ft along either the top or bottom edge. Shear reaction loads are estimated to be one-half of those values. However, neither of these includes an allowance for stress concentration.

Vibration Load Factors

The vibration load factors for equipment mounted on the draft curtain are as follows for the 18 gage, 16 ft long panel analyzed in Table H9:

On Draft Curtain

Perpendicular to curtain		$\pm 21 \text{ g}$
Horizontal, In Plane of Curtain		$\pm 11 \text{ g}$
Vertical	Up	$+ 10 \text{ g}$
	Down	$- 12 \text{ g}$

The effective weight W_m , to be used in Eq H13 to allow for any mass loading effects which reduce the vibration load factor for equipment mounted on the draft curtain, can be computed as follows.

The draft curtain can be considered as consisting of two 25 ft wide sections along each side and two 36 ft sections along the back. Thus, an average width is $(2 \times 25 + 36)/3 = 28.7 \text{ ft}$. The height of these sections varies from 16 ft in front of the curtain to 10 ft in back for a weighted average height of about 12 ft. Thus, for an 18 gage version with a surface weight of 3.46 psf, and allowing for a reduction by a factor of 4 in actual weight for the dynamically effective weight of a typical draft curtain panel section, the value of W_m will be $1/4 \times 28.7 \times 12 \times 3.46 = 298 \approx 300 \text{ lbs}$.

For equipment mounted on the lower girder of the roof truss (or 3 in. channel) supporting the draft curtain, the preceding load factors will be reduced by mass loading. The average effective weight of a typical section of the lower girder is assumed to be 25 percent of the total weight of the roof truss section (i.e., 50 percent of one-half of the weight of the roof truss). The weight of the individual roof truss sections can be derived from Table H6. The resulting effective weight, including an average effective weight of 70 lb for the 3 in. channel at the bottom of the draft curtain, is 960 lb for an average section between trusses.

Thus, the baseline load factor for equipment mounted on the lower girders supporting the draft curtain will be reduced from the preceding values by the ratio of 300 to $(960 + 300)$ or 0.238.

Table H9

Summary of Vibro-Acoustic Response Calculations for Draft Curtain

A. SUMMARY OF RESPONSE PARAMETERS FOR DRAFT CURTAIN, 11 Modes from 10 to 1173 Hz

Gage/ Length, ft.	= 18	14	Ps/X = 222	= Static Pressure/Deflection
Sp. Avg. rms Accel.	= 9.94 g's	ft. K	= NA	= Static Stress/[Ps·(a/h) ²], Approx.
Maximum rms Velocity	= 14.92 in/sec.	Fp	= 2.15	= Peak/rms factor for random noise
Maximum rms Stress	= 4,063 psi	Ff	= 0.75	= Reduced strength due to fatigue
Maximum rms Displ.	= 0.075 in.			
Surface Density	= 0.0247 psi	Equiv. Static Pressure		
Length	= 192 in.	Ps, psf	= 33.7 psf	REACTION LOAD
h(Dyn.Equiv.Thick'ns)	= 3.939 in.			
Fundamental Freq.	= 9.69 Hz	LOAD FACTOR		221 lb./ft.
Dyn. Magnif. Factor	= 25	21.4 g's		

B. FREQUENCY RESPONSE CHARACTERISTICS FOR DRAFT CURTAIN

long. & lateral	AVG.M.S.ACCEL. Value	La	Veloci	Strs/Vel	Stress	Displ.	Freq.	Peak	10·Log(J ²)	Peak		
J ² m,n				psi/				Accel.	Jm ²	Reaction		
	g ²	dB re:1g	(in/s) ²	(in/sec)	(psi) ²	(in) ²	Hz.	g's		Load		
										lb./ft.		
		-20										
	0.08	0.03	-15.74	17.14	272.4	1.27E+06	4.62E-03	9.69	0.35	-3.973	-3.636	6.36
	0.12	1.18	0.73	47.57	272.4	3.53E+06	8.02E-04	38.8	2.34	-11.96	1.4336	21.20
	0.10	5.91	7.72	46.95	272.4	3.48E+06	1.56E-04	87.2	5.23	-12.59	1.3288	31.60
	0.16	27.36	14.37	68.73	272.5	5.10E+06	7.24E-05	155	11.25	-10.97	1.5727	50.98
	0.14	30.02	14.77	30.89	272.5	2.29E+06	1.33E-05	242	11.78	-11.61	1.4859	42.72
	0.10	15.64	11.94	7.76	272.5	5.76E+05	1.62E-06	349	8.50	-13.09	1.4426	25.70
	0.07	8.58	9.34	2.30	272.4	1.71E+05	2.58E-07	475	6.30	-14.39	1.5290	16.32
	0.06	4.66	6.69	0.73	272.4	5.43E+04	4.82E-08	620	4.64	-15.52	1.5492	10.52
	0.05	2.68	4.28	0.26	272.4	1.95E+04	1.08E-08	785	3.52	-16.53	1.5379	7.09
	0.04	1.60	2.04	0.10	272.4	7.63E+03	2.77E-09	969	2.72	-17.44	1.4873	4.93
	0.03	1.04	0.18	0.05	272.4	3.39E+03	8.43E-10	1,173	2.19	-18.26	1.5241	3.62
	0.02	0.68	-1.64	0.02	272.4	1.58E+03	2.76E-10	1,395	1.78	-19.01	1.4971	2.69
	0.02	0.47	-3.31	0.01	272.4	7.80E+02	9.93E-11	1,638	1.47	-19.70	1.5010	2.05
	0.02	0.31	-5.06	0.01	272.4	3.87E+02	3.67E-11	1,899	1.20	-20.34	1.5195	1.56
	0.02	0.21	-6.78	0.00	272.4	1.98E+02	1.42E-11	2,180	0.99	-20.94	1.4924	1.19

Table H10

**Summary of Vibration Response Parameters for Alternative Gages
and Lengths of Draft Curtain**

Gage*	Length, ft	10	12	14	16	Avg.
18 Gage	f_o , Hz	24.8	17.2	12.7	9.7	16.1
$I = 1.325 \text{ in}^4/\text{ft}$	P_s , psf	104	68	48	34	63.5
$w = 3.46 \text{ psf}$	LF, g	22	21	22	21	21.5
	R/b lb/ft	192	202	216	221	208
20 Gage	f_o , Hz	24.2	16.8	12.3	9.5	15.7
$I = 0.959 \text{ in}^4/\text{ft}$	P_s , psf	101	66	46	33	61.5
$w = 2.61 \text{ psf}$	LF, g	29	28	29	28	28.5
	R/b lb/ft	191	200	212	219	206

* Based on properties specified for Vulcraft Type 3N20 or 3N18 Acoustical Deck

On Lower Support Girders

Perpendicular to Curtain		$\pm 5.0 \text{ g}$
Horizontal, In Plane of Curtain		$\pm 2.5 \text{ g}$
Vertical	Up	$+ 1.5 \text{ g}$
	Down	$- 3.5 \text{ g}$

These baseline load factors may be reduced further for equipment with a weight, W_e , more than about 10 percent of the value for the total effective weight W_m ($960+300/2$) = 1260 lb for the lower girder and draft curtain weight per section.

The baseline load factor for equipment attached to the top girder of the trusses forming the draft curtain can be derived from the roof load factors in Table H6C. For this particular area, the average load factor is $\pm 2.8 \text{ g}$, slightly lower than the average of $\pm 3.1 \text{ g}$ over all of the roof trusses.

The corresponding average value of effective weight for equipment mounted on the top girders supporting the draft curtain is 5300 lb, slightly higher than the average value of 5017 lb over all roof truss sections listed in Table H7.

***Vibration Loads for 20 Versus 18 Gage and for
Different Lengths of the Draft Curtain***

Table H10 provides a summary of the key vibration response parameters for both an 18 and a 20 gage version of the draft curtain and for segments of different lengths. Only the equivalent static pressure, P_s , varies significantly with length. However, the highest average load factor, 28.5 g, occurs as expected for the lightest gage.

HV System

Three aspects of the HV system are of concern relative to vibro-acoustic loads. They are: (a) the vibro-acoustic loads on the HV system enclosure panels, (b) the vibro-acoustic loads on the air ducts, and (c) the vibration load factors for the HV mechanical equipment.

Vibro-Acoustic Loads on HV Enclosure

A typical HV (e.g., blower motor/plenum) enclosure cabinet will consist of 18 gage galvanized steel panels braced at the edges and mid-span with 1 in. x 1 in. x 1/8 in. steel angles. Typical panel sizes, according to a representative manufacturer's brochure, are 4 ft x 4 ft and 2 ft x 4 ft. A Q of 25 was assumed for all enclosure panel modes.

Table H11 summarizes the vibro-acoustic response parameter for an 18 gage 4 ft x 4 ft panel and a 2 ft x 4 ft panel. The equivalent static pressures are 2.8 psf and 7.5 psf and the load factors are 5.4 g and 7.0 g respectively for the different panel sizes. The approximate vibration reaction loads along each edge can be approximated from the product of the load factor and the dynamically effective weight of these panels which have a surface weight for 18 gage steel of 1.94 psf, or

$$48'' \times 48'' \text{ panel, } R = 5.4 \times \frac{1}{4} \times 48 \times 48 \times \frac{1.94}{144} = 42 \text{ lb}$$

$$24'' \times 48'' \text{ panel, } R = 7.0 \times \frac{1}{4} \times 24 \times 48 \times \frac{1.94}{144} = 27 \text{ lb}$$

Fatigue of the enclosure panels is not likely for such a modest load, although some problems such as fastener loosening or local cracking around fasteners may occur in time. The vibro-acoustic load is low due to the low fundamental resonance frequencies of the enclosure panels and the low acoustic excitation at such low frequencies. In this case, stiffening of the enclosure walls to minimize any possible fatigue problems could actually make the net vibro-acoustic response greater. Evaluation of response for different gage thicknesses did not change the overall result significantly.

Vibro-Acoustic Loads on HV Ducts

The HV ducts inside the AMD vary widely in size and orientation from cross sections as small as 8 in. x 14 in. with a span of 90 in. up to 36 in. x 36 in. with a 133 in. span. The vibro-acoustic response of each size of sidewall of these ducts was analyzed assuming a dynamic magnification factor of 30 and 18 gage thick walls. (Standard practice would ordinarily dictate use of 20 gage for ducts with widths less than 30 in.)

To determine the vibro-acoustic response of each sidewall of a duct, the net acoustic load on each wall was approximated by assuming that the acoustic pressure on the inside wall was equal to the incident pressure on the outside but with a phase shift due to the propagation delay of the sound on the back side caused by its diffracted sound propagation path around the opposite duct wall. A simple mass-law sound attenuation law was also applied to allow for the sound transmission loss of this diffracted sound after it passed through the opposite duct wall.

Table H11

Summary of HV Enclosure Panel Vibro-Acoustic Response Parameters

A) HVAC ENCLOSURE, 48 in.,x 48 in., 18 Gage, 378 Modes from 4 to 1004 Hz

Sp. Avg.rms Accel.	=	2.50 g's	K	=	0.2866
Maximum rms Velocity	=	13.32 in/sec.	Fp	=	2.15
Maximum rms Stress	=	1,994 psi	Ff	=	0.75
Maximum rms Displ.	=	0.454 in.			
Surface Density	=	0.0135 psi	Equiv. Static Pressure		
a(48in.)/b(48in.)	=	1.0000	Ps,psf = 2.8 psf		
h	=	0.0478 in.			
Fundamental Freq.	=	3.9 Hz	Load Factor =		
Dyn. Magnif. Factor	=	25	5.4 g's		

B) HVAC ENCLOSURE, 48 in.,x 24 in., 18 Gage, 185 Modes from 10 to 1004 Hz

Sp. Avg.rms Accel.	=	3.24 g's	K	=	0.6125
Maximum rms Velocity	=	13.32 in/sec.	Fp	=	2.15
Maximum rms Stress	=	2,808 psi	Ff	=	0.75
Maximum rms Displ.	=	0.183 in.			
Surface Density	=	0.0135 psi	Equiv. Static Pressure		
a(24in.)/b(48in.)	=	0.5000	Ps,psf = 7.5 psf		
h	=	0.0478 in.			
Fundamental Freq.	=	9.9 Hz	Load Factor =		
Dyn. Magnif. Factor	=	25	7.0 g's		

These two corrections are a highly simplified version of a complex process but serve to provide a better approximation for the net acoustic loading. Applying these corrections changed the effective pressure on the outside from the incident pressure P_1 (including surface reflection) to an effective value P_{eff} given by the rms net pressure difference $\langle P_1 - P_4 \rangle$ across the duct where P_4 is the pressure on the inside wall. The net result is that

$$P_{eff} = \sqrt{(P_1 - P_4)^2} = \sqrt{P_1^2 - 2P_1P_4 + P_4^2}$$

$$P_{eff} = P_1 \sqrt{1 - \frac{2\cos\left(\frac{2\pi f \Delta X}{c_0}\right)}{1 + \tau} + \frac{1}{(1 + \tau)^2}}$$

where

ΔX = Duct height + 2 x duct width (width dimension is distance between opposite walls of duct side under consideration)

c_o = Speed of sound in air, 1126 ft/sec

τ = $2\pi fw/\rho_w c_o$

f = Frequency

w = Surface weight of duct wall

ρ_w = Weight density of air

A few cases were also analyzed in which the pressure on the inside of the duct was set equal to zero. This variation did not change the results significantly. The results of this analysis of the vibro-acoustic response of the duct walls are summarized in Table H12. It is important to note that this analysis only

Table H12

Summary of Vibro-Acoustic Response Parameters
for 18 Gage Galvanized Steel Walls of HV Ducts

Duct Size in	Panel Size		f_o^* Hz	P_s psf	LF g	σ^{**} psi	X_{pk}^{***} in.	$W/120^\dagger$ in.	R/W^\ddagger lb/ft	Diffraction Included
	W in.	L in.								
8 x 14	8	90	71.6	156	24	7990	0.18	0.067	88	Yes
10 x 12	10	90	46.0	111	32	8835	0.28	0.083	117	Yes
12 x 12	12	90	32.1	58	23	6640	0.33	0.10	84	Yes
8 x 14	14	90	23.7	36	19	5625	0.35	0.12	69	Yes
12 x 16	16	90	18.3	27	21	5435	0.37	0.13	77	Yes
16 x 42	42	90	3.1	1.9	6.5	2280	0.49	0.35	24	Yes
16 x 50	50	90	2.4	1.4	5.4	2085	0.54	0.42	20	Yes
12 x 12	12	90	32.1	46	20.5	5250	0.23	0.10	75	No
8 x 14	14	90	23.7	33	20	5110	0.30	0.12	73	No
20 x 24	20	133	11.6	17.4	24	5530	0.52	0.17	128	Yes
22 x 24	22	133	9.6	10.2	17	3915	0.48	0.18	90	Yes
24 x 24	24	133	8.1	7.7	17	3535	0.50	0.20	92	Yes
30 x 30	30	133	5.3	4.1	16.6	2855	0.53	0.25	90	Yes
36 x 36	36	133	3.8	2.7	9.5	2690	0.57	0.30	57	Yes

* Fundamental resonance frequency for one side of duct wall with specified panel size.

** rms stress in duct wall. Peak stress will be 2.15 times greater 10 percent of the time.

*** Effective peak displacement allowing a peak/rms deflection of 2.15 and an additional increase of 1/0.75 for fatigue effect.

† Nominal desirable limit in deflection based on panel width.

‡ Conservative estimate of reaction load/ft along each joint.

considers the response of each surface of the duct walls vibrating as a panel. Chapter 8 presents the duct response when the entire duct is treated as a beam. This duct response data is summarized in Table 24a and 24b. In this case, the acoustic loading can be based on the net load of the incident sound on the widest surface assuming that the duct is located up against a wall and thus has no significant acoustic load on the opposite duct wall.

As indicated in Table H12, the acoustic loads vary markedly; the equivalent pressures and load factors decrease sharply as the duct height (i.e., the short dimension normal to the direction of arrival of the incident sound) increases. The ducts with smaller cross sections have higher panel resonance frequencies which are closer to the peak frequencies of the acoustic excitation and thus have higher equivalent static pressures. This is also apparent by comparing the estimated peak deflection, X_{pk} , to a normally acceptable deflection based conservatively on 1/120th of the panel width W , the smaller of the two panel dimensions. It is clear that for the smaller ducts, the peak deflection, X_{pk} is of the order of three times $W/120$. Note that X_{pk} is a value expected to be exceeded less than 10 percent of the time and is increased, as explained in Appendix D, by the ratio 1/0.75 to allow for fatigue effects. Nevertheless, this is a clear indication of the potential for acoustically induced fatigue damage to the HV ducts at any location (e.g., joints) where there will be stress concentrations. It is recommended, therefore, that particular attention be given to the use of high strength, highly damped joints and taking steps to minimize any additional dead weight loads on the HV duct walls.

While the results in Table H12 are quantitative, they are necessarily approximate and can only be considered as providing definite qualitative indications of the high potential for troublesome acoustically-induced fatigue failures of the HV duct walls unless proper design steps are taken to minimize such fatigue. One of the steps implicit in these results is that a heavier gauge ducting than normally used should be considered for the smaller cross section ducts which will tend to have the greater potential for fatigue damage. Such recommendations for the use of heavier gauge duct thickness are given in Chapter 7, Tables 21a and 21b.

Reaction Loads at HV Joints. Reaction loads per foot at HV duct joints are conservatively estimated by dividing the product of the peak total reaction load per side by the length in feet of the joints on each side of a given duct wall. The peak total reaction load is the Load Factor (LF) times the dynamically effective weight of the duct wall which is equal to the area times the surface weight (0.0135 psi for 18 gage steel) times 1/4. This product is then multiplied by two to account for the load at one joint for two adjacent duct walls, and divided by two for the two joints at each end. This conservative estimate assumes that all of the vibration reaction load on each duct wall side is taken up only at the joints. These loads per foot are also listed in Table H12. For example, for the first duct, the estimated reaction load along each 8 in. joint on one of the two 8 in. x 90 in. panel sides is:

$$\frac{R}{b} = \frac{LF W L w \frac{1}{4} 12 \text{ in/ft}}{2W} \times 2$$

$$= \frac{24 \times 8 \times 90 \times 0.0135 \times \frac{1}{4} \times 12}{2 \times 8} \times 2 = 88 \text{ lb/ft}$$

Vibration Response of HV Mechanical Equipment Unit

A vibration analysis of the HV mechanical equipment unit was carried out assuming the entire unit and an associated maintenance catwalk would be mounted on two W8 x 28 beams located 6 ft and 12 ft respectively from roof truss 3 and spanning roof trusses C and D. The HV unit, with a base of 10 ft by 8 ft and a weight of 2700 lb, was centered on these two W8 x 28 beams (the 10 ft dimension running parallel to the I-beams). The 6 ft wide by 20 ft long 2900 lb catwalk extends from 6 ft outside roof truss 3 to 14 ft inside roof truss 3; the center was located 5 ft from truss D.

The entire system was reduced to a lumped mass, 3 degree of freedom system illustrated in Figure H2A and B. Part A represents the lumped mass model and Part B illustrates the equivalent mechanical mobility analog circuit for this system. Damping is not shown but is incorporated, inherently, in the spring elements by using a complex stiffness as was done previously in the Vibration Load Factors for Pipe Hangers Supported from Bar Joists Section for the pipe hanger model. As indicated in the figure, the driving force F_1 for the system is the acoustic load on the roof deck, and V_1 is the velocity response of this portion of the roof and the desired response at the base of the HV unit is the velocity V_3 .

As shown in the figure, the three lumped masses, M_1 , M_2 and M_3 , correspond to the weights of:

- (1) The section of the roof deck/bar joists over the HV unit
- (2) The sections of roof truss C and D
- (3) The two W8 x 28 support beams, catwalk and HV unit.

The three springs, represented by compliances C_1 , C_2 and C_3 (a compliance C , in in/lb, is the inverse of a stiffness K in lb/in) correspond to the stiffness of:

- (1) The roof deck/bar joist
- (2) The sections of roof truss C and D
- (3) The two W8 x 28 support beams.

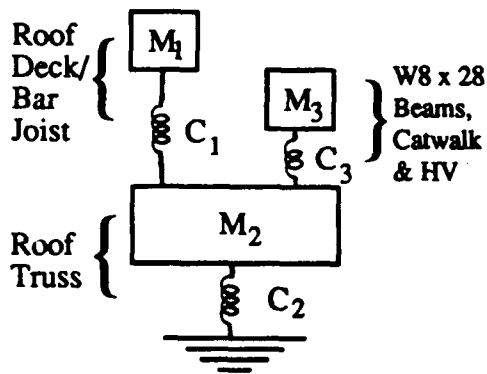
These mass and compliance parameters were established as follows.

1. $M_1, C_1 =$ Roof Deck/Bar Joist

$M_1 g =$ Weight of one bay of roof between roof trusses 3 and 4, C and D = 6085 lb (see Table H6A) where $g = 386 \text{ in/sec}^2$

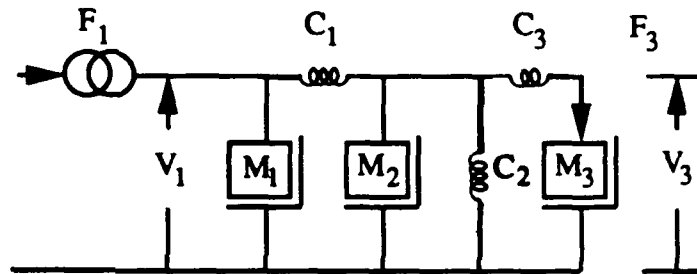
$$\text{Since } f_1 = \frac{1}{2\pi} \sqrt{\frac{1}{M_1 C_1}}$$

$$C_1 = \frac{g}{[M_1 g (2\pi f_1)^2]} = 1.66 \times 10^{-5} \text{ in/lb}$$



Model Shown
Without Damping
Elements

$$\text{Modes} - f_i = \frac{1}{2\pi} \sqrt{1/M_i C_i}$$



F_1 = Driving Force of Acoustic Load on Roof Deck

V_1 = Velocity Response of Roof Deck/Bar Joist

V_3 = Velocity Response of HV Mounting Point

F_3 = Force Driving HV/Catwalk Mounting Beam

M_1 = Mass of Roof Deck/Bar Joist

C_1 = Compliance of Roof Deck/Bar Joist

M_2 = Mass of Roof Truss Section

C_2 = Compliance of Truss Section

M_3 = Mass of W8 x 28/Catwalk/ HV

C_3 = Compliance of W8 x 28 Beams

(a) Lumped mass model

(b) Equivalent mechanical mobility analog circuit

Figure H2. Lumped mass mobility model for HV system.

2. $M_2, C_2 =$ Section of Roof Truss

$$M_2g = \frac{1}{2} [\text{weight of truss C (3-4)} + \text{weight of truss D (3-4)}]$$

$$= \frac{1}{2} [4374 + 3432] \text{ (see Table H6A)}$$

$$= 3903 \text{ lb}$$

From the analysis of roof C in Chapter 7 (p 87)

Mode No.	1	2	3	4
$f_2, \text{ Hz}$	= 24.6	32	55.4	72.1
$\therefore C_2, \text{ in/lb}$	= 4.14×10^{-6}	2.45×10^{-6}	8.16×10^{-7}	4.82×10^{-7}

3. M_3, C_3 - HV, Catwalk and two W8 x 28 Beams

The analysis is carried out for the dynamic response of just one of the two W8 x 28 beams.

$$M_3g = \frac{1}{2} [\text{wt of HV} + \text{wt of W8 x 28 beams} + \text{wt of portion of catwalk carried by W8 x 28 beams}]$$

or

$$M_3g = \frac{1}{2} [2700 + (25)(28)(2) + 1500] = 2800 \text{ lb}$$

Without the HV or catwalk, the fundamental resonance frequency of one W8 x 28 beam will be:

$$f_3 = \frac{\pi}{2L^2} \sqrt{\frac{EI}{w/12g}}$$

where

$$L = \text{Length of beam (25 x 12 = 300 in)}$$

$$E = 3 \times 10^7 \text{ psi for steel}$$

$$I = 98.0 \text{ in}^4 \text{ for W8 x 28 beam}$$

$$w = \text{weight/ft} = 28 \text{ lb/ft for beam}$$

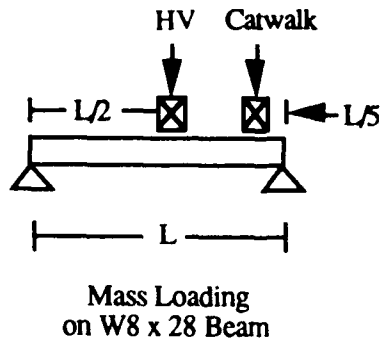
or

$$f_3 = 12.2 \text{ Hz}$$

When the weights of the HV system and catwalk are added as lumped masses to the beam (see sketch), its fundamental frequency will decrease due to mass loading to f_3' according to:

$$f_3' = \frac{f_3}{\sqrt{1 + \frac{\sum \Phi^2(Y_i) W_i}{W_b/2}}} \quad [\text{Eq H10}]$$

where $\Phi_i(Y_i)$ = beam mode shape for i th mass at Y_i .



For a simply supported beam, $\Phi_i(Y_i) = \sin(\pi Y/L)$, and splitting the lumped masses evenly between the two W8 x 28 beams,

$$\therefore \text{for HV, } \Phi^2(Y_1)W_1 = \sin^2\left(\frac{\pi}{2}\right) \times \left(\frac{2700}{2}\right) = 1350 \text{ lb}$$

$$\text{For catwalk, } \Phi^2(Y_2)W_2 = \sin^2\left(\frac{\pi}{5}\right) \left(\frac{1500}{2}\right) = 259 \text{ lb}$$

Substituting these into Eq H10, $f_3 = 5.14 \text{ Hz}$

$$\therefore C_3 = \frac{g}{[W_3(2\pi f_3')^2]} = 1.32 \times 10^{-4} \text{ in/lb}$$

From an analysis of the mobility diagram in Figure H2, and including the effects of damping, it can be shown that for this simple lumped mass model the ratio of the acceleration A_3 at the base of the HV unit to the acceleration A_1' at the roof deck/bar joists alone (when the latter are tied to rigid supports as was assumed in deriving the roof deck/bar joist vibration environment) is given by:

$$\frac{A_3}{A_1'} = \frac{\frac{C_2}{C_1}}{\sqrt{[P - (\frac{K}{S})(MS + m(MH - NI))]^2 + [Q - (\frac{K}{S})(NS + m(NH + MI))]^2}} \quad [\text{Eq H11}]$$

where

$$H = 1 - \left(\frac{\omega}{\omega_1}\right)^2, \quad \omega_1 = 2\pi f_1 = \frac{1}{\sqrt{M_1 C_1}}$$

$$I = \frac{\omega}{\omega_1 Q_1}, \quad Q_1 \text{ assumed} = 15$$

$$K = \left(\frac{\omega}{\omega_2}\right)^2, \quad \omega_2 = \frac{1}{\sqrt{M_2 C_2}}$$

$$M = 1 - \left(\frac{\omega}{\omega_3}\right)^2, \quad \omega_3 = \frac{1}{\sqrt{M_3 C_3}}$$

$$N = \frac{\omega}{\omega_3 Q_3}, \quad Q_3 \text{ assumed} = 20$$

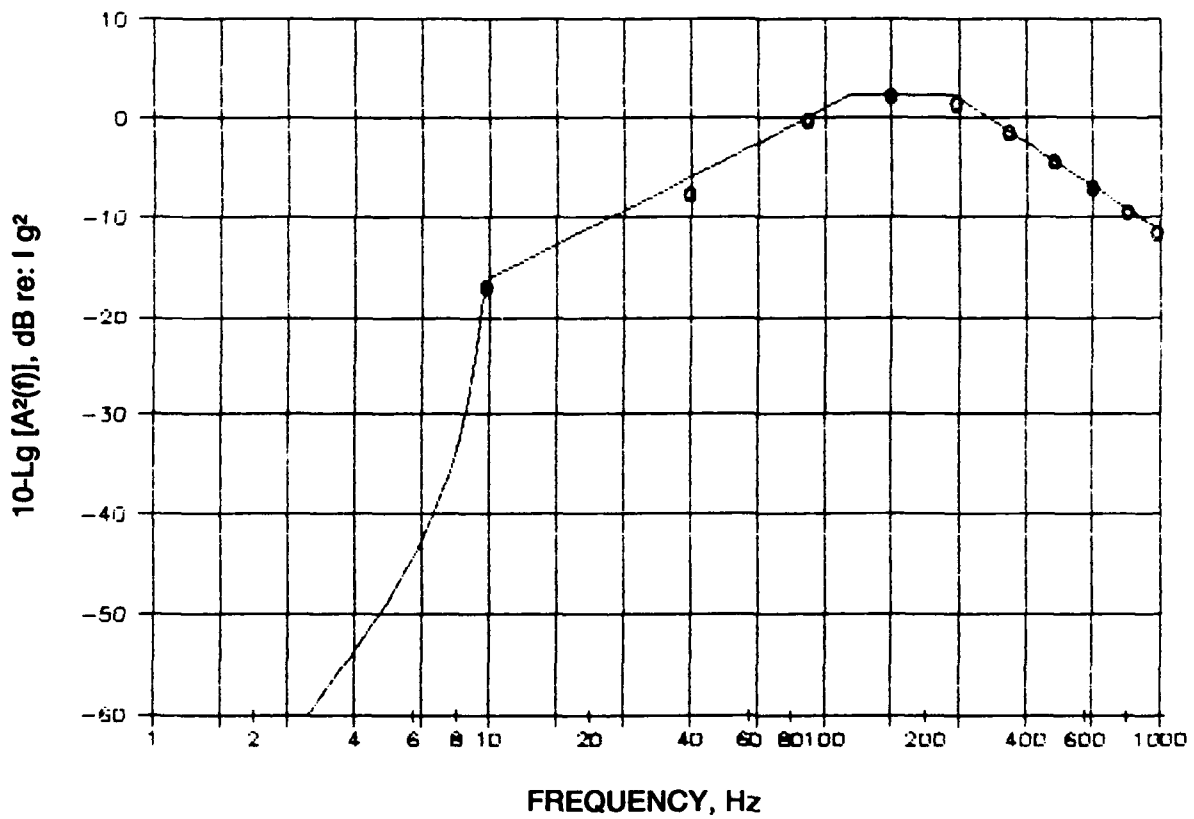
$$P = 1 - \left(\frac{\omega}{\omega_4}\right)^2, \quad \omega_4 = \frac{1}{\sqrt{M_3(C_2 + C_3)}}$$

$$Q = \frac{\omega}{\omega_4 Q_4}, \quad Q_4 = Q_3$$

$$m = \frac{M_1}{M_2}$$

To apply this expression, the acceleration peaks of the response spectrum of the roof deck/bar joists, developed in Table H5, were enveloped by a continuous spectrum as illustrated in Figure H3. Below the fundamental frequency (9.85 Hz for the 16K6 bar joists), the input spectrum was rolled off as expected for a single degree of freedom system with a Q of 15.

This input acceleration, A_1' , shown in Figure H3 on a log scale as $10 \log$ (Mean Square Acceleration in g^2) was used, along with the square of the value of A_3/A_1' , obtained from Eq H11, to define the envelope of the estimated mean square acceleration peaks, $A_3^2(f)$, as a function of frequency, at the base of the HV unit. Mounting the HV unit on the W8 x 28 beams provides, in effect, vibration isolation from the general vibration of the roof trusses.



(o) = response peaks from Table H5 (-) = continuous envelope used for analysis

Figure H3. Acceleration response spectrum for roof deck used as input to mobility model for HV vibration response.

However, at frequencies above the highest fundamental frequency used in the mobility model in Figure H2 (about 72 Hz for f_2), it was assumed that the actual HV vibration was no less than 20 dB below (lower by a factor of 10 in vibration amplitude) from the roof deck/bar joist vibration. This empirical adjustment to the estimated HV vibration response accounts, in a very approximate way, for the limited vibration isolation provided at higher modes of the entire structure that is not accounted for by the lumped mass model.

Once the envelope of mean square acceleration $\bar{A}_3^2(f)$ response spectrum at the base of the HV was determined, it was converted into an Acceleration Spectral Density Spectrum $APSD_3(f)$ using:

$$APSD_3(f) = \frac{2Q_3 \bar{A}_3^2(f)}{\pi f} \quad [\text{Eq H12}]$$

This response APSD spectrum was then integrated, numerically, over frequency to determine the overall mean square acceleration \bar{A}_3^2 at the HV base. The vibration load factor at this point was then computed, as for all other cases in this report, by multiplying the rms acceleration by 2.15 for a peak response:

$$LF = 2.15\sqrt{\bar{A}_3^2} \quad [\text{Eq H13}]$$

The results of applying this analysis are shown in Table H13 for the four different values for the roof truss frequencies f_2 , cited earlier in this appendix and in Chapter 7 of the main body of the report.

The results were found to be relatively insensitive to the dynamic magnification factors assumed. Based on these results, it is recommended that the HV unit be designed for the following vibration load factors.

Vertical Direction	Up	+ 0.3 g
	Down	- 2.3 g
Horizontal Direction		± 0.63 g

Table H13

Summary of Calculated Vibration Response Parameters at Base of HV

f_2 Hz	LF g	Peak Displacement in.
24.6	1.26	0.020
32	1.24	0.018
55.4	1.20	0.008
72.1	1.20	0.008

METHODOLOGY FOR DEVELOPMENT OF RANDOM VIBRATION TEST SPECIFICATIONS

Given the structural response spectrum in terms of mean square (MS), rms or peak accelerations at each predicted mode for various structures, appropriate vibration test specifications are defined as follows for potentially vibration-sensitive equipment in terms of acceleration power spectral density (APSD) curves.

Each response at a modal frequency f_n can be described by the response APSD (f) of the structure that serves as input to any component (neglecting any mass loading effect) mounted on the structure. That is, the peak acceleration response A_p at the n th resonance frequency, f_n , would be given by:

$$A_p(f_n) = F_p \sqrt{\frac{\pi}{2} \text{APSD}_s(f_n) \frac{f_n}{Q}} \quad [\text{Eq H14}]$$

where F_p is the peak to rms ratio (2.15) (see Appendix D). Solving for this structural response APSD_s (the input APSD to the test component),

$$\text{APSD}_s(f_n) = \frac{2}{\pi} \frac{Q}{f_n} \left[\frac{A_p(f_n)}{F_p} \right]^2 = \frac{2}{\pi} \overline{A^2(f_n)} \times \frac{Q}{f_n} \quad [\text{Eq H15}]$$

where

$A_p(f_n)$ = Peak acceleration at modal frequency f_n

$\overline{A^2(f_n)}$ = Mean square acceleration at f_n

Q = Resonance Amplification Factor

A conservative design or test envelope for the APSD (f) at any frequency f is then obtained by constructing an approximate envelope of these resonance response APSD (f_n) peaks. This is the procedure employed in constructing the random vibration test envelopes.

The rms acceleration \bar{a} for each test envelope is the square root of the integral of the APSD (f) curve from 5 to 2000 Hz given by:

$$\bar{a} = \sqrt{\int_5^{2000} \text{APSD}(f) df} \cdot g' / s \quad [\text{Eq H16}]$$

Electrical Equipment Mounted on Tube Between Girts

The APSD spectrum for the electrical and fire protection equipment components to be mounted on a tube spanning the wall girts was estimated using the following procedures.

- Mounting Tube Cross Section 3" x 3" x 3/16"
 Length 90 " (7.5 ft)
 I 2.60 in⁴
 w 6.86 lb/ft
- Fundamental Resonance of Unloaded Tube

$$f_1 = \left(\frac{\pi}{2L^2} \right) \sqrt{\frac{EI}{\left(\frac{w}{12g} \right)}} = 44.5 \text{ Hz}$$

Estimated reduction in resonance frequency with 20 lb equipment mounted:

$$f_i = \frac{f_1}{\sqrt{1 + \frac{M_e}{M_t}}}$$

where

M_e = equipment weight = 20 lb

M_t = generalized weight of tube $6.86 \times 7.5/2 = 25.7$ lb

resulting in

$$f_i = 33.4 \text{ Hz}$$

The APSD specification for this location was then estimated by accounting for a resonant response of the mounting tube at this frequency. This was based on the APSD input to the mounting tube, derived from the estimated wall acceleration response, reduced by a factor of 5 to account for the mass loading to the wall panels.

Electrical Equipment Mounted on Columns

In this case, the APSD for light components (e.g., less than 50 lb) mounted on the columns was estimated from the APSD for the wall panels reduced by a factor of 10 to account for the mass loading effect of the columns.

In all cases, the estimated APSD levels in the two orthogonal directions in the plane of the vibrating surface (e.g., on the plane of the wall, roof panels, etc.) are reduced by a factor of 4 from the estimated response levels in the direction normal to the vibrating surface. This reduces the corresponding rms accelerations for the test specifications for these directions by a factor of 2. These reduced in-plane response levels are based on experience in estimating trends in vibration response of a variety of structural systems.

ADDITIONAL CONSIDERATIONS FOR FATIGUE

Alternate operating power conditions were considered for the main engines. This made it necessary to examine the potential increase in acoustically-induced fatigue failure of sensitive AMD secondary structures (or equipment) if the power condition was increased from 6820 rpm to as high as 8060 rpm, or decreased to as low as 5883 rpm based on the data in the Baseline Environment for Reference Source Position Section. Such changes in operating conditions would be expected to change maximum sound levels inside the AMD and relative vibration stress levels of secondary structure as follows:

rpm		ΔL , dB*	$\sigma/\sigma_{\text{baseline}}$ **
8060	Maximum power	+10.3	3.27
6820	Baseline	0	1.0
5883	Reduced power	- 8.5	0.37

* Change in sound level, dB
 ** Relative stress

The above estimates of changes in sound level are based on the following empirical relationship between sound level and rpm.

$$\Delta L = 0.0138(n - n_0) - 3.7 \times 10^{-7}(n^2 - n_0^2) \quad [\text{Eq H17}]$$

where

ΔL = change in sound level, in dB, from baseline

n = new rpm

n_0 = baseline rpm of 6820

The corresponding change in relative stress, assuming a linear response of the structure to different sound levels is:

$$\frac{\sigma}{\sigma_{\text{baseline}}} = 10^{\frac{\Delta L}{20}} \quad [\text{Eq H18}]$$

For a typical S-N curve for steel (see Figure 25), the change in fatigue life, N , for a change in stress σ can be estimated from:

$$N_2 = N_1 \left(\frac{\sigma_2}{\sigma_1} \right)^{-\alpha_N} \quad [\text{Eq H19}]$$

where

σ_2 = failure stress after N_2 cycles

σ_1 = failure stress after N_1 cycles.

The S-N slope parameter α_N has a typical value of about 14 (it varies over a range of about 11 to 29).

Thus, applying the above values for stress σ_2 relative to the baseline value σ_1 , the number of cycles to failure N_2 at the new stress level relative to the baseline value N_1 would be expected to be as follows:

rpm	σ_2/σ_1	N_2/N_1^*
8060	3.27	6.3×10^{-8}
6820	1.0	1.0
5883	0.37	1.1×10^6

* Based on $\alpha_N = 14$ in Eq H19

Clearly, the changes in rpm cause drastic changes in expected fatigue life. The estimated number of fatigue cycles for the baseline operation as developed in Adjustments to RMS Response to Define Effective Static Load section of the main body of this report was of the order of 1 million cycles for the fundamental vibration frequency (~20 Hz) of the wall panels.

Thus, decreasing the rpm to 5883 would increase the probable number of life cycles to about $1.1 \times 10^6 \times 10^6 \sim 10^{12}$ cycles, clearly indicating that operation at this reduced rpm would not be expected to cause any fatigue for any practical operating time of the AMD.

In contrast, if the rpm is increased to 8060, the above figures suggest that the revised number of cycles to failure would be less than 1. This is clearly a case of extrapolation of the S-N curve beyond reasonable limits, but it *does* clearly indicate that operation of the test system at this higher rpm for any significant length of time inside the AMD would be likely to cause significant fatigue damage to secondary structures and vibration sensitive equipment within a very short period of time - quite possibly during the first operating cycle. This pessimistic view concerning potential fatigue failure of AMD secondary structures for operation at 8060 rpm cannot readily be refined or moderated without acquisition of actual vibro-acoustic response, preferably on a completed prototype facility or very similar facility using a test engine. Alternatively, high intensity acoustic tests could be conducted in a laboratory on prototype AMD secondary structural elements such as wall or roof panels.

The increase in sound level and the stress ratio relative to the stresses at the baseline (BL) of 6820 rpm was calculated for several levels of engine fan speed. These values along with the allowable number of cycles are calculated using Equation H19. This information is summarized in Table H14 for values of α_N of 14 and 11. Table H14 illustrates the impact of operating the engines at fan speeds above the 6820 rpm.

Table H14
Engine Power Level Calculations

Percent Fan Speed (%)	Engine Fan Speed (RPM)	ΔL , Change in Sound Power Level (dB)	σ/σ_{BL} Stress Ratio	Estimated Number of Cycles to Failure	
				$\alpha_N = -14$ (Best Est.) (No)	$\alpha_N = -11$ (No)
100.0	8532	13.89	4.950	0.0002	0.03
95.0	8105	10.63	3.399	0.0436	1.71
94.5	8060	10.28	3.264	0.0769	2.67
94.0	8020	9.96	3.149	0.128	3.98
93.0	7935	9.29	2.914	0.376	9.31
92.0	7849	8.61	2.694	1.13	22.2
91.0	7764	7.92	2.490	3.40	52.6
90.0	7679	7.24	2.301	10.3	126
89.0	7593	6.54	2.122	31.9	305
88.0	7508	5.84	1.958	98.3	738
87.0	7423	5.13	1.806	305	1799
86.0	7338	4.43	1.665	957	4414
85.0	7252	3.70	1.532	3067	11021
84.0	7167	2.98	1.410	9780	27413
83.0	7062	2.09	1.272	41465	85283
82.0	6996	1.52	1.191	1.03E05	1.75E05
81.0	6911	0.78	1.095	3.39E05	4.44E05
80.0	6826	0.04	1.005	1.12E06	1.14E06
79.9	6821	0.00	1.000	1.20E06	1.20E06 BL *
79.0	6740	-0.71	0.921	3.78E06	2.95E06
78.0	6655	-1.46	0.845	1.27E07	7.65E06
77.0	6570	-2.22	0.774	4.30E07	2.00E07
76.0	6484	-2.99	0.709	1.49E08	5.30E07
75.0	6399	-3.76	0.649	5.14E08	1.40E08
74.0	6314	-4.53	0.593	1.79E09	3.73E08
73.0	6228	-5.32	0.542	6.36E09	1.01E09
72.0	6143	-6.10	0.495	2.25E10	2.73E09
71.0	6058	-6.89	0.452	8.03E10	7.42E09
67.0	5716	-10.12	0.312	1.46E13	4.44E11
56.0	4777	-19.44	0.107	4.83E19	5.87E16
38.0	3242	-36.06	0.016	2.11E31	8.22E25
37.7	3218	-36.34	0.015	3.28E31	1.16E26 Idle **
37.0	3157	-37.04	0.014	1.01E32	2.81E26

* Baseline (BL) is for a fan speed of 6821 rpm.

** Idle is for a fan speed of 3218 rpm.

APPENDIX I: Equipment Response Calculations

The stiffness of the roof truss braces, assuming they are simply supported at both ends, is given by the following equation:

$$k = \frac{48EI}{L^3} \quad [\text{Eq 11}]$$

For the braces between roof trusses 4 and 5, and C and D, I is twice the moment of inertia of the double angle 4 x 3-1/2 x 1/4 in., or 8.36 in⁴, and L is the diagonal span of 41.6 feet. With these values k becomes 96.8 lb/in. The mass is taken as 5/8 the total mass of the 4 x 3-1/2 x 1/4 in. members, lumped in the center, and this becomes 1.67 lb-s²/in. The natural frequency is calculated from the following equation:

$$f_n = \frac{1}{2\pi} \sqrt{\frac{k}{m}} = \frac{1}{2\pi} \sqrt{\frac{96.8 \text{ lb/inch}}{1.67 \text{ lbs}^2/\text{inch}}} = 1.21 \text{ hz} \quad [\text{Eq 12}]$$

Tables I1 through I9 show equipment response calculations for the items indicated in table titles and subtitles.

Table I1
Calculated Weight for Horizontal Wind Brace Supports

Location Between Trusses	Double Angle Members	Member Weight (lb/ft)	Diagonal Length (ft)	Total Weight (lb)	Effective Weight (lb)	
					1/2	5/8
B - C & 3 - 4	5 x 5 x 5/16" 4 x 3-1/2 x 3/8"	20.6 18.2	41.60 41.60	1614	807	1009
E - F & 3 - 4	4 x 3-1/2 x 1/4" 5 x 5 x 5/16"	12.4 20.6	41.60 41.60	1373	686	858
B - C & 4 - 5	4 x 3 x 1/4" 4 x 3 x 1/4"	11.6 11.6	41.60 41.60	965	482	603
C - D & 4 - 5	4 x 3-1/2 x 1/4" 4 x 3-1/2 x 1/4"	12.4 12.4	41.60 41.60	1032	516	645
D - E & - 5	4 x 3-1/2 x 1/4" 4 x 4 x 1/4"	12.4 13.2	41.60 41.60	1065	532	666
E - F & 4 - 5	4 x 3 x 1/4" 4 x 3 x 1/4"	11.6 11.6	41.60 41.60	965	482	603
B - C & 5 - 6	5 x 3-1/2 x 1/4" 5 x 3-1/2 x 1/4"	14.0 14.0	43.83 43.83	1227	613	767
E - F & 5 - 6	5 x 3-1/2 x 1/4" 5 x 3-1/2 x 1/4"	14.0 14.0	43.83 43.83	1227	613	767

Table I2
Effective Acceleration Calculations for Each Modal Contribution
for Equipment Supported by the Roof Bar Joists

Note: $a_T = a_{pk} \times T$ for each support motion frequency (f)

Table I2a
Horizontal Wind Truss Support

f (Hz)	a_{pk} (g)	T	a_T (g)	a_T^2 (g ²)
9.85	0.13	0.200058	0.062018	0.003846
39.4	0.89	0.1	0.089	0.007921
88.65	2.11	0.1	0.211	0.044521
157.6	2.78	0.1	0.278	0.077284
246.25	2.52	0.1	0.252	0.063504
354.6	1.83	0.1	0.183	0.033489
482.65	1.32	0.1	0.132	0.017424
630.4	0.96	0.1	0.096	0.009216
797.85	0.73	0.1	0.073	0.005329
9.85	0.57	0.1	0.057	0.003249
1191.85	0.46	0.1	0.046	0.002116

Table I2 (Cont'd)

Table I2b
Horizontal Ductwork (35-140lb)

f (Hz)	a _{pk} (g)	T	a _T (g)	a _T ² (g ²)
9.85	0.31	0.270059	0.083718	0.007009
39.4	0.89	0.1	0.089	0.007921
88.65	2.11	0.1	0.211	0.044521
157.6	2.78	0.1	0.278	0.077284
246.25	2.52	0.1	0.252	0.063504
354.6	1.83	0.1	0.183	0.033489
482.65	1.32	0.1	0.132	0.017424
630.4	0.96	0.1	0.096	0.009216
797.85	0.73	0.1	0.073	0.005329
9.85	0.57	0.1	0.057	0.003249
1191.85	0.46	0.1	0.046	0.002116

Table I2c
Horizontal Ductwork (110-320lb)

f (Hz)	a _{pk} (g)	T	a _T (g)	a _T ² (g ²)
9.85	0.31	0.244058	0.075658	0.005724
39.4	0.89	0.1	0.089	0.007921
88.65	2.11	0.1	0.211	0.044521
157.6	2.78	0.1	0.278	0.077284
246.25	2.52	0.1	0.252	0.063504
354.6	1.83	0.1	0.183	0.033489
482.65	1.32	0.1	0.132	0.017424
630.4	0.96	0.1	0.096	0.009216
797.85	0.73	0.1	0.073	0.005329
9.85	0.57	0.1	0.057	0.003249
1191.85	0.46	0.1	0.046	0.002116

Table I2d
Exhaust Horizontal Ductwork (45-130lb only)

f (Hz)	a _{pk} (g)	T	a _T (g)	a _T ² (g ²)
9.85	0.31	0.390059	0.120918	0.146214
39.4	0.89	0.1	0.089	0.007921
88.65	2.11	0.1	0.211	0.044521
157.6	2.78	0.1	0.278	0.077284
246.25	2.52	0.1	0.252	0.063504
354.6	1.83	0.1	0.183	0.033489
482.65	1.32	0.1	0.132	0.017424
630.4	0.96	0.1	0.096	0.009216
797.85	0.73	0.1	0.073	0.005329
9.85	0.57	0.1	0.057	0.003249
1191.85	0.46	0.1	0.046	0.002116

Table I2 (Cont'd)

Table I2e
Exhaust Fans (1,2,11 & 12) and Attached Ductwork

f (Hz)	a _{pk} (g)	T	a _T (g)	a _T ² (g ²)
9.85	0.31	0.230058	0.071318	0.005086
39.4	0.89	0.1	0.089	0.007921
88.65	2.11	0.1	0.211	0.044521
157.6	2.78	0.1	0.278	0.077284
246.25	2.52	0.1	0.252	0.063504
354.6	1.83	0.1	0.183	0.033489
482.65	1.32	0.1	0.132	0.017424
630.4	0.96	0.1	0.096	0.009216
797.85	0.73	0.1	0.073	0.005329
9.85	0.57	0.1	0.057	0.003249
1191.85	0.46	0.1	0.046	0.002116

Table I2f
Exhaust Fans (10 & 20) and Attached Ductwork

f (Hz)	a _{pk} (g)	T	a _T (g)	a _T ² (g ²)
9.85	0.31	0.680045	0.210814	0.044443
39.4	0.89	0.1	0.089	0.007921
88.65	2.11	0.1	0.211	0.044521
157.6	2.78	0.1	0.278	0.077284
246.25	2.52	0.1	0.252	0.063504
354.6	1.83	0.1	0.183	0.033489
482.65	1.32	0.1	0.132	0.017424
630.4	0.96	0.1	0.096	0.009216
797.85	0.73	0.1	0.073	0.005329
9.85	0.57	0.1	0.057	0.003249
1191.85	0.46	0.1	0.046	0.002116

Table I2g
Fire Protection Pipe (6 in. full pipe support at the bar joists)

f (Hz)	a _{pk} (g)	T	a _T (g)	a _T ² (g ²)
9.85	0.31	0.200058	0.062018	0.003846
39.4	0.89	0.1	0.089	0.007921
88.65	2.11	0.1	0.211	0.044521
157.6	2.78	0.1	0.278	0.077284
246.25	2.52	0.1	0.252	0.063504
354.6	1.83	0.1	0.183	0.033489
482.65	1.32	0.1	0.132	0.017424
630.4	0.96	0.1	0.096	0.009216
797.85	0.73	0.1	0.073	0.005329
9.85	0.57	0.1	0.057	0.003249
1191.85	0.46	0.1	0.046	0.002116

Table I3

Ductwork Support Reaction Calculations and Isolator Selection

Table I3a
HV Ductwork Support Reactions (Area A - South Side)

	Node	X (in.)	Y (in.)	Z (in.)	Length (in.)	Wgt/in. (lb/in.)	Wgt/ Sect (lb)	Wgt/ Iso (lb)	No. of Iso	Rec Iso Type
	1	12	114	0	12	3.68	44			
Girt	2	0	114	0	38	3.68	140	92	2	I
		0	152	0	38	3.68	140			
Girt	3	0	190	0	38	3.68	140	147	2	H
	4	0	228	0	5	2.71	14			
		0.5	233	0	43	2.71	117			
Girt	5	4.8	276	0	12	2.71	33	102	2	I
	6	6	288	0	31	1.73	54			
		6	319	0	43	1.73	75			
Girt	7	6	362	0	34	1.73	59	70	2	I
	8	6	396	0	4	1.73	7			
		10	396	0	38	1.73	66			
B.J.	9	48	396	0	67	1.73	115	91	2	F
		115	396	0	67	1.73	115			
B.J.	10	181	396	0	84	1.73	146	130	2	G
		265	396	0	84	1.73	146			
B.J.	11	349	396	0	99	1.73	171	158	2	G
		349	396	98.5	24	1.73	41			
	12	349	396	122	75	2.14	159			
B.J.	13	343	432	187			0	191	3	G _F ^G
	14	144	432	196	37	2.54	94			
B.J.	15	181	432	196	81	2.54	206	150	2	G
		262	432	196	81	2.54	206			
B.J.	13	343	432	196	73					
	13	343	432	205	71	2.34	166			
					2	2.34	5			
	16	346	399	270	69	2.13	147			
B.J.	17	346	399	339	67	2.13	142	147	2	G
		346	399	405.5	67	2.13	142			
B.J.	18	346	399	472	67	2.13	143	142	2	G
		346	399	539	67	2.13	143			
B.J.	19	346	399	606				130	3	G _F ^G
	20	12	114	612	12	2.93	35			
Girt	21	0	114	612	38	2.93	111	73	2	I
		0	152	612	38	2.93	111			
Girt	22	0	190	612	38	2.93	111	117	2	I
		0	228	612	5	2.29	11			
	23	0.4	233	612	43	2.29	99			
Girt	24	4	276	612	12	2.29	28	89	2	I
	25	5	288	612	31	1.66	51			
		5	319	612	43	1.66	71			
Girt	26	5	362	612	33	1.66	55	67	2	I
	27	5	395	612	5	1.66	8			
		10	395	612	38	1.66	63			
B.J.	28	48	395	612	67	1.66	110	87	2	F
		115	395	612	67	1.66	110			
B.J.	29	181	395	612	84	1.66	138	124	2	G
		265	395	612	82	1.66	135			

Table 13 (Cont'd)

B.J.	19	346	395	612						
	19	346	395	618	46	1.68	77			
	30	350	394	664	28	1.22	33			
		350	394	691.5	74	1.22	89			
B.J.	31	350	394	765	74	1.22	89	89	2	F
		350	394	838.5	74	1.22	89			
B.J.	32	350	394	912	16	1.22	19	69	2	F
	33	350	394	928	24	1.22	29			
		326	394	928	39	1.22	47			
B.J.	34	287	394	928	15	1.22	18	38	2	F
	35	272	394	928	9	1.22	10			
		272	385.5	928	24	1.22	29			
Girt	36	272	362	928	43	1.22	52	40	2	J
		272	319	928	31	1.22	38			
	37	272	288	928	12	1.48	18			
Girt	38	272	276	928.8	43	1.48	64	60	2	I
		272	233	931.7	5	1.48	7			
	39	272	228	932	38	1.73	66			
Girt	40	272	190	932	38	1.73	66	70	2	I
		272	152	932	38	1.73	66			
Girt	41	272	114	932	12	1.73	21	43	2	J
	42	272	114	920						

Table 13b
HV Ductwork Support Reactions (Area A - North Side)

	Node	X (in.)	Y (in.)	Z (in.)	Length (in.)	Wgt/in. (lb/in.)	Wgt/ Sect (lb)	Wgt/ Iso (lb)	No. of Iso	Rec Iso Type
	1	12	114	0	12	3.68	44			
Girt	2	0	114	0	38	3.68	140	92	2	I
		0	152	0	38	3.68	140			
Girt	3	0	190	0	38	3.68	140	147	2	H
	4	0	228	0	5	2.71	14			
		0.5	233	0	43	2.71	117			
Girt	5	4.8	276	0	12	2.71	33	102	2	I
	6	6	288	0	31	1.73	54			
		6	319	0	43	1.73	75			
Girt	7	6	362	0	34	1.73	59	70	2	I
	8	6	396	0	4	1.73	7			
		10	396	0	38	1.73	66			
B.J.	9	48	396	0	67	1.73	115	91	2	F
		115	326	0	67	1.73	115			
B.J.	10	181	396	0	84	1.73	146	130	2	G
		265	396	0	84	1.73	146			
B.J.	11	349	396	0	99	1.73	171	158	2	G
		349	396	98.5	24	1.73	41			
	12	349	396	122	75	2.14	159			
B.J.	13	343	432	187			0	191	3	G _F
	14	144	432	196	37	2.54	94			
B.J.	15	181	432	196	81	2.54	206	150	2	G
		262	432	196	81	2.54	206			
B.J.	13	343	432	196	73					
	13	343	432	205	71	2.34	166			
					2	2.34	5			
	16	346	399	270	69	2.13	147			

Table 13 (Cont'd)

B.J.	17	346	399	339	67	2.13	142	147	2	G
		346	399	405.5	67	2.13	142			
B.J.	18	346	399	472	67	2.13	143	142	2	G
		346	399	539	67	2.13	143			
B.J.	19	346	399	606				130	3	G ^G _F
	20	12	114	612	12	2.93	35			
Girt	21	0	114	612	44	2.93	129	82	2	I
		0	158	612	44	2.93	129			
Girt	22	0	202	612	26	2.93	76	105	2	I
		0	228	612	3	2.29	6			
		0.4	231	612	66					
Girt	24	4	259	612	29	2.29	66	78	2	I
	25	5	288	612	14	1.66	23			
		5	302	612	43	1.66	71			
Girt	26	5	345	612	50	1.66	83	81	2	I
	27	5	395	612	5	1.66	8			
		10	395	612	38	1.66	63			
B.J.	28	48	395	612	67	1.66	110	87	2	F
		115	395	612	67	1.66	110			
B.J.	29	181	395	612	84	1.66	138	124	2	G
		265	395	612	82	1.66	135			
B.J.	19	346	395	612						
	19	346	395	618	46	1.68	77			
	30	350	394	664	28	1.22	33			
		350	394	691.5	74	1.22	89			
B.J.	31	350	394	765	74	1.22	89	89	2	F
		350	394	838.5	74	1.22	89			
B.J.	32	350	394	912	16	1.22	19	69	2	F
	33	350	394	928	24	1.22	29			
		326	394	928	39	1.22	47			
B.J.	34	287	394	928	15	1.22	18	38	2	F
	35	272	394	928	9	1.22	10			
		272	385.5	928	24	1.22	29			
Girt	36	272	362	928	43	1.22	52	40	2	J
		272	319	928	31	1.22	38			
	37	272	288	928	12	1.48	18			
Girt	38	272	276	928.8	43	1.48	64	60	2	I
		272	233	931.7	5	1.48	7			
	39	272	228	932	38	1.73	66			
Girt	40	272	190	932	38	1.73	66	70	2	I
		272	152	932	38	1.73	66			
Girt	41	272	114	932	12	1.73	21	43	2	J
	42	272	114	920						

Table I3 (Cont'd)

Table I3c
EF-3 & 13 Fan and Duct (Area A - North Side)

	Node	X (in.)	Y (in.)	Z (in.)	Length (in.)	Wgt/in. (lb/in.)	Wgt/ Sect (lb)	Wgt/ Iso (lb)	No. of Iso	Rec Iso Type
Floor	1	0	2	0				20	2	
		0	52.5	0	50.5	0.78	40			
Girt	2	0	103	0	50.5	0.78	40	38	2	J
		0	149.5	0	46.5	0.78	36			
Girt	3	0	196	0	46.5	0.78	36	32	2	J
	4	0	228	0	32.0	0.78	25			
		0	224.5	0	3.5	0.78	3			
Girt	5	0	253	0	28.5	0.78	22	28	2	J
	6	0	288	0	35.0	0.78	27			
		0	296	0	8.0	0.78	6			
Girt	7	0	339	0	43.0	0.78	34	34	2	J
		0	382	0	43.0	0.78	34			
Girt	8	0	425	0	43.0	0.78	34	33	2	J
	9	0	443	0	18.0	0.78	14			
		23	443	0	23.0	0.78	18			
B.J.	10	64	443	0	41.0	0.78	32	42	2	J
	11	80	443	0	16.0	0.78	13			
	12	80	484	0	41.0	0.98	40			
Fan on							Min.	26	4	
B.J.							Max.	30	4	J

Table I3d
EF-4 & 14 Fan and Duct (Area A - South Side)

	Node	X (in)	Y (in)	Z (in.)	Length (in.)	Wgt/in (lb/in.)	Wgt/ Sect (lb.)	Wgt/ Iso (lb.)	No of Iso	Rec Iso Type
Floor	1	0	2	0				20	2	
		0	52.5	0	50.5	0.78	40			
Girt	2	0	103	0	50.5	0.78	40	37	2	J
		0	146.5	0	43.5	0.78	34			
Girt	3	0	190	0	43.5	0.78	34	34	2	J
	4	0	228	0	38.0	0.78	30			
		0	233	0	5.0	0.78	4			
Girt	5	0	276	0	43.0	0.78	34	34	2	J
	6	0	288	0	12.0	0.78	9			
		0	319	0	31.0	0.78	24			
Girt	7	0	362	0	43.0	0.78	34	31	2	J
		0	398	0	36.0	0.78	28			
Girt	8	0	434	0	36.0	0.78	28	29	2	J
	9	0	447	0	13.0	0.78	10			
		26	447	0	26.0	0.78	20			
B.J.	10	64	447	0	38.0	0.78	30	39	2	J
	11	80	447	0	16.0	0.78	13			
	12	80	484	0	37.0	0.98	36			
Fan on							Min.	26	4	
B.J.							Max.	30	4	J

Table I3 (Cont'd)

Table I3e
EF-5 & 15 Fan and Duct (Area A - North Side)

	Node	X (in)	Y (in)	Z (in.)	Length (in.)	Wgt/in (lb/in.)	Wgt/ Sect (lb.)	Wgt/ Iso (lb.)	No of Iso	Rec Iso Type
Floor	1	0	2	0				65	2	
		0	52.5	0	50.5	2.58	130			
Girt	2	0	103	0	50.5	2.58	130	103	2	I
		0	132	0	29.0	2.58	75			
Girt	3	0	161	0	29.0	2.58	75	82	2	I
		0	195.5	0	34.5	2.58	89			
	4	0	228	0	32.5	2.58	84			
Girt	5	0.1	230	0	2.0	2.16	4	80	2	I
		2.3	263	0	33.1	2.16	71			
	6	4	288	0	25.1	2.16	54			
Girt	7	4	296	0	8.0	1.73	14	63	2	I
		4	329	0	33.0	1.73	57			
Girt	8	4	362	0	33.0	1.73	57	68	2	I
		4	407	0	45.0	1.73	78			
Girt	9	4	452	0	45.0	1.73	78	77	2	I
		4	484	0	32.0	1.73	55			
	10	16	484	0	12.0	1.73	21			
B.J.	11	60	484	0	44.0	1.73	76	122	2	I
	12	85	484	0	25.0	1.73	43			
	13	85	540	0	56.0	2.21	124			
Fan on							Min.	90	4	
B.J.							Max.	100	4	I

Table I3f
EF-8 & 18 Fan and Duct (Area A - South Side)

	Node	X (in)	Y (in)	Z (in.)	Length (in.)	Wgt/in (lb/in.)	Wgt/ Sect (lb.)	Wgt/ Iso (lb.)	No of Iso	Rec Iso Type
Floor	1	0	2	0				65	2	
		0	52.5	0	50.5	2.58	130			
Girt	2	0	103	0	50.5	2.58	130	121	2	I
		0	146.5	0	43.5	2.58	112			
Girt	3	0	190	0	43.5	2.58	112	111	2	I
	4	0	228	0	38.0	2.58	98			
		0	233	0	5.0	2.16	11			
Girt	5	3.2	276	0	43.1	2.16	93	86	2	I
	6	4	288	0	12.0	2.16	26			
		4	319	0	31.0	1.73	54			
Girt	7	4	362	0	43.0	1.73	75	76	2	I
		4	407	0	45.0	1.73	78			
Girt	8	4	452	0	45.0	1.73	78	77	2	I
	9	4	484	0	32.0	1.73	55			
		16	484	0	12.0	1.73	21			
B.J.	10	60	484	0	44.0	1.73	76	122	2	I
	11	85	484	0	25.0	1.73	43			
	12	85	540	0	56.0	2.21	124			
Fan on							Min.	90	4	
B.J.							Max.	100	4	I

Table I3 (Cont'd)

Table I3g
EF-6,7,16 & 17 Fan and Duct

	Node	X (in)	Y (in)	Z (in.)	Length (in.)	Wgt/in (lb/in.)	Wgt/ Sect (lb.)	Wgt/ Iso (lb.)	No of Iso	Rec Iso Type
Floor	1	0	2	0				65	2	
		0	52.5	0	50.5	2.58	130			
Girt	2	0	103	0	50.5	2.58	130	121	2	I
		0	146.5	0	43.5	2.58	112			
Girt	3	0	190	0	43.5	2.58	112	111	2	I
	4	0	228	0	38.0	2.58	98			
		0.3	233	0	5.0	2.16	11			
Girt	5	3.2	276	0	43.1	2.16	93	86	2	I
	6	4	288	0	12.0	2.16	26			
		4	319	0	31.0	1.73	54			
Girt	7	4	362	0	43.0	1.73	75	75	2	I
	8	4	406	0	44.0	1.73	76			
B.J.	9	48	406	0	44.0	1.73	76	117	2	I
	10	73	406	0	25.0	1.73	43			
	11	73	458	0	52.0	2.21	115			
Fan on B.J.						Min.		90	4	
						Max.		100	4	I

Table I3h
EF-9 & 19 Fan and Duct

	Node	X (in)	Y (in)	Z (in.)	Length (in.)	Wgt/in (lb/in.)	Wgt/ Sect (lb.)	Wgt/ Iso (lb.)	No of Iso	Rec Iso Type
Floor	1	20	2	102				19	2	
		20	52.5	102	50.5	0.73	37			
Girt	2	20	103	102	50.5	0.73	37	34	2	J
		20	146.5	102	43.5	0.73	32			
Girt	3	20	190	102	43.5	0.73	32	32	2	J
	4	20	228	102	38.0	0.73	28			
		20	233	102	5.0	0.73	4			
Girt	5	20	276	102	43.0	0.73	32	32	2	J
	6	20	288	102	12.0	0.73	9			
		20	319	102	31.0	0.73	23			
Girt	7	20	362	102	43.0	0.73	32	32	2	J
	8	20	397	102	35.0	0.73	26			
		20	397	92	10.0	0.73	7			
B.J.	9	20	397	46	46.0	0.73	34	33	2	J
		20	397	1	45.0	0.73	33			
	10	20	397	0	1.0	0.73	1			
B.J.	11	64	397	0	44.0	0.73	32	52	2	I
	12	80	397	0	16.0	0.73	15			
	13	80	456	0	59.0	0.95	56			
Fan on B.J.						Min.		25	4	
						Max.		30	4	J

Table I3 (Cont'd)

Table I3i
EF-10 & 20 Fan and Duct

	Node	X (in)	Y (in)	Z (in.)	Length (in.)	Wgt/in (lb/in.)	Wgt/ Sect (lb.)	Wgt/ Iso (lb.)	No of Iso	Rec Iso Type
Floor	1	0	2	0				17	2	
		0	52.5	0	50.5	0.68	34			
Girt	2	0	103	0	50.5	0.68	34	32	2	J
		0	146.5	0	43.5	0.68	29			
Girt	3	0	190	0	43.5	0.68	29	29	2	J
	4	0	228	0	38.0	0.68	26			
		0	233	0	5.0	0.68	3			
Girt	5	0	276	0	43.0	0.68	29	29	2	J
	6	0	288	0	12.0	0.68	8			
		0	319	0	31.0	0.68	21			
Girt	7	0	362	0	43.0	0.68	29	27	2	J
		0	398	0	36.0	0.68	24			
Girt	8	0	434	0	36.0	0.68	24	24	2	J
		0	470	0	36.0	0.68	24			
Girt	9	0	506	0	36.0	0.68	24	26	2	J
	10	0	525	0	19.0	0.68	13			
		22	525	0	22.0	0.68	15			
B.J.	11	64	525	0	42.0	0.68	28	38	2	J
	12	80	525	0	16.0	0.68	11			
	13	80	568	0	43.0	0.87	37			
Fan on B.J.							Min.	7	4	
							Max.	26	4	S

Table I3j
EF-31 Fan and Duct (Area A - South Side)

	Node	X (in)	Y (in)	Z (in.)	Length (in.)	Wgt/in (lb/in.)	Wgt/ Sect (lb.)	Wgt/ Iso (lb.)	No of Iso	Rec Iso Type
Floor	1	0	2	0				17	2	
		0	52.5	0	50.5	0.68	34			
Girt	2	0	103	0	50.5	0.68	34	32	2	J
		0	146.5	0	43.5	0.68	29			
Girt	3	0	190	0	43.5	0.68	29	29	2	J
	4	0	228	0	38.0	0.68	26			
		0	233	0	5.0	0.68	3			
Girt	5	0	276	0	43.0	0.68	29	29	2	J
	6	0	288	0	12.0	0.68	8			
		0	319	0	31.0	0.68	21			
Girt	7	0	362	0	43.0	0.68	29	27	2	J
		0	398	0	36.0	0.68	24			
Girt	8	0	434	0	36.0	0.68	24	24	2	J
		0	470	0	36.0	0.68	24			
Girt	9	0	506	0	36.0	0.68	24	27	2	J
	10	0	526	0	20.0	0.68	14			
		23	526	0	23.0	0.68	16			
B.J.	11	66	526	0	43.0	0.68	29	34	2	J
	12	77	526	0	11.0	0.68	7			
	13	77	567	0	41.0	0.76	31			
Fan on B.J.							Min.	25	4	
							Max.	30	4	J

Table 13 (Cont'd)

Table 13k
EF-32 Fan and Duct (Area C - South Side)

	Node	X (in)	Y (in)	Z (in.)	Length (in.)	Wgt/in (lb/in.)	Wgt/ Sect (lb.)	Wgt/ Iso (lb.)	No of Iso	Rec Iso Type
Floor	1	0	2	0				14	2	
		0	52.5	0	50.5	0.57	29			
Girt	2	0	103	0	50.5	0.57	29	27	2	J
		0	146.5	0	43.5	0.57	25			
Girt	3	0	190	0	43.5	0.57	25	25	2	J
	4	0	228	0	38.0	0.57	22			
		0	233	0	5.0	0.57	3			
Girt	5	0	276	0	43.0	0.57	24	24	2	J
	6	0	288	0	12.0	0.57	7			
		0	319	0	31.0	0.57	18			
Girt	7	0	362	0	43.0	0.57	24	22	2	J
		0	398	0	36.0	0.57	20			
Girt	8	0	434	0	36.0	0.57	20	20	2	J
		0	470	0	36.0	0.57	20			
Girt	9	0	506	0	36.0	0.57	20	22	2	J
	10	0	526	0	20.0	0.57	11			
		23	526	0	23.0	0.57	13			
B.J.	11	66	526	0	43.0	0.57	24	30	2	J
	12	77	526	0	11.0	0.57	6			
	13	77	567	0	41.0	0.70	29			
Fan on							Min.	25	4	
B.J.							Max.	30	4	J

Table 13l
EF-29 & 30 Duct

	Node	X (in)	Y (in)	Z (in.)	Length (in.)	Wgt/in (lb/in.)	Wgt/ Sect (lb.)	Wgt/ Iso (lb.)	No of Iso	Rec Iso Type
Valve										
Room	1	0	156	0						
Roof		0	193	0	37.0	0.52	19			
Girt	2	0	230	0	37.0	0.52	19	18	2	J
		0	263	0	33.0	0.52	17			
Girt	3	0	296	0	33.0	0.52	17	17	2	J
		0	329	0	33.0	0.52	17			
Girt	5	0	362	0	33.0	0.52	17	20	2	J
		0	407	0	45.0	0.52	23			
Girt	6	0	452	0	45.0	0.52	23	21	2	J
		0	488	0	36.0	0.52	19			
Girt @										
Roof	7	0	524	0	36.0	0.52	19	19	2	J
Top of										
Duct	8	0	560	0	36.0	0.52	19			

Table 14

**Effective Acceleration Calculations for Each Modal
Contribution for Equipment Supported by the Wall Girts**

Table 14a
Vertical Ductwork (110-160lb)

f (Hz)	a _{pk} (g)	T	a _T (g)	a _T ² (g ²)
11	0.66	0.225058	0.148538	0.022064
44	1.8	0.1	0.18	0.0324
99	3.95	0.1	0.395	0.156025
176	4.91	0.1	0.491	0.241081
275	3.88	0.1	0.388	0.150544
396	2.8	0.1	0.28	0.0784
539	1.96	0.1	0.196	0.038416
704	1.43	0.1	0.143	0.020449
891	1.09	0.1	0.109	0.011881
1100	0.85	0.1	0.085	0.007225

Table 14b
Vertical Ductwork (40-135lb)

f (Hz)	a _{pk} (g)	T	a _T (g)	a _T ² (g ²)
11	0.66	0.340059	0.224439	0.050373
44	1.8	0.1	0.18	0.0324
99	3.95	0.1	0.395	0.156025
176	4.91	0.1	0.491	0.241081
275	3.88	0.1	0.388	0.150544
396	2.8	0.1	0.28	0.0784
539	1.96	0.1	0.196	0.038416
704	1.43	0.1	0.143	0.020449
891	1.09	0.1	0.109	0.011881
1100	0.85	0.1	0.085	0.007225

Table 14c
Vertical Ductwork (17-50lb)

f (Hz)	a _{pk} (g)	T	a _T (g)	a _T ² (g ²)
11	0.66	0.310059	0.204639	0.041877
44	1.8	0.1	0.18	0.0324
99	3.95	0.1	0.395	0.156025
176	4.91	0.1	0.491	0.241081
275	3.88	0.1	0.388	0.150544
396	2.8	0.1	0.28	0.0784
539	1.96	0.1	0.196	0.038416
704	1.43	0.1	0.143	0.020449
891	1.09	0.1	0.109	0.011881
1100	0.85	0.1	0.085	0.007225

Table I4d
Hot Water and Heating Pipes (95-125lb)

f (Hz)	a _{pk} (g)	T	a _T (g)	a _T ² (g ²)
11	0.66	0.200058	0.132038	0.017434
44	1.8	0.1	0.18	0.0324
99	3.95	0.1	0.395	0.156025
176	4.91	0.1	0.491	0.241081
275	3.88	0.1	0.388	0.150544
396	2.8	0.1	0.28	0.0784
539	1.96	0.1	0.196	0.038416
704	1.43	0.1	0.143	0.020449
891	1.09	0.1	0.109	0.011881
1100	0.85	0.1	0.085	0.007225

Table I4e
Vertical Fire Protection Pipe

f (Hz)	a _{pk} (g)	T	a _T (g)	a _T ² (g ²)
11	0.66	0.380059	0.250839	0.06292
44	1.8	0.1	0.18	0.0324
99	3.95	0.1	0.395	0.156025
176	4.91	0.1	0.491	0.241081
275	3.88	0.1	0.388	0.150544
396	2.8	0.1	0.28	0.0784
539	1.96	0.1	0.196	0.038416
704	1.43	0.1	0.143	0.020449
891	1.09	0.1	0.109	0.011881
1100	0.85	0.1	0.085	0.007225

Table I4f
Beakon Fire Protection Lighting

f (Hz)	a _{pk} (g)	T	a _T (g)	a _T ² (g ²)
11	0.66	0.265059	0.174939	0.030604
44	1.8	0.1	0.18	0.0324
99	3.95	0.1	0.395	0.156025
176	4.91	0.1	0.491	0.241081
275	3.88	0.1	0.388	0.150544
396	2.8	0.1	0.28	0.0784
539	1.96	0.1	0.196	0.038416
704	1.43	0.1	0.143	0.020449
891	1.09	0.1	0.109	0.011881
1100	0.85	0.1	0.085	0.007225

Table I5

Steam and Condensate Pipe Support Reactions Calculations

Table I5a

10 in. Steam Pipe Support Reactions

Node	X (in)	Y (in)	Length (in)	Tributary Length (in)	Weight/ft (lb/ft)	Weight/ Isolator (lb)	Vertical (V) Guided (G) or Anchor (A)	
2	6	0	42				G	
4	48	0	180	111	40.48	374	V	
13	228	0	228	204	40.48	688	A	Max.A
25	456	0	199.5	213.75	40.48	180	G	Max.G
35	656	0	193.5	196.5	40.48	663	V	
44	849	0	205.5	199.5	40.48	168	G	
54	1055	0	193.5	199.5	40.48	673	V	
63	1248	0	114	153.75	40.48	130	G	Min.G
70	1362	0	114	114	40.48	385	V	
77	1434	42	249	181.5	40.48	612	V	
89	1434	291	169	209	40.48	705	V	
98	1531	363	310	239.5	40.48	808	V	Max.V

Table I5b

6 in. Condensate Pipe Support Reactions

Node	X (in)	Y (in)	Length (in)	Tributary Length (in)	Weight/ft (lb/ft)	Weight/ Isolator (lb)	Vertical (V) Guided (G) or Anchor (A)	
2	60	42					G	
			80	111	39.87	369	V	Min.V
13	228	0	228	204	39.87	678	A	
25	456	0	199.5	213.75	39.87	178	G	
35	656	0	193.5	196.5	39.87	653	V	
44	849	0	205.5	199.5	39.87	166	G	
54	1055	0	193.5	199.5	39.87	663	V	
63	1248	0	186	189.75	39.87	158	G	
73	1434	0	134	160	39.87	532	V	
81	1506	62	212	173	39.87	575	V	
91	1506	274	144	178	39.87	591	V	
99	1578	346	216	180	39.87	598	V	
111	1794	346						

Table I6

Pipe Weight and Frequency Calculations

Table I-6a
Pipe Weight and Frequency Calculations

Member Spec.	I (in ⁴)	Wgt/ft (lb/ft)	Length (in)	k (lb/in)	Eff Mass (lbs/in)	f (Hz)	React (lb)	Wgt/iso (lb)
Steam & Condensate								
10" Sch 40	161	40.48	310	7782	1.691	10.8	1046	523
Steam	161	40.48	249	15017	1.359	16.7	840	420
	161	40.48	205.5	26715	1.121	24.6	693	347
	161	40.48	180	39753	0.982	32.0	607	304
4" Steam	7.23	10.79	144	3487	0.209	20.5	129	65
Supply	7.23	10.79	90	14281	0.131	52.6	81	40
	7.23	10.79	132	4527	0.192	24.4	119	59
6" Sch 80	40.5	39.87	216	5787	1.161	11.2	718	359
Condensate	40.5	39.87	206	6671	1.107	12.4	684	342
	40.5	39.87	194	7988	1.043	13.9	645	322
	40.5	39.87	180	10000	0.967	16.2	598	299
2" Cond	0.666	5.1	144	321	0.099	9.1	61	31
Return	0.666	5.1	84	1618	0.058	26.6	36	18
Heating/Hot Water								
6" HWR	28.1	31.49	144	13551	0.611	23.7	378	189
	28.1	31.49	133	17199	0.565	27.8	349	175
	28.1	31.49	96	45736	0.407	53.3	252	126
Vertical	28.1	31.49	90	55506	0.382	60.7	236	118
4" HW	7.23	16.31	144	3487	0.317	16.7	196	98
	7.23	16.31	133	4425	0.292	19.6	181	90
	7.23	16.31	96	11768	0.211	37.6	130	65
Vertical	7.23	16.31	180	1785	0.396	10.7	245	122
	7.23	16.31	90	14281	0.198	42.8	122	61
Catwalk	7.23	16.31	108	8265	0.237	29.7	147	73
2" HW	0.666	5.1	180	164	0.124	5.8	77	38
Vertical	0.666	5.1	90	1316	0.062	23.2	38	19
Fire Protection Overhead Sprinkler Pipe								
Vertical Pipe								
Empty 6"	28.1	18.97	48	365885	0.123	274.8	76	38
Empty 6"	28.1	18.97	120	23417	0.307	44.0	190	95
Full 6"	28.1	31.49	120	23417	0.509	34.1	315	157
Horizontal Pipe								
Empty 6"	28.1	18.97	96	45736	0.245	68.7	152	76
Empty 6"	28.1	18.97	144	13551	0.368	30.5	228	114
Full 6"	28.1	31.49	144	13551	0.611	23.7	378	189
Empty 4"	7.23	10.79	120	6025	0.175	29.6	108	54
Full 4"	7.23	16.31	120	6025	0.264	24.1	163	82

Table I6a (cont'd)
Pipe Weight and Frequency Calculations

Member Spec.	I (in ⁴)	Wgt/ft (lb/ft)	Length (in)	k (lb/in)	Eff Mass (lbs/in)	f (Hz)	React (lb)	Wgt/iso (lb)
Empty 3"	3.02	7.58	120	2517	0.123	22.8	76	38
Full 3"	3.02	10.78	120	2517	0.174	19.1	108	54
Empty 2.5"	1.53	5.79	120	1275	0.094	18.6	58	29
Full 2.5"	1.53	7.86	120	1275	0.127	15.9	79	39
Fire Protection Oscillating Monitor Pipe								
Horizontal Pipe								
Full 6"	28.1	31.49	132	17593	0.560	28.2	346	173
Full 6"	28.1	31.49	168	8534	0.713	17.4	441	220
Full 4"	7.23	16.31	84	17566	0.185	49.1	114	57
Full 4"	7.23	16.31	168	2196	0.369	12.3	228	114
Vertical Pipe								
Full 6"	28.1	31.49	54	256973	0.229	168.5	142	71
Full 6"	28.1	31.49	90	55506	0.382	60.7	236	118
Horizontal Pipe Over the Rear Hangar Door								
Full 6"	28.1	31.49	90	55506	0.382	60.7	236	118
Full 6"	28.1	31.49	144	13551	0.611	23.7	378	189

Table I6b
Weight of Pipes

Nominal	Size	Outside Dia (in.)	Inside Dia (in.)	Empty Weight (lb.)	Full Weight (lb.)
	10	10.75	10.02	40.48	74.65
Sch 80	6	6.625	5.761	28.57	39.87
Sch 40		6.625	6.065	18.97	31.49
	4	4.5	4.026	10.79	16.31
	3	3.5	3.068	7.58	10.78
	2.5	2.875	2.469	5.79	7.86
	2	2.375	2.067	3.65	5.10

Table I7

**Effective Acceleration Calculations for Each Modal
Contribution for Equipment Supported by the Roof Truss**

Table I7a
Steam and Condensate Pipe Guided Supports

f (Hz)	Bar Joist a_{pk} (g)	Roof Truss a_{pk} (g)	T	a_T (g)	a_T^2 (g ²)
9.85	0.31	0.184808	0.240058	0.044365	0.001968
39.4	0.89	0.530577	0.1	0.053058	0.002815
88.65	2.11	1.257885	0.1	0.125788	0.015823
157.6	2.78	1.657308	0.1	0.165731	0.027467
246.25	2.52	1.502308	0.1	0.150231	0.022569
354.6	1.83	1.090962	0.1	0.109096	0.011902
482.65	1.32	0.786923	0.1	0.078692	0.006192
630.4	0.96	0.572308	0.1	0.057231	0.003275
797.85	0.73	0.435192	0.1	0.043519	0.001894
9.85	0.57	0.339808	0.1	0.033981	0.001155
1191.85	0.46	0.274231	0.1	0.027423	0.000752

Table I7b
Steam and Condensate Pipe Guided Supports

f (Hz)	Bar Joist a_{pk} (g)	Roof Truss a_{pk} (g)	T	a_T (g)	a_T^2
9.85	0.31	0.184808	0.230058	0.042517	0.001808
39.4	0.89	0.530577	0.1	0.053058	0.002815
88.65	2.11	1.257885	0.1	0.125788	0.015823
157.6	2.78	1.657308	0.1	0.165731	0.027467
246.25	2.52	1.502308	0.1	0.150231	0.022569
354.6	1.83	1.090962	0.1	0.109096	0.011902
482.65	1.32	0.786923	0.1	0.078692	0.006192
630.4	0.96	0.572308	0.1	0.057231	0.003275
797.85	0.73	0.435192	0.1	0.043519	0.001894
9.85	0.57	0.339808	0.1	0.033981	0.001155
1191.85	0.46	0.274231	0.1	0.027423	0.000752

Table I8

**Effective Acceleration Calculations for Each Modal
Contribution for Oscillating Monitor Fire Protection Pipes**

f (Hz)	Bar Joist a_{pk} (g)	Roof Truss a_{pk} (g)	T	a_T (g)	a_{T2} (g ²)
11	0.66	0.4455	0.272059	0.121202	0.01469
44	1.8	1.215	0.1	0.1215	0.014762
99	3.95	2.66625	0.1	0.266625	0.071089
176	4.91	3.31425	0.1	0.331425	0.109843
275	3.88	2.619	0.1	0.2619	0.068592
396	2.8	1.89	0.1	0.189	0.035721
539	1.96	1.323	0.1	0.1323	0.017503
704	1.43	0.96525	0.1	0.096525	0.009317
891	1.09	0.73575	0.1	0.073575	0.005413
1100	0.85	0.57375	0.1	0.057375	0.003292

Table 19

**Effective Acceleration Calculations for Each Modal Contribution
for Equipment Supported by the W8 x 28 Beams
That Support the Heating and Ventilating Unit and Catwalk**

Table 19a HV Unit						Table 19a (cont'd) HV Unit					
f (Hz)	a _{pk} (g)	a _{pk} ² (g ²)	T	a _T (g)	a _T ² (g ²)	f (Hz)	a _{pk} (g)	a _{pk} ² (g ²)	T	a _T (g)	a _T ² (g ²)
1.047	0.00232	5.382E-06	1.346284	0.003123	9.8E-06	6.31	0.08967	0.00804071	0.11992	0.010753	0.000116
1.096	0.00245	6.002E-06	1.392472	0.003412	0.000012	6.607	0.05348	0.00286011	0.108246	0.005789	0.000034
1.148	0.00259	6.708E-06	1.447661	0.003749	0.000014	6.918	0.03545	0.0012567	0.1	0.003545	0.000013
1.202	0.00274	7.508E-06	1.51287	0.004145	0.000017	7.244	0.02521	0.00063554	0.1	0.002521	6.4E-06
1.259	0.0029	8.410E-06	1.592146	0.004617	0.000021	7.586	0.01898	0.00036024	0.1	0.001898	3.6E-06
1.318	0.00308	9.486E-06	1.688017	0.005199	0.000027	7.943	0.0174	0.00030276	0.1	0.00174	3.0E-06
1.38	0.00327	0.00001069	1.807776	0.005911	0.000035	8.318	0.01949	0.00037986	0.1	0.001949	3.8E-06
1.445	0.00348	0.00001211	1.960453	0.006822	0.000047	8.71	0.02224	0.00049462	0.1	0.002224	4.9E-06
1.514	0.0037	0.00001369	2.16362	0.008005	0.000064	9.12	0.02612	0.00068225	0.1	0.002612	6.8E-06
1.585	0.00395	0.0000156	2.43562	0.009621	0.000093	9.55	0.03221	0.00103748	0.1	0.003221	0.00001
1.66	0.00423	0.00001789	2.828965	0.011967	0.000143	10	0.04323	0.00186883	0.1	0.004323	0.000019
1.738	0.00453	0.00002052	3.432584	0.01555	0.000242	10.471	0.05501	0.0030261	0.1	0.005501	0.00003
1.82	0.00486	0.00002362	4.485907	0.021802	0.000475	10.965	0.06053	0.00366388	0.1	0.006053	0.000037
1.905	0.00524	0.00002746	6.723158	0.035229	0.001241	11.482	0.06172	0.00380936	0.1	0.006172	0.000038
1.995	0.00566	0.00003204	14.97054	0.084733	0.00718	12.023	0.06294	0.00396144	0.1	0.006294	0.00004
2.089	0.00614	0.0000377	38.42013	0.2359	0.055649	12.589	0.06418	0.00411907	0.1	0.006418	0.000041
2.188	0.00669	0.00004476	8.078557	0.054046	0.002921	13.163	0.06545	0.0042837	0.1	0.006545	0.000043
2.291	0.00732	0.00005358	4.313324	0.031574	0.000997	13.804	0.06674	0.00445423	0.1	0.006674	0.000045
2.399	0.00805	0.0000648	2.852166	0.02296	0.000527	14.454	0.06805	0.0046308	0.1	0.006805	0.000046
2.512	0.0089	0.00007921	2.079971	0.018512	0.000343	15.136	0.0694	0.00481636	0.1	0.00694	0.000048
2.63	0.00992	0.00009841	1.604851	0.01592	0.000253	15.849	0.07077	0.00500839	0.1	0.007077	0.00005
2.754	0.01115	0.00012432	1.282495	0.0143	0.000204	16.596	0.07216	0.00520707	0.1	0.007216	0.000052
2.884	0.01265	0.00016002	1.050776	0.013292	0.000177	17.378	0.07358	0.00541402	0.1	0.007358	0.000054
3.02	0.01451	0.00021054	0.877156	0.012728	0.000162	18.197	0.07503	0.0056295	0.1	0.007503	0.000056
3.162	0.01687	0.0002846	0.742948	0.012534	0.000157	19.055	0.07651	0.00585378	0.1	0.007651	0.000059
3.311	0.01996	0.0003984	0.636031	0.012695	0.000161	19.953	0.07802	0.006087	0.1	0.007802	0.000061
3.467	0.02409	0.00058033	0.54936	0.013234	0.000175	20.893	0.07956	0.00633	0.1	0.007956	0.000063
3.631	0.02986	0.00089162	0.477697	0.014264	0.000203	21.878	0.08113	0.006582	0.1	0.008113	0.000066
3.802	0.03828	0.00146536	0.41841	0.016006	0.000256	22.909	0.08273	0.006844	0.1	0.008273	0.000068
3.981	0.05142	0.00264402	0.367872	0.018916	0.000358	23.988	0.08436	0.007117	0.1	0.008436	0.000071
4.074	0.04597	0.00211324	0.345536	0.015884	0.000252	25.119	0.08602	0.007399	0.1	0.008602	0.000074
4.169	0.0559	0.00312481	0.324914	0.018163	0.00033	26.303	0.08772	0.007695	0.1	0.008772	0.000077
4.266	0.06977	0.00486785	0.30583	0.021339	0.000455	27.542	0.08945	0.008001	0.1	0.008945	0.00008
4.365	0.0901	0.00811801	0.288178	0.025935	0.000674	28.84	0.09121	0.008319	0.1	0.009121	0.000083
4.467	0.12185	0.01484742	0.271638	0.033099	0.001096	30.2	0.09301	0.008651	0.1	0.009301	0.000087
4.571	0.17617	0.03103587	0.25629	0.045151	0.002039	31.623	0.09485	0.008997	0.1	0.009485	0.00009
4.677	0.28294	0.08005504	0.242028	0.068479	0.004689	33.113	0.09672	0.009355	0.1	0.009672	0.000094
4.786	0.54194	0.29369896	0.228641	0.12391	0.015354	34.674	0.09862	0.009726	0.1	0.009862	0.000097
4.898	1.0905	1.18919025	0.216074	0.235629	0.055521	36.308	0.10057	0.010114	0.1	0.010057	0.000101
5.012	1.2147	1.47549609	0.204374	0.248253	0.06163	38.019	0.10255	0.010517	0.1	0.010255	0.000105
5.129	1.13193	1.28126552	0.193377	0.218889	0.047913	39.811	0.10457	0.010935	0.1	0.010457	0.000109
5.248	1.08801	1.18376576	0.183122	0.199239	0.039696	41.687	0.10663	0.01137	0.1	0.010663	0.000114
5.37	1.22712	1.50582349	0.173472	0.212871	0.045314	43.652	0.10874	0.011824	0.1	0.010874	0.000118
5.495	0.97652	0.95359131	0.16439	0.16053	0.02577	45.709	0.11088	0.012294	0.1	0.011088	0.000123
5.623	0.43151	0.18620088	0.155341	0.067247	0.004522	47.863	0.11307	0.012785	0.1	0.011307	0.000128
5.754	0.22489	0.05057551	0.147792	0.033237	0.001105	50.119	0.1153	0.013294	0.1	0.01153	0.000133
6.026	0.18152	0.03294951	0.133023	0.024146	0.000583	52.481	0.11757	0.013823	0.1	0.011757	0.000138

Table 19 (cont'd)

Table 19a (cont'd)
HV Unit

f (Hz)	HV Unit a_{pk} (g)	a_{pk}^2 (g ²)	T	a_T (g)	a_T^2 (g ²)
54.954	0.11989	0.014374	0.1	0.011989	0.000144
57.544	0.12225	0.014945	0.1	0.012225	0.000149
60.256	0.12466	0.01554	0.1	0.012466	0.000155
63.096	0.12712	0.016159	0.1	0.012712	0.000162
66.069	0.12963	0.016804	0.1	0.012963	0.000168
69.183	0.13218	0.017472	0.1	0.013218	0.000175
72.444	0.13479	0.018168	0.1	0.013479	0.000182
75.858	0.13745	0.018893	0.1	0.013745	0.000189
79.433	0.14016	0.019645	0.1	0.014016	0.000196
83.176	0.14292	0.020426	0.1	0.014292	0.000204
87.096	0.14574	0.02124	0.1	0.014574	0.000212
91.201	0.14861	0.022085	0.1	0.014861	0.000221
95.499	0.15154	0.022964	0.1	0.015154	0.00023
100	0.15453	0.02388	0.1	0.015453	0.000239
104.71	0.15758	0.024831	0.1	0.015758	0.000248
109.65	0.16069	0.025821	0.1	0.016069	0.000258
114.82	0.16385	0.026847	0.1	0.016385	0.000268
120.23	0.16701	0.027892	0.1	0.016701	0.000279
125.89	0.16858	0.028419	0.1	0.016858	0.000284
131.83	0.16858	0.028419	0.1	0.016858	0.000284
138.04	0.16858	0.028419	0.1	0.016858	0.000284
144.54	0.16858	0.028419	0.1	0.016858	0.000284
151.36	0.16858	0.028419	0.1	0.016858	0.000284
158.49	0.16859	0.028423	0.1	0.016858	0.000284
165.96	0.16858	0.028419	0.1	0.016858	0.000284
173.78	0.16858	0.028419	0.1	0.016858	0.000284
181.97	0.16858	0.028419	0.1	0.016858	0.000284
190.55	0.16858	0.028419	0.1	0.016858	0.000284
208.93	0.16858	0.028419	0.1	0.016858	0.000284
218.78	0.16858	0.028423	0.1	0.016858	0.000284
229.09	0.16859	0.028419	0.1	0.016859	0.000284
239.88	0.16858	0.028419	0.1	0.016858	0.000284
251.19	0.16718	0.027949	0.1	0.016718	0.000279
263.03	0.16369	0.026794	0.1	0.016369	0.000268
275.42	0.15959	0.025469	0.1	0.015959	0.000255
288.4	0.1556	0.024211	0.1	0.01556	0.000242
302	0.15171	0.023016	0.1	0.015171	0.00023
316.23	0.14791	0.021877	0.1	0.014791	0.000219
331.13	0.14422	0.020799	0.1	0.014422	0.000208
346.74	0.14061	0.019771	0.1	0.014061	0.000198
363.08	0.13709	0.018794	0.1	0.013709	0.000188
380.19	0.13366	0.017865	0.1	0.013366	0.000179
398.11	0.13032	0.016983	0.1	0.013032	0.000179
416.87	0.12706	0.016144	0.1	0.012706	0.00017
436.52	0.12388	0.015346	0.1	0.012388	0.000161
457.09	0.12078	0.014588	0.1	0.012078	0.000153
478.63	0.11776	0.013867	0.1	0.011776	0.000139
501.19	0.11482	0.013184	0.1	0.011482	0.000132

Table 19b
Horizontal Steam Supply Attached to the Catwalk

f (Hz)	HV Unit a_{pk} (g)	Catwalk= $a_{pk} \times 0.6$ (g)	T	a_T (g)	a_T^2 (g ²)
1.047	0.00232	0.001392	1.269826	0.001768	3.1E-06
1.096	0.00245	0.00147	1.303517	0.001916	3.7E-06
1.148	0.00259	0.001554	1.343117	0.002087	4.4E-06
1.202	0.00274	0.001644	1.389005	0.002284	5.2E-06
1.259	0.0029	0.00174	1.443523	0.002512	6.3E-06
1.318	0.00308	0.001848	1.50766	0.002786	7.8E-06
1.38	0.00327	0.001962	1.585145	0.00311	9.7E-06
1.445	0.00348	0.002088	1.67992	0.003508	0.000012
1.514	0.0037	0.00222	1.799551	0.003995	0.000016
1.585	0.00395	0.00237	1.949128	0.004619	0.000021
1.66	0.00423	0.002538	2.146464	0.005448	0.00003
1.738	0.00453	0.002718	2.412439	0.006557	0.000043
1.82	0.00486	0.002916	2.793435	0.008146	0.000066
1.905	0.00524	0.003144	3.371139	0.010599	0.000112
1.995	0.00566	0.003396	4.373546	0.014853	0.000221
2.089	0.00614	0.003684	6.479267	0.020057	0.000403
2.188	0.00669	0.004014	13.7684	0.055266	0.00305
2.291	0.00732	0.004392	49.64517	0.218042	0.047542
2.399	0.00805	0.00483	8.613373	0.041683	0.001731
2.512	0.0089	0.00534	4.475127	0.023897	0.000571
2.63	0.00992	0.005952	2.932652	0.017455	0.000305
2.754	0.01115	0.00669	2.126072	0.014223	0.000202
2.884	0.01265	0.00759	1.632949	0.012394	0.000154
3.02	0.01451	0.008706	1.30208	0.011336	0.000129
3.162	0.01687	0.010122	1.065946	0.01079	0.000116
3.311	0.01996	0.011976	0.888844	0.010645	0.000113
3.467	0.02409	0.014454	0.751891	0.010868	0.000118
3.631	0.02986	0.017916	0.642846	0.011517	0.000133
3.802	0.03828	0.022968	0.554966	0.012746	0.000162
3.981	0.05142	0.030852	0.482649	0.014891	0.000222
4.074	0.04597	0.027582	0.451045	0.012441	0.000155
4.169	0.0559	0.003354	0.42215	0.014159	0.0002
4.266	0.06977	0.041862	0.395666	0.016568	0.000274
4.365	0.0901	0.05406	0.371338	0.020075	0.000403
4.467	0.12185	0.07311	0.348731	0.025496	0.00065
4.571	0.17617	0.105702	0.327903	0.03466	0.001201
4.677	0.28294	0.169764	0.308677	0.052402	0.002746
4.786	0.54194	0.325164	0.29074	0.094518	0.008937
4.898	1.0905	0.6543	0.273998	0.179277	0.03214
5.012	1.2147	0.72882	0.258494	0.188395	0.035493
5.129	1.13193	0.679158	0.243994	0.165711	0.02746
5.248	1.08801	0.652806	0.230536	0.150495	0.022649
5.37	1.22712	0.736272	0.217927	0.160453	0.025745
5.495	0.97652	0.585912	0.206108	0.120761	0.014583
5.623	0.43151	0.258906	0.195025	0.050493	0.00255
5.754	0.22489	0.134934	0.184629	0.024913	0.000621
6.026	0.18152	0.108912	0.165645	0.018041	0.000325
6.31	0.08967	0.053802	0.148906	0.008011	0.000064
6.607	0.05348	0.032088	0.134071	0.004302	0.000019
6.918	0.03545	0.02127	0.120869	0.002581	6.6E-06
7.244	0.02521	0.015126	0.10908	0.00165	2.7E-06

Square Root of the
Sum of the Squares (SRSS)

3.1153 0.6270

Table 19 (cont'd)

Table 19b (cont'd)
Horizontal Steam Supply Attached to the Catwalk

f (Hz)	HV Unit a_{pk} (g)	Catwalk= $a_{pk} \times 0.6$ (g)	T	a_T (g)	a_T^2 (g ²)
7.5e6	0.01898	0.011388	0.1	0.001139	1.3E-06
7.943	0.0174	0.0174	0.1	0.001044	1.1E-06
8.318	0.01949	0.011694	0.1	0.001169	1.4E-06
8.71	0.02224	0.013344	0.1	0.001334	1.8E-06
9.12	0.02612	0.015672	0.1	0.001567	2.5E-06
9.55	0.03221	0.019326	0.1	0.001933	3.7E-06
10	0.04323	0.025938	0.1	0.002594	6.7E-06
10.471	0.05501	0.033006	0.1	0.003301	0.000011
10.965	0.06053	0.036318	0.1	0.003632	0.000013
11.482	0.06172	0.037032	0.1	0.003703	0.000014
12.023	0.06294	0.037764	0.1	0.003776	0.000014
12.589	0.06418	0.038508	0.1	0.003851	0.000015
13.183	0.06545	0.03927	0.1	0.003927	0.000015
13.804	0.06674	0.040044	0.1	0.004004	0.000016
14.454	0.06805	0.04083	0.1	0.004088	0.000017
15.136	0.0694	0.04164	0.1	0.004164	0.000017
15.849	0.07077	0.042462	0.1	0.004246	0.000018
17.378	0.07358	0.044148	0.1	0.004415	0.000019
18.197	0.07503	0.045018	0.1	0.004502	0.00002
19.055	0.07651	0.045906	0.1	0.004591	0.000021
19.953	0.07802	0.046812	0.1	0.004681	0.000022
20.893	0.07956	0.047736	0.1	0.004774	0.000023
21.878	0.08113	0.048678	0.1	0.004868	0.000024
22.909	0.08273	0.049638	0.1	0.004964	0.000025
23.988	0.08436	0.050616	0.1	0.005062	0.000026
25.119	0.08602	0.051612	0.1	0.005161	0.000027
26.303	0.08772	0.052632	0.1	0.005263	0.000028
27.542	0.08945	0.05367	0.1	0.005367	0.000029
28.84	0.09121	0.054726	0.1	0.005473	0.00003
30.2	0.09301	0.055806	0.1	0.005581	0.000031
31.623	0.09485	0.056912	0.1	0.005691	0.000032
33.113	0.09672	0.058032	0.1	0.005803	0.000034
34.674	0.09862	0.059172	0.1	0.005917	0.000035
36.308	0.10057	0.060342	0.1	0.006034	0.000036
38.019	0.10255	0.06153	0.1	0.006153	0.000038
39.811	0.10457	0.062742	0.1	0.006274	0.000039
41.687	0.10663	0.063978	0.1	0.006398	0.000041
43.652	0.10874	0.065244	0.1	0.006524	0.000043
45.709	0.11088	0.066528	0.1	0.006653	0.000044
47.863	0.11307	0.067842	0.1	0.006784	0.000046
50.119	0.1153	0.06918	0.1	0.006918	0.000048
52.481	0.11757	0.070542	0.1	0.007054	0.00005
54.954	0.11989	0.071934	0.1	0.007193	0.000052
57.544	0.12225	0.07335	0.1	0.007335	0.000054
60.256	0.12466	0.074796	0.1	0.00748	0.000056
63.096	0.12712	0.076272	0.1	0.007627	0.000058
66.069	0.12963	0.077778	0.1	0.007778	0.00006
69.183	0.13218	0.079308	0.1	0.007931	0.000063
72.444	0.13479	0.080874	0.1	0.008087	0.000065
75.858	0.13745	0.08247	0.1	0.008247	0.000068
79.433	0.14016	0.084096	0.1	0.00841	0.000071
83.176	0.14292	0.085752	0.1	0.008575	0.000074
87.096	0.14574	0.087444	0.1	0.008744	0.000076
91.201	0.14861	0.089166	0.1	0.008917	0.00008
95.499	0.15154	0.090924	0.1	0.009092	0.000083

Table 19b (cont'd)
Horizontal Steam Supply Attached to the Catwalk

f (Hz)	HV Unit a_{pk} (g)	Catwalk= $a_{pk} \times 0.6$ (g)	T	a_T (g)	a_T^2 (g ²)
100	0.15453	0.092718	0.1	0.009272	0.000086
104.71	0.15758	0.094548	0.1	0.009455	0.000089
109.65	0.16069	0.096414	0.1	0.009641	0.000093
114.82	0.16385	0.098318	0.1	0.009831	0.000097
120.93	0.16701	0.100206	0.1	0.0101021	0.0001
125.89	0.16858	0.101148	0.1	0.010115	0.000102
131.83	0.16858	0.101148	0.1	0.010115	0.000102
138.04	0.16858	0.101148	0.1	0.010115	0.000102
144.54	0.16858	0.101148	0.1	0.010115	0.000102
151.36	0.16858	0.101148	0.1	0.010115	0.000102
158.49	0.16858	0.101148	0.1	0.010115	0.000102
165.96	0.16858	0.101148	0.1	0.010115	0.000102
173.78	0.16858	0.101148	0.1	0.010115	0.000102
181.97	0.16858	0.101154	0.1	0.010115	0.000102
190.55	0.16858	0.101148	0.1	0.010115	0.000102
199.53	0.16858	0.101148	0.1	0.010115	0.000102
208.93	0.16718	0.101148	0.1	0.010115	0.000102
218.78	0.16369	0.101154	0.1	0.010115	0.000102
229.09	0.15959	0.101148	0.1	0.010115	0.000102
239.88	0.1556	0.101148	0.1	0.010115	0.000102
251.19	0.15171	0.100308	0.1	0.10031	0.000101
263.03	0.14791	0.098214	0.1	0.09821	0.000096
275.42	0.14422	0.095754	0.1	0.09575	0.000092
288.4	0.1556	0.09336	0.1	0.009336	0.000087
302	0.15171	0.091026	0.1	0.009103	0.000083
316.23	0.14791	0.088746	0.1	0.008875	0.000079
331.13	0.14422	0.086532	0.1	0.008653	0.000075
346.74	0.14061	0.084366	0.1	0.008437	0.000071
363.08	0.13709	0.082254	0.1	0.008225	0.000068
380.19	0.13366	0.080196	0.1	0.00802	0.000064
398.11	0.13032	0.078192	0.1	0.007819	0.000061
416.87	0.12706	0.076236	0.1	0.007624	0.000058
436.52	0.12388	0.074328	0.1	0.007433	0.000055
457.09	0.12078	0.072468	0.1	0.007247	0.000053
478.63	0.11776	0.070656	0.1	0.007066	0.00005
501.19	0.11482	0.068892	0.1	0.006889	0.000047

SRSS 0.4867

Table 19 (cont'd)

Table 19c Hot Water and Heating Pipes Attached to the Catwalk						Table 19cb (cont'd) Hot Water and Heating Pipes Attached to the Catwalk					
f (Hz)	HV Unit a _{pk} (g)	Catwalk= a _{pk} x 0.6 (g)	T	a _T (g)	a _T ² (g ²)	f (Hz)	HV Unit a _{pk} (g)	Catwalk= a _{pk} x 0.6 (g)	T	a _T (g)	a _T ² (g ²)
1.047	0.00232	0.001392	1.125247	0.001566	2.5E-06	9.55	0.03221	0.019326	0.121112	0.002341	5.5E-06
1.096	0.00245	0.00147	1.138911	0.001674	2.8E-06	10	0.04323	0.025938	0.109298	0.002835	8.0E-06
1.148	0.00259	0.001554	1.154489	0.001794	3.2E-06	10.471	0.05501	0.033006	0.1	0.003301	0.000011
1.202	0.00274	0.001644	1.171922	0.001927	3.7E-06	10.965	0.06053	0.03618	0.1	0.003632	0.000013
1.259	0.0029	0.00174	1.191815	0.002074	4.3E-06	11.482	0.06172	0.037032	0.1	0.003703	0.000014
1.318	0.00308	0.001848	1.214154	0.002244	5.0E-06	12.023	0.06294	0.037764	0.1	0.003776	0.000014
1.38	0.00327	0.001962	1.239719	0.002432	5.9E-06	12.589	0.06418	0.038508	0.1	0.003851	0.000015
1.445	0.00348	0.002088	1.269051	0.00265	7.0E-06	13.183	0.06545	0.03927	0.1	0.003927	0.000015
1.514	0.0037	0.002222	1.303339	0.002893	8.4E-06	13.804	0.06674	0.040044	0.1	0.004004	0.000016
1.585	0.00395	0.00237	1.342426	0.003182	0.00001	14.454	0.06805	0.04083	0.1	0.004083	0.000017
1.66	0.00423	0.002538	1.388484	0.003524	0.000012	15.136	0.0694	0.04164	0.1	0.004164	0.000017
1.738	0.00453	0.002718	1.442377	0.00392	0.000015	15.849	0.07077	0.042462	0.1	0.004246	0.000018
1.82	0.00486	0.002916	1.506754	0.004394	0.000019	16.596	0.07216	0.043296	0.1	0.00433	0.000019
1.905	0.00524	0.003144	1.583451	0.004978	0.000025	17.378	0.07358	0.044148	0.1	0.004415	0.000019
1.995	0.00566	0.003396	1.678144	0.005699	0.000032	18.197	0.07503	0.045018	0.1	0.004502	0.00002
2.089	0.00614	0.003684	1.795585	0.006615	0.000044	19.055	0.07651	0.045906	0.1	0.004591	0.000021
2.188	0.00669	0.004014	1.94577	0.00781	0.000061	19.953	0.07802	0.046812	0.1	0.004681	0.000022
2.291	0.00732	0.004392	2.140862	0.009403	0.000088	20.893	0.07956	0.047736	0.1	0.004774	0.000023
2.399	0.00805	0.00483	2.405674	0.011619	0.000135	21.878	0.08113	0.048678	0.1	0.004868	0.000024
2.512	0.0089	0.00534	2.782761	0.01486	0.000221	22.909	0.08273	0.049638	0.1	0.004964	0.000025
2.63	0.00992	0.005952	3.358228	0.019988	0.0004	23.988	0.08436	0.050616	0.1	0.005062	0.000026
2.754	0.01115	0.00669	4.347098	0.029082	0.000846	25.119	0.08602	0.051612	0.1	0.005161	0.000027
2.884	0.01265	0.00759	6.421654	0.04874	0.002376	26.303	0.08772	0.052632	0.1	0.005263	0.000028
3.02	0.01451	0.008706	13.41402	0.116782	0.013638	27.542	0.08945	0.05367	0.1	0.005367	0.000029
3.162	0.01687	0.010122	54.82281	0.554917	0.307932	28.84	0.09121	0.054726	0.1	0.005473	0.00003
3.311	0.01996	0.011976	8.801083	0.105402	0.0111	30.2	0.09301	0.055806	0.1	0.005581	0.000031
3.467	0.02409	0.014454	4.529715	0.065472	0.004287	31.623	0.09485	0.05691	0.1	0.005691	0.000032
3.631	0.02986	0.017916	2.950947	0.052869	0.002795	33.113	0.09672	0.058032	0.1	0.005803	0.000034
3.802	0.03828	0.022968	2.137292	0.049089	0.00241	34.674	0.09862	0.059172	0.1	0.005917	0.000035
3.981	0.05142	0.030852	1.641224	0.050635	0.002564	36.308	0.10057	0.060342	0.1	0.006034	0.000036
4.074	0.04597	0.027582	1.459114	0.040245	0.00162	38.019	0.10255	0.06153	0.1	0.006153	0.000038
4.169	0.0559	0.03354	1.307457	0.043852	0.001923	39.811	0.10457	0.062742	0.1	0.006274	0.000039
4.266	0.06977	0.041862	1.179378	0.049371	0.002438	41.687	0.10663	0.063978	0.1	0.006398	0.000041
4.365	0.0901	0.05406	1.069921	0.05784	0.003345	43.652	0.10874	0.065244	0.1	0.006524	0.000043
4.467	0.12185	0.07311	0.974562	0.07125	0.005077	45.709	0.11088	0.066528	0.1	0.006653	0.000044
4.571	0.17617	0.105702	0.105702	0.891644	0.094249	47.863	0.11307	0.067842	0.1	0.006784	0.000046
4.677	0.2894	0.169764	0.818973	0.139032	0.01933	50.119	0.1153	0.06918	0.1	0.006918	0.000048
4.786	0.54194	0.325164	0.754288	0.245267	0.060156	52.481	0.11757	0.070542	0.1	0.007054	0.00005
4.898	1.0905	0.6543	0.696447	0.455686	0.207649	54.954	0.11989	0.071934	0.1	0.007193	0.000052
5.012	1.2147	0.72882	0.644934	0.470041	0.220939	57.544	0.12225	0.07335	0.1	0.007335	0.000054
5.129	1.13193	0.679158	0.598447	0.40644	0.165193	60.256	0.12466	0.074796	0.1	0.00748	0.000056
5.248	1.08801	0.652806	0.556685	0.363407	0.132065	63.096	0.12712	0.076272	0.1	0.007627	0.000058
5.37	1.22712	0.736272	0.518713	0.381914	0.145858	66.069	0.12963	0.077778	0.1	0.007778	0.00006
5.495	0.97652	0.585912	0.484094	0.283637	0.08045	69.183	0.13218	0.079308	0.1	0.007931	0.000063
5.623	0.43151	0.258906	0.452453	0.117143	0.013722	72.444	0.13479	0.080874	0.1	0.008087	0.000065
5.754	0.22489	0.134934	0.423466	0.05714	0.003265	75.858	0.13745	0.08247	0.1	0.008247	0.000068
6.026	0.18152	0.108912	0.372203	0.040537	0.001643	79.433	0.14016	0.084096	0.1	0.00841	0.000071
6.31	0.08967	0.053802	0.328697	0.017685	0.000313	83.176	0.14292	0.085752	0.1	0.008575	0.000074
6.607	0.05348	0.032088	0.2914	0.00935	0.000087	87.096	0.14574	0.087444	0.1	0.008744	0.000076
6.918	0.03545	0.02127	0.25916	0.005512	0.00003	91.201	0.14861	0.089166	0.1	0.008917	0.00008
7.244	0.02521	0.015126	0.231097	0.003496	0.00012	95.499	0.15154	0.09024	0.1	0.009092	0.000083
7.586	0.01898	0.011388	0.20653	0.002352	5.5E-06	100	0.15453	0.092718	0.1	0.009272	0.000086
7.943	0.0174	0.01044	0.18503	0.001932	3.7E-06	104.71	0.15758	0.094548	0.1	0.009455	0.000089
8.318	0.01949	0.011694	0.166022	0.001941	3.8E-06	109.65	0.16069	0.096414	0.1	0.009641	0.000093
8.71	0.0224	0.13344	0.14924	0.001991	4.0E-06	114.82	0.16385	0.09831	0.1	0.009831	0.000097
9.12	0.02612	0.015672	0.134367	0.002106	4.4E-06	120.23	0.16701	0.100206	0.1	0.010021	0.0001

Table I9 (cont'd)

Table I9c (cont'd)
Hot Water and Heating Pipes Attached to the Catwalk

f (Hz)	HV Unit a_{pk} (g)	Catwalk= $a_{pk} \times 0.6$ (g)	T	a_T (g)	a_T^2 (g ²)
125.89	0.16858	0.101148	0.1	0.010115	0.000102
131.83	0.16858	0.101148	0.1	0.0115	0.000102
138.04	0.16858	0.101148	0.1	0.010115	0.000102
144.54	0.16858	0.101148	0.1	0.010115	0.000102
151.36	0.16858	0.101148	0.1	0.010115	0.000102
158.49	0.16858	0.101148	0.1	0.010115	0.000102
165.96	0.16858	0.101148	0.1	0.010115	0.000102
173.78	0.16858	0.101148	0.1	0.010115	0.000102
181.97	0.16858	0.101148	0.1	0.010115	0.000102
190.55	0.16858	0.101148	0.1	0.010115	0.000102
199.53	0.16858	0.101148	0.1	0.010115	0.000102
208.93	0.16858	0.101148	0.1	0.010115	0.000102
218.78	0.16859	0.101154	0.1	0.010115	0.000102
229.09	0.16858	0.101148	0.1	0.010115	0.000102
239.88	0.16858	0.101148	0.1	0.010115	0.000102
251.19	0.16718	0.100308	0.1	0.020031	0.000101
263.03	0.16369	0.098214	0.1	0.009821	0.000096
275.42	0.15959	0.095754	0.1	0.009575	0.000092
288.4	0.1556	0.09336	0.1	0.009336	0.000087
302	0.15171	0.091026	0.1	0.009103	0.000083
316.23	0.14791	0.088746	0.1	0.008875	0.000079
331.13	0.14422	0.086532	0.1	0.008653	0.000075
346.74	0.14061	0.084366	0.1	0.008437	0.000071
363.08	0.13709	0.082254	0.1	0.008225	0.000068
380.19	0.13366	0.080196	0.1	0.00802	0.000064
398.11	0.13032	0.078192	0.1	0.007819	0.000061
416.87	0.12706	0.076236	0.1	0.007624	0.000058
436.52	0.12388	0.074328	0.1	0.007433	0.000055
457.09	0.12078	0.072468	0.1	0.007247	0.000053
478.63	0.11776	0.070656	0.1	0.007066	0.00005
501.19	0.11482	0.068892	0.1	0.006889	0.000047

SRSS 1.1950

APPENDIX J: Qualification of Alternate Isolators

Several special cases of Amber/Booth isolators that exceed the maximum stiffness requirements of Table 22a through 22c, have been evaluated to determine if they are acceptable substitutes for those meeting these requirements. Exceeding the maximum stiffness requirement means that the transmissibility will increase, which will in turn increase the effective vertical and horizontal load in the isolators. This increased load is normally very small. What follows is the discussion related to each special case.

Horizontal Wind Braces

The Amber/Booth BSA-2-1600 isolator is being used as a E isolator to support the horizontal wind braces. In Table 22a, for a transmissibility of 0.20 the maximum stiffness is 797 lb/in, but the stiffness of the BSA-2-1600 isolator is 800 lb/in. This difference is of course negligible, but as a check the impact of the greater stiffness was evaluated by assuming a greater transmissibility of 0.23, which increases the maximum acceptable stiffness to 894 lb/in, which is well beyond the 800 lb/in needed for this isolator. This increase in transmissibility only increases the maximum vertical isolated load by 1 lb to 1409 lb. The increased load is well below the capacity of the isolator and the load on the supporting bar joist is also only increase by 1 lb. Therefore the BSA-2-1600 isolator is acceptable as a E isolator. Table 22a summarizes these calculations for the worst case of the isolator being attached to three bar joists, such that the mass loading benefits are minimized.

4 in. Horizontal Steam Supply Pipe

The Amber/Booth SW-2-250 isolator is being used where there should be a J isolator to support the four in. horizontal steam supply pipe to a bar joist at the roof. In Table 22a, for a transmissibility of 0.20 the maximum acceptable stiffness is 74 lb/in, but the stiffness of the SW-2-250 isolator is 125 lb/in. The transmissibility will increase to 0.39 for the 125 lb/in isolator. This increased in transmissibility will increase the maximum vertical isolated load by only 1 lb to 102 lb. The increased load is well below the 250 lb capacity of the isolator and will only increase the load on the supporting bar joist by 1lb. Therefore the SW-2-250 isolator is acceptable for supporting this pipe. Table 22a summarizes these calculations.

4 in. Fire Protection Oscillating Monitor Pipe

The four in. fire protection oscillating monitor pipe should be supported with the I isolator which has a maximum stiffness of 134 lb/in. This pipe is being supported with a Amber/Booth SW-1-300 isolator that has a stiffness of 300 lb/in. The minimum weight per isolator is 65 lb at the location just before the pipe drops down to the oscillating monitor at the floor of the building. The SW-1-300 is unacceptable at this location. At all other support locations the minimum weight per isolator is 85 lb. For this minimum load the transmissibility becomes 0.40, and the maximum vertical isolated load increases by 4 lb to 234 lb, well below the 300 lb capacity of the isolator. For the support location where the pipe drops down to the monitor at the floor a 50 lb weight should be added to the pipe to increase the weight per isolator by 25 lb, thus bringing the weight per isolator to 90 lb. With this additional weight the load per isolator now falls within the 85 lb minimum requirement at all locations and the SW-1-300 becomes acceptable for supporting this pipe at all locations. Table 22b summarizes these calculations. The minimum support spacing requirements used to determine the weight per isolator must be followed as discussed in Chapter 8 of this report.

Fire Protection Beacon Light

Amber/Booth BSA-1-25 isolators are being used as C isolators to support the fire protection beacon lights. For a transmissibility of 0.36 the maximum acceptable stiffness is 23 lb/in, but the stiffness of the BSA-1-25 isolator is 25 lb/in. This will increase the transmissibility to 0.40, does not increase the maximum vertical isolated load. This load remains 21 lb which is below the 25 lb isolator capacity. Therefore the BSA-1-25 isolator is acceptable for supporting this light. Table 22b summarizes these calculations.

Exhaust Fan Number 6 Horizontal Ductwork

Chapter 8 specifies the isolators that should be installed for the isolation of HV ductwork. As described in that Chapter 8 the horizontal ductwork in the roof truss area that exhausts fans 5, 6, 7, 8, 9, 15, 16, 17, 18, and 19 requires a I isolator, at those locations supported to a bar joist as indicated in Table I3c to I3k. However an H isolator has been installed for supporting the duct for Exhaust Fan 6 to the bar joist. This is a larger isolator with a greater stiffness than the recommended I isolators and thus this installation must be evaluated here. The specific isolator installed is a Amber/Booth SW-2-500 which has a stiffness of 250 lb/in. At this location the calculated weight per isolator is 117 lb as shown in Table I3g. For the purpose of this analysis a minimum weight of 105 lb and maximum of 130 lb per isolators was used. A transmissibility of 0.39 results in a maximum allowable stiffness of 292 lb and a maximum vertical isolated load of 179 lb. These calculations are summarized in Table 22a. The SW-2-500 with a stiffness of 250 lb falls below the 292 lb/in requirement, and it has a capacity of 540 lb which of course is well beyond the 179 lb applied load. Therefore this isolator is acceptable, even though it is larger than the appropriate isolator.

USACERL DISTRIBUTION

Chief of Engineers

ATTN: CEHEC-IM-LH (2)
ATTN: CEHEC-IM-LP (2)
ATTN: CERD-L
ATTN: CEMP-C
ATTN: CEMP-ET
ATTN: CEMRD-MD-MF
ATTN: CEMRO-ED-MB

HQ TAC/DES
(CETSO/ESEN)
Langley AFB, VA 23665

AFRCE-SAC (2)
ATTN: HQ SAQ/DEEQ
Offutt AFB, NE 68113

ASD/YS-SM
Wright-Patterson AFB, OH 45433-6503

US Army Engineer Districts
ATTN: Omaha 68102-4910

Fort Belvoir, VA
ATTN: CECC-R 22060-5580

CEWES, ATTN: Library 39180-6199

NAVFAC
ATTN: Naval Civil Engr Lab 93043

HQ AFCESA/RALC
Tyndall AFB, FL 32403-6001

351 SPTG/DEE
Whiteman AFB, MO 65305-5000

US Government Printing Office 20401
Receiving/Depository Section (2)

Nat'l Institute of Standards & Tech 20899

Defense Technical Info Center 22304
ATTN: DTIC-FAB (2)

24
+1
08/92